ACOMEN 2017

September 18-22, Ghent, Belgium

GHENT
UNIVERSITY

Book of Abstracts

Editors:
Marián Slodička, Ghent University
Karel van Bockstal, Ghent University

Organising committee:
C. Geuzaine (Univ. de Liège, Belgium)
S. Pop (UHasselt, Belgium)
K. Van Bockstal (Ghent Univ., Belgium)

Scientific committee:
J. Kačur (Comenius Univ., Bratislava, Slovakia)
G. S. Dulikravich (Florida Inte. Univ., USA)
P. Šolín (University of Nevada, Reno, USA)
S. Majid Hassanizadeh (Utrecht University, The Netherlands)
E. Zuazua (Universidad Autónoma de Madrid, Spain)
C. Geuzaine (Univ. de Liège, Belgium)
S. Pop (UHasselt, Belgium)

Sponsors and partners:

ISBN: xxxxxx

Welcome word from Marián Slodička, Conference Chair

Dear participants,

First of all, I wish to welcome you to the city of Ghent. We will have more than one hundred talks during this week!

This is already the seventh edition of the international conference on Advanced COmputational Methods in ENgineering. Like the previous editions of the conference, themes are concentrated on mathematical modeling, simulation and numerical methods for solving scientific problems from various engineering disciplines. I would like to thank all of its participants because they turn every ACOMEN into an interesting, learning-full and pleasant event.

Another important factor of the success of ACOMEN are the highstanding invited main lectures given by world-wide recognized experts in their respective research fields: Susanne C. Brenner (Louisiana State University), Zdzisław Brzeźniak (University of York), Martin Burger (University of Münster), Charles Elliott (University of Warwick), Ralf Hiptmair (ETH Zürich), Michael Klibanov (University of North Carolina at Charlotte), Peter Knabner (Universität Erlangen-Nürnberg, and Alfio Quarteroni (Ecole Polytechnique Federale de Lausanne).

I also thank the session chairs and organizers of the mini symposia for their engagement; Markus Bause, Thomas Carrao, Ivan Cimrák, Rob De Staelen, Abdellatif El Badia, Peter Frolkovič, Christophe Geuzaine, Thomas Henneron, Matteo Icardi, Mohammad Issa, Iveta Jančigová, Klaus Kaiser, Serge Nicaise, Florin Adrian Radu, Hendrik Rogier, Ruth V. Sabariego, and Jochen Schütz.

Special thanks goes to the organizational team of this edition, all technical staff working behind the scenes, and in particular Karel van Bockstal, conference secretary. Should you have any questions or specific needs during our meeting, we are more than glad to help you at the conference reception desk.

I hope you will enjoy your stay!

Kind regards,
Marián Slodička

Plenary speakers

Susanne C. Brenner
Louisiana State University

Zdzisław Brzeźniak
University of York

Martin Burger
University of Münster

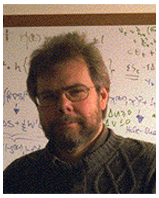

Charles Elliot
University of Warwick

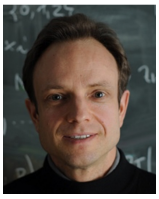

Ralf Hiptmair
ETH Zürich

Michael Klibanov
University of North Carolina at Charlotte

Peter Knabner
Universität Erlangen-Nürnberg

Alfio Quarteroni
École Polytechnique Fédérale de Lausanne

Contents

Plenary Talks

Book of abstracts of the 7th International Conference
on Advanced Computational Methods
in Engineering, ACOMEN 2017
18–22 September 2017.

C^0 Interior Penalty Methods

Susanne C. Brenner[1]

[1] *Department of Mathematics and Center for Computation & Technology, Louisiana State University, Baton Rouge, LA 70803, USA*

e-mails: brenner@math.lsu.edu

Abstract

C^0 interior penalty methods are discontinuous Galerkin methods for fourth order problems. In this talk we will present a simple analysis of C^0 interior penalty methods for the biharmonic problem and discuss the applications of C^0 interior penalty methods to two nonlinear problems for plates.

Key words: buckling, discontinuous Galerkin, obstacle, plate, variational inequalities
MSC 2010: 65N30, 65K15, 74S05, 49J40

Let Ω be a bounded convex polygonal domain in $\mathbb{R}^2$ and $f \in L_2(\Omega)$. Consider the following model biharmonic problem with the boundary conditions of clamped plates:

$$a(u,v) = (f,v) \qquad \forall\, v \in H_0^2(\Omega), \tag{1}$$

where

$$a(u,v) = \int_\Omega D^2u : D^2v\, dx, \qquad (f,v) = \int_\Omega fv\, dx,$$

and $D^2u : D^2v$ is the Frobenius inner product of the Hessian matrices for u and v.

Let $\mathcal{T}_h$ be a simplicial triangulation of Ω, $\mathcal{E}_h$ be the set of the edges in $\mathcal{T}_h$ and $V_h \subset H_0^1(\Omega)$ be a Lagrange finite element space of order ≥ 2 associated with $\mathcal{T}_h$. The C^0 interior penalty method for (1), introduced in [19], determines an approximation $u_h \in V_h$ by

$$a_h(u_h,v) = \int_\Omega fv\, dx, \tag{2}$$

where

$$\begin{aligned} a_h(w,v) = &\sum_{T\in\mathcal{T}_h}\int_T D^2w : D^2v\, dx + \sum_{e\in\mathcal{E}_h}\int_e \left\{\!\!\left\{\frac{\partial^2 w}{\partial n^2}\right\}\!\!\right\}\left[\!\!\left[\frac{\partial v}{\partial n}\right]\!\!\right] ds \\ &+ \sum_{e\in\mathcal{E}_h}\int_e \left\{\!\!\left\{\frac{\partial^2 v}{\partial n^2}\right\}\!\!\right\}\left[\!\!\left[\frac{\partial w}{\partial n}\right]\!\!\right] ds + \sigma\sum_{e\in\mathcal{E}_h}\frac{1}{|e|}\int_e \left[\!\!\left[\frac{\partial w}{\partial n}\right]\!\!\right]\left[\!\!\left[\frac{\partial v}{\partial n}\right]\!\!\right] ds. \end{aligned}$$

Here $\{\!\{\partial^2 v/\partial n^2\}\!\}$ (resp., $[\![\partial v/\partial n]\!]$) denotes the mean (resp., jump) of the second (resp. first) normal derivative across an edge, $|e|$ denotes the length of the edge e, and $\sigma > 0$ is a penalty

parameter. Note that simple modifications of V_h or $a_h(\cdot,\cdot)$ would allow other boundary conditions to be handled [6, 4].

For σ sufficiently large, the bilinear form $a_h(\cdot,\cdot)$ satisfies

$$a_h(v,v) \geq C_b \|v\|_h^2 \qquad \forall\, v \in V_h, \tag{3}$$

where

$$\|v\|_h^2 = \sum_{T\in\mathcal{T}_h} |v|_{H^2(T)}^2 + \sum_{e\in\mathcal{E}_h} |e|^{-1} \|[\![\partial v/\partial n]\!]\|_{L_2(e)}^2,$$

and the unique solution of (2) satisfies

$$\|u-u_h\|_h \leq Ch\|f\|_{L_2(\Omega)}. \tag{4}$$

The error analysis for C^0 interior penalty methods can be carried out in terms of the standard nodal interpolation operator $\Pi_h : H_0^2(\Omega) \longrightarrow V_h$ and an enriching operator $E_h : V_h \longrightarrow H_0^2(\Omega)$ defined by local averaging. The operator E_h enjoys the following properties (cf. [11, 2]):

$$\sum_{k=0}^{2} h^k |v - E_h v|_{H^k(\Omega)} \leq Ch^2 \|v\|_h \qquad \forall\, v \in V_h, \tag{5}$$

$$|a_h(\Pi_h\zeta, v) - a(\zeta, E_h v)| \leq Ch|\zeta|_{H^3(\Omega)}\|v\|_h \qquad \forall\, \zeta \in H^3(\Omega)\cap H_0^2(\Omega),\ v \in V_h, \tag{6}$$

$$|\zeta - E_h\Pi_h\zeta|_{H^2(\Omega)} \leq Ch|\zeta|_{H^3(\Omega)} \qquad \forall\, \zeta \in H^3(\Omega)\cap H_0^2(\Omega). \tag{7}$$

We have, by (3),

$$\|\Pi_h u - u_h\|_h \leq C \sup_{v\in V_h} \frac{a_h(\Pi_h u - u_h, v)}{\|v\|_h}, \tag{8}$$

and, by (1), (2), (5) and (6),

$$\begin{aligned} a_h(\Pi_h u - u_h, v) &= a_h(\Pi_h u, v) - (f, v) \\ &\leq a(u, E_h v) - (f, v) + Ch|u|_{H^3(\Omega)}\|v\|_h \\ &= (f, E_h v - v) + Ch|u|_{H^3(\Omega)}\|v\|_h \\ &\leq C(h^2\|f\|_{L_2(\Omega)} + h|u|_{H^3(\Omega)})\|v\|_h \leq Ch\|f\|_{L_2(\Omega)}\|v\|_h. \end{aligned} \tag{9}$$

The error estimate (4) then follows from (8), (9), the triangle inequality and a standard interpolation error estimate for Π_h (cf. [10]).

C^0 interior penalty methods have certain advantages over classical finite element methods: (i) They are simpler than conforming finite element methods (especially in three dimensions). (ii) The lower order C^0 interior penalty methods are as simple as classical nonconforming finite element methods and the higher order ones can capture smooth solutions efficiently. (iii) Unlike mixed finite element methods, they preserve the symmetric positive definite property of the continuous problem.

Since the underlying finite element spaces are precisely the ones for second order problems, there are two other advantages: (i) Multigrid methods for the Laplace equation can be incorporated as preconditioners for C^0 interior penalty methods [12]. (ii) The isoparametric approach, originally developed for second order problems, can be extended to C^0 interior penalty methods for fourth order problems on curved domains [8].

Note that the post-processed solution $E_h u_h$ satisfies

$$\begin{aligned} |u - E_h u_h|_{H^2(\Omega)} &\leq |u - E_h \Pi_h u|_{H^2(\Omega)} + |E_h(\Pi_h u - u_h)|_{H^2(\Omega)} \\ &\leq |u - E_h \Pi_h u|_{H^2(\Omega)} + C(|\Pi_h u - u|_{H^2(\Omega)} + |u - u_h|_{H^2(\Omega)}) \\ &\leq Ch(|u|_{H^3(\Omega)} + \|f\|_{L_2(\Omega)}) \leq Ch\|f\|_{L_2(\Omega)} \end{aligned} \tag{10}$$

by (4), (5), (7), and a standard interpolation error estimate. Thus the C^0 interior penalty methods are also relevant for computing conforming approximations of u.

The estimates (4) and (10) can be extended to nonconvex polygonal domains and other boundary conditions, where h is replaced by h^α and the index of elliptic regularity α is determined by the interior angles at the corners of Ω and the boundary conditions [1].

Domain decomposition methods and multigrid methods for C^0 interior penalty methods were investigated in [17, 12, 18], and an adaptive algorithm was developed in [5]. The enriching operator E_h plays a key role in the constructions and analyses of these methods. indicate that the performance of the adaptive algorithm based on this

C^0 interior penalty methods have been applied to the von Kármán model for plate buckling in [7] and to the obstacle problem for clamped Kirchhoff plates in [15, 14]. The estimates (5)–(7) are again fundamental to the analyses of these methods. Surprisingly, the residual based error estimator in [5] can also be applied directly to the obstacle problem [3].

One can also apply C^0 interior penalty methods to elliptic distributed optimal control problems with pointwise state constraints by reformulating these problems as obstacle problems for simply supported plates [16, 9, 13].

Finally we note that C^0 interior penalty methods have been extended to fourth order problems with variable coefficients in [20] and variants of C^0 interior penalty methods can be found in [22, 21].

References

[1] H. Blum and R. Rannacher. On the boundary value problem of the biharmonic operator on domains with angular corners. *Math. Methods Appl. Sci.*, 2:556–581, 1980.

[2] S.C. Brenner. C^0 Interior Penalty Methods. In J. Blowey and M. Jensen, editors, *Frontiers in Numerical Analysis-Durham 2010*, volume 85 of *Lecture Notes in Computational Science and Engineering*, pages 79–147. Springer-Verlag, Berlin-Heidelberg, 2012.

[3] S.C. Brenner, J. Gedicke, L.-Y. Sung, and Y. Zhang. An a posteriori analysis of C^0 interior penalty methods for the obstacle problem of clamped Kirchhoff plates. *SIAM J. Numer. Anal.*, 55:87–108, 2017.

[4] S.C. Brenner, S. Gu, T. Gudi, and L.-Y. Sung. A quadratic C^0 interior penalty method for linear fourth order boundary value problems with boundary conditions of the Cahn-Hilliard type. *SIAM J. Numer. Anal.*, 50:2088–2110, 2012.

[5] S.C. Brenner, T. Gudi, and L.-Y. Sung. An a posteriori error estimator for a quadratic C^0 interior penalty method for the biharmonic problem. *IMA J. Numer. Anal.*, 30:777–798, 2010.

[6] S.C. Brenner and M. Neilan. A C^0 interior penalty method for a fourth order elliptic singular perturbation problem. *SIAM J. Numer. Anal.*, 49:869–892, 2011.

[7] S.C. Brenner, M. Neilan, A. Reiser, and L.-Y. Sung. A C^0 interior penalty method for a von Kármán plate. *Numer. Math.*, 135:803–832, 2017.

[8] S.C. Brenner, M. Neilan, and L.-Y. Sung. Isoparametric C^0 interior penalty methods for plate bending problems on smooth domains. *Calcolo*, 49:35–67, 2013.

[9] S.C. Brenner, M. Oh, S. Pollock, K. Porwal, M. Schedensack, and N. Sharma. A C^0 interior penalty method for elliptic distributed optimal control problems in three dimensions with pointwise state constraints. In S.C. Brenner, editor, *Topics in Numerical Partial Differential Equations and Scientific Computing*, volume 160 of *The IMA Volumes in Mathematics and its Applications*, pages 1–22, Cham-Heidelberg-New York-Dordrecht-London, 2016. Springer.

[10] S.C. Brenner and L.R. Scott. *The Mathematical Theory of Finite Element Methods* (*Third Edition*). Springer-Verlag, New York, 2008.

[11] S.C. Brenner and L.-Y. Sung. C^0 interior penalty methods for fourth order elliptic boundary value problems on polygonal domains. *J. Sci. Comput.*, 22/23:83–118, 2005.

[12] S.C. Brenner and L.-Y. Sung. Multigrid algorithms for C^0 interior penalty methods. *SIAM J. Numer. Anal.*, 44:199–223, 2006.

[13] S.C. Brenner and L.-Y. Sung. A new convergence analysis of finite element methods for elliptic distributed optimal control problems with pointwise state constraints. *SICON*, to appear.

[14] S.C. Brenner, L.-Y. Sung, H. Zhang, and Y. Zhang. A quadratic C^0 interior penalty method for the displacement obstacle problem of clamped Kirchhoff plates. *SIAM J. Numer. Anal.*, 50:3329–3350, 2012.

[15] S.C. Brenner, L.-Y. Sung, and Y. Zhang. Finite element methods for the displacement obstacle problem of clamped plates. *Math. Comp.*, 81:1247–1262, 2012.

[16] S.C. Brenner, L.-Y. Sung, and Y. Zhang. A quadratic C^0 interior penalty method for an elliptic optimal control problem with state constraints. In O. Karakashian X. Feng and Y. Xing, editors, *Recent Developments in Discontinuous Galerkin Finite Element Methods for Partial Differential Equations*, volume 157 of *The IMA Volumes in Mathematics and its Applications*, pages 97–132, Cham-Heidelberg-New York-Dordrecht-London, 2013. Springer. (2012 John H. Barrett Memorial Lectures).

[17] S.C. Brenner and K. Wang. Two-level additive Schwarz preconditioners for C^0 interior penalty methods. *Numer. Math.*, 102:231–255, 2005.

[18] S.C. Brenner and K. Wang. An iterative substructuring algorithm for a C^0 interior penalty method. *Elect. Trans. Numer. Anal.*, 39:313–332, 2012.

[19] G. Engel, K. Garikipati, T.J.R. Hughes, M.G. Larson, L. Mazzei, and R.L. Taylor. Continuous/discontinuous finite element approximations of fourth order elliptic problems in structural and continuum mechanics with applications to thin beams and plates, and strain gradient elasticity. *Comput. Methods Appl. Mech. Engrg.*, 191:3669–3750, 2002.

[20] T. Gudi, H.S. Gupta, and N. Nataraj. Analysis of an interior penalty method for fourth order problems on polygonal domains. *J. Sci. Comp.*, 54:177–199, 2013.

[21] J. Huang, X. Huang, and W. Han. A new C^0 discontinuous Galerkin method for Kirchhoff plates. *Comput. Methods Appl. Mech. Engrg.*, 199:1446–1454, 2010.

[22] G.N. Wells, E. Kuhl, and K. Garikipati. A discontinuous Galerkin method for the Cahn-Hilliard equation. *J. Comput. Phys.*, 218:860–877, 2006.

Book of abstracts of the 7th International Conference
on Advanced Computational Methods
in Engineering, ACOMEN 2017
18–22 September 2017.

Finite element method approximation of stochastic Landau-Lifshitz-Gilbert Equations.

Zdzisław Brzeźniak[1]

[1] *Department of Mathematics, University of York, UK*

e-mails: zdzislaw.brzezniak@york.ac.uk

Abstract

I will discuss finite element based space-time discretisations of the stochastic Landau-Lifshitz-Gilbert Equations. I will explain that the sequence of numerical solutions converges, for vanishing discretisation parameters, to a weak martingale solution. I will begin with recalling a few theoretical results regarding finite element approximations, compactness arguments, the Skorokhod Theorem, and the maximal regularity. The main part of my talk is based on a joint works with Lubo Baňas, Misha Neklyudov and Andreas Prohl [3, 4, 5] and with Ben Goldys and T Jegaraj [6].

Key words: stochastic Landau-Lifshitz-Gilbert equations, finite element method, time discretization, Itô-Stratonovich differential
MSC 2010: 82D40 (35R60 37A25 37A30 37M25 60H15 65Cxx

1 Historical background

Let us begin with the following paraphrase of a passage from the famous paper [7] by W Faris and G Jona-Lasinio. An example of primary importance in physics is provided by ferromagnetism. Since the seminal works by Weiss [18], Landau and Lifshitz [12], and Gilbert [8], it is well known that the behaviour of magnetization field M of a ferromagnetic material below the so called Curie temperature is usually described in terms of the Laundau-Lifshitz-Gilbert equations (LLGEs). However, this equation is known to be approximate in more than one aspect. It takes into account only approximately the microscopic nature of the classical fields. In addition, quantum effects and other sources of fluctuations are completely ignored. It is therefore of interest to know which properties described by these equations survive perturbations, in particular small stochastic perturbations which imitate some of the neglected effects. This latter problem is also of special importance in connection with some modern theories where one would like to determine physically interesting measures invariant under the flow generated by the LLGEs and stable under small perturbations. Another reason for studying stochastic perturbations of the LLGEs comes from the physical observations, see Neel [15] and Brown [2], that the physical experiments indicate that there must be a hidden mechanism which makes the magnetization to jump between stationary states. These stationary states are locally stable in the deterministic description and therefore, had the deterministic picture been completely accurate, such jumping behaviour would be impossible, see also the very nice article [11] by Kohn, Reznikoff and Vanden-Eijnden. The proposed model for the

hidden mechanism is a heat bath or an external noise, and the phenomenon is often called the *noise induced magnetization reversal*. The external noise is usually modelled by a time derivative of the Brownian Motion. Once the works by Neel and Brown have become known to the scientific community, there was a huge interest in the physical community in trying to explain physical experiments using the ideas of stochastic perturbations of the LLGES, see for instance papers [13] by Lyberatos and Chantrell, [9] Grinstein and Koch, [16] by Rikvold et al and [14] by Martens et al. In most of these works a simple one-particle ferromagnetic material was studied, which resulted in the reduction of the original LLGEs (which are genuine partial differential equations, with a first order derivative in time and a second order derivatives in space), to ordinary differential equations on the 2-dimensional sphere. This sphere constraint is a consequence of the assumption that the system is well below the Curie temperature and thus the magnetization has a length not changing in time.

2 Brief description

In this lectures I will address the following question: The numerical approximations of the solutions to the stochastic Landau-Lifshitz-Gilbert equations and its convergence.

We anticipate that the main audience of these lectures will be young researchers (advanced PhD students and postdocs) in the Stochastic Analysis (including the quickly growing community of researchers in Stochastic Partial Differential Equations) who would like to learn the theory of finite element approximation of Stochastic Partial Differential Equations on the concrete example of the stochastically perturbed Laundau-Lifshitz-Gilbert equations as well as researchers in Partial Differential Equations who would like to learn some aspects of stochastic models of PDEs.

We consider a a domain $D \subset \mathbb{R}^d$, $d = 1, 2, 3$, consisting of ferromagnetic material whose the magnetic moment at $x \in D$ and time t is denoted by $u(t, x)$. For temperatures not too high (below the Curie point) it hold that

$$|u(t, x)| = 1, \quad x \in D, \quad t \geq 0.$$

A configuration $u : D \to \mathbb{S}^2 \subset \mathbb{R}^3$, $u \in \mathbb{H}^1$, of magnetic moments minimizes the energy functional

$$\mathcal{E}_0(u) = \frac{a}{2} \int_D |\nabla u|^2 dx + \int_D \phi(u) dx - \int_D H \cdot u dx \tag{1}$$

consisting of *exchange*, *anisotropy* and *external* energies, where H is a given external field, and $\phi : \mathbb{S}^2 \to \mathbb{R}$ represents the anisotropy of the material, e.g. $\phi(u) = \frac{\beta}{2}(u_1^2 + u_2^2)$, $u = (u_1, u_2, u_3) \in \mathbb{S}^2$. When $H = 0$ the minimum of $\mathcal{E}_0$ subject to Neumann boundary conditions is attained at constant functions $\zeta_\pm(x) = (0, 0, \pm 1)$, $x \in D$. With the so-called effective field defined as

$$\mathcal{H}_0(u) = -\nabla_u \mathcal{E}_0(u) = a\Delta u - \phi'(u) + H, \tag{2}$$

where the gradient $\nabla_u \mathcal{E}_0(u)$ is (formally) with respect to the L^2-inner product, the Landau-Lifshitz-Gilbert equations read as follows

$$\begin{cases} \frac{\partial u}{\partial t} = \lambda_1 u \times \mathcal{H}(u) - \lambda_2 u \times (u \times \mathcal{H}(u)) & \text{on} \quad (0, \infty) \times D \\ \frac{\partial u}{\partial n} = 0 & \text{on} \quad \partial(0, \infty) \times D \end{cases} \tag{3}$$

where $\lambda_2 > 0$, $\lambda_1 \in \mathbb{R}$, and we assume that the initial data satisfies $|u_0| = 1$ on D. Following Néel [15], we will consider the energy perturbed by noise

$$\mathcal{E}(u) = \mathcal{E}_0(u) - \int_D \langle e \circ dW, u \rangle \tag{4}$$

where $e \circ dW = \sum_{j=1}^{N} e_j \circ dW_j$ for some $e_j \in \mathbb{H}^1$, $j = 1, \cdots, N$ and an $\mathbb{R}^N$-valued Brownian Motion W. An important problem is to study noise-induced transition between minima of $\mathcal{E}_0$ (the magnetization reversal). The Stochastic Landau-Lifshitz-Gilbert-Equations are obtained formally by considering a noisy perturbation of the effective field, i.e.

$$\mathcal{H}(u) = -\nabla_u \mathcal{E}(u) = \mathcal{H}_0(u) + \circ e dW = \Delta u - \phi'(u) + \circ e dW. \tag{5}$$

Rigorously, these can be written in the following Itô-Stratonovitch form

$$du = u \times \mathcal{H}_0(u)\, dt - \alpha u \times (u \times \mathcal{H}_0(u))\, dt + G(u)e \circ dW \tag{6}$$

where $G(u) = \lambda_1 u \times \cdot - \lambda_1 u \times (u \times \cdot)$ and $G(u)e \circ dW$ is the Stratonovitch differential:

$$G(u)e \circ dW \quad = \quad \frac{1}{2} \sum_j \left[G'(u)e_j \cdot G(u)e_j \right] dt + \sum_j G(u)e_j\, dW_j$$

In my lecture I will speak about numerical solvability (via finite element method) of the above problem as well as about the solution to the magnetization reversal problem, see [3, 4, 5] and [6].

References

[1] D. V. Berkov, *Magnetization Dynamics Including Thermal Fluctuations: Basic Phenomenology, Fast Remagnetization Processes and Transitions Over High-energy Barriers*, in H. Kronmüller and S. Parkin (eds.), Handbook of Magnetism and Advanced Magnetic Materials, Vol. 2 Micromagnetism, Wiley, 2007

[2] W. F. Brown, Magnetostatic principles in ferromagnetism, North Holland, Amsterdam, 1962.

[3] Z. Brzeźniak, L. Baňas, M. Neklyudov and A. Prohl, Stochastic Ferromagnetism — Analysis and Numerics, de Gruyter Studies in Mathematics **58**, ISBN: 978-3-11-030710-8, 2013

[4] Z. Brzeźniak, L. Baňas, M. Neklyudov and A. Prohl, *A convergent finite-element-based discretization of the stochastic Landau-Lifshitz-Gilbert equation*, IMA J. Numer. Anal. **34**, no. 2, 502-549 (2014)

[5] L. Baňas, Z. Brzeźniak and A. Prohl, *Computational studies for the stochastic Landau-Lifshitz-Gilbert equation*, SIAM J. SCI. COMPUT. Vol. **35**, No. 1, pp. B62-B81 (2013)

[6] Z. Brzeźniak, B. Goldys and T. Jegaraj, *Large deviations and transitions between equilibria for stochastic Landau-Lifshitz-Gilbert equation*, to appear in Arch Rational Mech Anal (2017), doi:10.1007/s00205-017-1117-0

[7] W. Faris and G. Jona Lasinio, *Large fluctuations for a nonlinear heat equation with noise*, J. Phys. A 15 (1982), no. 10, 3025–3055:

[8] T. L. Gilbert, *A Lagrangian formulation of the gyromagnetic equation of the magnetization field*, Phys. Rev., **100** (1955), 1243

[9] G. Grinstein and R. H. Koch, *Switching probabilities for single-domain magnetic particles*, Phys. Rev. B **71**, 184427 (2005)

[10] T. Kamppeter, F. G. Mertens et. al., *Stochastic vortex dynamics in two-dimensional easy-plane ferromagnets: Multiplicative versus additive noise*, Phys. Rev. B **59**, no. 17 (1999), 11349–11357

[11] R. V. Kohn, M. G. Reznikoff and E. Vanden-Eijnden, *Magnetic elements at finite temperature and large deviation theory*, J. Nonlinear Sci. **15** (2005), 223–253

[12] L. Landau and E. Lifshitz, *On the theory of the dispersion of magnetic permeability in ferromagnetic bodies*. Phys. Z. Sowj. **8, 153** (1935); terHaar, D. (eds.) Reproduced in: Collected Papers of L. D. Landau, pp. 101–114. New York: Pergamon Press 1965

[13] A. Lyberatos, R.W. Chantrell, *Thermal fluctuations in a pair of magnetostatically coupled particles*, J. Appl. Phys. **73**, pp. 6501–6503 (1993).

[14] K. Martens, D. L. Stein, and A. D. Kent, *Magnetic reversal in mesoscopic ferromagnetic rings*, Phys. Rev. B **73**, 054413 (2006)

[15] L. Néel, *Théorie Du Trainage Magnétique Des Ferromagnétiques En Grains Fins Avec Applications Aux Terres Cuites*, Ann. Geophys. **5**, pp. 99-136 (1949).

[16] P. A. Rikvold, G. Brown S. J. Mitchell, and M. A. Novotny, *Dynamics of magnetization reversal in models of magnetic nanoparticles and ultrathin films*, in Nanostructured Magnetic Materials and Their Applications, edts. D. Shi, B. Aktas, L. Pust, and F. Mikailov, Springer Lecture Notes in Physics **593**, 164–182 (2002)

[17] A. Visintin, *On Landau-Lifshitz' equations for ferromagnetism*, Japan J. Appl. Math. **2** no. 1 (1985), 69–84

[18] P. Weiss, L'hypothése du champ moleculaire et la proprieté ferromagnétique, J. Phys., 6, 661, (1907)

Book of abstracts of the 7th International Conference
on Advanced Computational Methods
in Engineering, ACOMEN 2017
18–22 September 2017.

Undersampled Dynamic Tomography and Motion Estimation

Martin Burger[1]

[1] *Applied Mathematics Münster , WWU Münster*

e-mails: martin.burger@wwu.de

Abstract

We discuss variational methods for the reconstruction of moving objects from (highly) undersampled dynamic tomography problems. The main idea is to incorporate physical motion models at a reasonable amount of complexity and estimate appropriate motion vectors together with the evolving image in order to obtain a suitable correlation in time. This leads to nonsmooth large scale optimization problems to be solved with alternating minimization and convex splitting techniques. The modelling of the motion vector fields in the variational image reconstruction has a direct impact on the efficiency of alternating minimization problems, optimal schemes can be split into separate variational problems for each time step and parallelized directly.

Key words: Dynamic Imaging, Inverse Problems, Variational Reconstruction, Convex Optimization

1 Introduction

Tomographic imaging is increasingly evolving from a static to a dynamic imaging modality, which leads to a variety of interesting questions. In particular concerns about radation doses and needs to measure fast prevent one from measuring suitably sampled tomographic images at every time step. Hence, images cannot be reconstructed with reasonable resolution at different time steps and novel reconstruction methods are needed that directly reconstruct the whole time sequence, taking benefit of the strong correlation of images in time.

We are interested in reconstructing a sequence of density images u_k, $k = 0, \dots, N$ from indirect data f_k satisfying the relation

$$f_k = R_k u_k, \tag{1}$$

where R_k is a subsampled version of the Radon transform, i.e. a set of line integrals changing in time. State-of-the art image reconstruction would compute approximations of the u_k by solving variational problems of the form

$$u_k \in \arg\min_u D(R_k u, f_k) + \alpha J(u_k), \tag{2}$$

where D is a suitable fidelity term quantifying the differences between the measured data f_k and the forward projected $R_k u$. J is a convex functional such as the frequently used total variation or variants thereof and $\alpha > 0$ is a regularization parameter. In situations of strong undersampling of angular measurements the quality of image reconstructions deteriorates and novel dynamic reconstruction methods need to be developed.

2 Motion Models and Variational Reconstruction

In order to incorporate the standard information that u_k is a density subject to motion we incorporate a standard mechanical model of the form

$$u_k(x) = u_{k-1}(y_k(x)) \det(\nabla y_k(x)), \qquad k = 1, \dots, N, \tag{3}$$

where y_k is a deformation vector field. This Lagrangian formulation seems suitable in three-dimensional image reconstruction in many tomographic setups, an alternative Eulerian formulation could be formulated in terms of continuity equations connecting subsequent time steps with the velocity fields describing the motion (cf. [2]). Note that in the case of small motion between time steps, i.e. $y_k(x) = x - v_k(x)$ with v_k small it may be suitable to approximate the motion at leading order by the discretized transport equation

$$u_k = u_{k-1} - \nabla \cdot (u_{k-1} v_k), \qquad k = 1, \dots, N. \tag{4}$$

A formulation completely equivalent to (3) arises if one indeed tracks all motion back to the original reference state u_0, i.e. ,

$$u_k(x) = u_0(z_k(x)) \det(\nabla z_k(x)), \qquad k = 1, \dots, N, \tag{5}$$

where $z_1 = y_1$ and $z_k = y_k \circ z_{k-1}$ for $k > 1$.

At the level of describing the motion there is a one-to-one relation between the y_k in (3), the z_k in (5), and the velocities in a transport equation. There is a significant difference however in deriving variational reconstruction methods based on these models, since in such we want to put some suitable prior (regularization) on the unknowns, e.g. small elastic or hyperelastic energy of the motion field. Obviously it makes a difference whether we put a prior on y_k or z_k, both with respect to modelling (it clearly seems more feasible to assume smallness of y_k than smallness of z_k for large k) as well as with respect to the numerical solution. In order to unify the notation let us denote the unknown deformation vectors by w_k (meaning y_k in the first and z_k in the second case) and $\mathbf{w} = (w_k)$. A variational model

$$(\mathbf{u}, \mathbf{w}) \in \arg \min_{(\mathbf{u}, \mathbf{w}) \in C} \sum_{k=0}^{N} (D(R_k u_k, f_k) + \alpha_k J(u_k)) + \sum_{k=1}^{N} \beta_k H(w_k) \tag{6}$$

with the constraint set C described by either (3) or (5), and α_k respectively β_k being nonnegative regularization parameters. We mention that it may become suitable to choose $\alpha_k = 0$ for $k > 1$, since the images u_k are determined completely by u_0 and the deformations $\mathbf{w}$.

3 Minimization Strategies

The general variational model (6) is a large scale optimization problem, with $N+1$ images and N vector fields to be reconstructed. Thus, we end up with around $(4N + 1)M$ unknowns and even for moderate images sizes like $M = 128^3$ Voxels and 20 time steps, this leads to about 10^8 degrees of freedom in the optimization. The fact that J and sometimes also H involve nonsmooth terms and hence need to be treated by appropriate convex minimization methods prevent the application of straight-forward gradient type methods. In order to efficiently minimize the problem after discretization it is natural to apply an alternating minimization strategy, which enforces to eliminate the constraint by expressing u_k, $k \geq 1$, in terms of u_0

and w_k. In both cases we can write $u_k = T_k(u_0, \mathbf{w})$, via iterated substitution in the case of (3) and directly in the case of (5). state model (5). The alternating minimization thus reads

$$u_0^{m+1} \in \arg\min_{u_0} \sum_{k=0}^{N} (D(R_k T_k(u_0, \mathbf{w}^m), f_k) + \alpha_k J(T_k(u_0, \mathbf{w}^m)))$$

$$\mathbf{w}^{m+1} \in \arg\min_{\mathbf{w}} \sum_{k=0}^{N} (D(R_k T_k(u_0^{m+1}, \mathbf{w}), f_k) + \alpha_k J(T_k(u_0^{m+1}, \mathbf{w}))) + \sum_{k=1}^{N} \beta_k H(w_k),$$

where $C(\mathbf{w}^m)$ is the constraint set defined by (3) respectively (5) with given deformation field $\mathbf{w}^m$. Note that the with given deformation field, the first step is a state-of-the art image reconstruction problem for the single variable u_0, for which appropriate convex optimization techniques can be applied (cf. [4]). At the level of the second subproblem we observe the main difference between the two models (3) and (5). In the second case we can write $T_k(u_0, \mathbf{w}) = \tilde{T}_k(u_0, w_k)$, hence we can compute the deformation fields in a decoupled way via

$$w_k^{m+1} \in \arg\min_{w_k} D(R_k \tilde{T}_k(u_0^{m+1}, w_k), f_k) + \alpha_k J(T_k(u_0^{m+1}, w_k)) + \sum_{k=1}^{N} \beta_k H(w_k).$$

Hence, we obtain a memory-friendly and also easily parallelizable algorithm, which has been implemented for the setup in Positron-Emission Tomography (PET) in [3]. In the first case, which seemed more natural with respect to modelling, the motion estimation, i.e. the second substep in the alternating minimization does not decouple and the efficient minimization remains an open problem. In [1] the approach was used successfully for a two-dimensional tomography problem with different undersampling strategies, leading to strong improvements compared to the state of the art.

Acknowledgements

This work has been supported by ERC via Grant EU FP 7 - ERC Consolidator Grant 615216 LifeInverse and by the German Science Foundation DFG via EXC 1003 Cells in Motion Cluster of Excellence, Münster, Germany.

References

[1] M. Burger, H. Dirks, L. Frerking, A. Hauptmann, T. Helin, S. Siltanen, *A variational reconstruction method for undersampled dynamic X-ray tomography based on physical motion models*, Preprint, arXiV (2017).

[2] M. Burger, H. Dirks, C. Schönlieb, *A variational model for joint motion estimation and image reconstruction*, Preprint, arXiV (2016) .

[3] M. Burger, J. Modersitzki, S. Suhr, *A nonlinear variational approach to motion-corrected reconstruction of density images*, Preprint, arXiV (2015) .

[4] H. Dirks, *A flexible primal-dual toolbox*, Preprint, arXiV (2016) .

Book of abstracts of the 7th International Conference
on Advanced Computational Methods
in Engineering, ACOMEN 2017
18–22 September 2017.

Numerical solution of PDEs on surfaces and evolving domains

C. M. Elliott[1]

[1] *Mathematics Institute, University of Warwick*

e-mails: c.m.elliott@warwick.ac.uk

Abstract

This is an abstract for a talk to be given at the 6th International Conference on Advanced Computational Methods in Engineering, ACOMEN 2017, to be held from 18 to 22 September 2017 in Ghent, Belgium.

Key words: Evolving domains and surfaces, evolving finite element spaces, implicit surface approach, numerical cell biology, unfitted finite element method,
MSC 2010: 35, 65N30, 92C37

1 Introduction

Many physical models give rise to the need to solve partial differential equations in time dependent regions. For example, the complex morphology of biological membranes and cells coupled with biophysical mathematical models present significant computational challenges, [17, 19, 21]. Naturally such problems also arise in fluids and material science, for example [12, 18]. Our motivational examples will be to applications in cell biology.

In this talk we discuss the mathematical and computational issues associated with the formulation of PDEs in time dependent domains in both flat and curved space. Here we are thinking of problems posed with time dependent d-dimensional hypersurfaces $\Gamma(t)$ in $\mathbb{R}^{d+1}$. The surface $\Gamma(t)$ may be the boundary of the bounded open bulk region $\Omega(t)$. In this setting we may also view $\Omega(t)$ as $(d+1)$-dimensional sub-manifold in $\mathbb{R}^{d+2}$. Using this observation we may develop a theory applicable to both surface and bulk equations. We will present an abstract framework for treating the theory of well- posedness of solutions to abstract parabolic partial differential equations on evolving Hilbert spaces using generalised Bochner spaces, [1]. This theory is applicable to variational formulations of PDEs on evolving spatial domains including moving hyper-surfaces, [2]. See [11] for a survey of various approaches to the formulation and computation of parabolic equations on hypersurfaces.

Our setting is abstract and not restricted to evolving domains or surfaces. We can show well-posedness to a certain class of parabolic PDEs under some assumptions on the parabolic operator and the data. For example we may study a surface heat equation, an equation posed on a bulk domain, a novel coupled bulk-surface system and an equation with a dynamic boundary condition, [2].

We will describe how the theory may be used in the development and numerical analysis of evolving surface finite element spaces which unifies the discretisation methodology for evolving surface (ESFEM) and bulk equations, [6, 9, 15, 16].

In applications often the domain has to be computed. See [3] for an account of numerical methods for computing the solution to geometric evolution equations such as motion by mean curvature. Evolving surface triangulations by velocity fields which have arbitray tangenial components give rise to ALE ESFEM, [22, 20]. Recently methods for computing parametrisations with non physical tangential components which evolve triangulations whilst maintaining good mesh properties have been proposed in [14, 13].

If there is time we may discuss unfitted finite element and implicit surface approaches, [4, 5, 7, 8, 18].

We give some computational examples from cell biology involving the coupling of surface evolution to processes on the surface.

Acknowledgements

The work was partially supported by the Royal Society via a Wolfson Research Merit Award.

References

[1] A. Alphonse, C.M. Elliott and B. Stinner *An abstract framework for parabolic PDEs on evolving spaces* Portugaliae Mathematica **72** (2015) 1–46

[2] A. Alphonse, C.M. Elliott and B. Stinner*On some linear parabolic PDEs on moving hypersurfaces* Interfaces and Free Boundaries **17** (2015) 157–187

[3] K. P. Deckelnick, G. Dziuk and C. M. Elliott *Computation of geometric partial differential equations and mean curvature flow* Acta Numerica **14** (2005) 139–232

[4] K. P. Deckelnick, G. Dziuk, C. M. Elliott and C.-J. Heine *An h−narrow band finite element method for elliptic equations on implicit surfaces* IMAJ Num. Anal. **30** (2010) 351–376

[5] K. P. Deckelnick, C. M. Elliott and T. Ranner *Unfitted finite element methods using bulk meshes for surface partial differential equations* SIAM J. Numerical Analysis **52** (2014) 2137–2162

[6] G. Dziuk and C.M. Elliott *Finite elements on evolving surfaces* IMAJ Num. Anal. **27** (2007) 262–292

[7] G. Dziuk and C.M. Elliott *Eulerian finite element method for parabolic equations on implicit surfaces* Interfaces Free Boundaries **10** (2008) 119–138

[8] G. Dziuk and C.M. Elliott *An Eulerian approach to transport and diffusion on evolving surfaces* Computing and Visualization in Science **13** (2010) 17–28

[9] G. Dziuk and C. M. Elliott *Fully discrete evolving surface finite element method* SIAM J. Numer. Anal. **50** 5 (2012) 2677–2694

[10] G. Dziuk and C. M. Elliott *Finite element methods for surface partial differential equations* Acta Numerica **22** (2013) 289–396

[11] G. Dziuk and C. M. Elliott *L2 estimates for the evolving surface finite element method* Math. Comp. **82** (2013) 1–24

[12] C. Eilks and C. M. Elliott *Numerical simulation of dealloying by surface dissolution via the evolving surface finite element method* J. Comp. Phys. **227** (2008) 9727–9741

[13] C. M. Elliott and H. Fritz, *On algorithms with good mesh properties for problems with moving boundaries based on the Harmonic Map Heat Flow and the DeTurck trick* SMAI Journal of Computational Mathematics **2** (2016) 141–176

[14] C. M. Elliott and H. Fritz, *On approximations of the curve shortening flow and of the mean curvature flow based on the DeTurck trick* IMA Journal Numerical Analysis **37** (2017) 543–603

[15] C. M. Elliott and T. Ranner *Evolving surface finite element method for the Cahn-Hilliard equation* Numerische Mathematik **129** (2014) 483–534

[16] C. M. Elliott and T. Ranner *A unified theory for continuous in time evolving finite element space approximations to partial differential equations in evolving domains* arXiv preprint arXiv:1703.04679

[17] C. M. Elliott and B. Stinner *Modelling and computation of two phase geometric biomembranes using surface finite elements* J. Comp. Phys. **229** (2010) 6585–6612

[18] C. M. Elliott, B. Stinner, V. M. Styles and R. Welford *Numerical computation of advection and diffusion on evolving diffuse interfaces* IMAJ Num. Anal. **31** (2011) 786–812

[19] C. M. Elliott and B. Stinner *Computation of two-phase biomembranes with phase dependent material parameters using surface finite elements* Communications in Computational Physics **13** (2) (2012) 325–360

[20] C. M. Elliott and C. Venkataraman *Error analysis for an ALE evolving surface finite element method* Num. Methods for PDEs **31** (2015) 459–499

[21] C. M. Elliott, B. Stinner and C. Venkataraman *Modelling cell motility and chemotaxis with evolving surface finite elements* Journal Royal Society Interface **9**(76) (2012) 3027–3044

[22] C.M. Elliott and V.M. Styles *An ALE ESFEM for solving PDEs on evolving surfaces* Milan Journal Mathematics **80** (2012) 469–501

Book of abstracts of the 7th International Conference on Advanced Computational Methods in Engineering, ACOMEN 2017 18–22 September 2017.

Operator Preconditioning: Theory and Applications

Ralf Hiptmair[1]

[1] *Seminar for Applied Mathematics, ETH Zürich, CH-8092 Zürich*

e-mails: hiptmair@sam.math.ethz.ch

Abstract

We review applications of a very general concept of operator preconditioning to finite element and boundary element Galerkin discretizations.

Key words: Operator preconditioning, equivalent operators, finite elements, boundary elements, Calderón preconditioning, dual meshes

1 Abstract Theory

On two reflexive Banach spaces V, W we consider two continuous sesqui-linear forms $a \in L(V \times V, \mathbb{C})$ and $b \in L(W \times W, \mathbb{C})$. Let $V_h \subset V$ and $W_h \subset W$ be finite-dimensional subspaces, on which a and b satisfy inf-sup-conditions with constants $c_A, c_B > 0$ Further, there is a stable pairing connecting the spaces V_h and W_h: we assume the existence of a continuous sesqui-linear form $d \in L(V \times W, \mathbb{C})$ that satisfies another inf-sup-condition

$$\sup_{w_h \in W_h} \frac{|d(v_h, w_h)|}{\|w_h\|_W} \geq c_D \|v_h\|_V \quad \forall v_h \in V_h \; . \tag{1}$$

Picking bases $\{b_1, \ldots, b_N\}$, $N := \dim V_h$, of V_h and $\{q_1, \ldots, q_M\}$, $M := \dim W_h$, of W_h, we can introduce the Galerkin-matrices

$$\mathbf{A} := (a(b_i, b_j))_{i,j=1}^{N} \quad , \quad \mathbf{D} := (d(b_i, q_j))_{i,j=1}^{N,M} \quad , \quad \mathbf{B} := (b(q_i, q_j))_{i,j=1}^{M} \; .$$

Theorem ([7]) *If, in the setting outlined above,* $\dim V_h = \dim W_h$*, then*

$$\kappa(\mathbf{D}^{-1}\mathbf{B}\mathbf{D}^{-T}\mathbf{A}) \leq \frac{\|a\| \, \|b\| \, \|d\|^2}{c_A c_B c_D^2} \; ,$$

where $\kappa(\cdot)$ *stands for the spectral condition number of a square matrix.*

Remark. The bound of Thm. 1 is completely independent of the choice of bases for V_h and W_h. The choice of Galerkin spaces V_h and W_h only enters through the constants c_A, c_B, and c_D.

2 Equivalent Operator Preconditioning

This is the classical variant of operator preconditioning, probably independently discovered and proposed several times. The main idea is discussed, among others, in [5, 1] and the survey articles [2, 12]. For applications to non-linear monotone operators see [6, 11].

Now, the role of the space V of Section 1 is played by a Hilbert space H with inner product $(\cdot,\cdot)_H$. As before, a is a bounded sequi-linear form on H that satisfies an inf-sup condition on a finite-dimensional subspace $H_h \subset H$. We equip H_h with a basis $\{b_1,\ldots,b_N\}$, $N := \dim H_h$. Specializing the generic setting of the previous section we make the intriguing choice

$$V = W = H \quad , \quad V_h = W_h = H_h \quad , \quad b(\cdot,\cdot) = d(\cdot,\cdot) = (\cdot,\cdot)_H \ . \tag{2}$$

To begin with this means $\mathbf{D} = \mathbf{B} = \left(\left(b_i, b_j\right)_H\right)_{i,j=1}^N$, the symmetric positive definite Riesz matrix for the inner product on H_h. Moreover, $c_B = c_D = \|b\| = \|d\| = 1$ is immediate and the assertion of Theorem 1 simplifies to

$$\left\|\mathbf{D}^{-1}\mathbf{A}\right\|_{H_h\mapsto H_h} \le \|a\| \ , \quad \left\|\mathbf{A}^{-1}\mathbf{D}\right\|_{H_h\mapsto H_h} \le c_A^{-1} \quad \Rightarrow \quad \kappa(\mathbf{D}^{-1}\mathbf{A}) \le \|a\|\, c_A^{-1} \ , \tag{3}$$

where $\|\cdot\|_{H_h\mapsto H_h}$ is based on the norm on $\mathbb{C}^N$ induced by $(\cdot,\cdot)_H$ and the coefficient isomorphism.

Compact equivalent operators [1]. If a is H-elliptic, $a(u,u) \ge c_A \|u\|_H^2$ for all $u \in H$, and is of the form

$$a(u,v) = (u,v)_H + (Ku,v)_H \quad \text{with } \textit{compact} \quad K : H \to H \ , \tag{4}$$

then the well-known property of compact operators that their eigenvalues accumulate at 0 only, bestows *superlinear convergence* on the **c**onjugate **g**radient method for the **n**ormal equtions (CGN) applied to solve linear systems of equations with coefficient matrix $\mathbf{A}$ and preconditioner $\mathbf{D}$.

Bilinear forms complying with (4) arise from the variational formulations of second-order convection-diffusion and reaction-diffusion equations. For instance, with $H = H_0^1(\Omega)$, $\Omega \subset \mathbb{R}^d$ a bounded domain,

$$a(u,v) := \int_\Omega \mathbf{grad}\, u \cdot \mathbf{grad}\, v + \boldsymbol{\beta} \cdot \mathbf{grad}\, u\, v \,\mathrm{d}\boldsymbol{x} \ , \quad u, v \in H_0^1(\Omega) \ . \tag{5}$$

In this case $(\cdot,\cdot)_H$ is related to the principal part of the underlying elliptic partial differential operator.

Saddle point problems [2, Sect. 8.2]. Consider the mixed variational formulation of second-order elliptic boundary value problems with Dirichlet boundary conditions. Here we have $H = \boldsymbol{H}(\mathrm{div};\Omega) \times L^2(\Omega)$ and the Galerkin matrix induced by the corresponding inner product can serve as a "block-diagonal" preconditioner for the indefinite saddle point matrix, if stable pairs of conforming finite element spaces are used.

Another example is the variational formulation of the Stokes problem, where $H = (H_0^1(\Omega))^d \times L_0^2(\Omega)$, $\Omega \subset \mathbb{R}^d$. The indefinite matrix arising from a stable conforming finite element method can be preconditioned by the block-diagonal s.p.d. matrix related to the inner product of H.

Complex variational problems. Let H be a Hilbert space over $\mathbb{C}$ and assume that $(\cdot,\cdot)_H = (\cdot,\cdot)_1 + (\cdot,\cdot)_0$ with two sesqui-linear forms $(\cdot,\cdot)_*$, and that $a(u,v) = (u,v)_1 + \imath\,(u,v)_0$, $u, v \in H$, $\imath^2 = 1$. For instance, in frequency-domain eddy current models we encounter $H = \boldsymbol{H}(\mathbf{curl};\Omega)$, $a(\boldsymbol{u},\boldsymbol{v}) := (\mathbf{curl}\,\boldsymbol{u}, \mathbf{curl}\,\boldsymbol{v})_{L^2(\Omega)} + i\,(\boldsymbol{u},\boldsymbol{v})_{L^2(\Omega)}$.

>From $a(u,u) \geq \frac{1}{\sqrt{2}} \|u\|_H^2$ for all $u \in H$ we conclude that $c_A \geq \frac{1}{2}\sqrt{2}$ and $\|a\| \leq 1$ is evident. When splitting a variational problem involving the sesqui-linear form $a(\cdot,\cdot)$ into real and imaginary parts, we end up with a saddle point problem on the real Hilbert space $H_{\mathbb{R}} \times H_{\mathbb{R}}$ related to the bi-linear form (subscripts tag real/imaginary parts)

$$\widetilde{a}\left(\begin{pmatrix} u_R \\ u_I \end{pmatrix}, \begin{pmatrix} v_R \\ v_I \end{pmatrix}\right) := a(u_R, v_R) + a(u_I, v_R) + a(u_R, v_I) - a(u_I, v_I) \ .$$

It goes without saying that $\widetilde{a}$ inherits stability and continuity constants from a. We thus find $\kappa\left(\begin{pmatrix} \mathbf{D}^{-1} & \\ & \mathbf{D}^{-1} \end{pmatrix} \widetilde{\mathbf{A}}\right) \leq \frac{1}{2}\sqrt{2}$, $\mathbf{D}$ the Galerkin Riesz matrix of H. Thus, fast convergence of the preconditioned minimal residual Krylov iterative solver is guaranteed.

3 Dual-Mesh Calderón Preconditioning

Now we are concerned with first-kind boundary integral equations on $\Gamma := \partial\Omega$ related to second-order partial differential equations with constant coefficients [14, Ch. 3]. In the scalar case ("**potential problems**") their weak formulations involve the symmetric positive (semi-) definite bilinear forms a_V and a_W defined on the trace spaces $H^{-\frac{1}{2}}(\Gamma)$ and $H^{\frac{1}{2}}(\Gamma)$, respectively, see [13, Ch. 7]. For Galerkin discretization of a_V we employ the **b**oundary **e**lement (BE) space $\mathcal{S}^{-1,0}(\Gamma_h)$ of piecewise constant functions on a triangular mesh Γ_h of Γ. On shape-regular families of meshes the spectral condition numbers of the resulting Galerkin matrices will grow like $O(h^{-1})$, h the minimal meshwidth, which calls for preconditioning.

Application of operator preconditioning is motivated by the key observation that the $L^2(\Gamma)$ inner product establishes duality of $H^{-\frac{1}{2}}(\Gamma)$ and $H^{\frac{1}{2}}(\Gamma)$. Hence, using the notations of Theorem 1, we may choose

$$V = H^{-\frac{1}{2}}(\Gamma) \ , \quad a = a_V \ , \quad W = H^{\frac{1}{2}}(\Gamma) \ , \quad b = a_W \ , \quad d = (\cdot,\cdot)_{L^2(\Gamma)} \ , \quad V_h = \mathcal{S}^{-1,0}(\Gamma_h) \ .$$

The requirement $W_h \subset H^{\frac{1}{2}}(\Gamma)$ entails continuity for a piecewise polynomial BE space W_h. We also want (1) to be satisfied with c_D depending only on shape-regularity of Γ_h.

This challenge was successfully tackled in [15] relying on a dual mesh $\widetilde{\Gamma}_h$. Its construction relies on the barycentric refinement $\widetilde{\Gamma}_h$ of the so-called primal mesh Γ_h, another triangular surface mesh created by adding barycenters of cells and midpoints of edges of Γ_h as new vertices. Then W_h is chosen as a subspace of the BE space $\mathcal{S}^{0,1}(\widetilde{\Gamma}_h)$ of piecewise linear continuous functions on $\widetilde{\Gamma}_h$: we retain values at barycenters as degrees of freedom, and set values at vertices of Γ_h and midpoints of edges to match the average of the values in the barycenters of adjacent cells of the primal mesh.

For **electromagnetic scattering**, we face the **e**lectric **f**ield **i**ntegral **e**quation (EFIE) posed on the tangential trace space $\boldsymbol{H}^{-\frac{1}{2}}(\mathrm{div}_\Gamma, \Gamma)$ [4], which enjoys *self-duality* with respect to the skew-symmetric pairing $d(\mathbf{u},\mathbf{v}) := \int_\Gamma (\mathbf{u} \times \mathbf{v}) \cdot \mathbf{n} \, \mathrm{d}S$. A Γ_h-piecewise linear BE subspace is the space $\mathcal{E}(\Gamma_h)$ of rotated surface edge element functions, also known as RWG space. This suggests the choices

$$V = W = \boldsymbol{H}^{-\frac{1}{2}}(\mathrm{div}_\Gamma, \Gamma) \quad a = b = a_{EF} \ , \quad V_h = \mathcal{E}(\Gamma_h)$$

for operator preconditioning, where a_{EF} is the indefinite sesqui-linear form underlying the variational EFIE. Again, the BE space $W_h \subset \boldsymbol{H}^{-\frac{1}{2}}(\mathrm{div}_\Gamma, \Gamma)$ has to be chosen as an edge element space on the dual mesh $\widehat{\Gamma}_h$ by imposing suitable constraints on functions in $\mathcal{E}(\widetilde{\Gamma}_h)$. This ensures (1) with c_D a function of shape-regularity and (local) quasi-uniformity only [3].

If Γ is a manifold with boundary (**screen**), then the bilinear forms of the variational scalar first-kind boundary integral equations are elliptic on the "trace spaces with zero boundary conditions" $\widetilde{H}^{-\frac{1}{2}}(\Gamma)$ and $\widetilde{H}^{\frac{1}{2}}(\Gamma)$ [14, Sect 3.5.3]. Those are not dual to each other but in L^2-duality to $H^{\frac{1}{2}}(\Gamma)$ and $H^{-\frac{1}{2}}(\Gamma)$. Only recently, [9] proposed integral representations of bilinear forms $a_{\overline{W}}$ and $a_{\overline{W}}$ that are elliptic on those spaces and amenable to Galerkin boundary element discretization. This paves the way for dual mesh based operator preconditioning as explained above,see [8, 10] for details.

References

[1] O. Axelsson and J. Karátson, *Mesh independent superlinear PCG rates via compact-equivalent operators*, SIAM J. Numer. Anal., 45 (2007), pp. 1495–1516.

[2] O. Axelsson and J. Karátson, *Equivalent operator preconditioning for elliptic problems*, Numer. Algorithms, 50 (2009), pp. 297–380.

[3] A. Buffa and S. Christiansen, *A dual finite element complex on the barycentric refinement*, Math. Comp., 76 (2007), pp. 1743–1769.

[4] A. Buffa and R. Hiptmair, *Galerkin boundary element methods for electromagnetic scattering*, in Topics in Computational Wave Propagation. Direct and inverse Problems, M. Ainsworth, P. Davis, D. Duncan, P. Martin, and B. Rynne, eds., vol. 31 of Lecture Notes in Computational Science and Engineering, Springer, Berlin, 2003, pp. 83–124.

[5] V. Faber, T. A. Manteuffel, and S. V. Parter, *On the theory of equivalent operators and application to the numerical solution of uniformly elliptic partial differential equations*, Adv. in Appl. Math., 11 (1990), pp. 109–163.

[6] I. Faragó and J. Karátson, *Numerical solution of nonlinear elliptic problems via preconditioning operators: theory and applications*, vol. 11 of Advances in Computation: Theory and Practice, Nova Science Publishers, Inc., Hauppauge, NY, 2002.

[7] R. Hiptmair, *Operator preconditioning*, Computers and Mathematics with Applications, 52 (2006), pp. 699–706.

[8] R. Hiptmair, C. Jerez-Hanckes, and C. Urzúa-Torres, *Optimal operator preconditioning for hypersingular operator over 3d screens*, Tech. Rep. 2016-09, Seminar for Applied Mathematics, ETH Zürich, Switzerland, 2016.

[9] R. Hiptmair, C. Jerez-Hanckes, and C. Urzua-Torres, *Closed-form exact inverses of the weakly singular and hypersingular operators on disks*, Preprint arXiv:1703.08556 [math.AP], arXiv, March 2017. Submitted to Integral Equations and Operator Theory.

[10] R. Hiptmair, C. Jerez-Hanckes, and C. UrzÃža-Torres, *Optimal operator preconditioning for weakly singular operator over 3d screens*, Tech. Rep. 2017-13, Seminar for Applied Mathematics, ETH Zürich, Switzerland, 2017.

[11] J. Karátson, *Operator preconditioning with efficient applications for nonlinear elliptic problems*, Cent. Eur. J. Math., 10 (2012), pp. 231–249.

[12] R. C. Kirby, *From functional analysis to iterative methods*, SIAM Rev., 52 (2010), pp. 269–293.

[13] W. McLean, *Strongly Elliptic Systems and Boundary Integral Equations*, Cambridge University Press, Cambridge, UK, 2000.

[14] S. Sauter and C. Schwab, *Boundary Element Methods*, vol. 39 of Springer Series in Computational Mathematics, Springer, Heidelberg, 2010.

[15] O. Steinbach, *Stability estimates for hybrid coupled domain decomposition methods*, vol. 1809 of Lecture Notes in Mathematics, Springer-Verlag, Berlin, 2003.

Book of abstracts of the 7th International Conference
on Advanced Computational Methods
in Engineering, ACOMEN 2017
18–22 September 2017.

Phaseless Inverse Scattering and Global Convergence for Coefficient Inverse Problems

Michael V. Klibanov[1]

[1] *Department of Mathematics and Statistics, University of North Carolina at Charlotte, Charlotte, NC 28223, USA*

e-mails: mklibanv@uncc.edu

Abstract

Recent results of the group of the speaker on phaseless coefficient inverse scattering problems and globally convergent numerical methods for coefficient inverse scattering problems will be presented. Results of performances of developed algorithms on experimental data will be presented as well.

Key Words: phaseless inverse scattering problems, globally convergent numerical methods

MSC 2010: Mathematics Subject Classification: 35R30.

1 Phaseless Coefficient Inverse Scattering Problems

The Phaseless Coefficient Inverse Scattering Problem amounts to the determination of an unknown coefficient of either Schrodinger or Helmholtz equation from measurements of the absolute value of the complex valued wave field outside of the scatterers. Phase is not measured. Since 2014 a significant progress has been made in works of M.V. Klibanov and V.G. Romanov in addressing this problem. More precisely, uniqueness theorems were proved, reconstruction procedures were established and numerical results were obtained. In parallel, the Phaseless Coefficient Inverse Scattering Problem was addressed by R.G. Novikov from a different standpoint. These works constitute the first solution of a long standing problem posed by. K. Chadan and P.C. Sabatier in 1977 in Chapter 10 of their well known book "Inverse Problems in Quantum Scattering Theory", Springer, New York, 1977

2 Globally Convergent Numerical Methods for Coefficient Inverse Scattering Problems

The second topic of my talk is globally convergent numerical methods for Coefficient Inverse Scattering Problems (CISPs). This topic is pretty much connected with the first one. CIPs are both highly nonlinear and ill-posed. These two factors cause very substantial challenges in the development of numerical methods for them. This is especially true for the most difficult case of CIPs with single measurement data (as opposed to infinitely many measurements). Until recently the only idea for those methods was the least squares minimization. However,

this approach inevitably suffers from the phenomenon of multiple local minima and ravines. The latter makes computational results unreliable.

Our research group has pioneered two types of globally convergent numerical methods for CIPs with single measurement data. The first type is the so-called "tail functions" method. The second type is the so-called "convexification" method. The main advantage of these numerical techniques over all other available ones is that a small neighborhood of the solution is reached without any a priori knowledge of that neighborhood. Both the convergence theory and numerical results will be presented. Of a particular interest are multiple results for experimental data collected by our group.

Acknowledgements

This work was supported by US Army Research Laboratory and US Army Research Office grant W911NF-15-1-0233 and by the Office of Naval Research grant N00014-15-1-2330. The authors are grateful to Mr. Steven Kitchen for his excellent work on data collection.

Book of abstracts of the 7th International Conference
on Advanced Computational Methods
in Engineering, ACOMEN 2017
18–22 September 2017.

Micro-Macro Models for Reactive Flow and Transport Problems in Complex Media

Peter Knabner[1]

[1] *Department of Mathematics, Friedrich-Alexander University of Erlangen-Nürnberg*

e-mails: peter.knabner@math.fau.de

Abstract

In porous media and other complex media with different length scales, (periodic) homogenization has been successfully applied for several decades to arrive at macroscopic, upscaled models, which only keep the microscopic information by means of a decoupled computation of "effective" parameters on a reference cell. The derivation of Darcy's law for flow in porous media is a prominent example. Numerical methods for this kind of macroscopic models have been intensively discussed and in general are considered to be favourable compared to a direct microscale computation. On the other hand, if the interplay of processes becomes to complex, e.g. the scale seperation does not act in a proper way, the porous medium itself is evolving, ..., the upscaled models obtained may be *micro-macro* models in the sense, that the coupling of the macroscopic equations and the equations at the reference cell is both ways, i.e. at each macroscopic point a reference cell is attached and the solution in the reference cell depends on the macroscopic solution (at that point) and the macroscopic solution depends on the microscopic solutions in the reference cells. At the first glance such models seam to be numerically infeasible due to their enormous complexity (in $d + d$ spatial variables). If on the other hand this barrier can be overcome, micro-macro models are no longer a burden but a chance by allowing more general interaction of processes (evolving porous media, multiphase flow, general chemical reactions, ...), where the microscopic processes "compute" the constitutive laws, which need longer be assumed (similar to the concept of heterogeneous homogenization). We will discuss various examples and in particular numerical approaches to keep the numerical complexity in the range of pure macroscopic models.

Micro-macro models appear in particular in evolving porous media: In [1], [2] models have been derived by (formal) periodic homogenization (two-scale asymptotic expansion) dealing with surface reactions like mineral precipitation/dissolution at the surface of the porous medium, possibly allowing for e.g. electrostatics by an interaction potential, given or to be determined. The free boundary situation at the pore scale and then in the upscaled model can be either handled in a phase field setting or as a sharp interface. We follow the latter approach using a level set approach which is also numerically accessible. In doing so, the interplay between flow, transport, and evolving geometry is focused on. As a result of the averaging procedure, a fully coupled mirco-macro model in new principle variables is maintained. Moreover, time and space dependent coefficient functions are explicitly characterized by means of supplementary fully coupled cell problems. So even the single processes are stationary the dynamics of the inner boundaries (in each reference cell attached to each macroscopic spatial point) renders the full problem time-dependent. For a geometry evolution in one parameter, the level set equations reduce

to an ordinary differential equation and the model resembles the established coupling approach of the porosity to the porous medium evolution, with the important difference that not only porosity is effected, but also the diffusity and the permeability tensor (in an exactly computable way). This approach offers a rigorous approach to a wide range of processes and application, coping with phenomena like clogging (by biofilm expansion), karst formation, ...

There are situations when the description of the evolving medium by smooth surfaces is not appropriate: In soil science, aggregate formations and turnover is an important principle process, where the evolving medium is a complex agglomerate composed of mineral and organic particles, in particular of bacteria and their products (EPS) forming a structure of hardly any surface regularity. Here a discrete description of the medium evolution is advisable. This can be done with a cellular automation concept. The processes in the fluid domain are still described in a continuum mechanic frame work [3].

Mirco-macro models of large complexity can also occur in a rigid porous media, if surface reactions with "many" species are involved. An example is the carbohydrate metabolism in plant cells including the process of metabolic channeling, which takes place at the outer membrane of the mitochondria. An important contribution in such models is the mathematical description of reactions and transport processes in the cell via suitable reaction kinetics for multi-substrate enzyme reactions. An effective model for the microscopic problem which describes the behaviour of the metabolism on the cell level has been derived in [4], [6].

To make these approaches also numerically feasible, several problems have to be addressed. Spatial discretizations are supposed to be locally mass conservative, therefore we choose mixed FEM or dG approaches (because of its compatibility with a (roughly) changing geometry [3]. To avoid a remeshing at every timestep and for each (of the many) micro-problems, cut cell (fictitious domain) approaches shall be integrated. The overall treatment of the arising nonlinear system shall be monolithic (all-in-once) as far as possible. Therefore only at the iterative linearised level (exact) decoupling strategies (Schur-complement) will be used to take advantage of the then "embarrassingly" parallel nature. Thus high performance computing for micro-macro problems using massive parallelisation for the pore-scale cell problems will render the problem treatable. This concept–for a rigid porous media, but for diffusion-reaction systems with many species–is in the process of being worked out in the PhD thesis of T. Elbinger [7], [5].

References

[1] N. Ray, T. Elbinger, P. Knabner, *Upscaling flow and transport in an evolving porous medium with general interaction potentials*, SIAM Journal on Applied Mathematics **75 (5)** (2015) 2170–2192.

[2] N. Ray, T. van Noorden, F. Frank, P. Knabner, *Multiscale modeling of colloid and cluid dynamics in porous media including an evolving microstructure*, Transport in Porous Media **95 (3)** (2012) 669–696.

[3] N. Ray, A. Rupp, A. Prechtel, *Discrete-continuum multiscale model for transport, biomass development and solid restructuring in porous media*, Advances in Water Resources (2017).

[4] M. Gahn, M. Neuss-Radu, P. Knabner, *Derivation of an effective model for metabolic processes in living cells including substrate channeling*, Vietnam Journal of Mathematics **45** (2017) 265–293.

[5] T. Elbinger, M. Gahn, M. Neuss-Radu, P. Knabner, *Simulation of processes in living cells: towards the modelling of metabolic channeling*, 2nd International Conference on Multi-scale Computational Methods for Solids and Fluids (2015) 44–47.

[6] M. Gahn, M. Neuss-Radu, P. Knabner, *Homogenization of reaction-diffusion processes in a two-component porous medium with nonlinear flux conditions at the interface*, SIAM Journal on Applied Mathematics **76** (2016) 819–1843.

[7] T. Elbiner, *Numerical investigation of reactive flows in plant cells*, PhD Thesis, in preparation (2017).

Book of abstracts of the 7th International Conference on Advanced Computational Methods in Engineering, ACOMEN 2017
18–22 September 2017.

Mathematical and numerical modeling of multiphysics problems, with application to the cardiovascular system

Alfio Quarteroni[1]

[1] *CMCS, Institute of Mathematics, Ecole Polytechnique Fédérale de Lausanne, and MOX, Politecnico di Milano*

e-mails: alfio.quarteroni@epfl.ch

Abstract

Mathematical and numerical modeling of the cardiovascular system (CS) is a research topic that has attracted increasing interest from both the mathematical and bioengineering communities over the past 20 years. This because cardiovascular diseases (CVD) have an increasing impact in our lives. As a matter of fact, CVD are the major cause of death worldwide, leading to more than 17.3 million deaths per year, a number that is expected to grow to more than 23.6 million by 2030. In Europe, nowadays they correspond to nearly half of all deaths (47%).

CS features two principal components, the arterial circulation and the heart function with its electrical and mechanical activities. Geometric complexity, lack of data to feed the mathematical models, multiphysics and multiscale nature of the processes at hand, represent major challenges when trying to reproduce both function and malfunction.

In this presentation we will address some of the basic processes of the CS modeling. We first start with modeling stand-alone core components describing a single functionality, like e.g. the artery fluid-dynamics, the heart electrical activity, the fluid dynamics in the left ventricle, etc. Each core model needs to be efficiently approximated numerically, often by specifically devised methods. The next step is the integration of the core models into global, coupled integrated models apt at describing a meaningful and coherent part of the CS system. This step requires the introduction of suitable coupling conditions and of appropriate numerical strategies for a stable, reliable, and computationally effective solution of the global problem.

Modeling the cardiac function is a particularly challenging task that comprises several core cardiac models – electrophysiology, solid and fluid mechanics, microscopic cellular force generation, and valve dynamics – which are then coupled and finally embedded into the systemic and pulmonary blood circulations. It is a multiscale system of Partial Differential Equations and Ordinary Differential Equations featuring multiphysics interactions among the core models.

Clinical data are essential for CS models. Clinical radiological images (such as Computer Tomography and Magnetic Resonance Imaging) are necessary to construct the computational domains. The procedure of geometric reconstruction is difficult and, especially for the heart, requires advanced mathematical and numerical tools.

Boundary data are also difficult to obtain. When the computational domain results from an artificial truncation, specific physical quantities (e.g. fluid velocity or pressure) should be provided at those locations of the arterial tree corresponding to the artificial boundaries. However, this would require invasive measurements that cannot be easily

carried out. Finally, the huge inter- and intra-patient data variability and uncertainty represent further sources of concern toward model calibration and validation.

In spite of all these difficulties, mathematical models can, from one side, provide a better understanding of the physical and quantitative processes governing the CS, and on the other side, open new frontiers in therapeutic planning and the design of implantable devices (such as e.g. medical stents and cardiac defibrillators).

In this presentation, several numerical results to highlight the effectiveness of the numerical strategies here presented. A few cases of clinical relevance will also be presented and discussed.

All our numerical results have been obtained using the *Finite Element library LifeV*, see `www.lifev.org` for more details.

Key words: cardiovascular models, clinical applications, finite element analysis,multiphysics and multiscale problems, scientific computing

References

[1] L. Formaggia, A. Quarteroni, and A. Veneziani, editors. *Cardiovascular mathematics. Modeling and simulation of the circulatory system*, volume 1 of *MS&A*. Springer-Verlag Italia, Milan, 2009.

[2] A. Quarteroni, editor. *Modeling the heart and the circulatory system*, volume 14 of *MS&A*. Springer-Verlag Italia, Milan, 2015.

[3] A. Quarteroni, A. Veneziani, and C. Vergara. Geometric multiscale modeling of the cardiovascular system, between theory and practice. *Comput. Methods Appl. Mech. Engrg.*, 302:193–252, 2016.

[4] A. Quarteroni, T. Lassila, S. Rossi, and R. Ruiz-Baier. Integrated heart—coupling multiscale and multiphysics models for the simulation of the cardiac function. *Comput. Methods Appl. Mech. Engrg.*, 314:345–407, 2017.

[5] A. Quarteroni, A. Manzoni, and C. Vergara. The cardiovascular system: Mathematical modeling, numerical algorithms, clinical applications. *Acta Numerica*, 26:–, 2017. in press.

Minisymposia

MS 1 Poromechanics: advances in numerical simulation and applications

Organiser: Markus Bause, Florin Adrian Radu

Description: Since recently there is an emerging interest in analyzing and simulating poromechanics that belongs to the classical but still largely unsolved problems. Poromechanics has challenging applications of practical interest covering many branches of science and technology, in particular, the geosciences (e.g. geothermal energy, oil and gas recovery, fracturing), environmental sciences (e.g. long-term disposal of waste, remediation of contaminated sites), mechanical engineering (e.g. vibroacoustics and vehicle engineering) and the life sciences (e.g. biomechanis and medicine). Mathematical models for poromechanics are built upon the work of Biot and couple mechanical deformation with fluid flow. They involve non-linear, possible degenerate, systems of partial differential equations. This complicates their mathematical analyses and the design of efficient numerical schemes. In this minisymposium recent advances in mathematical modelling of poromechanics as well as in the development of reliable discretization schemes and solver technology for the coupled systems are discussed. A special focus will be on problems with multiphase or reactive flow phenomena. Further, applications of practical relevance belong also to the scope of interest.

Book of abstracts of the 7th International Conference
on Advanced Computational Methods
in Engineering, ACOMEN 2017
18–22 September 2017.

Space-time finite element approximation of the Biot poroelasticity system with iterative coupling

Markus Bause[1], **Florin A. Radu** [2] **and Uwe Köcher**[1]

[1] *Faculty of Mechanical Engineering, Helmut Schmidt University, Hamburg, Germany*

[2] *Department of Mathematics, University of Bergen, Bergen, Norway*

e-mails: bause@hsu-hh.de, Florin.Radu@math.uib.no, koecher@hsu-hh.de

Abstract

In this work the numerical approximation of the Biot system of poroelaticity by an optimized artificial fixed-stress iterative coupling scheme is addressed. For the numerical approximation of the subproblems of fluid flow and mechanical deformation families of space-time finite element methods are used. The convergence of the iteration scheme is proved and its numerical performance properties are illustrated.

Key words: Poroelasticity, iterative coupling, space-time finite element methods
MSC 2010: 65M60, 65M12

1 Introduction

The modelling of coupled mechanical deformation and flow in porous media has become of increasing importance in several branches of natural sciences and technology including power engineering (e.g., geothermal exploration, lithium-ion batteries), environmental engineering, petroleum and reservoir engineering, biomechanics and medicine. The numerical simulation of coupled mechanical deformation and fluid flow is complex due to the structure of the model equations and continues to remain a challenging task. Recently, iterative coupling techniques have attracted researchers' interest; cf., e.g., [1, 2] and the references therein. The appreciable advantage of these approaches is that by coupling the model components iteratively highly developed simulation techniques for each subproblem can be used fully.

2 Model and space-time finite element discretization

Here we study the approximation of the Biot system of poroelasticity

$$-\nabla\cdot\boldsymbol{\sigma}(\boldsymbol{u},p)=\rho_b\boldsymbol{g}\,,\qquad \partial_t\left(\frac{1}{M}p+\nabla\cdot(b\boldsymbol{u})\right)+\nabla\cdot\boldsymbol{q}=f\,,\quad \boldsymbol{q}=-\frac{\boldsymbol{K}}{\eta}\left(\nabla p-\rho_f\boldsymbol{g}\right)\,,\tag{1}$$

equipped with the initial conditions $p(0)=p_0$ and $\boldsymbol{u}(0)=\boldsymbol{u}_0$ and appropriate boundary conditions, by the artificial fixed-stress iterative coupling scheme

$$\left(\tfrac{1}{M}+L\right)\partial_t p^{k+1}+\nabla\cdot\boldsymbol{q}^{k+1}=f-b\nabla\cdot\partial_t\boldsymbol{u}^k+L\partial_t p^k\,,\qquad \boldsymbol{q}^{k+1}=-\boldsymbol{K}\nabla p^{k+1}\,,\tag{2}$$

$$-\nabla\cdot\left(2\mu\boldsymbol{\varepsilon}(\boldsymbol{u}^{k+1})+\lambda\nabla\cdot\boldsymbol{u}^{k+1}\boldsymbol{I}\right)=\rho_b\boldsymbol{g}-b\nabla p^{k+1}\,.\tag{3}$$

In Eqs. (2) and (3) an optimization in terms of an acceleration of the iteration process comes through the adaptation of the numerical stabilization or tuning parameter L. For the discretization in time of the subproblems (2) and (3) continuous and discontinuous Galerkin methods are proposed. Mixed finite element methods are applied for the spatial discretization of the subproblem of fluid flow; cf. [3]. The convergence of the iterative coupling scheme is proved; cf. [1]. Efficient solution techniques for solving the arising algebraic systems of equations are addressed; cf. [4]. The convergence and performance properties of the approaches are illustrated by numerical experiments. In particular, the optimality of the choice of the tuning parameter L, that is proposed by the analyses, is studied carefully.

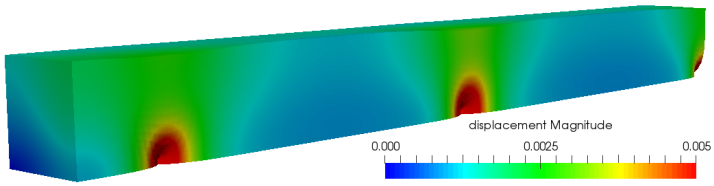

Figure 1: Simulation of poroelasticity in reservoir engineering.

Finally, future applications of the methods to the fully dynamic Biot-Allard model of poroelasticity that captures elastic waves in the porous medium by coupling the hyperbolic elastic wave equation with the parabolic flow problem are discussed. This requires an extension of the space-time finite element techniques to wave phenomena; cf. [5].

Acknowledgements

This work was supported by the German Academic Exchange Service (DAAD) under the grant ID 57238185, by the Research Council of Norway under the grant ID DAADppp255715 and the Toppforsk projekt under the grant ID 250223.

References

[1] M. Bause, F. Radu, U. Köcher, *Space-time finite element approximation of the Biot poroelasticity system with iterative coupling*, Comp. Methods Appl. Mech. Engrg., **320** (2017), 745–768, doi: 10.1016/j.cma.2017.03.017.

[2] M. Bause, U. Köcher, *Iterative coupling of variational space-time methods for Biot's system of poroelasticity*, in B. Karasözen et al. (eds.), *Numerical Mathematics and Advanced Applications ENUMATH 2015*, Springer, 2016, 143–151.

[3] M. Bause, F. A. Radu, U. Köcher, *Error analysis for discretizations of parabolic problems using continuous finite elements in time and mixed finite elements in space*, Numer. Math., **under review** (2015), arXiv:1504.04491v2, 1–47.

[4] M. Bause, U. Köcher, *Variational time discretization for mixed finite element approximations of nonstationary diffusion problems* J. Comput. Appl. Math., **289** (2015), 208–224.

[5] U. Köcher, M. Bause, *Variational space-time discretisations for the wave equation*, J. Sci. Comput., **61** (2014), 424–453.

Book of abstracts of the 7th International Conference
on Advanced Computational Methods
in Engineering, ACOMEN 2017
18–22 September 2017.

Robust iterative schemes for unsaturated poromechanics

Jakub W. Both[1], Kundan Kumar[1], Jan M. Nordbotten[1] and Florin A. Radu[1]

[1] *Department of Mathematics, University of Bergen, Norway*

e-mails: jakub.both@uib.no, kundan.kumar@uib.no, jan.nordbotten@uib.no, florin.radu@uib.no

Abstract

In this work, we propose a novel, robust linearization scheme for the nonlinear Biot's equations, modeling unsaturated, deformable porous media, which we discretize in space by the finite element method and in time by the backward Euler method. The nonlinear, coupled system of equations is decoupled and linearized by the simultaneous application of a Fixed Stress Splitting concept and the L-scheme. We demonstrate numerically the robustness of the scheme and compare its performance with the linearization via Newton's method, which is known to lack robustness and is nevertheless usually the method of choice.

Key words: Poromechanics, Fixed Stress Splitting, L-Scheme, Anderson acceleration

1 Introduction

The coupling of fluid flow and mechanical deformation in unsaturated porous media is relevant for many applications ranging from modeling rainfall-induced land subsidence in environmental engineering to understanding the swelling of cement-based materials in civil engineering. Due to the involved models' nonlinear, coupled character, the numerical solution of the corresponding discretized problem is challenging and requires in particular a robust linearization method. Newton's method is commonly the method of choice although it is known to lack robustness due to its limitation to local convergence. Numerical examples for this problem show, indeed, that Newton's method might fail to converge and should not be chosen irrespective of the example. Instead, we propose a novel, robust linearization scheme, which decouples the separate mechanics and flow problems and applies an inexact Newton's method to the flow problem, see Section 3.

2 Mathematical model – Nonlinear Biot's equations

In this work, we consider porous media assuming infinitesimal deformations, incompressible solid grains and the presence of two fluids. One fluid phase is assumed to be incompressible, whereas the other fluid phase is assumed to be a passive phase, which can be neglected.

Following the work of Coussy [1], the corresponding governing equations are given by

$$-\boldsymbol{\nabla}\cdot\left[2\mu\boldsymbol{\varepsilon}(\boldsymbol{u})+\lambda\boldsymbol{\nabla}\cdot\boldsymbol{u}\boldsymbol{I}-\alpha p_E\boldsymbol{I}\right] = \rho_b\boldsymbol{g}, \tag{1}$$

$$\phi_0\partial_t s_w+\alpha s_w\partial_t\boldsymbol{\nabla}\cdot\boldsymbol{u}+\boldsymbol{\nabla}\cdot\boldsymbol{q}_w = 0, \tag{2}$$

$$\boldsymbol{q}_w+\boldsymbol{\lambda}_w\left(\boldsymbol{\nabla}p_w-\rho_w\boldsymbol{g}\right) = \boldsymbol{0}, \tag{3}$$

where the primal variables $\boldsymbol{u}$, p_w, $\boldsymbol{q}_w$ denote mechanical displacement, fluid pressure and fluid flux, respectively. For the saturation $s_w = s_w(p_w)$ and mobility $\boldsymbol{\lambda}_w = \boldsymbol{\lambda}_w(s_w)$, we employ the van Genuchten model. The pore pressure p_E is given by $p_E(s_w,p_w) = s_w p_w - \int_0^{s_w} s_w^{-1}(S)\,dS$. The Lamé parameters μ, λ, the initial porosity ϕ_0, the Biot constant α, the fluid density ρ_w, the bulk density ρ_b and the gravitational acceleration $\boldsymbol{g}$ are constant.

3 Numerical solution

In order to discretize Eq. (1)-(3) in space, we employ linear Galerkin finite elements for the displacement $\boldsymbol{u}$, and lowest order Raviart-Thomas mixed finite elements for pressure p_w and flux $\boldsymbol{q}_w$. Additionally, we employ the backward Euler method for time discretization.

In order to linearize robustly the discretized system of equations, we propose the following strategy. First, we decouple the discrete problem by employing the concept of the Fixed Stress Splitting scheme [2], automatically linearizing the cross-coupling. Simultaneously, we employ the L-scheme [3] in order to linearize the decoupled flow problem. A similar strategy has been rigorously shown to be globally converging for nonlinear Biot's equations involving nonlinear mechanics, nonlinear compressibility and a linear coupling [4]. Due to the resulting scheme's fixed point character, only linear convergence can be expected. In order to accelerate the convergence, we apply Anderson acceleration [5].

In this talk, we demonstrate numerically the robustness of the scheme for cases the standard Newton's method fails to converge.

Acknowledgements

J.W. Both wishes to thank Meltzer foundation for the grant 2017/05/LMH to participate at ACOMEN 2017.

References

[1] O. Coussy, *Poromechanics*, Wiley and Sons (2004).

[2] J.W. Both, M. Borregales, J.M. Nordbotten, K. Kumar, F.A. Radu, *Robust fixed stress splitting for Biot's equations in heterogeneous media*, Appl. Math. Lett. **68** (2017) 101–108.

[3] F. List, F.A. Radu, *A study on iterative methods for solving Richards' equation*, Comput. Geosci. **20** (2016) 341–353.

[4] M. Borregales, F.A. Radu, K. Kumar, J.M. Nordbotten, *Robust iterative schemes for non-linear poromechanics*, arXiv:1702.00328.

[5] H.F. Walker, P. Ni, *Anderson Acceleration for Fixed-Point Iterations* SIAM J. Numer. Anal. **49** (2011) 1715–1735.

Book of abstracts of the 7th International Conference
on Advanced Computational Methods
in Engineering, ACOMEN 2017
18–22 September 2017.

A new iterative algorithm based on the fixed-stress split scheme for solving the Biot's problem

Francisco Gaspar[1], Kundan Kumar[2], Florin Adrian Radu[2] and Carmen Rodrigo[3]

[1] *Centrum Wiskunde & Informatica, Amsterdam, The Netherlands*

[2] *Department of Mathematics, University of Bergen, Norway*

[3] *Department of Applied Mathematics, University of Zaragoza, Spain*

e-mails: Gaspar@cwi.nl, kundan.kumar@uib.no, florin.radu@uib.no, carmenr@unizar.es

Abstract

In recent years, intensive research has been focused on the design of efficient methods for solving the large linear systems arising from the discretization of the Biot's model, since in real simulations it is the most consuming part. There are mainly two approaches, the fully coupled methods and the iterative coupling methods. At each time step, the fully coupled methods solve simultaneously the system of equations for all the unknowns, whereas iterative coupling methods solve sequentially the equations for fluid flow and geomechanics, until a converged solution within a prescribed tolerance is achieved. A big advantage of these methods is their flexibility since two different codes for fluid flow and geomechanics can be linked for solving the Biot's model. Due to its unconditional stability, one of the most frequently used schemes of this type is the so-called fixed stress split method. This sequential-implicit method basically consists in solving the flow problem first fixing the volumetric mean total stress, and then the mechanic part is solved from the values obtained at the previous flow step. In this work, we propose a new algorithm based on this method, which results in a very appealing alternative due to its parallelizable properties. The convergence of this iterative scheme is proved and illustrated by numerical experiments.

Book of abstracts of the 7th International Conference
on Advanced Computational Methods
in Engineering, ACOMEN 2017
18–22 September 2017.

Assessing solute macrodispersion in heterogeneous porous formations using random walk particle tracking

Rinako Hamada[1], **Kazuya Inoue**[1], **Yasuteru Kobi**[1] **and Tsutomu Tanaka**[1]

[1] *Graduate School of Agricultural Science, Kobe University*

e-mails: 175a014a@stu.kobe-u.ac.jp, mornel@kobe-u.ac.jp,
160a006a@stu.kobe-u.ac.jp, ttanaka@kobe-u.ac.jp

Abstract

This study presents advective-dispersive solute transport processes using random walk particle tracking in heterogeneous porous formations to assess macrodispersion phenomena. Laboratory solute transport experiments were also conducted to validate the numerical results based on different stochastic models. The most noticeable quantitative outcome was relevant to particle transfer between different hydraulic conductivities and its stochastic modeling.

Key words: random walk particle tracking, macrodispersion, spatial moment analysis, heterogeneous porous media

1 Introduction

Dispersion of solutes in transport by groundwater is governed primarily by the spatial variability of the hydraulic conductivity. The rate of spreading of a solute plume is quantified in terms of macrodispersion, leading to the non-Fickian behavior of transport in heterogeneous porous media [1, 2]. The aims of this study are to assess macrodispersion phenomena in heterogeneous porous formations using random walk particle tracking and to validate the results based on laboratory-scale solute transport experiments.

2 Random walk particle tracking (RWPT)

Simulation of advective and dispersive mass transport may proceed by changing particle positions with time via an Itô interpretation, give as [1]

$$\boldsymbol{X}_p(t+\Delta t) = \boldsymbol{X}_p(t) + \boldsymbol{A}(\boldsymbol{X}_p, t)\Delta t + \boldsymbol{B}(\boldsymbol{X}_p, t)\Xi(t)\sqrt{\Delta t} \tag{1}$$

where $\boldsymbol{X}_p(t)$ is the i-component of the particle location at time t, Δt is the time step, and Ξ contains three normally distributed random numbers with zero mean and unit variance. The vector $\boldsymbol{A}$ represents the deterministic drift determined by the fluid flow velocity and contains contributions from the dispersion tensor. The matrix $\boldsymbol{B}$ represents the direction displacement

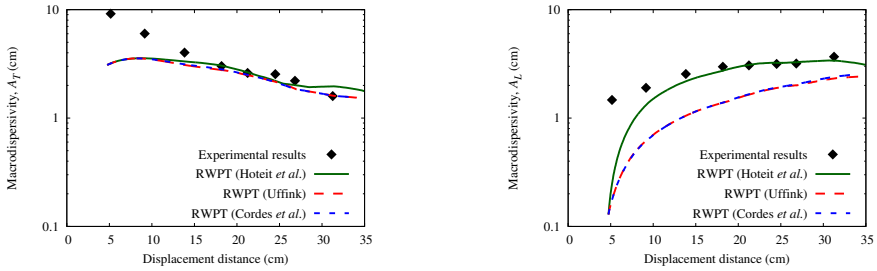

Figure 1: Variation of transverse (left) and longitudinal (right) macrodispersivities.

distance for the random process $\Xi(t)\sqrt{\Delta t}$, which expresses Brownian motion. RWPT was linked with spatial moments to identify longitudinal (A_L) and transverse (A_T) macrodispersivities using three stochastic models [1, 2, 3] expressing particle transfer between different hydraulic conductivities.

3 Laboratory-scale solute transport experiments

Laboratory experiments with dye were conducted in a $1 \times 1 \times 0.03$ m sandbox with $0.03 \times 0.03 \times 0.03$ m blocks having different hydraulic conductivities. A methodology using spatial moment analysis linked with image processing of a dye tracer behavior was developed to identify the changes in longitudinal and transverse macrodispersivities caused by the presence of heterogeneities with the correlation length of 0.18 m.

4 Results and discussion

Estimation results of transverse and longitudinal macrodispersivities obtained in solute transport experiments are plotted in Figure 1 as a function of the displacement distance of the centroid of dye tracer. Numerical results using RWPT are also shown in the same figure for three different stochastic models. Three models show smaller transverse macrodispersivities than experimental results at an earlier stage of the displacement distance. This attributes to the effect of initial injection of dye tracer. On the other hand, experimental values were in good agreement with Hoteit's model [2], especially in longitudinal macrodispersivity. It is inferred that solutes governed by other models [1, 3] have a tendency to migrate into higher hydraulic conductivity areas in this experimental scale, leading to smaller degree of solute spreading in the longitudinal direction.

Acknowledgements

This work has been partially supported by JSPS KAKENHI Grant Numbers JP16K07941.

References

[1] G. Uffink, *Analysis of Dispersion by the Random Walk*, Ph.D Dissertation, Delft University of Technology, 1990.

[2] H. Hoteit, R. Mose, Younes. A., Lehmann, F., Ph. Ackerer, *Three-dimensional modeling of mass transfer in porous media using the mixed hybrid finite elements and the random-walk methods*, Math. Geol., **34(4)**(2002), 435–456.

[3] C. Cordes, H. Daniels, G. Rouve, *A new very efficient algorithm for particle tracking in layered aquifers*, Proc. Inter. Conf. on Computer Methods and Water Resources (1991), 41–55.

Book of abstracts of the 7th International Conference
on Advanced Computational Methods
in Engineering, ACOMEN 2017
18–22 September 2017.

Finite element discretization Biot's consolidation model with strong mass conservation

Guido Kanschat[1] and Béatrice Rivière[2]

[1] *Interdisciplinary Center for Scientific Computing (IWR), Heidelberg University*

[2] *Computational and Applied Mathematics Department (CAAM), Rice University*

e-mails: kanschat@uni-heidelberg.de, riviere@caam.rice.edu

Abstract

A finite element discretization for Biot's consolidation model is derived. It features a projection-free continuity equation and thus provides strong mass conservation. The seepage velocity is modeled by a mixed method with Raviart-Thomas elements. The solid deformation is discretized by a divergence-conforming discontinuous Galerkin method. We present key features of the analysis and numerical evidence for the feasibility of the method.

Key words: Biot equations, consolidation, discontinuous Galerkin, divergence-conforming, mixed finite element method
MSC 2010: 65N30, 74F10

1 Biot's consolidation model

The consolidation model couples the deformation of a porous solid body to the flow of a fluid through its pores. The model is derived under the simplifying assumptions that inertial effects of the solid are irrelevent, thus the solid is at every time in static equilibrium with the fluid forces. Furthermore, we make the assumption of infinitesimally small strain and stress, such that the model is linear. Then, Biot's consolidation model reads

$$\frac{\partial}{\partial t}(c_s p + \alpha \nabla\cdot\mathbf{u}) + \nabla\cdot\mathbf{w} = f_1, \qquad \text{in } \Omega\times(0,T), \tag{1}$$

$$K^{-1}\mathbf{w} = -\nabla p, \qquad \text{in } \Omega\times(0,T), \tag{2}$$

$$-\nabla\cdot(\boldsymbol{\sigma} - \alpha p\mathbf{I}) = \mathbf{f}_2, \qquad \text{in } \Omega\times(0,T). \tag{3}$$

Here, α is the Biot-Willis constant, which represents the pressure-storage coupling coefficient. The constant c_s represents the compressibility of the fluid. The permeability K is a symmetric positive definite matrix. We assume here that the effective stress tensor satisfies Hooke's law:

$$\boldsymbol{\sigma} = \lambda(\nabla\cdot\mathbf{u})\mathbf{I} + 2\mu\varepsilon(\mathbf{u}),$$

where

$$\varepsilon(\mathbf{u}) = \frac{1}{2}(\nabla\mathbf{u} + (\nabla\mathbf{u})^T).$$

We note that in applications involving water as a fluid under moderate pressure, we have to deal with incompressibility, that is, $c_s \approx 0$. Then, in the conservative case ($f_1 = 0$), the continuity equation (1) reduces to

$$\alpha \frac{\partial}{\partial t} \nabla \cdot \mathbf{u} = -\nabla \cdot \mathbf{w},$$

from which we deduce that α must be related to unaccounted volume in the model and thus in the ideal case of a correct model $\alpha = 1$. In this case, we can say that every volume fraction vacated by the dolid is filled by fluid and vice versa.

2 Discretization

Our goal is the derivation of a discretization for equations (1) to (3) which is stable in the limits $c_s = 0$ and $\alpha = 0$. Furthermore, we strive to achieve the physically important property of conservation of mass. This is achieved by two means:

1. The Darcy problem in equations (1) and (2) is discretized by a mixed method with a certain pressure space Q_h. Hence, the pressure and the divergence of the seepage velocity $\mathbf{w}$ in (1) are in the same space.

2. The displacement space is chosen, such that its divergence is equal to the pressure space Q_h as well.

If these two conditions are met, even in the finite element formulation (1) holds pointwise. Choosing a discretization matching the second condition, we were guided by our previous work on Stokes-Darcy coupling [1, 2] and choose a divergence conforming discontinuous Galerkin method with the correct pressure space.

Acknowledgements

Computations were performed with the finite element library deal.II [3].

References

[1] G. Kanschat, B. Rivière, *A strongly conservative finite element method for the coupling of Stokes and Darcy flow* J. Comput. Phys. **229** (2010) 5933–5943. Springer, 2010.

[2] V. Girault, G. Kanschat, B. Rivière, *Error analysis for a monolithic discretization of coupled Darcy and Stokes problems*, J. Numer. Math. **22/2** (2014) 109–142.

[3] W. Bangerth, R. Hartmann, G. Kanschat, *Deal.II – a general purpose object oriented finite element library*, ACM Trans. Math. Softw. **33/4** (2007).

Book of abstracts of the 7th International Conference
on Advanced Computational Methods
in Engineering, ACOMEN 2017
18–22 September 2017.

A Globally Convergent Scheme for Non-equilibrium Models for Flow in Heterogeneous Porous Media

K. Mitra[1], I.S. Pop[2], C.J. van Duijn[1], D. Seus[3] and F.A. Radu[4]

[1] *Department of Mathematics and Computer Science, Eindhoven University of Technology*

[2] *Faculty of Science, Hasselt University*

[3] *Institute of Applied Analysis and Numerical Simulation , University of Stuttgart*

[4] *Department of Mathematics, University of Bergen*

e-mails: k.mitra@tue.nl, sorin.pop@uhasselt.be, C.J.v.Duijn@TUE.nl, david.seus@ians.uni-stuttgart.de, Florin.Radu@math.uib.no

Abstract

We consider a linear globally convergent scheme for non-linear differential equations rising in unsaturated flow through porous media. Particularly, the focus is on non-equilibrium effects, like hysteresis and dynamic capillary effect, which make the system pseudo-parabolic. Also a domain decomposition scheme using the aforementioned linearization technique is proposed that ensures numerical convergence for heterogeneous and layered/fractured porous domains. We discuss the convergence of the schemes and show numerical results that validate the theoretical findings.

Key words: L-scheme, Porous flows, Hysteresis, Capillarity, Domain decomposition,
MSC 2010: Numerical analysis, Functional Analysis

1 Introduction

The Richards equation is a commonly used model for unsaturated flow through porous media. Using the Darcy law in the mass balance equation, and bringing the resulting equation to a dimensionless form, for gravity driven flow one gets the equation:

$$\partial_t S(p) = \nabla \cdot [k(\mathbf{x}, S)\,(N_c \nabla p - \hat{g})]\,. \tag{1}$$

Here $\hat{g}$ is the unit vector of gravitational acceleration, N_c is the capillary number, and $k(\mathbf{x}, S)$ is a nonlinear function that is determined based on experiments. Two unknowns are involved: S, the water saturation ($0 < S < 1$) and p, the water pressure. Standard models assume that these are related by a nonlinear relationship determined, again, based on experiments:

$$-p = P_c(S). \tag{2}$$

However (2) does not take into account the hysteresis effects and dynamic effects [1] that are observed from experiments. A model incorporating such effects is proposed in [1]:

$$-p = P^+(S) - P^-(S) \cdot \operatorname{sign}(\partial_t S) - \tau f(S) \partial_t S. \tag{3}$$

(1) and (3) constitute a highly non-linear pseudo-parabolic system of equations which is difficult to solve numerically. Moreover, if the porous domain is layered then the variance of structural parameters may lead to discontinuities of the saturation at contact interfaces between homogeneous blocks. This posses significant problems for the convergence of the numerical method. Below we propose a linear scheme which is not limited by these issues.

2 Mathematical formulation and results

We discretize (1) in time. If time T is divided in N time-steps of size τ (i.e. $T = N\tau$) then for solving for the n^{th} time-step we use the following linear iteration:

$$Lp_n^i - \tau\nabla\cdot\left[k(\mathbf{x}, S_n^{i-1})N_c\nabla p_n^i\right] = Lp_n^{i-1} - \tau\mathcal{F}(S_n^{i-1}, p_n^{i-1}) - \tau\nabla\cdot\left[k(\mathbf{x}, S_n^{i-1})\hat{g}\right], \tag{4}$$

where the subscript n stands for n^{th} time-step and superscript i stands for i^{th} inner iteration, and $L > 0$ is a constant. In [2, 3], (1) and (2) were solved using $\mathcal{F}(S, p) = S - S_{n-1}$ and S_n^{i-1} was calculated in each step using inverse of $P_c(S)$ function, i.e. $S_n^{i-1} = (P_c)^{-1}(p_n^{i-1})$. It was shown in [2, 3] that convergence of the scheme can be guaranteed irrespective of initial guess choice and so p_n could be defined as $p_n = \lim p_n^i$. For solving (1) and (3) we use the relation:

$$S_n := S_n^i = S_{n-1} + \tau\mathcal{F}(S_{n-1}, p_{n-1}), \tag{5}$$

but in this case $\mathcal{F}(S, p)$ is the unique function that solves:

$$P^-(S)\Psi_\varepsilon(\mathcal{F}(S, p)) + \tau f(S)\mathcal{F}(S, p) = P^+(S) + p. \tag{6}$$

Here Ψ_ε is a regularized version of sign function. The convergence result is summarized in

Theorem *If f, P^+ and P^- are Lipschitz and $k \geq k_m > 0$ for all arguments, then there exists a $L_m > 0$ and $\tau_M > 0$ such that p_n^i solving (4) converges as $i \to \infty$ for all $L > L_m$ and $\tau < \tau_M$.*

We further extend the linearization procedure in combination with a domain decomposition approach for the system (1) and (2) and for the system (1) and (3). We consider two domains Ω_1 and Ω_2 sharing a common interface Γ, each of them having their own parameterization. The model is solved in each subdomain separately and the results are coupled through a Robin type boundary condition on Γ. At each time step, an L-type linearization is used. For brevity we omit the details. Numerically, convergence is observed for all the error metrics. Also, a comparison with conventional schemes reveals the robustness of our method.

Acknowledgements

This work has been funded by the NWO-FOM-Shell programme through the grant 14CSER016.

References

[1] S. M. Hassanizadeh, W. G. Gray, *Thermodynamic basis of capillary pressure in porous media*, Water Resour. Res. **29**(1993): 3389-3405

[2] I.S. Pop, F. Radu, P. Knabner, *Mixed finite elements for the Richards' equation: linearization procedure*, J. Comput. and Appl. Math. **168**, (2004): 365-373

[3] F. List, F. Radu, *A study on iterative methods for Richards' equation*, Computational Geoscience, Comput. Geosci. **20** (2016) 341-353.

Book of abstracts of the 7th International Conference
on Advanced Computational Methods
in Engineering, ACOMEN 2017
18–22 September 2017.

Numerical methods for porous media flow models Iterative schemes and domain decomposition approaches

Jakub Both[1], Kundan Kumar[1], Koondanibha Mitra[3,2], Jan Martin Nordbotten[1], Iuliu Sorin Pop[2,1], Florin Adrian Radu[1], Christian Rohde[4] and David Seus[4]

[1] *Department of Mathematics, University of Bergen, Norway*

[2] *Faculty of Sciences, Hasselt University, Belgium*

[3] *Dept. of Math. and Comp. Sci., TU Eindhoven, The Netherlands*

[4] *Department of Mathematics, University of Stuttgart, Germany*

e-mails: jakub.both@uib.no, kundan.kumar@uib.no, k.mitra@tue.nl, jan.nordbotten@uib.no, sorin.pop@uhasselt.be, florin.radu@uib.no, christian.rohde@mathematik.uni-stuttgart.de, david.seus@mathematik.uni-stuttgart.de

Abstract

Unsaturated porous media flow models are nonlinear, degenerate equations of parabolic type. This makes developing numerical schemes for such problems particularly challenging. We discuss a coupled iterative - domain decomposition approach for the numerical discretization of a porous medium flow model.

Key words: convergence analysis, degenerate parabolic problems, domain decomposition, linear iterative scheme, porous media flow model

1 Introduction

Porous media flows are encountered in numerous real-life applications. Examples in this sense are enhanced oil recovery, geological CO_2 storage, or design of fuel cells. Mathematical modelling and numerical simulation tools are essential for understanding and controlling such processes. Commonly, the resulting mathematical models are (systems of) nonlinear partial differential equations of evolution type, with nonlinearities that vanish or become unbounded depending on the solution of the equation.

We consider the Richards equation modelling unsaturated water flow in a porous medium. In a dimensionless setting, the porous medium is a bounded domain $\Omega \subset \mathbb{R}^d$ ($d \in \{1, 2, 3\}$) with Lipschitz continuous boundary, and $T > 0$ a maximal time. The Richards equation results after combining the mass balance equation with the Darcy law. Using the Kirchhoff transform and neglecting gravity terms, one has

$$\partial_t b(u) - \Delta u = f, \tag{1}$$

where u is the unknown "pressure" after the Kirchhoff transformation, f the source term and b a nonlinear, non-decreasing and Hölder continuous function in u that may also depend on x. Initial and boundary conditions complete (1).

Here $\partial_u b$ can become 0 or infinite, so implicit schemes are needed. These lead to nonlinear problems, for which robust and convergent numerical schemes have to be constructed, a challenging task in view of the character of the nonlinear function b.

2 A robust and convergent iterative scheme

If the medium consists of homogeneous blocks, applying domain decomposition schemes is meaningful. The original problem is decoupled into smaller size sub-problems, for which schemes with optimally chosen parameters can be employed. Assume that Ω consists of two adjacent sub-domains $\Omega_{1,2}$, separated by a common interface Γ. With $N \in \mathbb{N}$ and $\tau = T/N$ being a fixed time step, let $t_k = k\Delta t$ ($k = 0, \ldots, N$) and $u_k \approx u(t_k)$), an Euler implicit scheme for (1) reads

$$b(u_k) - \tau \Delta u_k = b(u_{k-1}) + \tau f_k, \tag{2}$$

where $f_k = f(t_k)$ is the source term at t_k. To define an iterative, domain decomposition scheme for approximating u_k we construct the sequence $(u^i_{k,1}, u^i_{k,2})$ ($i = 0, 1, \ldots$), where $u^i_{k,\ell}$ approximate the restriction of u_k to the sub-domain Ω_ℓ ($\ell = 1, 2$). With $\lambda > 0$ arbitrary and $L_\ell > 0$ sufficiently large (see [2], $u^i_{k,\ell}$ solves

$$\begin{aligned} L_\ell u^i_{k,\ell} - \tau \Delta u^i_{k,\ell} &= L_\ell u^{i-1}_{k,\ell} - b(u^{i-1}_{k,\ell}) + b(u^{i-1}_{k-1,\ell}) + \tau f_k && \text{in } \Omega_\ell, \\ -\nabla u^i_{k,\ell} \cdot \mathbf{n}_\ell &= g^i_\ell + \lambda u^i_{k,\ell} && \text{at } \Gamma, \end{aligned}$$

Here $\mathbf{n}_\ell$ is the unit normal at Γ pointing into $\Omega_{3-\ell}$, while $g^i_\ell := -2\lambda u^{i-1}_{k,3-l} - g^{i-1}_{3-\ell}$. Moreover, $u^0_{k,\ell} := u_{k-1,\ell}$. Observe that the problems are decoupled and linear.

In this presentation we discuss the convergence ($i \to \infty$) of $(u^i_{k,1}, u^i_{k,2})$ to the limit pair $(u_{k,1}, u_{k,2})$. In particular, one has $u_{k,1} = u_{k,2}$ and $\nabla u_{k,1} \cdot \mathbf{n}_1 + \nabla u_{k,2} \cdot \mathbf{n}_2 = 0$ at Γ, thus $u_{k,\ell}$ is the restriction of u_k to Ω_ℓ (see [3]).

Acknowledgements

Work supported by the Research Foundation - Flanders FWO (Odysseus project GoG1316N), the Norwegian Research Council (projects NRC 255510 (CHI) and NRC 255426 (IMMENS)) and the Shell-NWO/FOM CSER project 14CSER016.

References

[1] J. M. Nordbotten, M.A. Celia, *Geological Storage of CO2: Modeling Approaches for Large-Scale Simulation*, Wiley 2011.

[2] F.A. Radu, K. Kumar, J.M. Nordbotten, I.S. Pop, *A robust, mass conservative scheme for two-phase flow in porous media including Hoelder continuous nonlinearities*, IMA J. Numer. Anal., accepted.

[3] D. Seus, K. Mitra, I.S. Pop, F.A. Radu, C. Rohde, *A linear domain decomposition method for partially saturated flow in porous media*, in preparation.

Book of abstracts of the 7th International Conference
on Advanced Computational Methods
in Engineering, ACOMEN 2017
18–22 September 2017.

Newton based iterative methods for non-linear poromechanics

Florin Adrian Radu[1], Manuel Borregales[1], Carmen Rodrigo Cardiel[2], Francesco Gaspar[2] and Kundan Kumar[1]

[1] *Department of Mathematics, University of Bergen, Norway*

[2] *Department of Mathematics, University of Zaragoza, Spain*

e-mails: florin.radu@uib.no, manuel.borregales@uib.no, carmenr@unizar.es, fjgaspar@unizar.es, kundan.kumar@uib.no

Abstract

In this work we present monolithic and splitting schemes for solving the non-linear Biot model. The convergence of the schemes is shown rigorously. Illustrative numerical examples are presented to sustain the theoretical results.

Key words: Biot model, iterative splitting, Newton method, convergence analysis

1 Introduction

Fully coupled porous media flow and mechanics, i.e. poromechanics plays an important role in many relevant applications as e.g. energy storage in the subsurface, CO_2 sequestration or geothermal energy extraction. The most used mathematical model for poromechanics is the (quasi-static) linear Biot model [4]. Nevertheless, in many applications the linearity assumption is not realistic. In this work we consider a non-linear extension of the Biot model:

$$-\nabla \cdot [2\mu\varepsilon(\mathbf{u}) + a(\nabla\mathbf{u}) + h(\nabla\cdot\mathbf{u})] + \alpha\nabla\cdot(pI) = \mathbf{f}, \tag{1}$$

$$\partial_t\left(b(p) + \alpha\nabla\cdot\mathbf{u}\right) - \nabla\cdot\left(\frac{\mathbf{K}}{\mu_f}\nabla p - \rho_f\mathbf{g}\right) = g, \tag{2}$$

where $\mu > 0$ is the constant shear modulus, $\mathbf{u}$ is the displacement, $\varepsilon(\mathbf{u}) = \frac{1}{2}\left(\nabla\mathbf{u} + (\nabla\mathbf{u})^t\right)$, p is the fluid pressure, $\mathbf{I}$ is the identity matrix, α the Biot coefficient and $\mathbf{K}, \mathbf{g}$ and μ_f are the permeability, gravitational vector and viscosity, respectively. The coefficient functions $a(\cdot)$, $h(\cdot)$ and $b(\cdot)$, as well as the source terms $\mathbf{f}, g$ are supposed to be given.

Due the coupling and the non-linearities the system above is difficult to be solved (independent of the implicit discretization one choses). For the linear case we refer to [5] for a review of the splitting methods available and a discussion on their stability. The recommended splitting schemes are the fixed stress and the undrained split. For the convergence analysis of these scheme we refer to the recent papers [7, 3]. In the present work we focus on efficiently solving the non-linear system (1)-(2) by using Newton's method.

2 Iterative schemes based on Newton's method for the non-linear Biot model

We first discretize the system (1)-(2): we use backward Euler for the discretization in time and the finite element pair P^1-bubble/P^1, that is, the so-called MINI element. This pair of finite elements was proven to be stable for the linear Biot's model in [9]. One can solve the resulting fully discrete non-linear system either monolithically or by combining a linearization method with a splitting algorithm. For the case $a = 0$ and $h(\cdot), b(\cdot)$ monotone increasing we proposed in [2] a monolithic and a splitting scheme based on a linearization by the L-scheme. The idea of the L-scheme, see e.g. [6] is to solve a non-linearity $F(U)$ iteratively by linearizing in the following way

$$F(U^i) + L(U^{i+1} - U^i), \tag{3}$$

where i is the iteration index and $L > 0$ a free to chose parameter. The L-scheme is very robust but only linearly convergent. Moreover, it works only for monotone coefficient functions. We propose now new monolithic and splitting schemes based this time on the Newton scheme. For this, a non-linearity $F(U)$ will be solved by

$$F(U^i) + F'(U^i)(U^{i+1} - U^i), \tag{4}$$

with F' being the Jacobi matrix. The monolithic and splitting scheme will be rigorously analyzed, techniques from [3] and [8] being employed. The quadratic, but local convergence will be proved. Illustrative numerical results will be presented. This will include also simulations based on higher-order space time elements, extending our results for the linear case in [1].

Acknowledgements

F.A. Radu wish to thank Meltzer fundation for the grant 2017/3273 to participate at ACOMEN 2017.

References

[1] M. Bause, F. A. Radu, U. Koecher, *Space-time finite element approximation of the Biot poroelasticity system with iterative coupling,* CMAME 320 (2017): 745-768.

[2] M. Borregales, F.A. Radu, K. Kumar, J.M. Nordbotten, *Robust iterative schemes for non-linear poromechanics*, arXiv:1702.00328, 2017.

[3] J. Both, M. Borregales, F.A. Radu, K. Kumar, J.M. Nordbotten, *Robust fixed stress splitting for Biot's equations in heterogeneous media*, Appl. Math. Letters 68 (2017): 101-108.

[4] O. Coussy, *Poromechanics*, J. Willey & Sons, Ltd. 2004.

[5] J. Kim, H. Tchelepi, R. Juanes, *Stability and convergence of sequential methods for coupled flow and geomechanics: Fixed-stress and fixed-strain splits*, CMAME 200 (2011): 1591-1606.

[6] F. List, F.A. Radu, *A study on iterative methods for Richards' equation*, Comput. Geosci. 20 (2016): 341-353.

[7] A. Mikelic, M.F. Wheeler, *Convergence of iterative coupling for coupled flow and geomechanics,* Comput. Geosci. 17 (3) (2013): 455-461.

[8] F.A. Radu, I.S. Pop, *Newton method for reactive solute transport with equilibrium sorption in porous media*, J. Comput. and Appl. Math. 234 (2010): 2118-2127.

[9] C. Rodrigo, F.J. Gaspar, X. Hu, L. Zikatanov, *Stability and monotonicity for some discretizations of the Biot's consolidation model*, CMAME 298 (2016): 183-204.

MS 2 IMEX schemes for hyperbolic problems

Organiser: Klaus Kaiser, Jochen Schütz

Description: Developing algorithms for singularly perturbed problems can be challenging. This is in particular true for problems of (near-)hyperbolic type. In this minisymposium, we discuss recent advances toward the treatment of those problems with the aid of schemes of mixed implicit / explicit (IMEX) type.

Book of abstracts of the 7th International Conference
on Advanced Computational Methods
in Engineering, ACOMEN 2017
18–22 September 2017.

A unified IMEX strategy for hyperbolic systems with multiscale relaxation

Sebastiano Boscarino[1], **Lorenzo Pareschi**[2] **and Giovanni Russo**[1]

[1] *Department of Mathematics and Computer Science, University of Catania*

[2] *Department of Mathematics and Computer Science , University of Ferrara*

e-mails: boscarino@dmi.unict.it, lorenzo.pareschi@unife.it, russo@dmi.unict.it

Abstract

Several systems of evolutionary partial differential equations may contain stiff terms, which require an implicit treatment. Typical examples are hyperbolic systems with stiff hyperbolic or parabolic relaxation and kinetic equations in regimes close to fluid dynamic limit. In the hyperbolic-to-hyperbolic relaxation (HSHR) a natural treatment consists in adopting implicit-explicit (IMEX) schemes, in which the relaxation is treated by an implicit scheme, while the hyperbolic part is treated explicitly [1]. In the hyperbolic-to-parabolic relaxation (HSPR) standard methods relax to an explicit scheme for the parabolic limit, thus suffering from parabolic CFL restriction. This drawback can be overcome by a penalization method, consisting in adding and subtracting the same term, so that the system appears as the limit relaxed system plus a small perturbation, [2, 3]. In this talk we present a unified IMEX approach for systems which may admit both limits. This generalizes the two approaches: HSHR and HSPR. The methodology is illustrated in the case of the simple 2x2 system

$$\begin{aligned} u_t + v_x &= 0, \\ \varepsilon^\alpha v_t + \frac{1}{\varepsilon^\alpha} u_x &= -\frac{1}{\varepsilon}(v - f(u)) \end{aligned}$$

depending of an additional parameter α which modifies the nature of the asymptotic behaviour which can be either hyperbolic ($\alpha = 0$, gives HSHR) or parabolic ($\alpha = 1$, gives HSPR). The main idea is to treat the variable v in the first equation implicitly and to discretize the time by globally stiffly accurate IMEX schemes. The modified equation associated to the scheme has bounded characteristic speeds. This approach is capable to capture the correct asymptotic limit of the system independently of the scaling used. Several examples will be presented.

References

[1] S. Boscarino, G. Russo, *On a class of uniformly accurate IMEX RungeÐKutta schemes and applications to hyperbolic systems with relaxation*, SIAM J. Sci. Comput., 31 (2009), pp. 1926 -1945.

[2] S. Boscarino, L. Pareschi, G. Russo, *Implicit-Explicit Runge-Kutta schemes for hyperbolic systems and kinetic equations in the diffusion limit*, SIAM J. SCI. COMPUT., Vol. 35, No. 1, pp. A22-A51.

[3] S. Boscarino, G. Russo, *Flux-Explicit IMEX Runge-Kutta schemes for hyperbolic to parabolic relaxation problems*, SIAM J. NUMER. ANAL., Vol. 51, No. 1, pp. 163-190.

Book of abstracts of the 7th International Conference
on Advanced Computational Methods
in Engineering, ACOMEN 2017
18–22 September 2017.

Multiderivative time integrators for a hybridized discontinuous Galerkin method

Alexander Jaust[1], Jochen Schütz[1] and David C. Seal[2]

[1] *Faculty of Sciences, Hasselt University, Belgium*

[2] *Department of Mathematics, U.S. Naval Academy, USA*

e-mails: alexander.jaust@uhasselt.be, jochen.schuetz@uhasselt.be, seal@usna.edu

Abstract

The discretization-in-space of time-dependent partial differential equations may lead to stiff ordinary differential equations. Implicit time-stepping schemes can in such a case be beneficial as they do not suffer from severe time step restrictions. However, the computational complexity of standard schemes is enormous. In this work, we reduce the computational complexity by applying implicit multiderivative time integration schemes to the hybridized discontinuous Galerkin method. We present numerical schemes that are of high order in both time and space.

Key words: hybridized discontinuous Galerkin method, CFD, multiderivative time integrator, high-order method

This work is concerned with time-dependent partial differential equations (PDEs) on a domain Ω in convection-diffusion form, i.e.,

$$w_t + \nabla \cdot (f(w) - f_v(w, \nabla w)) = 0. \tag{1}$$

The system is assumed to be equipped with suitable initial and boundary conditions. This type of problem arises in many applications such as, e.g., in computational fluid dynamics. (Note that both Euler and Navier-Stokes equations are covered by this framework.)

After discretizing the PDE (1) in space one usually obtains an ordinary differential equation (ODE) with given initial data

$$\frac{\mathrm{d}}{\mathrm{d}t} y(t) = g(y), \quad y(0) = y_0. \tag{2}$$

If viscosity is dominating, or if the discretization uses a high-order of approximation order, this equation usually turns out to be stiff, so implicit solvers are methods of choice. It is often discretized using standard ODE time integrators such as multistage or multistep methods. These methods achieve a high order in time by computing intermediate stage values or by using a history of data points.

Another way to increase the accuracy of the method is achieved by using additional information in the form of additional derivatives of the solution y which can be expressed using

the original ODE (2). Combining this approach while still allowing for multiple stages and steps leads to the general class of multistep-multistage-multiderivative time integrators [3]. The methods can be constructed to have high accuracy in time, good stability properties, and a low number of stages. The last point is very important because the solution step associated to each stage is computationally expensive. The efficient application of explicit and implicit multiderivative schemes to 'standard' discontinuous Galerkin (DG) schemes has been presented, e.g., in [2, 4].

In contrast to 'standard' DG methods, hybridized discontinuous Galerkin (HDG) discretizations [1] introduce an additional hybrid unknown λ on the trace of the triangulation of Ω. This allows to apply static condensation techniques to decrease the size of the resulting system of equations that has to be solved. This makes the method especially interesting for stiff problems with implicit time integration techniques where the implicit solution steps are usually the most time and memory consuming part of the computation. Therefore, the HDG method is in particular suited to be coupled with implicit multiderivative time integrators.

We present the combination of multiderivative time integrators and the HDG method. We will apply an approach similar to the one presented in [4] where an auxiliary variable was introduced to obtain a stable and efficient discretization without the problem of increasing stencils that typically occurs in higher derivatives. The resulting scheme is verified by numerical experiments and the results are discussed.

Acknowledgements

This study was supported by the Special Research Fund (BOF) of Hasselt University.

References

[1] B. Cockburn, J. Gopalakrishnan and R. Lazarov, *Unified Hybridization of discontinuous Galerkin, Mixed, and Continuous Galerkin Methods for Second Order Elliptic Problems*, SIAM Journal on Numerical Analysis **47** (2009), 1319–1365

[2] D. C. Seal, Y. Güçlü and A. Christlieb, *High-Order Multiderivative Time Integrators for Hyperbolic Conservation Laws*, Journal of Scientific Computing **60** (2014), 101–140.

[3] E. Hairer and G. Wanner, *Multistep-multistage-multiderivative methods for ordinary differential equations*, Computing **11** (1973), 287–303.

[4] J. Schütz, D.C. Seal and A. Jaust, *Implicit multiderivative collocation solvers for linear partial differential equations with discontinuous Galerkin spatial discretizations*, CMAT preprint UP-17-02, 2017.

Book of abstracts of the 7th International Conference
on Advanced Computational Methods
in Engineering, ACOMEN 2017
18–22 September 2017.

A new stable splitting for singularly perturbed equations

Klaus Kaiser[1,2] **and Jochen Schütz**[1]

[1] *Faculty of Sciences, Hasselt University, Belgium*

[2] *Institut für Geometrie und Praktische Mathematik, RWTH Aachen University, Germany*

e-mails: kaiser@igpm.rwth-aachen.de, jochen.schuetz@uhasselt.be

Abstract

Singularly perturbed equations place stringent requirements on the numerical methods used to compute an approximation. One popular method are IMEX time integration schemes, for which the equation is needed to be split into a stiff and a non-stiff part.

In this work we present the RS-IMEX splitting for singularly perturbed equations, which is based on the singular limit of the equation. It is analyzed and compared with splittings from literature in terms of stability, efficiency and accuracy.

Key words: IMEX, isentropic Euler, incompressible Euler, asymptotic preserving

The incompressible Euler equations are an approximation of the compressible Euler equations for low Mach (ε) number flows. Furthermore, one can show that the compressible one transforms towards the incompressible one as $\varepsilon \to 0$. This can be understood best if we consider the isentropic Euler equations, assume that every quantity can be represented by an asymptotic expansion ($\mathbf{w} = \mathbf{w}_{(0)} + \varepsilon \mathbf{w}_{(1)} \dots$) and compute the formal limit $\varepsilon \to 0$ (see [7] for a more formal proof):

$$\begin{pmatrix} \rho \\ \rho\mathbf{u} \end{pmatrix}_t + \nabla \cdot \begin{pmatrix} \rho\mathbf{u} \\ \rho\mathbf{u} \otimes \mathbf{u} + \frac{p(\rho)}{\varepsilon^2} \cdot Id \end{pmatrix} = 0 \quad \overset{\varepsilon \to 0}{\longrightarrow} \quad \begin{pmatrix} 0 \\ \mathbf{u}_{(0)} \end{pmatrix}_t + \nabla \cdot \begin{pmatrix} \mathbf{u}_{(0)} \\ \mathbf{u}_{(0)} \otimes \mathbf{u}_{(0)} + \frac{p_{(2)}}{\rho_{(0)}} \cdot Id \end{pmatrix} = 0$$

Computing a suitable numerical approximation for low Mach number flows is quite difficult and topic of several recent publications, e.g. [3, 4, 6]. One special challenge is that the numerical method should show a similar behavior for $\varepsilon \to 0$ as the equation. This property is called asymptotic preserving (AP).

One way to obtain a suitable numerical method is to split the equation into a stiff and a non-stiff contribution,

$$\mathbf{w}_t + \nabla \cdot \mathbf{F}(\mathbf{w}) = \mathbf{w}_t + \nabla \cdot \left(\widehat{\mathbf{F}}(\mathbf{w}) + \widetilde{\mathbf{F}}(\mathbf{w}) \right),$$

and use an IMEX time integration scheme [1]. This means that the stiff part $\widetilde{\mathbf{F}}$ is handled with an implicit method and the non-stiff part $\widehat{\mathbf{F}}$ with an explicit method. Then the main task is to find a splitting which results in a stable, accurate and efficient method. In the past years several different splittings have been developed but they may suffer from stability problems and/or they are only designed for one special equation.

In this talk we present the main ideas and steps in the development of the *RS-IMEX* splitting. This splitting is given by

$$\widetilde{\mathbf{F}} = \mathbf{F}(\mathbf{w}_{(0)}) + \mathbf{F}'(\mathbf{w}_{(0)})(\mathbf{w} - \mathbf{w}_{(0)}) \qquad \text{and} \qquad \widehat{\mathbf{F}} = \mathbf{F} - \widetilde{\mathbf{F}},$$

where $\mathbf{w}_{(0)} = \lim_{\varepsilon \to 0} \mathbf{w}$ or in other words $\mathbf{w}_{(0)}$ corresponds to the solution of the limiting equation.

We apply the RS-IMEX splitting to different singularly perturbed equations combined with low and high order methods. Starting with a high order discretization of an ordinary differential equation, we prove the AP property and also show numerical results, thereby observing possible problems with order reduction [2, 8]. Continuing with a first order approximation of the isentropic Euler equation we prove the AP property and compare the splitting with a given one from literature [4, 6]. Finally, we consider a high order discretization of the isentropic Euler equations, prove again the AP property and show first numerical results [5].

The talk is closed with an overview on recent and future steps in the development of the splitting.

Acknowledgements

Klaus Kaiser has been partially supported by the German Research Foundation (DFG) through project NO 361/6-1; his study was supported by the Special Research Fund (BOF) of Hasselt University.

References

[1] U. M. Ascher and S. Ruuth and R. Spiteri, *Implicit-explicit Runge-Kutta methods for time-dependent partial differential equations*, Applied Numerical Mathematics **25** (1997), 151–167

[2] S. Boscarino, *Error analysis of IMEX Runge-Kutta methods derived from differential-algebraic systems*, SIAM Journal on Numerical Analysis **45** (2007) 1600–1621

[3] P. Degond and M. Tang, *All speed scheme for the low Mach number limit of the isentropic Euler equation*, Communications in Computational Physics **10** (2011) 1–31

[4] J. Haack and S. Jin and J.-G. Liu, *An all-speed asymptotic-preserving method for the isentropic Euler and Navier-Stokes equations*, Communications in Computational Physics **12** (2012) 955–980

[5] K. Kaiser and J. Schütz, *A high-order method for weakly compressible flows*, accepted for publication in Communications in Computational Physics (2016)

[6] K. Kaiser and J. Schütz and R. Schöbel and S. Noelle, *A new stable splitting for the isentropic Euler equations*, Journal of Scientific Computing **70** (2017) 1390–1407

[7] S. Klainerman and A. Majda, *Singular limits of quasilinear hyperbolic systems with large parameters and the incompressible limit of compressible fluids*, Communications on Pure and Applied Mathematics **34** (1981) 481–524

[8] J. Schütz and K. Kaiser, *A new stable splitting for singularly perturbed ODEs*, Applied Numerical Mathematics **107** (2016) 18–33

Book of abstracts of the 7th International Conference on Advanced Computational Methods in Engineering, ACOMEN 2017
18–22 September 2017.

High-order accurate implicit time integration methods applied to semidiscrete Discontinuous Galerkin approximations for unsteady low Mach number flows

Alessandra Nigro[1], Carmine De Bartolo[2], Andrea Crivellini[3], Matteo Franciolini[3], Alessandro Colombo[4] and Francesco Bassi[4]

[1] *Faculty of Science and Technology, Free University of Bozen*

[2] *Department of Mechanical, Energy and Management Engineering, University of Calabria*

[3] *Department of Industrial Engineering and Mathematical Science, Marche Polytechnic University*

[4] *Department of Industrial Engineering, University of Bergamo*

e-mails: alessandra.nigro@unibz.it, carmine.debartolo@unical.it, a.crivellini@univpm.it, m.franciolini@pm.univpm.it, alessandro.colombo@unibg.it, francesco.bassi@unibg.it

Abstract

In this work we investigate the use of implicit multi-stage multi-step Modified Extended BDF (MEBDF) and linearly implicit Rosenbrock-type Runge-Kutta schemes for the time integration of high-order Discontinuous Galerkin (DG) approximations of the Navier-Stokes equations, focusing the attention on unsteady compressible low Mach number flows. We show that, by adopting the Matrix-Free approach, it is possible to obtain a fourth-order accurate MEBDF method which is much less expensive than its Matrix-Explicit counterpart, making the time integration algorithm even more robust at low Mach numbers. We additionally employ a low-Mach number treatment of the dissipative term of the Roe numerical flux and we evaluate its impact on accuracy and efficiency of unsteady solutions obtained by using the eight-stage fifth-order accurate Rosenbrock scheme. Numerical experiments are performed on 2D inviscid isentropic vortex and laminar vortex shedding behind a circular cylinder and 3D ILES Taylor-Green vortex test cases. The proposed time integration algorithms compare favorably with the more commonly used five-stage fourth-order accurate Strong Stability Preserving Runge-Kutta scheme in terms of accuracy and efficiency. The numerical computations also show that the preconditioned Roe scheme allows to obtain accurate solutions on relatively coarse grids, although results indicate that effects of preconditioning reduce as the polynomial degree of the DG approximation increases.

Key words: Discontinuous Galerkin, Low Mach, Matrix-Free, Modified Extended Backward Differentiation Formulae, Rosenbrock-type Runge-Kutta schemes

1 Numerical results

We have studied two- and three-dimensional fluid flow problems at low and moderate levels of grid-induced and physics-induced stiffness. The convection of an inviscid isentropic vortex has been considered, for several free stream Mach numbers, to assess the effectiveness of the Matrix-Free approximation [1] for the three-stage fourth-order accurate MEBDF scheme (MF-MEBDF4) with respect to its Matrix-Explicit counterpart (ME-MEBDF4) [2]. The results of this analysis are shown in fig. 1(a) for $M_\infty = 0.14$. The potential of the proposed MF-MEBDF4 algorithm for efficient long-time simulations is demonstrated by computing 35 laminar vortex shedding behind a circular cylinder. For this test case $M_\infty = 0.1$ while the Reynolds number was varied from 100 to 400 to consider different wake patterns. Fig. 1(b) shows, for $Re = 100$, the time evolution of the difference between the lift coefficient of a numerical exact solution and the one computed by MF-MEBDF4 at the large time step size of $\Delta t = 2$. Finally, ILES of the Taylor-Green vortex at $M = 0.1$ and $Re = 1600$ have been performed using the eight-stage fifth-order accurate Rosenbrock scheme (ROS5) [3] to investigate the influence of the numerical flux on the accuracy and the efficiency of the solution. Figure 1(c) compares the time evolution of the enstrophy computed by using the Explicit Riemann Solver (ERS) and the preconditioned Roe numerical flux (pRoe) [4] with a reference numerical solution.

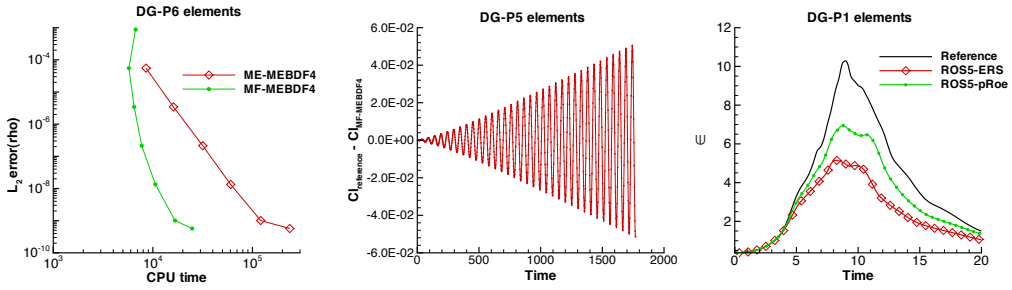

(a) Inviscid isentropic vortex (b) Laminar vortex shedding (c) ILES Taylor-Green vortex

Figure 1: An overview of the results.

References

[1] A. Crivellini and F. Bassi. An implicit matrix-free Discontinuous Galerkin solver for viscous and turbulent aerodynamic simulations. Computer & Fluids, 50: 81–93, 2011

[2] A. Nigro, A. Ghidoni, S. Rebay and F. Bassi. Modified Extended BDF scheme for the Discontinuous Galerkin solution of unsteady compressible flows. International Journal of Numerical Methods in Fluids, 76(9): 549–574, 2014

[3] F. Bassi, L. Botti, A. Colombo, A. Ghidoni and F. Massa. Linearly implicit Rosenbrock-type Runge-Kutta schemes applied to the Discontinuous Galerkin solution of compressible and incompressible unsteady flows. Computer & Fluids, Vol. 118: 305–320, 2015

[4] F. Bassi, C. De Bartolo, R. Hartmann and A. Nigro. A discontinuous Galerkin method for inviscid low Mach number flows. Journal of Compuational Physics, 228(11): 3996 – 4011, 2009

Book of abstracts of the 7th International Conference
on Advanced Computational Methods
in Engineering, ACOMEN 2017
18–22 September 2017.

On the stability of IMEX methods

Jochen Schütz[1], **Klaus Kaiser**[2] **and Sebastian Noelle**[2]

[1] *Faculty of Sciences, Hasselt University, Belgium*

[2] *Institut für Geometrie und Praktische Mathematik, RWTH Aachen University, Germany*

e-mails: jochen.schuetz@uhasselt.be, kaiser@igpm.rwth-aachen.de,
noelle@igpm.rwth-aachen.de

Abstract

The non-dimensionalized Euler or Navier-Stokes equations yield, for a small reference Mach number, a singularly perturbed system of equations. This system can be efficiently solved by a decoupling of stiff and non-stiff terms, treating the latter ones explicitly and the former ones implicitly. However, not any seemingly reasonable splitting yields a stable overall method. A criterion on how to choose a splitting that induces a uniformly stable algorithm is therefore of utmost important.

In this work, we consider prototype equations and explain the challenges one encounters when trying to find stable splittings and how to circumvent them. Stable and unstable splittings are discussed based on analytical and numerical investigations.

Key words: IMEX schemes, low Mach, finite volumes

The non-dimensionalized Navier-Stokes equations - for simplicity the isentropic ones - at low Mach number can be written as

$$\begin{aligned} \rho_t + \nabla \cdot \rho \mathbf{u} &= 0, \\ (\rho \mathbf{u})_t + \nabla \cdot (\rho \mathbf{u} \otimes \mathbf{u}) + \frac{1}{\varepsilon^2} \nabla p &= 0, \end{aligned}$$

for ρ density, $\mathbf{u}$ velocity and $p \equiv p(\rho)$ pressure. The characteristic speeds in normal directions of this equation are

$$\lambda_0 = \mathbf{u} \cdot \mathbf{n}, \qquad \lambda_\pm = \mathbf{u} \cdot \mathbf{n} \pm \frac{c}{\varepsilon}.$$

We have therefore in the limit $\varepsilon \to 0$ two completely different behaviors of characteristic speeds: One remains bounded, the others tend to infinity, giving rise to a system of mixed parabolic-hyperbolic type. If these waves were completely independent, one would treat the $O(1)$–wave explicitly, and the other ones implicitly to obtain a stable algorithm. However those waves are not independent of each other, and so one has to rely on a splitting of the equation into 'stiff' and 'nonstiff' parts [3, 2] which are treated implicitly and explicitly, respectively. This leads to so-called IMEX schemes [1].

In this talk we will, based on the work in [4], consider the singularly disturbed *linear* system of conservation laws

$$w_t + \nabla \cdot (A_\varepsilon w) = 0$$

for a given A_ε. We will discuss unconditional stability of IMEX schemes for this equation. We will show that for the one-dimensional equation, there exists an optimal splitting based on characteristic decomposition; stability of this splitting is shown analytically. Also, we show some unstable – though seemingly reasonable – splittings and discuss why they fail. Possible extensions to nonlinear equations will be discussed.

Acknowledgements

Klaus Kaiser has been partially supported by the German Research Foundation (DFG) through project NO 361/6-1; his study was supported by the Special Research Fund (BOF) of Hasselt University.

References

[1] U. M. Ascher and S. Ruuth and R. Spiteri, *Implicit-explicit Runge-Kutta methods for time-dependent partial differential equations*, Applied Numerical Mathematics **25** (1997), 151–167.

[2] J. Haack and S. Jin and J.-G. Liu, *An all-speed asymptotic-preserving method for the isentropic Euler and Navier-Stokes equations*, Communications in Computational Physics **12** (2012), 955–980.

[3] R. Klein, *Semi-Implicit Extension of a Godunov-Type Scheme Based on Low Mach Number Asymptotics I: One-Dimensional Flow*, Journal of Computational Physics **121** (1995), 213–237.

[4] J. Schütz and S. Noelle, *Flux Splitting for stiff equations: A notion on stability*, Journal of Scientific Computing **64** (2015), 522–540.

Book of abstracts of the 7th International Conference
on Advanced Computational Methods
in Engineering, ACOMEN 2017
18–22 September 2017.

Energy stable and high-order methods for gradient flows based on the Convex Splitting Runge–Kutta methods

Jaemin Shin[1], **Hyun Geun Lee**[2] **and June-Yub Lee**[3]

[1] *Institute of Mathematical Sciences, Ewha Womans University*

[2] *Department of Mathematics, Kwangwoon University*

[3] *Department of Mathematics, Ewha Womans University*

e-mails: jmshin@ewha.ac.kr, leeh1@kw.ac.kr, jyllee@ewha.ac.kr

Abstract

We introduce the recent development based on the convex splitting method to solve the gradient flow considering the energy stability. We present the Convex Splitting Runge–Kutta methods which provide a simple unified framework. The core idea is the combination of convex splitting methods and multi-stage implicit-explicit Runge–Kutta methods. The proposed methods are high-order accurate in time and the energy stability is completely proved when we consider the special design of implicit-explicit Runge–Kutta tables, called a *resemble* condition. We present numerical experiments with the Cahn–Hilliard equation which is a typical example for the gradient flow to show the numerical accuracy, stability, and efficiency of the proposed methods.

Key words: Energy stability, High-order accuracy, Gradient flow, Cahn–Hilliard equation, Implicit-explicit Runge–Kutta

References

[1] D. J. Eyre , *An unconditionally stable one-step scheme for gradient systems*, Unpublished article, 1998.

[2] J. Shin, H. G. Lee, J.-Y. Lee, *Convex Splitting Runge–Kutta methods for phase-field models*, Computers & Mathematics with Applications, **73** (2017) 2388–2403.

[3] J. Shin, H. G. Lee, J.-Y. Lee, *Unconditionally stable methods for gradient flow using Convex Splitting Runge–Kutta scheme*, Journal of Computational Physics, **347** (2017) 367–381.

Book of abstracts of the 7th International Conference
on Advanced Computational Methods
in Engineering, ACOMEN 2017
18–22 September 2017.

Investigation of a novel splitting scheme for the weakly compressible Euler equations

Jonas Zeifang[1], Andrea Beck[1], Klaus Kaiser[2] and Jochen Schütz[3]

[1] *Institute for Aerodynamics and Gas Dynamics, University of Stuttgart, Pfaffenwaldring 21, D-70329 Stuttgart*

[2] *IGPM, RWTH Aachen University, Templergraben 55, D-52062 Aachen*

[3] *Faculty of Sciences, Hasselt University, Agoralaan Gebouw D, BE-3590 Diepenbeek*

e-mails: zeifang@iag.uni-stuttgart.de, beck@iag.uni-stuttgart.de, kaiser@igpm.rwth-aachen.de, jochen.schuetz@uhasselt.be

Abstract

In this talk results of the application of the *RS-IMEX* splitting, introduced by Kaiser and Schütz [1], will be presented. After the presentation of the numerical framework which is based on a high order nodal discontinuous Galerkin spectral element method, investigations concerning efficiency in the low Mach number limit of the isentropic Euler equations will be shown. Furthermore, problems and solution strategies for the application of the splitting to the full Euler equations will be discussed.

Key words: discontinuous Galerkin, IMEX splitting, weakly compressible Euler equations

1 Introduction

The *RS-IMEX* splitting for a general hyperbolic equation system in conservation form relies on the linearization about an arbitrary reference state $\mathbf{w}_{ref}$. For the hyperbolic equation system

$$\partial_t \mathbf{w} + \nabla \cdot \mathbf{F}(\mathbf{w}) = 0$$

the *RS-IMEX* splitting is defined by

$$\mathbf{F}(\mathbf{w}) = \tilde{\mathbf{F}}(\mathbf{w}) + \hat{\mathbf{F}}(\mathbf{w}), \tag{1}$$

where

$$\tilde{\mathbf{F}}(\mathbf{w}) = \mathbf{F}(\mathbf{w}_{ref}) + \mathbf{F}'(\mathbf{w})(\mathbf{w} - \mathbf{w}_{ref}) \qquad \text{and} \qquad \hat{\mathbf{F}} = \mathbf{F}(\mathbf{w}) - \tilde{\mathbf{F}}(\mathbf{w}).$$

An application to the non-dimensional isentropic Euler equations shows that the eigenvalues of the stiff system with flux $\tilde{\mathbf{F}}$ are dependent on the Mach number ϵ and, therefore, are treated implicitly. The eigenvalues of the non-stiff system with flux $\hat{\mathbf{F}}$ are independent of the Mach number and, therefore, are treated explicitly. Motivated by the asymptotics of the isentropic Euler equations, the reference state can be chosen as the incompressible solution. Hence, the required solver is tripartite: An explicit and an implicit solver for the two parts of the split system and an incompressible solver for the reference solution. For spatial discretization a high order nodal discontinuous Galerkin spectral element method according to Hindenlang et al. [2] will be described. In the following, several aspects concerning the implicit temporal discretization for the stiff and the incompressible part will be highlighted.

2 Application to isentropic Euler equations

For the evaluation of efficiency and the demonstration of applicability in the low Mach number limit, two test cases are considered. For the two dimensional case, a traveling vortex is an exact solution to the isentropic Euler equations. It has been applied and calculated for different spatial resolutions with a fully explicit, a fully implicit and with the *RS-IMEX* splitting. Results suggest that for Mach numbers $\epsilon \leq 10^{-3} \ldots 10^{-4}$ an efficiency gain relating to the fully explicit scheme can be obtained with the *RS-IMEX* splitting. Relating to the fully implicit scheme, an efficiency gain is obtained even for $\epsilon \leq 10^{-2}$.

As a three dimensional test case the incompressible Taylor-Green-Vortex has been consistently extended to the non-dimensional compressible isentropic Euler equations. With these two different initial data sets the *RS-IMEX* splitting is able to achieve similar decay of the kinetic energy as a fully explicit scheme, both equipped with Lax-Friedrichs type Riemann solvers. This demonstrates the ability of the *RS-IMEX* splitting to reproduce a complex three dimensional behavior. Again, efficiency is compared with a fully explicit and a fully implicit scheme. Results show that a scaling in computational time $\propto \frac{1}{\epsilon}$ is obtained for the explicit scheme. In contrary, the *RS-IMEX* has only a very slight increase in computational effort as the Mach number decreases. For rather large Mach numbers ($\mathcal{O}(10^{-1})$) the *RS-IMEX* is computational more costly as more equations have to be solved. But, this is compensated for a decreasing Mach number as the time step can be chosen independent of the Mach number.

3 Application to Euler Equations

When applying eq. (1) to the Euler equations for an ideal gas one can obtain complex eigenvalues for the non-stiff system for special cases. Therefore, the reference solution has to be chosen carefully. We will show a simple choice for the reference solution which will prevent the eigenvalues from becoming complex. The functionality will be demonstrated with a three dimensional test case.
We will conclude with current results and an outlook.

Acknowledgements

This work has been supported by the International Research Training Group GRK 2160: Droplet Interaction Technologies (DROPIT)

References

[1] K. Kaiser, J. Schütz, *A high-order method for weakly compressible flows*, IGPM Preprint **456** 2016.

[2] F. Hindenlang, G.J. Gassner, C. Altmann, A.D.Beck, M. Staudenmaier, C.-D. Munz, *Explicit discontinuous Galerkin methods for unsteady problems*, Computers & Fluids **61** (2012) 86–93.

MS 3 Numerical methods for evolving surfaces

Organiser: Peter Frolkovič

Description: In this minisymposium we shall discuss recent developments in the Level-set and Lagrangian computational methods for curve and surface evolutions and show their usage in various applications.

Book of abstracts of the 7th International Conference
on Advanced Computational Methods
in Engineering, ACOMEN 2017
18–22 September 2017.

Numerical modelling of forest fire propagation

Martin Ambroz[1], Martin Balažovjech[1], Matej Medľa[1] and Karol Mikula[1]

[1] *Department of Mathematics, Faculty of Civil Engineering, Slovak University of Technology, Radlinskeho 11, 810 05 Bratislava, Slovak Republic*

e-mails: ambroz.martin.ml@gmail.com, balazovjech@math.sk, medla@math.sk, mikula@math.sk

Abstract

In this talk we present a new approach to wildland forest fire spread modelling. We evolve a surface curve, which represents the fire perimeter, i.e., the boundary between burned and unburned fuel. Such curve is evolved as a projection to a horizontal plane and is driven by our mathematical model. This mathematical model is based on the empirical laws of the fire spread influenced by the fuel, wind, terrain slope and the shape of the fire perimeter (geodesic and normal curvatures). For numerical solution we discretize the intrinsic partial differential equation by a semi-implicit scheme in curvature term and for the advective term we use so-called inflow-implicit/outflow-explicit approach which guarantee solvability of linear systems by efficient tridiagonal solver without any time step restriction. Fast treatment of a topological changes (splitting and merging curves) is shown on examples as well. We demonstrate the influence of the fire spread model parameters on a testing topography and finally, we reconstruct a real wildland fire.

Key words: curve evolution, surface curve, wildland fire modelling, geodesic curvature, normal curvature

1 Introduction

Our model is built on the the so-called Lagrangian approach to evolution of a surface curve, representing the fire perimeter. For the numerical computations we use its projection into a planar curve, where we follow [3, 4].

Let us have a planar curve Γ, $\Gamma : S^1 \to \mathbf{R}^2$, parametrized by $u \in S^1$, where S^1 is a circle with unit length, thus $u \in [0,1]$ and $\Gamma = \{\mathbf{x}(u);\ u \in S^1\}$, where $\mathbf{x}(u) = (x(u), y(u))$ is position vector of the curve Γ for parameter u.

Such curve could represent the fire perimeter in the case of a flat terrain [1]. Therefore we define a surface $\mathcal{M}$, that represents a local Earth topography. Let $\mathcal{M}$ be the two dimensional surface in $\mathbb{R}^3$, $\mathcal{M} = \{(x, y, \varphi(x, y)) \in \mathbb{R}^3,\ (x, y) \in \Omega\}$, represented by a graph of a function $\varphi : \Omega \subset \mathbb{R}^2 \to \mathbb{R}$ defined in a domain $\Omega \subset \mathbb{R}^2$. Let the curve $\mathcal{G} : S^1 \to \mathbb{R}^3$, parametrized by $u \in S^1$, where S^1 is a circle with unit length, thus $u \in [0,1]$, be a smooth surface curve on $\mathcal{M}$, that represents the fire perimeter on the surface $\mathcal{M}$. Let us denote by p the unit arc-length parametrization of the curve $\mathcal{G}$: $dp = G du$, where $G = |\mathcal{G}_u| > 0$. Furthermore, we suppose a constraint between planar curve Γ and the surface curve $\mathcal{G}$ as follows $\mathcal{G} = \{(x(u), y(u), z(u) = \varphi(x(u), y(u))) \in \mathbb{R}^3,\ (x(u), y(u)) \in \Gamma\}$, so that the curve Γ is a vertical projection of the surface curve $\mathcal{G}$.

2 Mathematical fire spread model

The fire spread rate is expressed by an external force $\mathcal{F}$, which includes heterogeneous burnability, wind and terrain slope effects. Besides that, the local fire spread is influenced by the shape of the fire perimeter. The geodesic curvature, K_g, smooths the curve. The curvature K_n of the curve evolving in a valley (or on a ridge) can increase (or decrease) the normal velocity $\mathcal{V}$. Such evolution of curve $\mathcal{G}$ can be described by following formula

$$\mathcal{V} = \mathcal{F}\left(1 - \delta_g \mathcal{K}_g + \delta_n \mathcal{K}_n\right), \tag{1}$$

where δ_g is a weight of the geodesic curvature and δ_n is a weight of the normal curvature influence to the fire spread. Such formula expresses the dominant role of the external force, that can be accelerated or slowed down by the geodesic and normal curvatures.

3 Evolution of the projected planar curve

We split general motion of any point $\mathbf{x}$ of the curve Γ into the normal and tangential directions, so we consider a general form of the planar curve evolution in the following form

$$\mathbf{x}_t = \beta \mathbf{N} + \alpha \mathbf{T}, \tag{2}$$

where β is a velocity in the normal direction $\mathbf{N}$ and α is a tangential velocity of the planar curve Γ, designed for asymptotically uniform grid point redistribution [2].

To find the relationship between the normal velocity $\mathcal{V}$ in the tangent plane and the projected curve Γ normal velocity β we follow [3]

$$\mathcal{V} = \mathcal{G}_t \cdot \mathcal{N} = (x_t, y_t, \varphi_t(x,y)) \cdot \mathcal{N} = (\mathbf{x}_t, \mathbf{x}_t \cdot \nabla\varphi) \cdot \mathcal{N} = \sqrt{\frac{1 + |\nabla\varphi|^2}{1 + (\nabla\varphi \cdot \mathbf{T})^2}}\beta. \tag{3}$$

Acknowledgements

This work was supported by the grants APVV-15-0522 and VEGA 1/0808/15.

References

[1] M. Balažovjech, K. Mikula, M. Petrášová, J. Urbán, *Lagrangean method with topological changes for numerical modelling of forest fire propagation, ALGORITMY 2012, Proceedings of contributed papers and posters, ISBN 978-80-227-3742-5, pp. 42-52.*

[2] K. Mikula, D. Ševčovič, *A direct method for solving an anisotropic mean curvature flow of planar curve with an external force, Mathematical Methods in Applied Sciences, Vol. 27, No. 13 (2004), pp. 1545-1565.*

[3] K. Mikula, D. Ševčovič, *Computational and qualitative aspects of evolution of curves driven by curvature and external force, Computing and Visualization in Science, Vol. 6, No. 4 (2004), pp. 211-225.*

[4] K. Mikula, D. Ševčovič, *Evolution of curves on surface driven by the geodesic curvature and external force, Applicable Analysis, Vol. 85, No. 4 (2006), pp. 345-362.*

Book of abstracts of the 7th International Conference
on Advanced Computational Methods
in Engineering, ACOMEN 2017
18–22 September 2017.

Semi-implicit methods for numerical solution of level set advection equation

Peter Frolkovič[1]

[1] *Department of Mathematics and Descriptive Geometry, Slovak University of Technology*

e-mails: peter.frolkovic@stuba.sk

Abstract

A new parametric class of semi-implicit numerical schemes for level set advection equation is derived and analyzed. The accuracy and stability study is provided by partial Lax-Wendroff procedure and numerical von Neumann stability analysis. The obtained schemes are 2^{nd} order accurate for variable velocity case when using dimension by dimension application of one-dimensional scheme for Cartesian grids. Extensions for unstructured grids and nonlinear case are given and discussed. A so-called Corner Transport Upwind semi-implicit scheme is presented that is 2^{nd} order accurate for variable velocity case, 3^{rd} order accurate for constant velocity and unconditional stable according to numerical stability analysis.

Key words: advection equation, higher order method, Cartesian grid, Lax-Wendroff procedure, von Neumann stability analysis

1 Introduction

In this work we present a new class of semi-implicit schemes for the numerical solution of model advection equation

$$\partial_t u(x,t) + \mathbf{V} \cdot \nabla u(x,t) = 0\,, \quad u(x,0) = u^0(x)\,.$$

This type of equation is a part of many mathematical models that are used in applications of level set methods for tracking of interfaces, see e.g. [1, 2, 3]. Standard methods for numerical solutions of advection equation are fully explicit schemes that have the well-known CFL stability restriction on the choice of time step that depends on a length of grid step size. Although such restriction is not considered as a disadvantage in general, it can be critical e.g. if geometric boundaries are resolved only implicitly. The presence of so-called arbitrary small cut cells can give locally arbitrary small grid size that results in an unrealistic CFL restriction if no modification of fully explicit numerical scheme is provided [2].

To resolve this issue some recent works [4, 5, 6] have proposed to use semi-implicit finite volume schemes for advection equation. The main idea is that the implicit time discretization is used only at inflow boundaries of computational cells [7]. In this talk we present semi-implicit numerical methods for linear advection equation on Cartesian grids and discuss some extensions for unstructured grids and nonlinear case.

The novel tool in this study is partial Lax-Wendroff (or Cauchy-Kowalevski procedure) that in its full form replaces the time derivatives of solution in Taylor series by the space derivatives of solution obtained from the equation. In our approach we apply the steps of such procedure only partially by allowing mixed time-space derivatives in Taylor series.

Using this procedure we derive a class of semi-implicit schemes following the approach of fully explicit κ-scheme [8] that includes as particular cases several popular numerical methods like Lax-Wendroff scheme. Such parametric formulation of numerical scheme gives an opportunity by special choices of parameter to improve the accuracy of scheme in special cases, to adapt the scheme near boundaries, or to optimize the scheme using so-called limiters [8].

The one-dimensional semi-implicit κ-scheme is 2^{nd} order accurate with unconditional numerical stability for variable velocity and for all considered values of κ. A special (velocity dependent) choice of κ exists that gives 3^{rd} order accuracy for constant velocity $\mathbf{V}$. The dimension by dimension extension of one dimensional semi-implicit κ-scheme for Cartesian grids gives a 2^{nd} order accurate scheme for variable velocity case when the analogous fully explicit κ-scheme is only 1^{st} order accurate.

Finally, we present a Corner Transport Upwind extension of semi-implicit κ-scheme by extending its stencil using diagonal corner values. The resulting scheme is unconditionally stable as indicated by numerical von Neumann stability analysis, it is 2^{nd} order accurate for variable velocity case and 3^{rd} order accurate if the velocity is constant. We provide several numerical experiments that illustrate these properties in computational practice.

Acknowledgements

This work was supported by grants VEGA 1/0728/15 and APVV-15-0522.

References

[1] J. Sethian. *Level Set Methods and Fast Marching Methods.* Cambridge UP, 1999.

[2] P. Frolkovič. Application of level set method for groundwater flow with moving boundary. *Adv. Water. Resour.*, 47:56–66, 2012.

[3] P. Frolkovič, D. Logashenko, and Ch. Wehner. Flux-based level-set method for two-phase flows on unstructured grids. *Comput. Vis. Sci.*, 18(1):31–52, 2016.

[4] P. Frolkovič, K. Mikula, and J. Urbán. Semi-implicit finite volume level set method for advective motion of interfaces in normal direction. *Appl. Num. Math.*, 95:214–228, 2015.

[5] Sandra May and Marsha Berger. An explicit implicit scheme for cut cells in embedded boundary meshes. *Journal of Scientific Computing*, pages 1–25, 2016.

[6] J. Hahn, K. Mikula, P. Frolkovič, and B. Basara. Semi-implicit level set method with inflow-based gradient in a polyhedron mesh. In *Finite Volumes for Complex Applications VIII, Lille, 2017*, to appear.

[7] K. Mikula, M. Ohlberger, and J. Urbán. Inflow-implicit/outflow-explicit finite volume methods for solving advection equations. *Appl. Numer. Math.*, 85:16–37, 2014.

[8] P. Wesseling. *Principles of Computational Fluid Dynamics.* Springer Series in Computational Mathematics, 2001.

Book of abstracts of the 7th International Conference on Advanced Computational Methods in Engineering, ACOMEN 2017 18–22 September 2017.

Semi-implicit method with inflow-based gradient for the G-equation model on a polyhedron mesh

Jooyoung Hahn[1], Karol Mikula[2], Peter Frolkovič[2] and Branislav Basara[1]

[1] *Advanced Simulation Technology, AVL LIST GmbH, Hans-List-Platz 1, 8020 Graz, Austria*

[2] *Department of Mathematics and Descriptive Geometry, Slovak University of Technology, Radlinskeho 11, 810 05 Bratislava, Slovakia*

e-mails: jooyoung.hahn@avl.com, karol.mikula@stuba.sk, peter.frolkovic@stuba.sk, branislav.basara@avl.com

Abstract

A semi-implicit scheme of inflow-based gradient (IBG) finite volume method is proposed to solve the G-equation model in premixed turbulent combustion. In order to overcome small time step caused by CFL restriction in polyhedron mesh, a semi-implicit method is used in IBG finite volume method inspired by [3, 4]. Moreover, a conventional approximation of turbulent transport term in the G-variance equation is reviewed and compared with a mathematically correct tangential diffusion term. A sub-face tessellation technique is introduced to prevent deteriorating the order of convergence in case of distorted hexahedron cells. The implementation is very straightforward and easily combined with a conventional finite volume code. A higher order of convergence in numerical examples on polyhedron meshes is illustrated for each velocity term in the G-equation. Some numerical results in real engine cases are also presented.

Key words: G-equation model, Level set method, Polyhedron mesh, Semi-implicit method, Turbulent premixed combustion

MSC 2010: 65M08, 65N08, 35F25, 35F30

1 Introduction

We propose a semi-implicit scheme with inflow-based gradient (IBG) finite volume method to numerically solve the G-equation model in premixed turbulent combustion. The governing equations are described by the Favre mean $\widetilde{G}$ and the fluctuation G'' of G field which is an implicit function whose zero level set represents the flame surface. The equations of $\widetilde{G}$ and $\widetilde{G''^2}$ are commonly called by the G-equation and G-variance equation, respectively; more detail formulations are in [6, 1]. Two equations are coupled and closed by the turbulent flame surface equations and the turbulent flame speed formulations.

The basic form of the G-equation is a standard level set equation containing the advection, normal speed, and mean curvature terms. Comparing to conventional algorithms to solve level set equations on a polyhedron mesh, the proposed scheme has mainly three advantages. The first is that it numerically shows higher order of convergence not only on a hexahedron mesh but also on a a polyhedron mesh in 3D. The second is that the proposed method can be

applicable to the simplest decomposed domains, that is, 1-ring face neighborhood structure, for a parallel computation. The third is that a time step restriction caused by the CFL condition is reduced by the proposed semi-implicit scheme. The first and second advantages are also observed in a propagation in normal direction [2]. In the G-equation, we propose a semi-implicit method to extend the algorithm in [2] with the advection and mean curvature terms on a polyhedron mesh.

The G-variance equation has the same advection term as the G-equation and we apply the same algorithm used in the G-equation. The G-variance equation also has a turbulent transport term which does not allow turbulent diffusion normal to the mean flame front. It can be approximated as a tangential diffusion term. We present the difference between the mathematically correct tangential diffusion term and the conventional one [5] in the combustion community. Moreover, the reason why it is necessary to obtain a higher order scheme to solve the G-equation is explained in a view of solving G-variance equation.

A higher order of convergence in numerical examples on polyhedron meshes is illustrated for each velocity term in the G-equation. A numerical comparison between different approximations of turbulent transport term in the G-variance equation is also presented.

Acknowledgements

The work was supported by grants VEGA 1/0808/15, VEGA 1/0728/15, APVV-0522-15.

References

[1] J. Ewald, N. Peters, *On Unsteady Premixed Turbulent Burning Velocity Prediction in Internal Combustion Engines*, Proceedings of the Combustion Institute **31** (2007) 3051–3058.

[2] J. Hahn, K. Mikula, P, Frolkovič, B. Basara, *Inflow-Based Gradient Finite Volume Method for a Propagation in a Normal Direction in a Polyhedron Mesh*, Journal of Scientific Computing (2017) 1–24. DOI: 10.1007/s10915-017-0364-4

[3] K. Mikula, M. Ohlberger, *A New Level Set Method for Motion in Normal Direction Based on a Semi-Implicit Forward-Backward Diffusion Approach*, SIAM Journal of Scientific Computing **32** (2010) 1527–1544.

[4] K. Mikula, M. Ohlberger, *Inflow-Implicit/Outflow-Explicit Scheme for Solving Advection Equations*, In: J.F. et al. (ed.) Finite Volumes for Complex Applications VI - Problems & Perspectives, Springer Proceedings in Mathematics 4 **1** (2011) 683–691.

[5] N. Peters, *Turbulent Combustion*, Cambridge University Press (2000).

[6] N. Peters, *The Turbulent Burning Velocity for Large-scale and Small-scale Turbulence*, Journal of Fluid Mechanics **384** (1999) 107–32.

Book of abstracts of the 7th International Conference
on Advanced Computational Methods
in Engineering, ACOMEN 2017
18–22 September 2017.

Atlas based image segmentation

Jozef Urbán[1] **and Karol Mikula**[2]

[1] *Department of Research and Development, TatraMed Software s.r.o.*

[2] *Department of Mathematics and Descriptive Geometry, Slovak University of Technology*

e-mails: jozo.urban@gmail.com, mikula@math.com

Abstract

The new automatic image segmentation algorithm extending conventional segmentation methods with an influence of prior knowledge of segmented shape is presented in this talk. Algorithm is applied to Active Contours and also to Geodesic Active Contours method. Original contributions are mainly: automatic solving of curve correspondence problem, registration of planar curves and estimation of prior shape, based on the current segmentation and computed eigenshapes calculated from atlas of shape patterns, using Principal Component Analysis.

Key words: image segmentation, atlas, PCA, prior shape estimation

Acknowledgements

This work has been partially supported by TatraMed Software s.r.o. and through the grant APVV – 0161 – 12.

MS 4 Recent advances on model order reduction techniques

Organiser: Thomas Henneron, Ruth V. Sabariego

Description: Model order reduction techniques are a trend topic in computational science and that due to the ever increasing demand of realistic simulations. We aim at accounting for multiple scales (in space and time), for multiple physical phenomena (mechanics, electromagnetism, thermal processes), for multiple parameters in optimisation applications, for nonlinearities... with an acceptable computational cost in terms of time and memory storage. These techniques provide a compact model of a complex physical problem that captures its main features, i.e. a minimum number of unknowns but preserving a good accuracy. With this dedicated session, we would like to go through the current know-how in different model order reduction techniques (purely mathematical or physically based such as Reduced Basis, Proper Orthogonal Decomposition, Proper Generalized Decomposition, ...) applied at a system-level simulation but with a detailed design at component-level (structural mechanics, fluid mechanics, electromagnetism, thermal processes...).

Book of abstracts of the 7th International Conference on Advanced Computational Methods in Engineering, ACOMEN 2017
18–22 September 2017.

Model Order Reduction on Control Problems of Navier-Stokes Equations

Cansu Evcin[1] and Ömür Uğur[1]

[1] *Insitute of Applied Mathematics, Middle East Technical University*

e-mails: cbilgir@metu.edu.tr, ougur@metu.edu.tr

Abstract

In this study, model reduction strategies on the distributed control of the Navier-Stokes equations are studied. Proper Orthogonal Decomposition (POD) is used to reduce the dimension of the both steady-state parametric and evolutionary models. Boundary conditions are implemented by the Nitsche method weakly in the Mixed Finite Element (MFE) technique. The Empirical Interpolation method (EIM) is applied to further reduce the computational complexity. We provide numerical comparisons to demonstrate the performance of these novel approaches.

Key words: Empirical interpolation, Model reduction, Navier-Stokes equations, Optimal control, Proper orthogonal decomposition.

1 Introduction

Optimal control problems governed by the incompressible Navier-Stokes equations present a computational challenge to scientific computing community. Although the mixed finite element (MFE) method [3] has the advantage of the knowledge about the pressure in the model, the resulting computational model leads to a large system of equations which must be solved at each step of the optimization algorithm. Therefore, solutions to these type of problems need to be simplified by some reduction techniques. In order to investigate the strategies to be discussed, we consider the following distributed control problem for the Navier-Stokes equations [1]

$$\begin{aligned} \text{minimise} \quad & J(y,u) = \frac{1}{2}||y - z_d||_Q^2 + \frac{\alpha}{2}||u||_Q^2 \\ \text{subject to} \quad & y_t - \nu\Delta y + (y\cdot\nabla)y + \nabla p = u \quad \text{in} \quad Q \\ & \nabla\cdot y = 0 \quad \text{in} \quad Q \\ & y = g \quad \text{on} \quad \partial\Omega_i \\ & y = 0 \quad \text{on} \quad \partial\Omega_w \\ & \nu\partial_\eta y - p\eta = 0 \quad \text{on} \quad \partial\Omega_o \\ & y(0,x) = y_0 \quad \text{in} \quad \Omega \end{aligned} \tag{1}$$

Here, $Q = (0,T) \times \Omega$, Ω is a subset of $\mathbb{R}^2$, and $\partial\Omega = \partial\Omega_i \cup \partial\Omega_w \cup \partial\Omega_o$. For the solution of the Navier-Stokes equations and the corresponding adjoint problem we use the Taylor-Hood finite element pair $P2$-$P1$. Implementation of the non-homogenous Dirichlet boundary condition is provided by the Nitsche method [4], which provides a straightforward application of the condition in the continuous projection stage of the Proper Orthogonal Decomposition (POD).

The model reduction in the control of Navier-Stokes equations are implemented by the POD in both cases: steady and unsteady state solutions. In the first case, we consider the parameter dependent steady problem and take the snapshots over the parameter's range. In the second case, since we consider the time- dependent problem, the snapshots are taken at certain times within the domain. In both cases, the pressure is also taken into account, unlike the general approach in literature, in the projection step.

The computational complexity of the nonlinear term in model reduction by the POD still remains problematic. To overcome this, the Empirical Interpolation method (EIM) [2] is applied to approximate the nonlinearities; this is also is in good harmony with the continuous projection of the POD.

The reduction in the cost function is also achieved in a similar way by the projection to the POD basis. The optimization is performed by the use of dolfin-adjoint [5] and IPOPT [6]. Also, FEniCS [7] for the automated solution of the partial differential equations is invoked in this study.

Acknowledgements

This work has been supported by the Scientific HR Development Program (OYP) and TUBITAK (The Scientific and Technological Research Council of Turkey).

References

[1] M. Hinze, K. Kunisch, *Second Order Methods For Optimal Control Of Time-Dependent Fluid Flow*, Siam J. Control Optim. **40** (2001) 925-946.

[2] M. Barrault, Y. Maday, N. C. Nguyen, A. T. Patera, *An Empirical Interpolation Method: Application to efficient reduced-basis discretization of partial differential equations*, C. R. Acad. Sci. Paris, Ser. I **339** (2004) 667-672.

[3] Z. Luo, J. Cheng, L. M. Navon, X. Yang, *Mixed Finite Element Formulation and Error Estimates Based On Proper Orthogonal Decomposition For The Nonstationary Navier-Stokes Equations*, Siam J. Numerical Analysis **47** (2008) 1-19.

[4] J. Benk, M. Ulbrich, M. Mehl, *The Nitsche Method of the Navier-Stokes Equations for Immersed and Moving Boundaries*, ICCFD7-1301 (2012).

[5] S. W. Funke, P. E. Farrell, *A framework for automated PDE-constrained optimisation*, arXiv:1302.3894, 2013.

[6] A. Wächter, L. T. Biegler, *On the Implementation of a Primal-Dual Interior Point Filter Line Search Algorithm for Large-Scale Nonlinear Programming*, Mathematical Programming **106**(1) (2006) 25-57.

[7] A. Logg, K. A. Mardal, G. N. Wells, *Automated Solution of Differential Equations by the Finite Element Method*, Springer, 2012.

Book of abstracts of the 7th International Conference
on Advanced Computational Methods
in Engineering, ACOMEN 2017
18–22 September 2017.

Proper orthogonal decomposition-based model reduction of a synchronous machine

Mehrnaz Farzam Far[1], Floran Martin[1] and Anouar Belahcen[1]

[1] *Department of Electrical Engineering and Automation, Aalto University*

e-mails: mehrnaz.farzam.far@aalto.fi, floran.martin@aalto.fi, anouar.belahcen@aalto.fi

Abstract

The aim of this paper is to investigate on various methods of reducing the computational complexity, cost, and time for a finite element model of an electrical machine with a nonlinear magnetostatic field. A novel method is introduced in order to facilitate the evaluation of the nonlinear problem.

Key words: interpolation, magnetostatic field, model order reduction, permanent magnet synchronous machine

1 Introduction

Numerical methods, such as the finite element method, along with modern computers facilitate the accurate field computation of various electrical machines models. Nevertheless, when the model order is large, the computation becomes intensive in terms of computational time and data storage capacity. Proper orthogonal decomposition combined with the discrete empirical interpolation method (POD-DEIM) [1]-[3] is an efficient tool to reduce the computational complexity of the model while maintaining the accuracy in an acceptable range.

We propose orthogonal interpolation method to reduce the computational complexity of an electrical machine finite element model. This method interpolates the nonlinear solutions with the right-singular vectors of the snapshot matrix [4]. The right-singular vectors are generated by the singular value decomposition (SVD) while decomposing the snapshot matrix into the subset of orthogonal bases: the left-singular vectors U, the norm matrix Σ, and the right-singular vectors V^T.

Assuming the snapshot matrix to represent correctly the system, the discrete projection operator is determined with U and its most energetic norm are tracked with the norm matrix Σ. The product of these two matrices remains unchanged for any input variables within the range of the snapshot matrix. Although this property is fundamental to applied model order reduction, the prediction of the system output is only dependent on the right-singular vectors in V. Hence, each right-singular vector corresponds to a specific input set within the snapshot matrix. In this orthogonal basis, any new input set can be expressed as a vector sum of orthogonal vectors. Each component of this new vector can be independently interpolated with the corresponding components of the right-singular vectors as a function of the original input quantities (current, rotor angle...).

2 Numerical application

The orthogonal interpolation method is applied to the finite element model of an interior permanent magnet machine with 1379 nodes. The snapshot matrix, of size 1379×5, is generated with a greedy algorithm [5], where only the current source is of interest. The accuracy of this method is proven by comparing its flux density distribution to the finite element model reference and POD-DEIM reduced model (Fig. 1).

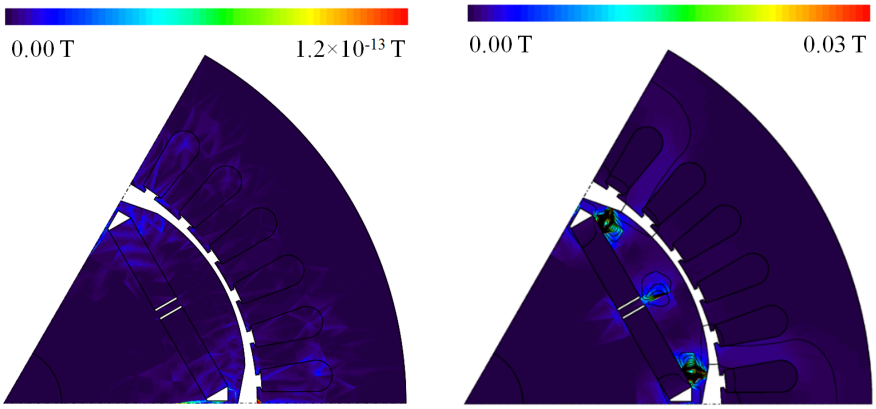

Figure 1: Different between the flux density distributions obtained from the finite element reference model and (a) orthogonal interpolation method of the vector potential (b) POD-DEIM (note the range difference). Shading: flux density distribution.

The implementation of orthogonal interpolation method and POD-DEIM to a rotating machine along with the accuracy and computational time comparison of these methods will be presented in the full paper.

References

[1] S. Chaturantabut, D. C. Sorensen, *Nonlinear model reduction via discrete empirical interpolation*, SIAM SCSC **32** (2010) 2737–2764.

[2] T. Henneron and S. Clenet, *Model-Order Reduction of Multiple-Input Non-Linear Systems Based on POD and DEI Methods*, IEEE. Trans. Mag. **51** (2015) 1–4.

[3] T. Henneron and S. Clenet, *Application of the PGD and DEIM to solve a 3-D non-linear magnetostatic problem coupled with the circuit equations*, IEEE Trans. Mag. **52** (2016) 1–4.

[4] L. Sirovich, *Turbulence and the dynamics of coherent structures. Part I: Coherent structures*, Quart. Appl. Math. **45** (1987) 561–571.

[5] S. Clenet, T. Henneron, N. Ida, *Reduction of a finite element parametric model using adaptive POD methods-Application to uncertainty quanti cation*, IEEE Trans. Mag. **52** (2015) 1–4.

Book of abstracts of the 7th International Conference
on Advanced Computational Methods
in Engineering, ACOMEN 2017
18–22 September 2017.

A reduced order accelerator for time-dependent reactor physics calculations

Carlo Fiorina[1] and Andreas Pautz[2]

[1] *EPFL, LRS, 1015 Lausanne, Switzerland*

[2] *PSI, LRS, 5232 Villigen, Switzerland*

e-mails: carlo.fiorina@epfl.ch, andreas.pautz@psi.ch

Abstract

This document describes an acceleration technique that proved to be effective for the segregated solution of the systems of partial differential equations that typically originate from an approximate deterministic solution of the Boltzmann equation describing the transport of neutrons. The technique is based on the projection of the problem on a limited number of basis functions.

1 Introduction

The space, energy and time dependency of neutron population in nuclear reactors is governed by a Boltzmann transport equation[1]. Such equation cannot normally be solved directly based on deterministic methods. Approximations are then introduced for treating the angular distribution of neutrons[1]. The most typical approximations are an expansion in spherical harmonics, a discretization of the solid angle (discrete ordinate methods), or the assumption of an isotropic behavior of neutrons (diffusion approximation). In addition, the energy dependency of neutrons is treated by grouping them into different energy groups (multi-group approach). These approximations can dramatically increase the number of equations, for which a coupled solution is normally obtained through Picard iteration. Several tens or hundreds of iterations are normally required at each time step, which calls for the use of accelerators. Predictors and other traditional acceleration techniques (e.g., Aitken) can effectively be used to limit the number of iterations[2]. In this work, an acceleration technique is proposed based on the projection of the problem on a limited number of orthogonal basis functions and on the solution of the obtained reduced-order model [3].

2 Description of the problem

The angular and energy approximations of the neutron transport equation lead to a system of linear partial differential equations that can be discretized using different techniques to obtain a set of matrix equations of the form:

$$A_{i,p}\phi_{i,p}\Big|_n = b_{i,p}\left(\phi_{j,q}\Big|_n, \phi_{i,p}\Big|_{n-1}\right) \qquad j \neq i,\ q \neq p \tag{1}$$

At each time step n, one equation of the form of Eq. 1 will be obtained for each energy group i, and for each direction or spherical harmonic p.

3 A reduced order acceleration

The proposed acceleration technique is based on the Galerkin projection of the Eqs. 1 on bases of orthogonal functions (one basis for equation). Such bases are gradually built during the Picard iterations at each time step. In particular:

1. A set of full-order solutions $\phi_{i,p}\Big|_0$ is obtained at the first iteration in the time step and used as a set of first basis functions $\Phi_{i,p,0}$, one for each energy i and moment/direction p ;

2. At each successive iteration, each of the Eqs. 1 is Galerkin projected on the corresponding available basis $\Phi_{i,p,k}$ (initially made of one single function $\Phi_{i,p,0}$ for each of the Eqs. 1), and the obtained reduced problem is solved;

3. After each reduced-order iteration, the initial residuals of the full-order problem are evaluated and compared to those of previous iterations. When/if the residuals stabilize (which means that the available bases are unsuited to achieve a higher level of accuracy), a new set of full-order solutions is computed. These solutions are then orthogonalized with respect to the available k basis functions $\Phi_{i,p,k}$ using a Gram-Schmidt procedure in order to obtain the new basis functions $\Phi_{i,p,k+1}$. A proper orthogonal decomposition can alternatively be selected for recalculating a basis based on the available basis functions and on the new snapshots.

4. The iterations are continued and, if necessary, the orthogonal basis expanded, till the required level of accuracy is achieved for the time step.

In this algorithm the full matrices $A_{i,p}$ are built only once for each time step and their projections over the respective bases are evaluated only when new functions are added to the bases. For most iterations, only the reduced-order source terms and the resulting reduced problems are solved for. This allows for extremely fast iterations.

Testing of such procedure for two representative cases [2] has shown a speed-up in the range of 30% to 50%, comparable or better compared to a standard Aitken acceleration.

The proposed algorithm can also be extended by: 1) storing the obtained basis functions for re-use in the following time steps, which can be highly effective in case small changes in shape are expected; 2) storing the obtained basis functions for re-use in other simulations, which can be of interest for repeated similar calculations; 3) gradually optimizing (training) the set of obtained basis functions for covering a set of most frequent simulations. Although these extensions proved to be extremely effective in some cases, their performance turned out to be extremely problem (and user) dependent, which make them unsuited for inclusion in production codes. Further investigation will be carried out in the future on this subject.

References

[1] A. Hébert, *Applied Reactor Physics*, Presses inter Polytechnique, 2009.

[2] C. Fiorina et al., *Development and verification of the neutron diffusion solver for the GeN-Foam multi-physics platform*, Ann. Nucl. En. **96** (2016) 212–222.

[3] A. Manzoni, A. Quarteroni, G. Rozza, , *Computational Reduction for Parametrized PDEs: Strategies and Applications*, Milan Journal of Mathematics **80** (2016) 283–309.

Book of abstracts of the 7th International Conference on Advanced Computational Methods in Engineering, ACOMEN 2017 18–22 September 2017.

Off-line/On-line approach based on POD and (D)EIM for the Model Order Reduction of Low frequency Electromagnetic devices based

T. Henneron[1], L. Montier[1,2], A. Pierquin[1] and S. Clénet[1]

[1] *Univ. Lille, Centrale Lille, Arts et Metiers ParisTech, HEI, EA 2697 - L2EP, F-59000 Lille, France*

[2] *EDF R&D, THEMIS, 1 Avenue du Général de Gaulle, 92140 Clamart, France*

e-mails: thomas.henneron@univ-lille1.fr, laurent.montier@ensam.eu, antoine.pierquin@univ-lille1.fr, stephane.clenet@lille.ensam.fr

Abstract

The Proper Orthogonal Decomposition (POD) combined with the (Discrete) Empirical Interpolation Method ((D)EIM) can be used to build a reduced model and speed up the solution of a Finite Element model. In order to define a reduced model effective on the full operating range of an electrical device, an Offline/Online approach based on the expertise of the engineer is proposed.

Key words: (Discrete) Empirical Interpolation Method, Low frequency electromagnetic problem, Proper Orthogonal Decomposition, Offline/Online approach.

1 Introduction

To model low frequency electromagnetic devices, the Finite Element (FE) method combined with a time-stepping scheme is widely used to discretize Maxwell's equations. Then, with a fine mesh and a small time step, the computational time of the large-scale system obtained from the discretization of the Non-Linear Partial Differential Equations can be prohibitive. To reduce the time of numerical simulations, Model Order Reduction methods have been developed in the literature. In the case of non-linear problems, the Proper Orthogonal Decomposition [1] is combined with the (Discrete) Empirical Interpolation Method to keep an effective reduced model with a good speed up [2]. These both approaches are based on the snapshot technique which consists on solving the FE model for a set of given parameters. The efficiency of a reduced model depends on the choice of the snapshots. In order to build a reduced model effective on the full operating range of an electrical device, several methods can be used. We propose an approach based on the expertise of the engineer. In electrical engineering, typical tests are used to determine the parameters of equivalent circuit models which describe the behavior of the device on the whole operating range. Then, the idea is to consider the same approach to construct a reduced model. During the offline step, the snapshots extracted from classical tests made usually by engineers to characterize an electromagnetic device are concatenated. Then, a reduced basis is deduced in order to approximate the solution on the full operating range. On the online step, the reduced model can be used to study an

electrical device coupled with an external electrical circuit for different operating points. The offline/online approach has been applied for several low frequency electromagnetic devices like single and three phase transformers [3] and synchronous machine [4].

2 Offline/Online approach based on POD-(D)EIM model

By applying the POD-(D)EIM approach on a nonlinear Finite Element electromagnetic model, the general form of the differential algebraic equations to solve can be written:

$$M_r X_r(t) + K_r \frac{dX_r(t}{dt} = F_r(t) + \Psi^t G_{EIM}(\Psi X_r(t)). \quad (1)$$

Where M_r and K_r are square matrices of the reduced model and $F_r(t)$ is the source vector. The size of these matrices and vector is much smaller than the size of the full FE model. $X_r(t)$ is the unknown vector of the reduced basis such as $X_(t) = \Psi X_r(t)$ with $X(t)$ the unknown vector of the full FE model. To determine Ψ, the POD associated with the snapshot technique is used. The nonlinearities of the full model are approximated in the vector G_{EIM} by the (Discrete) Empirical Interpolation Method. This approach is based on the computation of a small number of nonlinear entries and on the interpolation of other terms. To build a reduced model effective on the full operating range of an electrical device, an offline/online approach is used. On the Offline step, extrem operating points are simulated in order to extract the solution and nonlinear vectors. From these snapshots, the reduced model is build in order to study different operating points. For a three phase transformer, we consider the device at no load and in short circuit on the offline step. Then, the reduced model of the transformer is built to study the evolution of the currents for different load. The speed up is about 16.

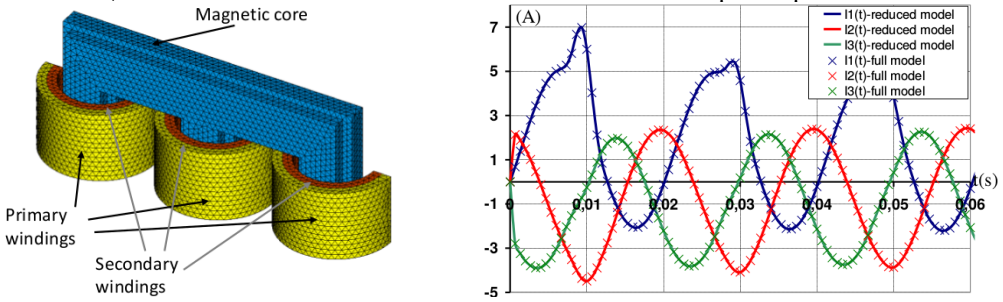

(a) geometry and mesh

(b) Primary currents with resistive load

Figure 1: Three phase transformer

References

[1] L. Sirovich, *Turbulence and the dynamics of coherent structures*, Q. Appl. Math. vol. XLV(3), (1987) 561–590.

[2] S. Chaturantabut and D. C. Sorensen, *Nonlinear Model Reduction via Discrete Empirical Interpolation*, SIAM J. Sci. Comput. vol. 32(5), (2010) 2737–2764.

[3] T. Henneron and S. Clénet, *Model-Order Reduction of Multiple-Input Non-Linear Systems Based on POD and DEI Methods*, IEEE Trans. Mag. vol. 51(3), (2015).

[4] L. Montier, T. Henneron, S. Clenet and B. Goursaud, *Transient simulation of an electrical rotating machine achieved through model order reduction*, Advanced Modeling and Simulation in Eng. Sci. vol. 3(10), (2016).

Book of abstracts of the 7th International Conference
on Advanced Computational Methods
in Engineering, ACOMEN 2017
18–22 September 2017.

Adaptive reduced-order modeling of thermo-mechanical systems

David Sachs[1], **Shobhit Jain**[1] **and Paolo Tiso**[1]

[1] *Institute for Mechanical Systems, ETH Zürich, Leonhardstrasse 21, 8092 Zürich, Switzerland*

e-mails: dsachs@student.ethz.ch, shjain@ethz.ch, ptiso@ethz.ch

Abstract

The thermal dynamics in thermo-mechanical systems exhibits a much slower time scale compared to the structural dynamics. We propose a method to reduce thermo-mechanical structural models with a slowly varying temperature distribution. The reduction bases corresponding to a set a-priori-determined static temperature configurations are interpolated over a non-compact Stiefel manifold [1] to obtain a basis for instantaneous temperature distribution. The method of multiple scales [2] is successively used to construct a reduced-order model which adapts according to the instantaneous temperature distribution of the structure, facilitating an efficient reduction in the number of unknowns.

Key words: Basis interpolation, Method of multiple scales, Model order reduction, Thermo-mechanical systems

References

[1] D. Amsallem, C. Farhat, Interpolation Method for Adapting Reduced-Order Models and Application to Aeroelasticity *AIAA journal*, (2008) 46(7): 1803-1813. DOI: 10.2514/1.35374

[2] J. Kevorkian, J. D. Cole, Multiple Scale and Singular Perturbation Methods *Springer*, New York(1996), Vol. 114, ed: JE. Marsden L. Sirovich F. John. ISBN: 978-1-4612-8452-9

Book of abstracts of the 7th International Conference on Advanced Computational Methods in Engineering, ACOMEN 2017 18–22 September 2017.

Model Order Reduction for Pattern Formation in Reaction-Diffusion Systems

Bülent Karasözen[1], Murat Uzunca[2], Tuğba Küçükseyhan[3] and Gülden Mülayim[4]

[1] *Institute of Applied Mathematics & Department of Mathematics, Middle East Technical University, Ankara, Turkey*

[2] *Department of Industrial Engineering, University of Turkish Aeronautical Association, Ankara, Turkey*

[3] *Department of Mathematics, Balıkesir University, Turkey*

[4] *Department of Mathematics, Adıyaman University, Turkey*

e-mails: bulent@metu.edu.tr, muzunca@thk.edu.tr, kucukseyhan@balikesir.edu.tr, gmulayim@adiyaman.edu.tr

Abstract

We compare three reduced order modelling (ROM) techniques: the proper orthogonal decomposition (POD), discrete empirical interpolation (DEIM) [2], and dynamical mode decomposition (DMD) [1] to reaction diffusion equations in biology. The formation of patterns in reaction-diffusion equations require highly accurate solutions in space and time and therefore require large computational time to reach the steady states. The three reduced order methods are applied to the diffusive FitzHugh-Nagumo equation [3] and the Brusselator model with cross diffusion [4]. DMD is an equation-free, data driven method which extracts dynamically relevant information content without explicitly knowing the dynamical operator. We use DMD as an alternative method to DEIM in order to approximate the nonlinear reaction terms. Application of the POD-DMD Galerkin projection gives rise to a linear system of equations. The high fidelity full order solutions (FOMs) are obtained by the discontinuous Galerkin discretization in space and semi-implicit Euler method in time. We compare the accuracy and CPU times of three reduced order model (ROM) solutions with the ones for FOM solutions. Numerical results show that POD is the most accurate whereas POD-DMD is the fastest.

Key words: Cross diffusion, FitzHugh-Nagumo model, pattern formation, reduced order modelling, Turing-Hopf bifurcation

1 Numeriacl results

The diffusive FitzHugh-Nagumo equation (FHNE) [3]

$$\begin{aligned} u_t &= d_1\Delta u - u^3 - u - v + \kappa \\ v_t &= d_2\Delta v - v + u \end{aligned}$$

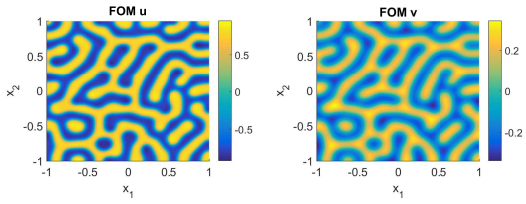

Figure 1: Labyrinth-like patterns for the FOM solutions

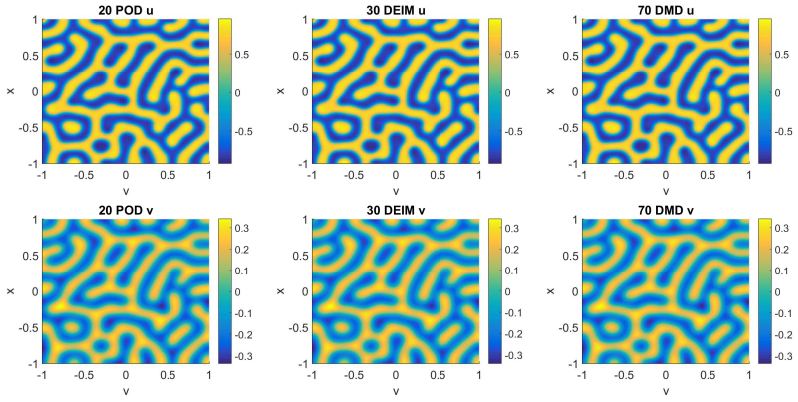

Figure 2: ROM solutions

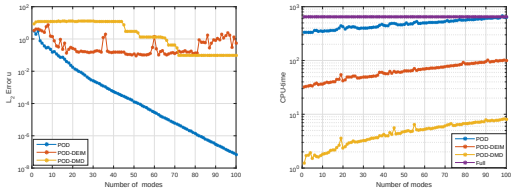

Figure 3: Relative errors between FOM and ROM solutions u (left), and CPU times with the same increasing number of POD, DEIM and DMD basis functions.

References

[1] S. Alla and J. N. Kutz *Nonlinear model reduction via dynamic mode decomposition* to appear in SIAM Journal on Scientific Computing (2016)

[2] S. Chaturantabut and D. C. Sorensen *Nonlinear model reduction via discrete empirical interpolation* SIAM Journal on Scientific Computing, **32(5)** (2015) 2737–2764 DOI:10.1137/090766498

[3] B. Karasözen, T. Küçükseyhan, and M. Uzunca, *Structure preserving integration and model order reduction of skew-gradient reaction–diffusion systems*, Annals of Operations Research (2015) 1-28 DOI: 10.1007/s10479-015-2063-6

[4] L. Zhigui, R. Ruiz-Baier, C. Tian *Finite volume element approximation of an inhomogeneous Brusselator model with cross-diffusion* Journal of Computational Physics, **256** (2014) 806-823 DOI: 10.1016/j.jcp.2013.09.009

Book of abstracts of the 7th International Conference on Advanced Computational Methods in Engineering, ACOMEN 2017 18–22 September 2017.

Approximation of Functions in Unbounded Domain by High Order Mapped Basis Sets using Double Exponential Transformation

Faisal Mumtaz[1] **and Fahhad H. Alharbi**[1,2]

[1] *College of Science and Engineering, Hamad Bin Khalifa University, Doha, Qatar*

[2] *Qatar Environment & Energy Research Institute, Qatar Foundation, Doha, Qatar*

e-mails: faimumtaz@hbku.edu.qa, falharbi@hbku.org.qa

Abstract

In this paper, an efficient approach to approximate functions in unbounded domain is presented. The method is based on double exponential domain transformation within spectral methods. The unbounded domain is mapped to bounded domain (0,1) using double exponential (DE) transformation. The transformation maintains the orthogonality which simplifies the calculations and increases computational efficiency. Sine series is chosen as the basis set to further improve the computational efficiency. Different functions with wide range of decay rates are considered for approximation. The results and the analyses show that the mapped sine series using DE transformation can be an efficient high-order tool to handle challenging physical problems on unbounded domains.

Key words: double exponential transformation, unbounded domain, spectral method

1 Introduction

Many phenomena occurring in the nature decay smoothly with increasing distance from some center. The physical domain of such problems extends towards infinities [1]. To tackle such problems numerically, three approaches have been used generally, namely domain truncation, using functions which are intrinsic to unbounded domain and domain mapping [1]. In domain truncation, the unbounded domain is chopped to convert it to a bounded domain. However, this introduces a truncation error. The second approach, which involves the use of functions which extend to infinites, fails to cover a wide range of decay rates. The third approach which is also the focus of this paper involves the domain mapping. This involves transforming the unbounded domain into bounded one using some coordinate transformation [1, 2].

It this work, we exploit the application of DE transformation for the efficient approximation of functions in unbounded domain. The DE transformation is given by:

$$x(u) = \sinh^{-1}(\tanh^{-1}(2u - 1)) \tag{1}$$

where $u \in (0, 1)$ and $x \in (-\infty, \infty)$. This is a particular case of mapping, where the unbounded domain is mapped to (0,1). The unbounded domain can be mapped to any bounded domain

(a,b) [3]. The choice of the domain (0,1) enables the use of simple basis set like sine series, which makes the analytical integrations possible and increases the computational efficiency. Furthermore, in this work, we have proposed a mapped basis set which maintains the orthogonality in both real and computational space. Maintaining orthogonality simplifies the calculations significantly, and hence increases the computational efficiency.

The proposed method is implemented to approximate different decaying functions with wide range of decay rates. In the analyses, we compare the proposed method with the globally converging Hermite polynomials. The results show that the proposed method is able to approximate a wide range of decay rates efficiently and accurately.

2 Proposed Method

If $F(x)$ is the function to be approximated, We propose a mapped basis set of the following form:

$$F(x) \approx \sum_{k=0}^{N} a_k \sin(k\pi u(x))\mu(u(x)) \tag{2}$$

where

$$\begin{aligned} a_k &= \int_{-\infty}^{\infty} F(x)P_k(u(x))\mu(u(x))dx \\ &= \frac{1}{2}\int_0^1 \frac{\sin(k\pi u)F(x(u))}{\mu(u)}du \end{aligned}, \tag{3}$$

and $\mu(u)$ is the auxiliary function to maintain the orthogonality and it follows directly from $x(u)$ where

$$\mu(u) = \sqrt{\frac{2}{\frac{dx}{du}}} \tag{4}$$

For the analysis of the results, we assess the approximation error vs. the number of basis used. We also analyze the range of decay rates that can be approximated to an accuracy for a fixed number of basis used. All the results are compared with the Hermite approximation. The results show that the DE transformation is efficient, accurate and outperforms Hermite approximation in all the cases.

Acknowledgements

This work is supported by Hamad Bin Khalifa University, Doha, Qatar.

References

[1] Jie Shen and Li-Lian Wang. Some recent advances on spectral methods for unbounded domains. *J. Commun. Comput. Phys*, 5:195–241, 2009.

[2] Raka Jovanovic, Sabre Kais, and Fahhad H Alharbi. Efficient method for localised functions using domain transformation and fourier sine series. *Molecular Physics*, 112(5-6):762–769, 2014.

[3] Masatake Mori. Discovery of the double exponential transformation and its developments. *Publications of the Research Institute for Mathematical Sciences*, 41(4):897–935, 2005.

Book of abstracts of the 7th International Conference on Advanced Computational Methods in Engineering, ACOMEN 2017
18–22 September 2017.

Multirate partial differential equations for the solution of field-circuit coupled problems

Andreas Pels[1], Johan Gyselinck[2], Ruth V. Sabariego[3] and Sebastian Schöps[1]

[1] *Graduate School of Computational Engineering and Institut für Theorie Elektromagnetischer Felder, Technische Universität Darmstadt, Germany*

[2] *BEAMS Department, Université libre de Bruxelles, Belgium*

[3] *Department of Electrical Engineering, EnergyVille, KU Leuven, Belgium*

e-mails: pels@gsc.tu-darmstadt.de, johan.gyselinck@ulb.ac.be, ruth.sabariego@esat.kuleuven.be, schoeps@gsc.tu-darmstadt.de

Abstract

Multirate partial differential equations (MPDEs) are a relatively new concept to deal with multirate phenomena. This abstract heads for the simulation of a low-frequency energy application with pulsed excitation, namely a buck converter, using MPDEs. A linear field-circuit coupled problem described in a single equation system is considered. The differential algebraic equations are rewritten as MPDEs and efficiently solved by a Galerkin ansatz and time discretization.

Key words: Multirate partial differential equations, Energy applications

1 Multirate formulation and solution

Consider the example of a simplified buck converter as in [2]. Its solution consists of fast periodically varying ripples and a slowly varying envelope as depicted in Fig. 1. This makes conventional time discretization inefficient as many steps are necessary to properly resolve the solution. The model of the buck converter consists of a circuit part and a finite element model of the coil which are strongly coupled, i.e., described in a single system of differential algebraic equations (DAEs) with dimension 15791 [3]. The DAEs with matrices $\mathbf{A}$ and $\mathbf{B}$ are equivalently rewritten as multirate partial differential equations (MPDEs) [1] by splitting the time into two time scales of different rate t_1 and t_2

$$\mathbf{A}\left(\frac{\partial \widehat{\mathbf{x}}}{\partial t_1}+\frac{\partial \widehat{\mathbf{x}}}{\partial t_2}\right)+\mathbf{B}\,\widehat{\mathbf{x}}(t_1,t_2)=\widehat{\mathbf{c}}(t_1,t_2)\,. \tag{1}$$

If $\widehat{\mathbf{c}}(t,t)=\mathbf{c}(t)$ is satisfied, the solution of the DAEs and MPDEs relate by $\mathbf{x}(t)=\widehat{\mathbf{x}}(t,t)$, where $\mathbf{c}(t)$ and $\mathbf{x}(t)$ are the excitation and solution of the DAEs, respectively. To solve the MPDEs, the solution is expanded into periodic basis functions $p_k(\tau)$ and coefficients $w_{j,k}(t_1)$

$$\widehat{x}_j(t_1,t_2)=\sum_{k=0}^{N_\mathrm{p}} p_k(\tau)w_{j,k}(t_1) \text{ with } \tau=\frac{t_2}{T_\mathrm{s}} \bmod 1. \tag{2}$$

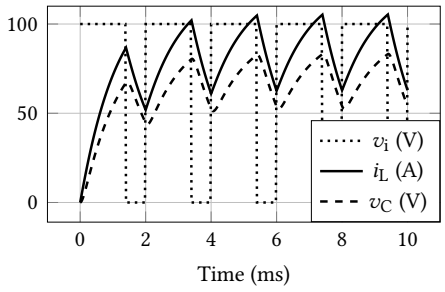

Figure 1: Solution of the simplified buck converter at $f_s = \frac{1}{T_s} = 500\,\text{Hz}$.

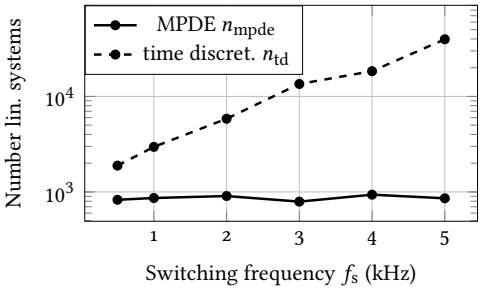

Figure 2: Comparison of number of solved equation systems versus switching frequency.

The time scale t_2 is associated with the fast periodically varying ripples, the time scale t_1 with the slowly varying envelope. Applying a Galerkin ansatz with respect to t_2, the MPDEs (1) reduce to DAEs in t_1 whose unknowns are the coefficients $w_{j,k}(t_1)$. These DAEs exhibit a much slower dynamic than the original ones as the fast periodically varying ripples are taken into account by the Galerkin ansatz. Therefore less time steps are needed for the solution. A drawback is the larger equation systems. As basis $p_k(\tau)$, the problem specific pulse width modulation (PWM) basis functions as introduced by Gyselinck et al. [2] are used.

2 Numerical results

The relative discrete ℓ^2-error of the MPDE solution towards a reference solution is calculated. The reference solution is obtained by conventional time discretization with fine rel./abs. tolerance of 10^{-6}. The simulation time interval is fixed to $t \in [0, 10]$ ms. For the MPDE approach, the number of basis functions and rel./abs. tolerance for time discretization are $N_p = 2$ and $tol = 10^{-2}$, respectively. Conventional time discretization (backward euler) is applied to the original DAE such that the same ℓ^2-error compared to the reference solution is obtained. The number of solved linear equation systems (n_{td} for conventional time discretization, n_{mpde} for MPDE approach) are compared, see Fig. 2. Increasing f_s, more ripples have to be resolved which leads to higher n_{td} in conventional time discretization while n_{mpde} stays almost constant. However, the actual efficiency of the MPDE approach depends on the efficiency of the linear solver and the switching frequency f_s.

Acknowledgements

This work is supported by the 'Excellence Initiative' of German Federal and State Governments and the Graduate School CE at TU Darmstadt.

References

[1] H. G. Brachtendorf, G. Welsch, R. Laur, A. Bunse-Gerstner, *Numerical steady state analysis of electronic circuits driven by multi-tone signals*, Electr. Eng., **79**(2), pp. 103–112, 1996.

[2] J. Gyselinck, C. Martis, R. V. Sabariego, *Using Dedicated Time-Domain Basis Functions for the Simulation of Pulse-Width-Modulation Controlled Devices – Application to the Steady-State Regime of a Buck Converter*, Electromotion 2013.

[3] I. A. Tsukerman, A. Konrad, J. D. Lavers, *A Method for Circuit Connections in Time-Dependent Eddy Current Problems*, IEEE Trans. Magn., **28**(2), pp. 1299–1302, 1992.

Book of abstracts of the 7th International Conference
on Advanced Computational Methods
in Engineering, ACOMEN 2017
18–22 September 2017.

Using the Proper Generalized Decomposition to solve Maxwell equations in thin laminated composites

Hermine Tertrais[1], Ruben Ibanez[2], Anais Barasinski[1] and Francisco Chinesta[2]

[1] *GeM, UMR CNRS, Centrale Nantes*

[2] *High Performance Computing Institute, Centrale Nantes*

e-mails: hermine.tertrais@ec-nantes.fr, ruben.ibanez-pinillo@ec-nantes.fr, anais.barasinski@ec-nantes.fr, francisco.chinesta@ec-nantes.fr

Abstract

Microwave heating relies on internal thermal sources which make it a good candidate for an alternate composite process. In this paper, an electromagnetic solver is proposed. Solving the problem in a laminated composite material requires a high degree of discretization in the thickness direction which is made possible by introducing the in-plane-out-of-plane decomposition approach using the Proper Generalized Decomposition (PGD).

Key words: Composite, microwave heating, Proper Generalized Decomposition

1 Introduction

To reduce long production cylce time of composite material, the microwave (MW) technology is considered by industrials [1] as volumetric heating saves time and energy. Today, the main drawback is that the physics involved during the process are not entirely understood and controlled. The challenge when simulating the propagation of the MW field in a laminated composite material concerns the need for a high-resolution in the thickness. In such materials, the in-plane dimensions are order of magnitude higher than the thickness one (typical aspect of ratio of tens of thousands). The use of the in-plane-out-of-plane separated representation within the PGD framework is an appealing and valuable route for solving 3D models while having a computational complexity of standard 2D models [2].

2 Electromagnetic Problem

In order to proceed with the in-plane-out-of-plane separated representation, we use a standard nodal formulation that is regularized in order to avoid spurious solutions [3]. This formulation for the electric field (1) is derived from the Maxwell equations with the Dirichlet boundary conditions associated on the whole domain boundary:

$$\nabla \times (\frac{1}{\mu} \nabla \times \mathbf{E}) - \overline{\epsilon^*}(\frac{1}{\mu\overline{\epsilon^*}\epsilon^*} \nabla \cdot (\epsilon^* \mathbf{E})) - \omega^2 \epsilon^* \mathbf{E} = 0 \text{ with } \mathbf{n} \times \mathbf{E} = \mathbf{E}^t, \quad (1)$$

where μ, ϵ and σ are the permeability, the permittivity and the conductivity of the material and $\mathbf{E}^t$ is the prescribed electric field assumed known. The weak formulation associated is solved using the in-plane-out-of-plane separated representation within the PGD framework which allows writing the electric field in the 3D separated form:

$$\mathbf{E}(x,y,z) \approx \sum_{i=1}^{N} \mathbf{X}_i(x,y) \circ \mathbf{Z}_i(z),$$

where the $\circ$ denotes the Hadamard rpoduct. Thus, the 3D solution is obtained from a set of N 2D and 1D problems. Therefore, we can reach extremely refined levels of resolution along the thickness direction (that has a characteristic size of few millimeters) without having any impact on the in-plane representation, and then in the computational efficiency [4].

3 Numerical Results

We consider a composite part placed in a wave-transparent ceramic mold (figure 1 (a)). The composite material is made of 20 unidirectionnal layers. Material properties of the mold are $\sigma = 0.008$, $\epsilon = 4\epsilon_0$, $\mu = \mu_0$,ϵ_0 and μ_0 being the permeability and permittivity of the vacuum and the 0-unidirectional layer is characterised by tensors which diagonales are $\sigma = [100 - 1 - 1]S/m$, $\epsilon = [90 - 10 - 10]\epsilon_0$, $\mu = \mu_0$. The dirichlet boundary conditions applied are $E_x = E_y = cos(2\pi nx)$ and $E_z = cos(2\pi ny)$ with $n = 10$.The mesh is composed of 1000 Q4 elements in the plane and 980 1D linear elements in the thickness. Figure 1 (right) highlights the amplitude decrease of the electric field when it propagates through the composite part.

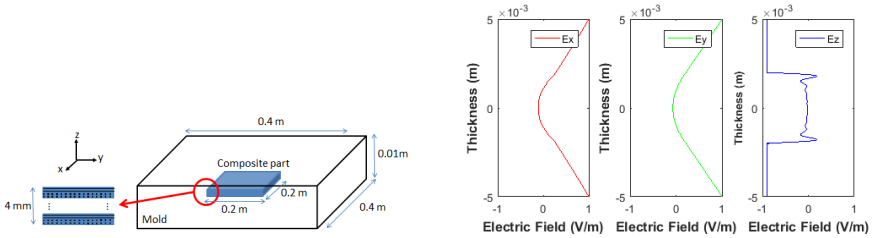

(a) Test case geometry

(b) Electric field amplitude through the thickness along $(x_{\text{middle}}, y_{\text{middle}}, z)$

Figure 1: Results.

References

[1] G. Hug, *Ph.D Thesis*, Arts et Metiers ParisTech, 2005.

[2] B. Bognet et al, *Advanced simulation of models defined in plate geometries: 3D solutions with 2D computational complexity*, Comput Methods Appl Mech Eng **201** (2012) 1–12.

[3] R. Otin, *Regularized Maxwell Equations and Nodal Finite Elements for Electromagnetic Field Computations*, Electromagnetics **30** (2010) 190–204.

[4] F.Chinesta et al, *Proper Generalized Decomposition for Advanced Numerical Simulation: A primer*, Springer, 2013.

MS 5 3rd Symposium on modelling of biological cells, fluid flow and microfluidics

Organiser: Ivan Cimrák, Iveta Jančigová

Description: The rapidly evolving area of microarrays, or lab-on-chips, offers an enormous increase in efficiency of laboratory experiments. The miniaturization of the experiments with resolution of several micrometers allows for better control of the experiments. These microarrays have numerous advantages such as faster analysis and response times of the system, massive parallelization due to compactness, lower fabrication costs. For the design of such microarrays, computational experiments can be effectively used. This symposium is devoted to topics that are related to the modelling of processes inside microfluidic channels. We especially welcome contributions, which address the models of fluid-structure interactions and those which cover processes on micro-scales where tracking of individual cells is possible. This approach allows for understanding of behaviour of individual cells and for monitoring the cells under exposure to modulated flow. We also welcome other contributions that concern blood flow modelling, modelling other cells in fluid, modelling microfluidic devices, computational methods for cell tracking, characterisation and identification and other related topics.

Book of abstracts of the 7th International Conference
on Advanced Computational Methods
in Engineering, ACOMEN 2017
18–22 September 2017.

Numerical Computation of the Immunotherapy Model Involving the Cervical Cancer Cells, Effector Cells, and IL-2 Compounds with Reaction-Diffusion

Fajar Adi-Kusumo[1], Sulasri Suddin[1], Lina Aryati[1] and Rara Sandhy Winanda[2]

[1] *Department of Mathematics, Faculty of Mathematics and Natural Sciences, Universitas Gadjah Mada, Yogyakarta, INDONESIA*

[2] *Department of Mathematics, Faculty of Mathematics and Natural Sciences, Ahmad Dahlan University, INDONESIA*

e-mails: f_adikusumo@ugm.ac.id, sulasri_suddin@yahoo.com, lina@ugm.ac.id, rarawinanda89@gmail.com

Abstract

Immunotherapy is one of the future treatment that can be used in most cases of cancer. The cervical cancer is one of the malignant cancer that triggers by a virus, which is known as *Human Papilloma Virus (HPV)*. The virus prevents some genes, e.g., p53 and pRb, which control the cell division and apoptosis to be activated. In this paper we consider the interactions between the cancer cells population, the effector cells population that is a part of the immune system, and IL-2 compounds which is a cytokine that can be used to stimulate the effector cells. The interactions between the cancer cells, effector cells, and IL-2 compounds do not only depend on the time but also the position in the cervix. Therefore, we add the reaction-diffusion term in our system to represent those situations. In this paper we consider the numerical computation of such system that show the effects of the immunotherapy on the tissues due to the time and the position. In this case we also consider the equilibrium condition that shows the long time behavior of the system.

Key words: cervical cancer, numerical computation, limit cycle, reaction-diffusion

Introduction and The Problem Formulation

Cervical cancer is one of the most dangerous disease which is mostly caused by the *Human Papilloma Virus (HPV)*. The virus is a family of the retrovirus DNA which consist some protein which has specific role in the infection and replication, [5]. The virus infection triggers the defect of the tissues called a lesion and plays an important role on the metastases of the diseases.

The mathematical model that show the dynamics of the cervical cancer on the tissues which shows the changes of the metastases behavior and the boundary of the pre-cancerous cells population, was studied in [1, 2]. In sub-cellular level, the cancer infections are mainly

caused by the mutation of the genes which is represented by the shifting behavior of the enzymes. There are some enzymes that can be used as the indicators of the mutation, e.g. p53, pRb, EBNA1, etc, see [3]. For the cervical cancer case, the HPV inactivates the enzymes p53 and pRb that increase the immortality and the proliferation of the cells.

The immunotherapy model of the cervical cancer that involves the interaction between the cancer cells, the effector cells and the IL-2 compound including the local and the global stability of the equilibria has been done in [7, 8]. In [4], the authors consider the periodic stimulation of the effector cells by the IL-2 compounds by adding a periodic perturbation in the system.

In cervical cancer case, the growth direction of the effector cells, the cancer cells, and the IL-2 compounds depend on the weakest parts of the cells in the tissue. Following the results in [6], we extend the system on [7, 8, 4] by adding the reaction-diffusion terms on each components.

Our system is a three dimensional system of partial differential equation. We separate the cells populations into three parts, those are the Cancer cells (T), the Effector cells (E) as parts of the immune system, and the IL-2 compounds (I_L) which is cytokines that stimulate the Effector cells. All of them are the functions with respect to the the time and the position. The immunotherapy in our system is represented by an external input on IL-2 compounds. We apply the numerical bifurcation analysis to study the existence and stability conditions of the equilibrium and the Runge-Kutta order 4 to determine the equilibria and the limit cycle of the system. The numerical simulation of the system is done by the PDEX5 toolbox of MATLAB.

References

[1] Noor-Asih, T. S., Adi-Kusumo, F., Aryati, L., Hardianti, M. S., The Metastasis Behavior in Cervical Cancer Model, *Far East Journal of Mathematical Sciences*, Vol 96 **(8)** (2015) 981-990.

[2] Asih, T. S., Lenhart, S., Wise, S., Aryati, L., Adi-Kusumo, F., Hardianti, M. S., Forde, J., The Dynamics of HPV Infection and Cervical Cancer Cells, *Bull Math Biol*, **78** (2016) 4-20

[3] Adi-Kusumo, F., Wiraya, A., Mathematical Modeling of the Cells Repair Regulations in Nasopharyngeal Carcinoma, *Mathematical Biosciences*, 277 (2016) 108-116

[4] Adi-Kusumo, F., Winanda, R. S., Bifurcation Analysis of the Cervical Cancer Cells, Effector cells, and IL-2 Compounds Interaction Model with Immunotherapy, *Far East Journal of Mathematical Sciences*, 99 (6), (2016) 869-883.

[5] Hakim, L., Biology dan Patogenesis Human Papillomavirus, *PKB New Perspective of Sexually Transmitted Problem*, 164-180, 2010.

[6] Ko, W., Inkyung, A., Stationary patterns and stability in a tumor- immune interaction model with immunotherapy, *J. Math. Anal. Appl.*, 383,(2011) pp. 307-329.

[7] Kirschner, D. and Panetta, J., Modelling Immunotherapy of Tumor Immune Interaction, *Journal of Mathematical Biology* **37**, (1998) 235-252.

[8] Kirschner, D. and Tsygvintsev, A., On the Global Dynamics of A Model for Tumor Immunotherapy, *Journal of Mathematical Biosciences and Engineering*, Vol 6 (3), (2009) 573-583.

Book of abstracts of the 7th International Conference
on Advanced Computational Methods
in Engineering, ACOMEN 2017
18–22 September 2017.

Relation between parameters of spring network model of red blood cell and membrane's bulk properties

Ivan Cimrák[1]

[1] *Department of Software Technologies, University of Žilina*

e-mails: ivan.cimrak@fri.uniza.sk

Abstract

In spring network models of red blood cells, the macroscopic elasticity of the membrane is determined by microscopic properties of individual components of the network. For example, the stiffness of individual springs forming triangular mesh influences the Young modulus of the modelled membrane. Recently, a new approach has been derived for area conservation modulus of a spring network model that is force-free and torque-free. We address this approach and derive the relation between network stiffness coefficients and continuum mechanical membrane properties, such as shear modulus and area compression modulus.

Key words: computational microfluidics, cell model, elasticity

1 Elasticity in spring network models

We consider a spring network model of red blood cell introduced in [1]. Model is based on a triangular mesh covering the surface of the cell. The surface is discretized with mesh points. The mechano-elastic properties of the membrane are represented with different types of bonds between neighboring mesh points generating repulsive or attractive forces. This way, the deformation of the object changes the relaxed distances between the mesh points and this induces forces acting against the change in the corresponding mesh points. These forces cause the mesh points to move in space and thus the temporal changes of the cell's shape are computed from the Newton's equations of motion given the deformation forces for each mesh point.

The definition of forces includes five different expressions mimicking the following elastic moduli of the membrane: stretching, bending, local area, global area and volume preservation. Concrete expressions can be found in [2]. In the original version of the local area modulus, forces in each mesh triangle ABC act in the direction towards its centroid T and have the same magnitude for each triangle vertex. This setting is however neither force-free nor torque-free.

Recently, in [3] the authors have adapted the expression for the local area modulus in order to preserve force-free and torque-free condition. For magnitude of force applied to vertex A of triangle ABC, they have suggested to use the following expression

$$F(A) = k_{al} \frac{|TA|}{|TA|^2 + |TB|^2 + |TC|^2} (S - S_0), \tag{1}$$

where k_{al} is the stiffness coefficient, S is the current area of the triangle and S_0 is the area of the triangle in a relaxed state.

2 Relation between model parameters and bulk properties

Experimental measurements performed on biological membranes provide their macroscopic properties such as shear modulus μ_0, Young modulus E, or area compression modulus K_A [4, 5]. In the case of simple spring networks where only linear stretching modulus is active, the relation between stretching stiffness coeficient k_s and bulk quantities is given by [6]

$$K_A = \sqrt{3}k_s/2, \qquad \mu_0 = \sqrt{3}k_s/4.$$

The previous results are valid for six-fold regular networks.

In the case of more complex networks, such relations are more complicated. In our work we consider linear stretching and local area modulus computed from (1) to be the only two elastic moduli. In that case we show that relations are

$$K_A = \sqrt{3}k_s/2 + k_{al}/2, \qquad \mu_0 = \sqrt{3}k_s/4.$$

Theoretical computations will be supported by computational simulations.

Acknowledgements

This work was supported by the Slovak Research and Development Agency under the contract No. APVV−15 − 0751.

References

[1] I. Cimrák, M. Gusenbauer, T. Schrefl, *Modelling and simulation of processes in microfluidic devices for biomedical applications*, Computers and Mathematics with Applications **64(3)** (2012) 278–288

[2] I. Cimrák, M. Gusenbauer, I. Jančigová, *An ESPResSo implementation of elastic objects immersed in a fluid*, Computer Physics Communications **185(3)** (2012) 900–907

[3] I. Jančigová, I. Cimrák, *Non-uniform force allocation for area preservation in spring network models*, International Journal for Numerical Methods in Biomedical Engineering **32(10)** (2016) e02757–n/a.

[4] S. Hénon, G. Lenormand, A. Richert, F. Gallet, *A New Determination of the Shear Modulus of the Human Erythrocyte Membrane Using Optical Tweezers*, Biophysical Journal **76(20)** (1999) 1145–1151.

[5] G. Tomaiuolo, *Biomechanical Properties of Red Blood Cells in Health and Disease towards Microfluidics*, Biomicrofluidics **8(5)** (2014) 051501.

[6] D. Boal, *Mechanics of the Cell*, Cambridge University Press, 2012.

Book of abstracts of the 7th International Conference
on Advanced Computational Methods
in Engineering, ACOMEN 2017
18–22 September 2017.

Force-free and torque-free elasticity in cell models

Iveta Jančigová and Ivan Cimrák

Department of Software Technologies, University of Žilina

e-mails: iveta.jancigova@fri.uniza.sk, ivan.cimrak@fri.uniza.sk

Abstract

Force-based models of elastic cells should be force- and torque-free. That is, in the absence of external stimuli, a relaxed cell should neither travel in space (force-free) nor rotate (torque-free). These properties are easier to achieve for local elastic forces such as local area conservation and more difficult for global forces such as surface or global volume conservation. We propose the force- and torque-free approaches to the global forces and discuss the tradeoff between exact fulfilment of these conditions and computational time and issues that arise from fulfilling the force-free condition.

Key words: computational microfluidics, cell model, elasticity, force-free, torque-free

1 Global forces in modeling of elastic cells

In modeling of elastic objects such as red blood cells, several elastic moduli are involved: stretching, bending, local area conservation, global area conservation and volume conservation [1]. In this work we focus on the last two and discuss the possibilities for defining them force- and torque-free so that they do not cause movement or rotation of the objects in relaxed state.

While the local elastic forces work to restore the local shape of the membrane, it is necessary to include global forces that conserve total surface and volume of the object. This can be done for example using forces of the following format for global area and volume conservation [2]:

$$\mathbf{F}_{ag}(A) = k_{ag}\frac{\Delta S}{S^0}\mathbf{t}_A \qquad \mathbf{F}_v(A) = k_v \Delta V S_{ABC}\mathbf{n}_{ABC}$$

where k_{ag} is the global area coefficient, S^0 is the relaxed area of the whole object, $\Delta S = S - S^0$ is the deviation from this area and $\mathbf{t}_A$ is the unit vector pointing from the centroid of the triangle ABC to the vertex A. Analogous forces are acting on nodes B and C. For volume force $\mathbf{F}_v$, k_v is the elastic coefficient, S_{ABC} is the current area of triangle ABC, ΔV is the difference between current volume and volume in the relaxed state and $\mathbf{n}_{ABC}$ is the unit normal vector to the plane ABC.

Note the direction of these forces. In each triangle, the global area force acts in the triangle plane, while the volume force acts in the direction perpendicular to the triangle plane. These global elastic moduli are neither force- nor torque-free, which can be demonstrated by both analytical calculation and simulation of cell without external stimuli, that exhibits very slow drifting and rotation. In other models, e.g. [3], we also see volume forces that are not force-free.

2 Consequences of force-free global area and volume

In [4], we have proposed a force-free and torque-free local area modulus and ideally, we would like to apply the same approach to the global forces as well:

$$\mathbf{F}_{ag}(A) = k_{ag} \cdot S_{ABC} \cdot \frac{\Delta S}{|\mathbf{t}_A|^2 + |\mathbf{t}_B|^2 + |\mathbf{t}_C|^2}\mathbf{t}_A \qquad \mathbf{F}_v(A_i) = k_v \cdot \frac{\Delta V}{\sum_{j=1}^{n} |\mathbf{t}_j|^2}\mathbf{t}_i$$

where k_{ag} is the global area coefficient, S_{ABC} is the area of triangle ABC (we weigh the forces by this area to avoid degeneration of the mesh), ΔS is the deviation of current surface area from relaxed surface area and $\mathbf{t}_A = \overrightarrow{AT}$, where T is the centroid of the triangle ABC. For volume force, k_v is the volume coefficient, ΔV is the difference between current volume and volume in the relaxed state, $\mathbf{t}_i = \overrightarrow{A_iT}$, T is the centroid of the object, A_i is a point of the mesh and the sum in the denominator of $\mathbf{F}_v$ runs over all discretisation points of the object.

These global forces are force- and torque- free, however, the practical implementation of this approach comes at a price of three loops over the nodes in every timestep: one to compute the current volume and current location of the centroid, one to calculate the sum of distances of the current nodes positions and the centroid and one to calculate the actual forces. (Note that in some cases it might be useful to use a street-fighting version of force-free volume force: calculate the resultant of all volume forces $\mathbf{F}_v^{total} = \sum \mathbf{F}_v$ applied in individual nodes and apply additional $-\frac{1}{n}\mathbf{F}_v^{total}$ in every node.)

Moreover, the volume forces now generally do not act in the directions perpendicular to the individual triangles. This means that the volume force can be split into the perpendicular and tangential portions and under certain circumstances, the tangential part may interfere with the in-plane acting global volume force. We will show examples, in which these forces act against each other - one is trying to decrease the size of the mesh triangle and the other to increase it. We will also discuss the implications for spring-network modeling.

Acknowledgements

This work was supported by the Slovak Research and Development Agency under the contract No. APVV−15 − 0751.

References

[1] M. Nakamura, S. Bessho, S. Wada, *Spring-network-based model of a red blood cell for simulating mesoscopic blood flow*, International Journal for Numerical Methods in Biomedical Engineering **29** (2013) 114–128.

[2] I. Cimrák, M. Gusenbauer, I. Jančigová, *An ESPResSo implementation of elastic objects immersed in a fluid*, Computer Physics Communications **185(3)** (2012) 900–907.

[3] D. A. Fedosov, *Multiscale Modeling of Blood Flow and Soft Matter*, phd thesis (2010).

[4] I. Jančigová, I. Cimrák, *Non-uniform force allocation for area preservation in spring network models*, International Journal for Numerical Methods in Biomedical Engineering **32(10)** (2016) doi:10.1002/cnm.2757.

Book of abstracts of the 7th International Conference
on Advanced Computational Methods
in Engineering, ACOMEN 2017
18–22 September 2017.

Analytical Solution for a 3D model of the airflow in the human upper respiratory tract

Supachara Kongnuan[1] **and Chatvarin Tasawang**[2]

[1] *Department of Mathematics and Statistics, Thammasat University, Thailand*

e-mails: suputchara@matstat.sci.tu.ac.th, Chatvarin.ts@gmail.com

Abstract

Understanding characteristic of the airflow behavior in the human respiratory tract is necessary for treatment of respiratory diseases. For this purpose, this paper aim to propose a three-dimensional mathematical model to describe the airflow in the human upper respiratory tract. The governing equations are composed of Navier-Stokes equations and the continuity equation. As the airflow is driven by the oscillating pressure gradient within the pulmonary, therefore one side of boundaries is set to be a periodic pressure function. Under the assumption that the airflow is axially symmetric, the governing equations are presented in the cylindrical coordinates system. Due to the requirement of high computing resource of a numerical method, we presented an efficient analytical method based on the Fourier-Bessel series form. The obtained airflow field is simulated on a three-dimensional geometry of a human respiratory tract. The simulated characteristic of the airflow show a good agreement to the fact of airflow behavior in the human airway ,the previous researches and other related publications. *Key words:*

human upper respiratory, three-dimensional mathematical model, Navier-Stokes equations, analytical solution, Fourier-Bessel series.

MSC 2010: 76D05, 9208

Book of abstracts of the 7th International Conference on Advanced Computational Methods in Engineering, ACOMEN 2017 18–22 September 2017.

Interior point method for the Stokes flow with stick-slip boundary conditions

Kučera Radek[1] **and Šátek Václav**[1]

[1] *IT4Innovations, VŠB - Technical University of Ostrava, 17. listopadu 15/2172, 708 33 Ostrava-Poruba, Czech Republic*

e-mails: radek.kucera@vsb.cz, vaclav.satek@vsb.cz

Abstract

The Stokes problem with the stick-slip boundary condition is solved by the mixed finite element method combined with the TFETI domain decomposition technique. An interior point method for the minimization subject to box and equality constraints is used as the main solver.

Key words: TFETI method, interior point method, stick-slip condition, Stokes problem.

1 Introduction

The contribution deals with the Stokes flow with the stick-slip boundary conditions. We consider the case when the slip of a fluid along the wall may occur only when the shear stress attains certain bound which is given a-priori and does not depend on the solution itself. The mathematical model of the velocity-pressure formulation leads to the so-called variational inequality of the second kind. This problem exhibits many attractive applications; see [9, 2] and references therein.

Our approximation uses the mixed finite element method based on the P1-bubble/P1 finite elements [1]. The stiffness matrices are generated by a vectorized code [5]. The finite element approximation is combined with the TFETI domain decomposition method [3]. The dual algebraic problem arising after the elimination of the velocity and the pressure components leads to the minimization of the quadratic, strictly convex function in terms of three Lagrange multipliers representing the gluing condition, the impermeability condition on the slip part of the boundary and the stick-slip condition. The third Lagrange multiplier is subject to box constraints and, due to the use of the TFETI method, all Lagrange multipliers have to satisfy linear equality constraints. The solution is computed by a path-following variant of the interior-point method [7] adapted for box and linear equality constraints [8]. Highly promising numerical experiments of the path-following algorithm for non-decomposed problems has been presented in [6].

The main idea of the algorithm consists on the use of the damped Newton method whose iterations lay in a neighborhood of a central path leading to the solution. The inner subproblems are given by linear systems with a block structure. These systems are reduced using the

Schur complement method so that a variant of the preconditioned projected conjugate gradient method (PPCGM) may be used. The PPCGM generates iterations in a subspace determined by the kernel of the matrix representing the equality constraints. An appropriate preconditioner eliminates ill conditioning of the reduced systems that arises typically in interior point methods when the iterations approach the solution. For that, we use the oblique projector. Our numerical experiments are performed by the decomposed problems taken from [6]. The first results computed with the TFETI active set strategy algorithm and a brief description of the simplified version of the TFETI path-following algorithm could be found in [4]. The main issue of this contribution is an experimental assessments of preconditioning variants that arise from the spectral analysis of the preconditioning technique [8].

Acknowledgements

This work was supported by The Ministry of Education, Youth and Sports from the National Programme of Sustainability (NPU II) project "IT4Innovations excellence in science - LQ1602".

References

[1] D. Arnold, F. Brezzi, and M. Fortin. A stable finite element for the Stokes equations. *Calcolo*, 21:337–344, 1984.

[2] M. Ayadi, L. Baffico, M. K. Gdoura, and T. Sassi. Error estimates for Stokes problem with Tresca friction conditions. *ESAIM: Mathematical Modelling and Numerical Analysis*, 48(5):113–126, 2014.

[3] Z. Dostál, D. Horák, and R. Kučera. Total FETI - an easier implementable variant of the FETI method for numerical solution of elliptic PDE. *Communications in Numerical Methods in Engineering*, 22(12):1155–1162, 2006.

[4] M. Jarošová, R. Kučera, and V. Šátek. A new variant of the path-following algorithm for the parallel solving of the Stokes problem with friction. In P. Iványi and B. H. V. Topping, editors, *Proceedings of the Fourth International Conference on Parallel, Distributed, Grid and Cloud Computing for Engineering*, Stirlingshire, UK, 2015. Civil-Comp Press, Paper 11.

[5] J. Koko. *Vectorized Matlab codes for the Stokes problem with P1-bubble/P1 finite element*, 2012. `http://www.isima.fr/~jkoko/Codes/StokesP1BubbleP1.pdf` [online].

[6] R. Kučera, J. Haslinger, V. Šátek, and M. Jarošová. Efficient methods for solving the Stokes problem with slip boundary conditions. *Math. Comput. Simulation*, (Available online 10 August 2016). `http://dx.doi.org/10.1016/j.matcom.2016.05.012`.

[7] R. Kučera, J. Machalová, H. Netuka, and P. Ženčák. An interior point algorithm for the minimization arising from 3d contact problems with friction. *Optim. Method Softw.*, 6(28):1195–1217, 2013.

[8] R. Kučera, V. Šátek, and M. Jarošová. Path-following interior point method for qpp with box and equality constraints: theory and applications. In preparation (2017).

[9] I. J. Rao and K.R. Rajagopal. The effect of the slip boundary condition on the flow of fluids in a channel. *Acta Mechanica*, 135:113–126, 1999.

Book of abstracts of the 7th International Conference
on Advanced Computational Methods
in Engineering, ACOMEN 2017
18–22 September 2017.

Magneto-Hydrodynamic Model for Simulation of Water Purification

Serge Polyakov[1] **and Tatiana Kudryashova**[1]

[1] *Keldysh Institute of Applied Mathematics, RAS, Moscow, Russia,*

e-mails: serge@imamod.ru, kudryashova@imamod.ru

Abstract

The present work is intended to introduce parallel approach to mathematical modeling of water treatment from iron impurities. We consider process of removing iron ions and iron oxides from water by means of a magnetic field. The 2D and 3D variants of this problem are studied. The model problem is considered in approximation of an incompressible fluid flow in a channel with rectangular cross section.The parallel code is realized on hybrid computer systems with Graphical Processing Units, classical microprocessors (Central Processing Units) and VPU (Video Processing Units). The proposed method integrates domain decomposition technique, parallel implementation via MPI technology, OpenMP and CUDA.

Key words: Mathematical modeling, numerical methods, parallel algorithms, water treatment processes.

Introduction

In this work, the influence of the magnetic field on the water purification is studied. Experiments show that the magnetic field increases the speed of chemical processes and the crystallization of dissolved substances in water, intensifies adsorption processes. It accelerates the coagulation of impurities and the precipitation of them. The influence of a magnetic field on water depends on the water composition, the magnetic field strength, velocity of water movement, the time of effect and other factors [1], [2].

In our study, we consider problem of capturing the iron ions and iron salts under magnetic processing of water flow in a nonmetallic pipe. Magneto-hydrodynamic model is formed. The model takes into account the direct effect of magnetic induction on the stream of water. In this case, currents of iron ions and/or iron salt ions appear and generate secondary electric field. We should consider this electrical field because it can substantially change the evolution of the impurity.

The paper deals with the two-dimensional plane-parallel flow. The flow is formed in the middle section of rectangular tube with a strong anisotropy of sides. The magnetic field acts in a transverse direction of flow and generates circular motions in this section of the tube. In this situation, the flow pattern is similar to the two-dimensional model and can be considered as an initial approximation for solving three-dimensional problem [3], [4]. The isothermal

laminar fluid flow is studied to simplify the analysis. The drift-diffusion approximation is used to describe the behavior of the fine dispersible impurities [5], [6].

Such processing is relevant to many industries. It is applied for heat energetics, agriculture, construction, medicine and others.

Acknowledgements

This work has been supported by Russian Foundation for Basic Researches (grants No 15-01-04620-a, 16-07-00206-a).

References

[1] V. I. Shvets, A. M Yurkevich, O. V Mosin., and D. A Skladnev, *Preparation of deuterated inosine suitable for biomedical application*, J. . Medical Sciences. **8** (1995) 231–232.

[2] T.G. Elizarova, *Quasi-gasdynamic equations*, Springer, 2009.

[3] B.N. Chetverushkin, *Kinetic Schemes and Quasi-Gasdynamic System of Equations*, Barcelona: CIMNE, 2008.

[4] A.A. Samarskii and P.N. Vabishchevich, *Numerical methods for solving inverse problems of mathematical physics*, Walter de Gruyter, 2007.

[5] S.V. Polyakov, *Exponential Difference Schemes with Double Integral Transformation for Solving Convection-Diffusion Equations*, J. . Mathematical Models and Computer Simulations. **5** (2013) 338–340.

[6] Tatiana Kudryashova, Sergey Polyakov, *Mathematical modeling of water purification process of iron containing impurities*, IARIA XPS Press, Wilmington, USA, 2016.

Book of abstracts of the 7th International Conference
on Advanced Computational Methods
in Engineering, ACOMEN 2017
18–22 September 2017.

Bicuspid aortic valve: A patient-specific modeling approach

D. Oliveira[1], S. Aguiar Rosa[2], J. Tiago[1] and A. Sequeira[1]

[1] *Math Department (CEMAT), Instituto Superior Tecnico, Lisboa, Portugal*

[2] *Cardiology Department, Hospital de Santa Marta (CHLC), Lisboa, Portugal*

e-mails: diana.oliveira@tecnico.ulisboa.pt, silviaguiarosa@gmail.com, jftiago@math.tecnico.ulisboa.pt, adelia.sequeira@math.tecnico.ulisboa.pt

Abstract

The congenital bicuspid aortic valve (BAV) disease leads to several complications, one of those being aortic dilation (AD). Different BAV phenotypes are correlated with diverse blood flow patterns, causing multiple AD phenotypes. A three dimensional realistic fluid-structure interaction (FSI) model of the aorta where different rigid BAV cusps are included is used to study such correlations. These cusps are built from patient-specific (PS) measures. We show that the application of such methodology can provide relevant results for these PS cases of disease: abnormal blood flow correlated with elevated patterns of wall shear stress (WSS) is observed.

Key words: aortic dilation, bicuspid aortic valve, fluid-structure interaction, patient-specific modeling

1 Introduction

BAV is a congenital heart malformation with great phenotypic heterogeneity, characterized either by the existence of two cusps instead of three, or by fusion of two of the cusps (being functionally bicuspid). It causes marked alterations on ascending aortic blood flow, and is associated with diverse complications such as AD [1]. BAV computational modeling with PS valve measurements is a crucial step towards a better understanding of this disease and related aortopathies. This work is devoted to the study of the influence of several phenotypes of BAV on aortic blood flow and its correlation with AD in PS geometries.

2 Methodology

The aortic lumen is reconstructed from PS computed tomography images and the aortic wall is virtually created using an open-source tool [2]. The BAV cusps are built in a peak systolic configuration using SOLIDWORKS. For its construction, PS measurements such as the shape of the BAV orifice or the length of the BAV raphe are retrieved from echocardiographic images.

An FSI approach is employed using the Arbitrary Lagrangian-Eulerian formulation [3]. Blood flow is governed by the Navier-Stokes equations that characterize Newtonian and incompressible fluids. The aortic wall tissue is assumed as a linear, elastic and isotropic material.

At the inlet, PS average velocity curves retrieved from Continuous Doppler echocardiography are applied. At the outlets, we impose linear absorbing boundary conditions [4] to avert spurious backflow due to the truncation of the computational domain.

Since the main goal of the work is to observe the influence of its shape in blood flow during systole, the displacement of the valve cusps is constrained in all directions and these are considered rigid.

To perform numerical simulations, a finite element method is employed using the software COMSOL Multiphysics through a P1-P1 stabilized discretization for the fluid and P2 for the solid.

3 Results

Figure 1 shows relevant hemodynamic results at peak systole for a PS BAV case.

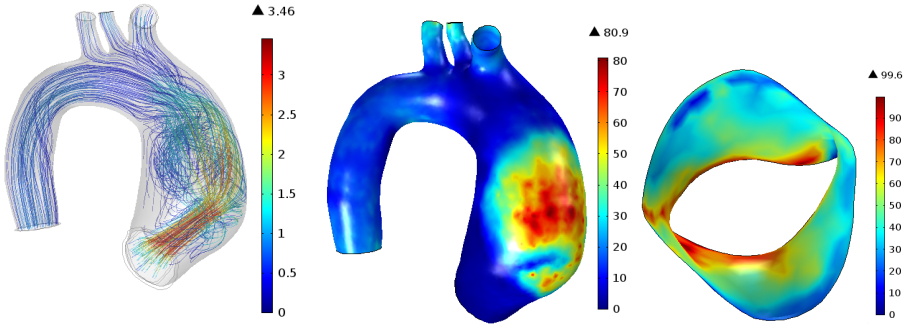

(a) Velocity field (m/s) (b) WSS - wall (dyn/cm^2) (c) WSS - cusps (dyn/cm^2)

Figure 1: Hemodynamic indicators obtained on a PS aortic complex for a BAV with two cusps without a raphe.

One can observe that a skewed high velocity blood jet (Figure 1(a)) hits the outer ascending aortic wall, subjecting this area to abnormally elevated WSS (Figure 1(b)). This issue can act as a maintaining AD factor in these patients. Alternatively, the WSS on the BAV leaflets (Figure 1(c)) is higher near the valve orifice, suggesting that the flow passage through the specific shape of these cusps will cause greater degeneration near the free edges.

References

[1] J. Kang et al., *Association Between Bicuspid Aortic Valve Phenotype and Patterns of Valvular Dysfunction and Bicuspid Aortopathy*, JACC: Cardiovascular Imaging **6(2)** (2013) 150–161.

[2] E. Faggiano et al., *An open-source tool for patient-specific fluid-structure vessel mesh generation*, The MATHCARD EU Project (2013).

[3] M. Fernandez, J. Gerbeau, *Algorithms for fluid-structure interaction problems. In Cardiovascular Mathematics*, 307–346, Springer, 2009.

[4] J. Janela et al., *Absorbing boundary conditions for a 3D non-Newtonian fluid-structure interaction model for blood flow in arteries*, INT J ENG SCI **48** (2010) 1332–1349.

MS 6 Novel trends and challenges in electromagnetic full-wave modelling

Organiser: Hendrik Rogier

Description: In the last decades, we have seen tremendous advances in electromagnetic full-wave modelling techniques, up to such a scale that commercial electromagnetic field solvers based on integral equations, finite elements and finite differences have become fully integrated as computer-aided engineering tools in most design processes of complex electronic systems. Yet, very complex and very large problems still represent major obstacles for mainstream full-wave simulators, making the analysis of such structures highly time consuming and their computer-aided optimization impossible. This mini-symposium provides an overview of the latest developments in electromagnetic field modelling research towards even more efficient and accurate solvers for large intricate simulation domains. Advanced preconditioning methods that avoid dense mesh and low frequency breakdown are presented, as well as local grid refinement techniques. In addition, the incorporation of stochastic frameworks into full-wave electromagnetic field solvers is discussed, including some pertinent design examples in the context of wearable antenna design.

Book of abstracts of the 7th International Conference on Advanced Computational Methods in Engineering, ACOMEN 2017
18–22 September 2017.

Calderon Preconditioners for the PMCHWT Integral Equation Based on the Quasi-Helmholtz Projectors

Y. Beghein[1], R. Mitharwal[2], K. Cools[3] and F. P. Andriulli[3]

[1] *Ghent University, Belgium*

[2] *IMT Atlantique, France*

[3] *University of Nottingham, UK*

e-mails: yves.beghein@ugent.be, rajendra.mitharwal@imt-atlantique.fr, Kristof.Cools@nottingham.ac.uk, francesco.andriulli@imt-atlantique.fr

Abstract

The Poggio-Miller-Chan-Harrington-Wu-Tsai (PMCHWT) is a widely used integral equation for simulating radiation and scattering from penetrable objects. This formulation, however, is plagued from mesh refinement and low-frequency ill-conditioning. Existing techniques for handling these problems, however, suffer from very low-frequency numerical cancellations or they require the detection of global loops. This work presents a new Calderon-like strategy for the PMCHWT which, leveraging on the quasi-Helmholtz projectors, solves both frequency and refinement ill-conditioning without detecting global loops. Moreover the technique is immune from very low-frequency numerical cancellations. Numerical results confirms all theoretical developments and show the practical impact of the new scheme.

Key words: Calderon preconditioning, Penetrable scatterers, PMCHWT integral equation.

1 Sketch of the formulation and numerical results

The PMCHWT integral equation reads

$$\begin{pmatrix} \mathcal{T}_k + \mathcal{T}_{k'}/\eta_r & -(\mathcal{K}_k + \mathcal{K}_{k'}) \\ \mathcal{K}_k + \mathcal{K}_{k'} & \mathcal{T}_k + \eta_r \mathcal{T}_{k'} \end{pmatrix} \begin{pmatrix} \boldsymbol{M}(\boldsymbol{r}) \\ \boldsymbol{J}(\boldsymbol{r}) \end{pmatrix} = - \begin{pmatrix} \eta_k \hat{\boldsymbol{n}}_{\boldsymbol{r}} \times \boldsymbol{H}^i(\boldsymbol{r}) \\ \hat{\boldsymbol{n}}_{\boldsymbol{r}} \times \boldsymbol{E}^i(\boldsymbol{r}) \end{pmatrix}$$

where for the definitions of the operators we refer the reader to [1] The first element of the formulation we propose follows from a Galerkin discretization of the equation via zeroth order Raviart-Thomas elements. The quasi helmholtz projectors are defined as in [1] as $\mathbf{P}^{\Sigma} = \Sigma \left(\Sigma^T \Sigma\right)^+ \Sigma^T$ and $\mathbf{P}^{\Lambda H} = \mathbf{I} - \mathbf{P}^{\Sigma}$ and the associated rescaling operators are $\mathbf{M} = \frac{1}{\sqrt{k/k_0}} \mathbf{P}^{\Lambda H} + i\sqrt{k/k_0} \mathbf{P}^{\Sigma}$ and $\mathbf{M}^{-1} = \sqrt{k/k_0} \mathbf{P}^{\Lambda H} + \frac{1}{i\sqrt{k/k_0}} \mathbf{P}^{\Sigma}$. This results in the following frequency preconditioned PMCHWT integral equation

$$\begin{pmatrix} \mathbf{Q}'_{jm} & \mathbf{Q}'_{jj} \\ \mathbf{Q}'_{mm} & \mathbf{Q}'_{mj} \end{pmatrix} \begin{pmatrix} \mathbf{x} \\ \mathbf{y} \end{pmatrix} = - \begin{pmatrix} \eta_k \mathbb{M}^{-1} \mathbf{G}^{-1} \mathbf{h}^i \\ \mathbb{M}^{-1} \mathbf{G}^{-1} \mathbf{e}^i \end{pmatrix} \tag{1}$$

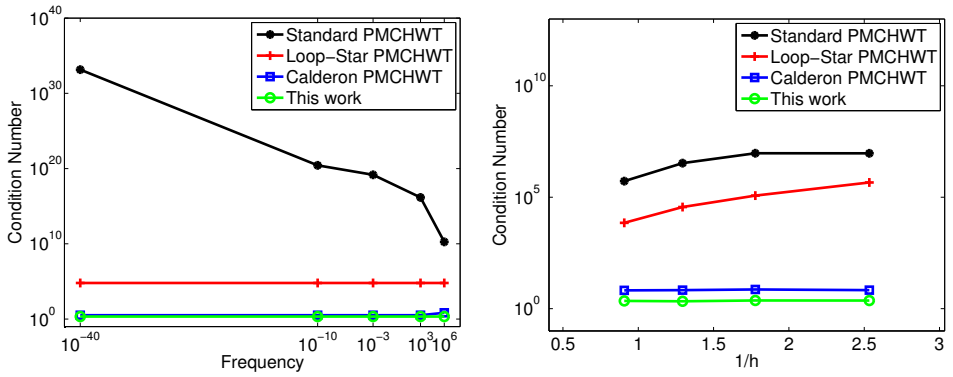

(a) Torus: Condition number w.r.t frequency.

(b) Torus: Condition Number of system matrix w.r.t. discretization density at 1 MHz.

Figure 1: Numerical results

where $\mathbf{Q}'_{\alpha\beta} = \mathbb{M}^{-1}\mathbf{G}^{-1}\mathbf{Q}_{\alpha\beta}\mathbf{M}$ with $\alpha = m, j$ and $\beta = m, j$ and where the blocks $\mathbf{Q}_{\alpha,\beta}$ represent the Galerking matrix blocks associated to (1). A similar strategy is possible on the dual mesh, resulting in the following dual qH-PMCHWT

$$\begin{pmatrix} \mathbb{Q}'_{jm} & \mathbb{Q}'_{jj} \\ \mathbb{Q}'_{mm} & \mathbb{Q}'_{mj} \end{pmatrix} \begin{pmatrix} \mathfrak{x} \\ \mathfrak{y} \end{pmatrix} = - \begin{pmatrix} \eta_k \mathbf{M}^{-1}\mathbb{G}^{-1}\mathfrak{h}^i \\ \mathbf{M}^{-1}\mathbb{G}^{-1}\mathfrak{e}^i \end{pmatrix} \tag{2}$$

where the operator matrices are defined following suitable duality rules [1]. It can be shown that the two new equations in (1) and (2) are immune from low-frequency breakdown and, moreover, it can be shown that they can be successfully combined in a Calderon fashion to obtain an equation immune from mesh refinement ill-conditioning which reads

$$\begin{pmatrix} \mathbb{Q}'_{jm} & \mathbb{Q}'_{jj} \\ \mathbb{Q}'_{mm} & \mathbb{Q}'_{mj} \end{pmatrix} \begin{pmatrix} \mathbf{Q}'_{jm} & \mathbf{Q}'_{jj} \\ \mathbf{Q}'_{mm} & \mathbf{Q}'_{mj} \end{pmatrix} \begin{pmatrix} \mathbf{x} \\ \mathbf{y} \end{pmatrix} = - \begin{pmatrix} \mathbb{Q}'_{jm} & \mathbb{Q}'_{jj} \\ \mathbb{Q}'_{mm} & \mathbb{Q}'_{mj} \end{pmatrix} \begin{pmatrix} \eta_k \mathbb{M}^{-1}\mathbf{G}^{-1}\mathbf{h}^i \\ \mathbb{M}^{-1}\mathbf{G}^{-1}\mathbf{e}^i \end{pmatrix}. \tag{3}$$

2 Numerical Results

The new formulation has been tested on a torus of external radius equal to 1.5m, internal radius equal to 0.5m and of dielectric constant $\epsilon_r = 3$. The fact that the new equation is immune from the low frequency breakdown is confirmed by Figure 1(a), while the mesh refinement breakdown immunity is verified in Figure 1(b).

References

[1] Y. Beghein, R. Mitharwal, K. Cools, F. P. Andriulli, *On a Low-Frequency and Refinement Stable PMCHWT Integral Equation Leveraging the Quasi-Helmholtz Projectors*, To appear.

Book of abstracts of the 7th International Conference
on Advanced Computational Methods
in Engineering, ACOMEN 2017
18–22 September 2017.

Coupling of FEM and Multiple Multipole Program for Computational Electromagnetics

Daniele Casati[1]

[1] *Seminar for Applied Mathematics, ETH Zurich*

e-mails: daniele.casati@sam.math.ethz.ch

Abstract

The Multiple Multipole Program (MMP) is a Trefftz method for computational electromagnetics, successfully employed in the code `OpenMaXwell` for many years.

MMP cannot handle nonlinearities in the material parameters. We propose to couple MMP with the Finite Element Method: FEM models the bounded nonlinear region, while MMP the unbounded exterior domain. Interface conditions on the boundary establish the good mathematical behavior of the joint solution.

Key words: finite element method, multiple multipole program, method of auxiliary sources, Trefftz method, computational electromagnetics
MSC 2010: 35Q61, 65N30, 65N80, 65Z05

1 Introduction

The Finite Element Method and the Multiple Multipole Program enjoy complementary capabilities. FEM requires a mesh of the computational domain of interest. This is expensive, but it can treat nonlinear materials. Moreover, FEM allows a purely local construction of the discrete system of equations.

On the other hand, MMP is a boundary method using basis functions that solve exactly the PDE: only integrals on a hypersurface have to be computed, and the obtained linear combination is valid in the whole domain where the PDE holds. At the same time, MMP performs better where the electromagnetic field is smooth, i.e. in the free space far from the physical sources and material interfaces: many basis functions, or basis functions with a complicated form, are needed to correctly model singularities of the field. In such situations, positioning the basis functions and choosing their orders are nontrivial tasks and require heuristic rules.

Thus, a natural way to combine the strengths of these methods arises when one needs to simulate the electromagnetic field of a material with nonlinear properties surrounded by free space: use FEM on a mesh defined in the material and MMP outside, matched with FEM on the subset of the mesh that covers the material surface.

However, while the basis functions of FEM have a finite support, the basis functions of MMP are global: this leads to computational issues. Many matrices that are assembled by FEM are symmetric and diagonally dominant, and therefore easy to invert; conversely, MMP always leads to dense matrices. The matrices of MMP, usually obtained by a collocation method, are rectangular, and the related linear systems are solved in a least-squares sense.

2 Mathematical Framework

The interface conditions on the surface of the material modeled by FEM are key to accurate coupled FEM-MMP solutions. Integrating by parts the variational form of the PDE solved by FEM, surface integrals appear, through which one can impose interface conditions by substituting the ansatz of MMP. However, not all interface conditions can be imposed in this way. We have explored two approaches to include the additional conditions.

The first approach is based on the collocation method, like MMP. Quadrature nodes on the intersections of the FEM elements with the boundary are selected as matching points. The number of points is chosen to make the system matrix almost square. This method proved reliable with nontrivial geometries, but so far lacks a rigorous mathematical foundation.

The other approach is a Galerkin method that introduces a weak formulation of the additional conditions. MMP basis functions (or their derivatives) are chosen as test functions. Usually, this can be done in a way that yields a symmetric linear system.

Future research will explore alternative ways to build the system coupling FEM and MMP.

3 Numerical Results

We have simulated electromagnetic fields in magnetostatics and wave scattering with different geometries and material parameters. When the material parameters are set equal to those of free space, the FEM-MMP coupling produces the expected results.

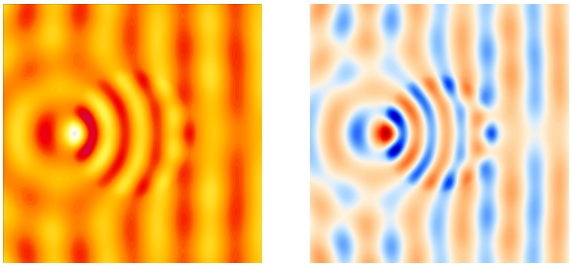

(a) `OpenMaXwell` (b) FEM-MMP Coupling

Figure 1: Photonic nanojet: magnitude of **H**-field at $t = 0$, $\epsilon_r = 2.5281$, $\frac{r}{\lambda} = 1.25$.

Figure 1 shows the photonic nanojet for a circle of dielectic material surrounded by free space. On the left, the well-established code `OpenMaXwell` was employed, modeling with MMP only. On the right, the coupling between FEM and MMP.

An extension to transient Maxwell equations will be considered in future research.

Acknowledgements

Supported through the grant 2000021_165674/1 by the Swiss National Science Foundation.

References

[1] J. Smajic, C. Hafner, J. Leuthold, *Coupled FEM–MMP for Computational Electromagnetics*, IEEE Trans. Magn **52**(3), 2015.

[2] C. Hafner, `OpenMaXwell`, http://openmax.ethz.ch/.

Book of abstracts of the 7th International Conference on Advanced Computational Methods in Engineering, ACOMEN 2017 18–22 September 2017.

Local Preconditioner for the Maxwell BETI Method

Kristof Cools[1] and Francesco P. Andriulli[2]

[1] *Dept. of Electrical and Electronic Engineering, University of Nottingham*

[2] *Microwave Department, TELECOM Bretagne*

e-mails: kristof.cools@nottingham.ac.uk, fracesco.andriulli@telecom-bretagne.eu

Abstract

The Boundary Element Tearing and Interconnect (BETI) method introduced by Langer et al. [3] and analysed in the context of the three-dimensional Maxwell system in Windisch [1] allows for a domain decomposition based solution of scattering and transmission problems. Like other domain decomposition methods its aim is twofold: to accelerate the solution by describing it in terms of linear systems with beneficial spectral problems, and (ii) to expose opportunities for parallelisation of the solution so that the deployment of multiple computing nodes can further accelerate the process. In order to arrive at a bounded condition number, both a preconditioner for the local Dirichlet problems and the global problem need to be provided. In this contribution, a Calderon based local preconditioner for the local problem will be described [2, 4]. The discretisation is detailed, and numerical experiments are presented to demonstrate its correctness and performance.

Key words: Calderón Preconditioning, Electromagnetic Scattering, Boundary Element Tearing and Interconnecting Method, Frequency Domain Analysis

1 Introduction

To lighten the notation only the case with a single interior domain will be discussed. The extension to the general case will require the careful bookkeeping of Lagrange multipliers, especially where three or more domains meet, but this is an issue orthogonal to the solution of the local problems.

Consider a bounded and connected domain Ω_1 with an unbounded complement Ω_0. The normal pointing *into* domain Ω_i is denoted $\hat{\boldsymbol{n}}_i$. The domain Ω_i is filled with a material characterised by an imepdance η_i and a wavenumber k_i. The single and double layer boundary integral operators are defined by

$$T_i\boldsymbol{j} = \frac{1}{ik_i}\hat{\boldsymbol{n}}_i \times \operatorname{grad}\int_\Gamma \frac{e^{-ik_iR}}{4\pi R}\operatorname{div}\boldsymbol{j}(\boldsymbol{r}')d\boldsymbol{r}' - ik_i\hat{\boldsymbol{n}}_i \times \int_\Gamma \frac{e^{-ik_iR}}{4\pi R}\boldsymbol{j}(\boldsymbol{r}')d\boldsymbol{r}' \tag{1}$$

$$K_i\boldsymbol{j} = \hat{\boldsymbol{n}}_i \times \int_\Gamma \operatorname{grad}\frac{e^{-ik_iR}}{4\pi R} \times \boldsymbol{j}(\boldsymbol{r}')d\boldsymbol{r}'. \tag{2}$$

Based on the representation theorem and the symmetric representations of the Poincare-Steklov operator for solutions in the respective domains, the boundary element tearing and interconnecting method as described in [1] leads to the following dual system for a set of Lagrange multipliers:

$$\begin{pmatrix} 1 & 0 \end{pmatrix} \begin{pmatrix} \frac{1}{\eta_0} T_0 & K_0^+ \\ -K_0^- & \eta_0 T_0 \end{pmatrix}^{-1} \begin{pmatrix} \lambda \\ 0 \end{pmatrix} + \begin{pmatrix} 1 & 0 \end{pmatrix} \begin{pmatrix} \frac{1}{\eta_1} T_1 & K_1^+ \\ -K_1^- & \eta_1 T_1 \end{pmatrix}^{-1} \begin{pmatrix} \lambda \\ 0 \end{pmatrix} = \dots \tag{3}$$

with $K_i^{\pm} = K_i \pm 1/2$ and where the Lagrange multiplier is a density supported by Γ. In the general case of multiple domains care needs to be taken to construct one Lagrange multiplier for every continuity constraint between the electric traces in each of the domains [1]. The solutions for the electric and magnetic traces, and any derived quantity of interest, can be readily computed when the above system is solved for $\boldsymbol{\lambda}$.

To efficiently solve this equation, fast algorithms are required, not only to compute the inverses of the block operators appearing in (3), but also to minimize the number of iterations required in the iterative solution of the global system. This contribution focuses on the implementation of a Calderon preconditioner [2] that allows (in combination with a matrix-vector product acceleration algorithm) to invert the local block operators in near linear time (w.r.t. the local number of DoFs).

The local systems are equivalent to computing the action of the Poincare-Steklov operator. The study of the mapping properties of this operator (e.g. [1]) and the numerical results on preconditioning this operator in a FEM setting [4] provide the motivation to apply a Calderon Multiplicative Preconditioner to these system. The Rao-Wilton-Glisson/Raviart-Thomas discretisation of the local variational problems is preconditioned by a different dual Buffa-Christiansen based discretisation of the same system.

We will detail how this discretisation is constructed and how to integrate the preconditioner in the solution process. Results will be shown that clearly demonstrate the efficiency of the preconditioner and its effect on the spectral distribution of the linear systems to be solved.

References

[1] M. Windisch, *Boundary Element Tearing and Interconnecting Methods for Acoustic and Electromagnetic Scattering*, Computation in Engineering and Science, TU Graz, 2011

[2] F.P. Andriulli, K. Cools, H. Bagci, F. Olyslager, A. Buffa, S. Christiansen, and E. Michielssen, *A Multiplicative Calderon Preconditioner for the EFIE*, IEEE Trans. on Antennas and Propagation **56(8)** (2008) 2398–2412.

[3] U. Langer and O. Steinbach, *Boundary Element Tearing and Interconnecting Methods*, Computing **71(3)** (2003) 205–228.

[4] D. Dobbelaere, D. De Zutter, J. Van Hese, J. Sercu, T. Boonen, H.Rogier, *A Calderon Multiplicative Preconditioner for the Electromagnetic Poincare-Steklov Operator of a Heterogeneous Domain with Scattering Applications*, Journal of Computational Physics **303** (2015) 335–371.

Book of abstracts of the 7th International Conference
on Advanced Computational Methods
in Engineering, ACOMEN 2017
18–22 September 2017.

Determination of a time-dependent convolution kernel from a boundary measurement in nonlinear Maxwell's equations

Marián Slodička[1] **and Michal Galba**[1]

[1] *Department of Mathematical Analysis, Ghent University*

e-mails: marian.slodicka@ugent.be, michal.galba@ugent.be

Abstract

A nonlinear hyperbolic Maxwell equation is studied, where an solely time dependent convolution kernel is unknown. Additional normal component measurement of Electric field along the whole boundary is used to recover the missing kernel.

The existence of a solution to this inverse problem is shown. Moreover, a constructive algorithm for approximations is designed and its convergence is established. Uniqueness is proven for a regular solution. Theoretical results are supported by a numerical experiment.

Key words: PDE's, Inverse problem, Maxwell's equations, convolution kernel, boundary measurement

Introduction

We assume that $\Omega \subset \mathbb{R}^3$ to be a bounded and connected domain where $\Omega \in C^{1,1}$ is either smooth or convex.

The starting point for the modelling of electromagnetic fields are the classical Maxwell's equations, which consist of four (Maxwell-Ampere's, Gauss electric, Faraday's and Gauss magnetic) laws

$$\begin{aligned} \nabla \times \boldsymbol{H} - \partial_t \boldsymbol{D} &= \boldsymbol{J} + \boldsymbol{J}^{app}, & \nabla \cdot \boldsymbol{D} &= \rho, \\ \partial_t \boldsymbol{B} + \nabla \times \boldsymbol{E} &= \boldsymbol{0}, & \nabla \cdot \boldsymbol{B} &= 0, \end{aligned} \tag{1}$$

The exact form of the constitutive relationships, that accomapny (1) depends on the situation under consideration. These dependencies can be linear (in linear materials) or nonlinear (in superconductors, nonlinear optics,...). Strictly speaking, from a physical point of view, relations may be hereditary. Applications can be found in chiral media [4], meta-materials [3, 2] or polarized media [5]. The authors of [1] have considered a nonlinear memory effect for polarization $\boldsymbol{P}$ of the type

$$\boldsymbol{P}(t) = (g * [\boldsymbol{E} + \boldsymbol{f}(\boldsymbol{E})])(t),$$

where the symbol $*$ stands for the convolution in time $(K * \boldsymbol{u}(\boldsymbol{x}))(t) = \int_0^t K(t-s)\boldsymbol{u}(\boldsymbol{x}, s)\,\mathrm{d}s$. The formulation from [1] can be interpreted as a generalization of the Debye or Lorentz polarization models in the sense that the polarization dynamics is driven by a nonlinear function of the electric field. In our paper we adopt a generalized Ohm's law of the following form

$$\boldsymbol{J} = \sigma * \boldsymbol{E} - 1 * \boldsymbol{g}(\boldsymbol{E}).$$

Further we assume that

$$\boldsymbol{D} = \varepsilon \boldsymbol{E} \quad \text{and} \quad \boldsymbol{B} = \mu \left(\boldsymbol{H} - 1 * \boldsymbol{f}(\boldsymbol{E}) \right)$$

with a positive variable permeability μ. Elimination of $\boldsymbol{H}$ in (1) leads to

$$\varepsilon \boldsymbol{E}_{tt} + (\sigma * \boldsymbol{E})_t + \nabla \times \left(\frac{1}{\mu} \nabla \times \boldsymbol{E} \right) = \boldsymbol{g}(\boldsymbol{E}) + \nabla \times \boldsymbol{f}(\boldsymbol{E}) - \boldsymbol{J}_t^{app}.$$

The conductivity term σ is assumed to be separable, i.e.

$$\sigma(\boldsymbol{x}, t) = \alpha(t) \tilde{\sigma}(\boldsymbol{x}),$$

where the given $\tilde{\sigma}(\boldsymbol{x})$ describes the heterogeneity of the material. We assume that $\tilde{\sigma}$ is constant along Γ with $\tilde{\sigma}|_\Gamma = \sigma^\Gamma$. The hereditary weight $\alpha(t)$ is unknown and is has to be determined. We consider boundary condition modelling a perfect contact (2) and initial data (3)

$$\boldsymbol{E} \times \boldsymbol{\nu} = \boldsymbol{0} \qquad \text{on } \Gamma, \tag{2}$$

$$\boldsymbol{E}(\boldsymbol{x}, 0) = \boldsymbol{E}_0(\boldsymbol{x}), \qquad \boldsymbol{E}_t(\boldsymbol{x}, 0) = \boldsymbol{V}_0(\boldsymbol{x}) \qquad \text{in} \Omega. \tag{3}$$

The inverse problem (IP) is to find a couple $\{\boldsymbol{E}(\boldsymbol{x}, t), \alpha(t)\}$. The missing data function $\alpha(t)$ will be recovered by means of the following measurement along Γ

$$\int_\Gamma \boldsymbol{E} \cdot \boldsymbol{\nu} \, \mathrm{d}\gamma = m(t), \qquad \text{(normal component measurement)}. \tag{4}$$

Acknowledgements

This work has been supported by the IAP P07/02 project of Belgian Science Policy (BELSPO).

References

[1] H.T. Banks and Gabriella A. Pinter. Maxwell-systems with nonlinear polarization. *Nonlinear Analysis: Real World Applications*, 4(3):483 – 501, 2003.

[2] Yunqing Huang, Jichun Li, and Qun Lin. Superconvergence analysis for time-dependent Maxwell's equations in metamaterials. *Numerical Methods for Partial Differential Equations*, 28(6):1794–1816, 2012.

[3] Yunqing Huang, Jichun Li, and Wei Yang. Solving metamaterial Maxwell's equations via a vector wave integro-differential equation. *Computers & Mathematics with Applications*, 63(12):1597 – 1606, 2012.

[4] Ioannis G. Stratis and Athanasios N. Yannacopoulos. Electromagnetic fields in linear and nonlinear chiral media: a time-domain analysis. *Abstract and Applied Analysis*, 2004(6):471–486, 2004.

[5] M. Zaslavsky and V. Druskin. Solution of time-convolutionary Maxwell's equations using parameter-dependent Krylov subspace reduction. *Journal of Computational Physics*, 229:4831–4839, 2010.

Book of abstracts of the 7th International Conference on Advanced Computational Methods in Engineering, ACOMEN 2017
18–22 September 2017.

A Novel Calderón Preconditioner for the Simulation of Conductive and High-Dielectric Contrast Media

Michiel Gossye[1], Dries Vande Ginste[1] and Hendrik Rogier[1]

[1] *Electromagnetics Group, Department of Information Technology, Ghent University*

e-mails: Michiel.Gossye@UGent.be, Dries.VandeGinste@UGent.be, Hendrik.Rogier@UGent.be

Abstract

We propose a novel Calderón preconditioner, based on the Poincaré-Steklov operator, to solve scattering problems involving (lossy) conductive and high-dielectric contrast media. The resulting system matrix is well-conditioned, independent of the specific material characteristics of the scattering media, as demonstrated by a numerical example.

Key words: Calderón preconditioning, electromagnetic scattering, Poincaré-Steklov operator, high-dielectric contrast media, boundary integral equations.

1 Formulation

The computational solution of electromagnetic scattering problems involving (piecewise) homogeneous structures can be obtained by the Method of Moments (MoM). The popularity of this method stems from the small system matrix dimensions when compared to other full-wave simulation algorithms. In general, this leads to a faster solution. However, the MoM system matrices notoriously suffer from dense-mesh and low-frequency breakdown, which worsens the convergence time and accuracy of the iterative solution. The introduction of a Calderón preconditioner in earlier research [1] solves this problem only partially, since the presence of conductive or high-dielectric contrast media still leads to bad conditioning [2]. For this reason, we introduce a Calderón preconditioned single-source equation that does not suffer from breakdown in these problematic cases.

The proposed method allows to model scattering problems with N bounded, disjunct domains $\mathcal{D}_l \in \mathbb{R}^3$, $l = 1,...,N$ with boundaries $\mathcal{S}_l$, characterized by a (complex) permittivity ε_l and permeability μ_l. These domains reside in a homogeneous background medium $\mathcal{D}_0$, defined by ε_0 and μ_0. We introduce an incident electromagnetic field $(\mathbf{e}^i, \mathbf{h}^i)$ with $e^{j\omega t}$ time dependency. In general, the field $(\mathbf{e}^s, \mathbf{h}^s)$, scattered by the media in $\mathcal{D}_l$, $l = 1,...,N$ cannot be determined analytically. Therefore, an equivalent problem is introduced, in which the medium inside each scattering domain is replaced by that of the exterior region. We impose fictitious magnetic currents $\mathbf{m}_l$, residing on $\mathcal{S}_l$, that generate the same scattered fields as in the original problem. This can be achieved by introducing a Poincaré-Steklov operator $\mathcal{P}_l$ that maps the tangential electric field on the tangential magnetic field at each boundary $\mathcal{S}_l$, and by imposing continuity of the tangential fields along $\mathcal{S}_l$. However, after discretization, the

resulting matrix equation is ill-conditioned and computationally expensive to solve. Hence, a Calderón preconditioner based on the electric field integral operator [1] is introduced. It can be shown that the accumulation points of the eigenvalue distribution of the preconditioned matrix are given by $\frac{1}{2} \pm \frac{1}{2}\sqrt{\frac{\varepsilon_0}{\varepsilon_l}}j$ and $\frac{1}{2} \pm \frac{1}{2}\sqrt{\frac{\mu_l}{\mu_0}}j$. When the permeability remains bounded, the system is well conditioned regardless of dielectric contrast, as long as $\varepsilon_l \nrightarrow -\varepsilon_0$ and $\mu_l \nrightarrow -\mu_0$.

2 Numerical Results

First, the method was verified by comparing the scattered fields of a single sphere to the Mie series solution. Second, electromagnetic scattering at a configuration consisting of four objects is considered to numerically validate the novel Calderón preconditioner, see Fig. 1(a). From Fig. 1(b), it is clear that dense-mesh breakdown does not occur, despite the presence of high-dielectric and conductive media.

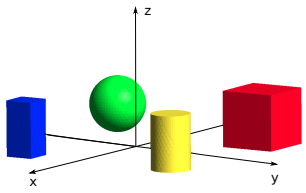

(a) Geometry of the scattering problem.

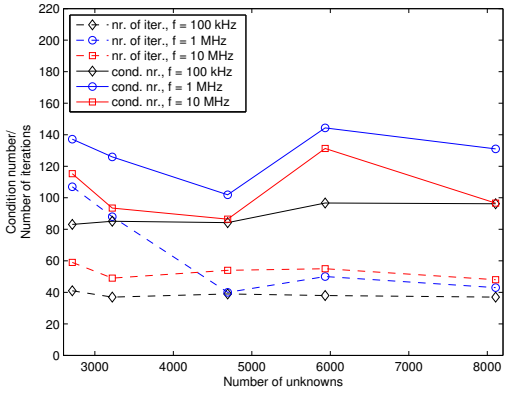

(b) Conditioning and number of iterations.

Figure 1: Scattering at a configuration consisting of a sphere ($\epsilon_r = 4$, radius = 1 m), cube ($\epsilon_r = 15$, length = 2 m), cuboid ($\epsilon_r = 100$, height = 2 m, length = 1 m) and cylinder (copper, height = 2 m, radius = 0.5 m). In (a), the geometry is visualized. In (b), the conditioning and number of iterations to reach convergence (relative error $\leq 10^{-5}$) are given as a function of the number of unknowns, for different frequencies.

Acknowledgements

The authors thank the Research Foundation Flanders (FWO) for supporting this research.

References

[1] K. Cools, F. P. Andriulli and E. Michielssen, *A Calderón multiplicative preconditioner for the PMCHWT integral equation*, IEEE Trans. Antennas Propag. **59** (2011) 4579–4587.

[2] P. Ylä-Oijala and S. P. Kiminki, *Challenges in developing efficient Calderón preconditioners for resonating or high material contrast penetrable objects*, J. Comput. Appl. Math. **289** (2015) 296–305.

Book of abstracts of the 7th International Conference on Advanced Computational Methods in Engineering, ACOMEN 2017 18–22 September 2017.

Stochastic Framework to Quantify Variability and Uncertainty in Wireless Links

Marco Rossi[1], **Dries Vande Ginste**[1] **and Hendrik Rogier**[1]

[1] *Dept. of Information Technology, Ghent University-imec*

e-mails: marco.rossi@ugent.be, dries.vandeginste@ugent.be, hendrik.rogier@ugent.be

Abstract

A stochastic framework is described to quantify the statistical distribution of the overall performance of wireless links. A generalized polynomial chaos expansion relates this distribution to variations in geometry and uncertainty in orientation and position of the receive and transmit antenna. A non-intrusive stochastic testing procedure is applied to evaluate the uncertainty on the efficiency of a wireless power transfer system.

Key words: statistics, generalized polynomial chaos, stochastic testing, electromagnetic theory

1 Stochastic framework

In a wireless link, the antenna geometries, positions and orientations will be random variables x_k. Therefore, the system performance y will be statistically distributed. Our aim is to calculate this probability density function (PDF) $d\mathcal{P}^y$, given the statistically independent input distributions $d\mathcal{P}^{x_k}$ describing the antenna variability and uncertainty. Let $\boldsymbol{x}$ be the vector containing all input random variables. To determine $d\mathcal{P}^y$, we approximate the relationship $y = f(\boldsymbol{x})$ by the generalized polynomial chaos (gPC) expansion

$$y \approx f^P(\boldsymbol{x}) = \sum_{\boldsymbol{l}=0}^{L} y_{\boldsymbol{l}}^{\boldsymbol{x}} \boldsymbol{\phi}_{\boldsymbol{l}}^{\boldsymbol{x}}(\boldsymbol{x}), \tag{1}$$

with $\boldsymbol{l} = [l_1, \ldots, l_K]$ a multi-index and with $l_1 + \ldots + l_K \leq L$. The set of expansion polynomials $\boldsymbol{\phi}_{\boldsymbol{l}}^{\boldsymbol{x}}(\boldsymbol{x})$ is composed of products of orthogonal polynomials $\phi_{l,k}(x_k)$, such that the Cameron-Martin theorem guarantees exponential convergence to $y = f(\boldsymbol{x})$. To determine the coefficients y_k^X, we enforce (1) in a set of testing points chosen according to the stochastic testing procedure [1].

The stochastic framework is now applied to quantify the uncertainty on the wireless power transfer efficiency PTE= $\eta_{\text{link}} \cdot \eta_{\text{match}} \cdot \eta_{\text{rect}}$ in a wireless power transfer (WPT) link between an MI-212-1.72.45 GHz horn antenna (transmit power 10 dBm at 2.45 GHz) and a dual-polarized textile patch antenna [2] at a distance d. A fast radiative near-field formalism [3] first computes the WPT link efficiency η_{link}, for arbitrary positions of transmitter

and receiver. On the latter antenna, a rectifier, voltage doubler and matching network deliver DC power. Harmonic balance simulation in ADS, yields the matching efficiency η_{match}, and the voltage doubler and rectifier efficiency $\eta_{\text{rect}} = P_{\text{inc}}/P_{\text{DC}}$, with $P_{\text{inc}} = \eta_{\text{match}} \cdot P_{\text{RX}}$ and $P_{\text{DC}} = V_{\text{out}}^2/R_L$.

The transmit antenna being a standard gain horn, we concentrate on random variations in dimensions and permittivity of the receive antenna. The radiation impedance $Z_{\text{RX}} = Z^{re} + jZ^{im}$ and the coefficients of the spherical harmonics expansion of the antenna pattern are expressed as gPC expansions as a function of length L, width W and relative permittivity ϵ_r. These parameters are then used to evaluate the radiative near-field link, following [3], and to calculate the wireless link efficiency η_{link} and the received power P_{RX}. The stochastic analysis accounts for random variations in the position (x, y) and rotation (θ, ϕ) of the receive antenna. The effect of all random variables on the overall PTE of the WPT system is given by

$$\text{PTE} = \sum_{\boldsymbol{l}_7=0}^{L_{\text{PTE}}} y_{\boldsymbol{l}_7}^{\boldsymbol{x}} \boldsymbol{\phi}_{\boldsymbol{l}_7}^{\boldsymbol{x}}(\mathbf{x}^{\text{WPT}}) \tag{2}$$

with $\mathbf{x}^{\text{WPT}} = [L, W, \epsilon_r, d, x, y, \theta, \phi]$ the vector of all random variables in the link. More details of the method are described in [2]

2 Results

Consider a WPT link between the standard gain horn and a rectenna on a substrate of thickness 3.94 mm and permittivity $\epsilon_r = 1.5259$ at 2.45 GHz with patch length $L = 45.3854$ mm and width $W = 44.4516$ mm, at a distance $d = 0.6$ m. L, W and $\epsilon_r$vary as independent Gaussian random variables with standard deviations $\sigma_L = 0.1628$ mm, $\sigma_L = 0.1268$ mm and $\sigma_{\epsilon_r} = 0.03190$. Antenna positions d, x, y and orientation angles θ and ϕ vary as Gaussian random variables with standard deviations $\sigma_d = 16.66$ mm, $\sigma_y = \sigma_x = 6.66$ mm and $\sigma_\theta = \sigma_\phi = 10°$. A median PTE of 0.6% is obtained, with the PTE being larger than 0.5% in 75% of the cases. The two-stage approach, where first stochastic antenna models are constructed based on full-wave simulations and then incorporated into the statistical radiative near-field link model to evaluate the distribution of the PTE reduces the simulation time to about 22 min. In contrast, a single gPC expansion directly applied to model the overall PTE requires more than 2 h. A validation based on the Monte Carlo method requires more than 41 h, since 10000 realizations need to be evaluated through full-wave simulations.

References

[1] P. Manfredi, D. Vande Ginste, D. De Zutter, and F. Canavero, "Generalized decoupled polynomial chaos for nonlinear circuits with many random parameters," *"IEEE Microw. Guided Wave Lett."*, vol. 25, no. 8, pp. 505–507, 2015.

[2] M. Rossi, G.-J. Stockman, H. Rogier, and D. Vande Ginste, "Stochastic analysis of the efficiency of a wireless power transfer system subject to antenna variability and position uncertainties," *Sensors*, vol. 16, no. 7, 2016.

[3] G. J. Stockman, H. Rogier, and D. Vande Ginste, "Efficient modeling of interactions between radiating devices with arbitrary relative positions and orientations," *IEEE Transactions on Electromagnetic Compatibility*, vol. 56, no. 6, pp. 1313–1321, Dec 2014.

Book of abstracts of the 7th International Conference
on Advanced Computational Methods
in Engineering, ACOMEN 2017
18–22 September 2017.

A Leapfrog Alternating-Direction Hybrid Implicit-Explicit FDTD Method for Local Grid Refinement

Arne Van Londersele[1], Daniël De Zutter[1] and Dries Vande Ginste[1]

[1] *Dept. of Information Technology, Ghent University-imec*

e-mails: arne.vanlondersele@ugent.be, daniel.dezutter@ugent.be, dries.vandeginste@ugent.be

Abstract

We propose a novel curl splitting technique to enhance the alternating-direction finite-difference time-domain (ADI-FDTD) method, as such allowing for a higher resolution in one or two dimensions. As our advocated approach leverages a hybrid implicit-explicit (HIE) update scheme it is named "leapfrog ADHIE-FDTD". The hybridization yields a time step that is solely bounded by the spatial steps in preferred dimensions.

Key words: Alternating-direction finite-difference time-domain (ADI-FDTD), hybrid implicit-explicit (HIE), electromagnetic theory

1 Formulation

The standard leapfrog ADI-FDTD method relies on a smart way to split the curl in Maxwell's equations without breaking the symmetry [1, 2]. Here, we propose a new type of curl splitting, resulting in a HIE scheme. Compared to ADI-FDTD, the novel scheme allows resolving structures that are fine in one or two dimensions, whilst explicit updating is used for the remaining coarsely discretized dimension(s), leading to increased accuracy and computational speed-up. Compared to the standard leapfrog Yee-FDTD and owing to the implicitization, the ADHIE-FDTD features a less stringent stability limit, rendering it computationally very efficient.

Suppose we want to resolve an object that is thin along the x-axis. Then, we propose to eliminate the x-dependence from the Courant limit by splitting the curl $C = C_0 + C_1 + C_2$ into the following three components:

$$C_0 = \begin{bmatrix} 0 & -\partial z & \partial y \\ \partial z & 0 & 0 \\ -\partial y & 0 & 0 \end{bmatrix}, \qquad C_1 = \begin{bmatrix} 0 & 0 & 0 \\ 0 & 0 & 0 \\ 0 & \partial x & 0 \end{bmatrix}, \qquad C_2 = \begin{bmatrix} 0 & 0 & 0 \\ 0 & 0 & -\partial x \\ 0 & 0 & 0 \end{bmatrix}. \tag{1}$$

The occurring derivatives are discretized by central differences on the conventional Yee lattice. The novel leapfrog ADHIE-FDTD update scheme is given by

$$\begin{bmatrix} \left(1 + \frac{\sigma Z \Delta\tau}{2}\right) I + \frac{\Delta\tau^2}{4\alpha} C_1 C_1^T & -\Delta\tau\, C \\ 0 & I + \frac{\Delta\tau^2}{4\alpha} C_2^T C_2 \end{bmatrix} \begin{bmatrix} Z^{-1}\mathbf{e}^{n+1} \\ \mathbf{h}^{n+0.5} \end{bmatrix}$$
$$= \begin{bmatrix} \left(1 - \frac{\sigma Z \Delta\tau}{2}\right) I + \frac{\Delta\tau^2}{4\alpha} C_1 C_1^T & 0 \\ -\Delta\tau\, C^T & I + \frac{\Delta\tau^2}{4\alpha} C_2^T C_2 \end{bmatrix} \begin{bmatrix} Z^{-1}\mathbf{e}^{n} \\ \mathbf{h}^{n-0.5} \end{bmatrix}, \tag{2}$$

where σ is the electrical conductivity, $Z = (\mu/\epsilon)^{1/2}$ the wave impedance, $\Delta\tau = c\Delta t$ the time step rescaled by the phase velocity $c = (\epsilon\mu)^{-1/2}$, and α is a tunable parameter.

It can be proven, following the reasoning described in [3], that a *sufficient* condition for numerical stability of the proposed scheme is given by

$$\Delta\tau < \frac{1-\alpha}{\sqrt{\frac{1}{\Delta y^2} + \frac{1}{\Delta z^2}}}\ , \quad \alpha \in]0, 1[\ . \tag{3}$$

Owing to the curl splitting (1), Δx has been eliminated from the stability limit (3). From (2) and (3), it is now clear that the parameter α controls the trade-off between accuracy and simulation speed. One the one hand, the smaller α, the larger the perturbation introduced by ADI and the larger the numerical error will be. On the other hand, a smaller α yields a larger maximum allowed time step $\Delta\tau$.

2 Results

To test the advocated method, we simulate the shielding effectiveness (SE) [4] of a thin metallic sheet of infinite dimensions placed in the yz-plane. The sheet has a thickness of 10 μm in the x-dimension and a conductivity $\sigma = 10^7$. It is illuminated by a z-oriented electric dipole placed at a distance of 150 mm before the shield. The simulation domain is terminated by means of perfectly matched layers (PML) and the grid contains $16 \times 16 \times 164$ cells. In ADHIE-FDTD, the cell size is given by $\Delta x = \Delta y = \Delta z = 1.875$ mm everywhere, except in the thin sheet, where $\Delta x_{\text{sheet}} = 0.15873$ μm. Consequently, locally, the refinement ratio along the x-axis is very large, i.e. $\Delta x/\Delta x_{\text{sheet}} > 10^4$.

When sweeping the parameter α from 0.25 to 0.90, we observe that the relative accuracy on the SE at a frequency of 10 GHz varies from 5% to a few tens of one percent, where standard Yee-FDTD was used as a reference method. This validates the accuracy of our technique. Moreover, whereas in Yee-FDTD, the time step has to be chosen at $c\Delta t = 159$ nm to resolve the thin sheet, in our ADHIE-FDTD this time step can be chosen between 0.1 mm up to 1 mm. As the required CPU time scales as $1/\Delta t$, the novel scheme is clearly much faster than traditional methods.

References

[1] F. Zheng, Z. Chen, and J. Zhang, "A finite-difference time-domain method without the Courant stability conditions," *IEEE Microwave and Guided Waves Letters*, vol. 9, no. 11, pp. 441–443, Nov. 1999.

[2] S.-C. Yang, Z. Chen, Y. Yu, and W.-Y. Yin, "An unconditionally stable one-step arbitrary-order leapfrog ADI-FDTD method and its numerical properties," *IEEE Transactions on Antennas and Propagation*, vol. 60, no. 4, pp. 1995–2003, Apr. 2012.

[3] B. Denecker, L. Knockaert, F. Olyslager, and D. De Zutter, "A new state-space-based algorithm to assess the stability of the finite-difference time-domain method for 3D finite inhomogeneous problems," *AEU - International Journal of Electronics and Communications*, vol. 58, no. 5, pp. 339–348, 2004.

[4] C. R. Paul, *Introduction to Electromagnetic Compatibility*, 2nd ed. John Wiley & Sons, Inc., 2006.

MS 7 Electrokinetic and electrochemical flows for batteries and fuel cells: analysis, simulation, upscaling

Organiser: Matteo Icardi, Thomas Carrao

Description: Charged particles and electrochemistry are present in a large number of important applications such as energy storage, automotive, consumer electronics, biological membranes. Here, a number of difficulties arise when coupling the fluid flow equations with electrostatic forces, electrochemical reactions, and porous structures. From the modelling perspective, due to the extreme complexity of the physics involved, depending on the scale of interest, many assumptions can be made, such as electro-neutrality, effective reaction rates, mean field approximations. Despite these assumptions the resulting PDE system is often non-linear and tightly coupled. The analysis of these equations and the development of robust numerical discretisation schemes are often challenging. Furthermore, issues like parametrisation, uncertainty and overall validity of the models at the different scales, make the actual simulation of these devices often not yet fully predictive.

Book of abstracts of the 7th International Conference on Advanced Computational Methods in Engineering, ACOMEN 2017 18–22 September 2017.

Theoretical and Computational Investigation of Charge Transport in All-Solid-State Thin Film Cells

Katharina Becker-Steinberger[1,2], Simon Schardt[1,3], Marie Preusse[1,3] and Arnulf Latz[1,2,4]

[1] *Electrochemical Multiphysics Modelling, Helmholtz Institute Ulm for Electrochemical Energy Storage (HIU)*

[2] *Institute of Engineering Thermodynamics, German Aerospace Center (DLR)*

[3] *Kahrlsruhe Institute of Technology (KIT),*

[4] *Institute of Electrochemistry, University of Ulm*

e-mails: Katharina.Becker-Steinberger@dlr.de, Simon.Schardt@kit.edu, Marie.Preusse@kit.edu, Arnulf.Latz@dlr.de

Abstract

We will present a rigorous, mathematical and physical derived model for charge transport in all-solid-state battery (ASSB) thin film cells based on the solid electrolyte (SE) model presented in [1]. Space charge layer (SCL) formation and charge transport in the SE is described by the continuity equation for the cation concentration, quasi-static momentum equation and Poisson's equation. The electric SCLs in the electrodes are approximated as an ideal plate capacitor. The charge transfer at the electrified electrode-SE interface is modeled by a Butler-Volmer like approach [2, 3]. The resulting model for a complete ASSB cell resolves the ionic SCL and couples to intercalation electrodes by taking account of the effects of the electric SCLs without detailed resolution. Long time behaviour is investigated by energy and entropy laws. Further, numerical results are presented.

Key words: all-solid-state batteries, Butler-Volmer approach, electro-reaction-diffusion systems, well-posedness

1 Introduction

SEs have experienced a growing interest in recent years as potential future components of safe next-generation high voltage batteries. The physical processes inside SEs are governed by the material properties of the utilized solids and the characteristics of the interfaces between the other components. Particularly, the processes at the interfaces resulting in SCLs are considered to be responsible for the present limitations of ASSBs.

The classical Poisson-Nernst-Planck (PNP) approach for ion transport in a self-consistent electric field is known to fail at the interfaces, since it neglects the high pressures induced by Maxwell-stress and it does not account for species interaction and volume constraints. But understanding and facing the various challenges of ASSBs requires fundamental knowledge of the underlying interfacial processes. For this reason, the rigorously derived transport model for SEs [1] is extended to ASSB thin film cells.

2 The Mathematical Model

Crystalline SEs are single ionic conductors containing one immovable constituent—the anions. Mass and charge transport within SEs is considered as a hopping mechanism, where cations move to adjactent free cation sides. As shown in [1], the barycentre in SEs moves relatively to the stationary anion lattice and ion transport is given only by one independent diffusional cation flux, which depends on the chemical potentials $\mu_\alpha, \alpha = +, -, v$ of all species. In the case of incompressible SEs the cation flux obeyes a gradient flow structure, where the driving force is given by the negative gradient of the effective electrochemical potential $\psi_{SE} = \tilde{\mu}_+(c_+, p) + \tilde{z}_+\phi$ of the SE

$$\boldsymbol{N}_+ = -L\nabla\psi_{SE} = -L\left(\frac{\partial\tilde{\mu}_+}{\partial c_+}\nabla c_+ + \frac{\partial\tilde{\mu}_+}{\partial p}\nabla p + \tilde{z}_+\nabla\phi\right).$$

Depending on the underlying free energy approach different driving forces may be derived. On the relevant time scale, the coupled system of partial differential equations (PDEs) for isothermal, incompressible SEs consists only of the continuity equation for the cation concentration c_+, a force balance to determine the pressure p, and Poisson's equation specifying the electric potential ϕ response on the charge density q

$$\begin{aligned}\partial_t c_+ + \nabla\cdot\frac{\rho}{\rho_-}\boldsymbol{N}_+ &= 0,\\ \nabla p &= -q\nabla\phi,\\ -\nabla\cdot\epsilon_0(1+\chi)\nabla\phi &= q.\end{aligned}$$

The ionic SCLs in the SE are explicitly resolved. On the other hand, since the thickness of the charge compensating electric SCLs in the electrodes is in the order of angstrom, they may be approximated as an ideal plate capacitor. The SE model is coupled to intercalation electrodes by a Butler-Volmer like approach as well as suitable jump conditions.

The resulting system of PDEs for charge transport in ASSB cells is a generalised electro-reaction-diffusion system on different domains.

3 Long-time Behaviour via Energy and Entropy Laws

The model equations include several model assumptions. The question arise, whether the derived model is still in conformity with thermodynamics. For that reason, we will apply the energy and entropy laws to show the thermodynamic correctness via existence of a weak Lyapunov function. In a way, it is an adoption of the second law of thermodynamics to a mathematical model.

References

[1] S. Braun, C. Yada, A.Latz, *Thermodynamically Consistent Model for Space-Charge-Layer Formation in a Solid Electrolyte* J. Phys. Chem. C, 1119 (2015) 22249–22746.

[2] A. Latz, J. Zausch, *Thermodynamic derivation of a Butler-Volmer model for intercalation in Li-ion batteries* Electrochim. Acta, **110** (2013) 358–362.

[3] J. Lück, A. Latz, *Theory of reactions at electrified interfaces* Phys. Chem. Chem. Phys 18(27) (2016) 17799–804.

Book of abstracts of the 7th International Conference
on Advanced Computational Methods
in Engineering, ACOMEN 2017
18–22 September 2017.

Adaptive finite element approaches for microscopic and macroscopic simulations of battery electrodes

Thomas Carraro[1] **and Sven Wetterauer**[1]

[1] *Institute for Applied Mathematics,*
Interdisciplinary Center for Scientific Computing (IWR), Heidelberg University

e-mails: thomas.carraro@iwr.uni-heidelberg.de,
sven.wetterauer@iwr.uni-heidelberg.de

Abstract

We present several approaches for adaptive solutions with finite elements of microscopic and macroscopic models for lithium ion battery electrodes.

Key words: Adaptive FEM, Goal oriented error estimation, XFEM, Li-ion battery eletrodes
MSC 2010: 65M60, 97N80, 97N40, 65M50

1 Introduction

A state of the art Lithium-ion cell consists of two porous electrodes (anode and cathode) whose porosity is filled with liquid electrolyte that serves as an ionic connection between the two electrodes, while in the crystal structure of the active material Lithium can be stored. The electrochemical phenomena that have to be taken into account in numerical simulations have a multiscale character and this aspect has to be considered in modelling and simulation.

2 Macroscopic problem

For the upscaling of the mathematical models of the electrochemical processes some auxiliary problems (called cell problems) have to be solved. Since this part of the model captures the microscopic effects, it needs appropriate numerical methods to describe the microscopic porous electrode microstructures, see Figure 1(a). We show numerical methods based on adaptive finite elements for the solution of the cell problems. In addition, we present an adaptive method for an upscaled Newman-type battery model based on the work [2].

3 Numerical methods

For the simulation of complex microstructures we show a 3D adaptive XFEM implementation [1] based on a goal oriented error estimator. Through this method, the mesh is refined only according to a "macroscopic" quantity of interest as needed on homogenization problems [3], see Figure 1(b). A central role in our microstructure simulations is played by the implicit

description of the material interface. We present an effective combination of spherical harmonical functions, level-set method and XFEM discretization to compute effective quantities needed for the upscaling, see Figures 1(b) and 1(d).

For the simulation of the macroscopic battery model, a time-space adaptive finite element method is under development and first numerical results are presented.

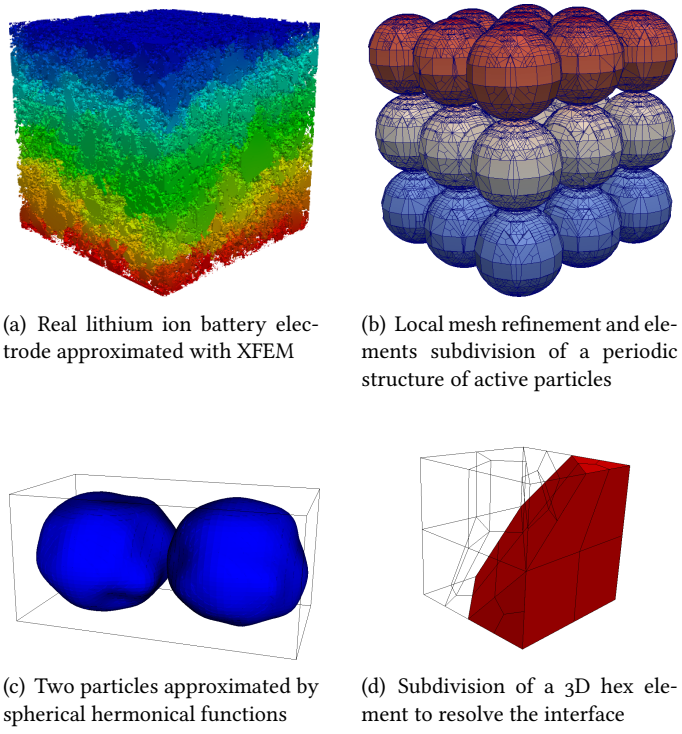

(a) Real lithium ion battery electrode approximated with XFEM

(b) Local mesh refinement and elements subdivision of a periodic structure of active particles

(c) Two particles approximated by spherical hermonical functions

(d) Subdivision of a 3D hex element to resolve the interface

Figure 1: Approximations of 3D microstructures with adaptive XFEM.

Acknowledgements

This work has been supported by the DFG grant CA 633/2-1 "*Multiscale modeling and numerical simulations of Lithium ion battery electrodes using real microstructures*" and the BMWi grant "*HiKoMat - Material development of hierarchically structured composite materials for electrochemical energy storage*".

References

[1] T. Carraro, S. Wetterauer, *On the implementation of the eXtended Finite Element Method (XFEM) for interface problems*, Archive of Numerical Software **4(2)** 2016 1–23.

[2] M. Ender, *An extended homogenized porous electrode model for lithium-ion cell electrodes*, Journal of Power Sources **282** (2015) 572–580.

[3] T. Carraro, C. Goll, *A Goal-Oriented Error Estimator for a Class of Homogenization Problems*, Journal of Scientific Computing **71(3)** (2017) 1169–1196.

Book of abstracts of the 7th International Conference
on Advanced Computational Methods
in Engineering, ACOMEN 2017
18–22 September 2017.

An Elliptic Problem with Strongly Nonlinear Interface Condition

Willy Dörfler[1]

[1] *Institute for Applied and Numerical Mathematics 2, Karlsruhe Institute for Technology (KIT)*

e-mails: willy.doerfler@kit.edu

Abstract

We consider a system of partial differential equations arising in the modeling of the electrochemical processes in Li-ion batteries. In this simplification it consists of two elliptic equations in two domains separated by an interface. At the interface holds a Neumann condition that depends exponentially on the jump of the solution at the interface (ButlerâĂŞVollmer equation). We prove unique existence of a solution and a comparison principle. We further discretise this problem with a finite element method and show its convergence. (Joint work with Markus Maier)

Book of abstracts of the 7th International Conference
on Advanced Computational Methods
in Engineering, ACOMEN 2017
18–22 September 2017.

Numerical Simulation of Flowing Slurry Electrodes

L. Feierabend[1], B. Oberschachtsiek[1], J. Wartmann[1], A. Kempf[2] and A. Heinzel[1]

[1] *The fuel cell research center ZBT GmbH, Duisburg, Germany,*

[2] *Chair of Fluid Dynamics, University of Duisburg-Essen*

e-mails: l.feierabend@zbt-duisburg.de, b.oberschachtsiek@zbt-duisburg.de, j.wartmann@zbt-duisburg.de, andreas.kempf@uni-due.de, a.heinzel@zbt-duisburg.de

Abstract

A numerical model to simulate the three-dimensional coupled transport and reaction phenomena in slurry electrodes is presented. The model can predict the influence of composition and flow conditions of the anodic zinc-electrolyte suspension on the overall performance of zinc-air flow batteries. The governing equations describing the electrolyte flow, concentration as well as potential distributions are discretized by finite volumes and are coupled to a Lagrangian description of the discrete zinc particles.

Key words: slurry electrode, multiphase flow, percolation, finite volume method, discrete element method

1 Introduction

The investigated slurry electrode is composed of microscopic zinc particles suspended in a gelled aqueous electrolyte solution. Within the battery cell, the suspension is transported through flow channels, which are bounded by a separator, a current collector and, if applicable, electrochemically inactive channel walls. During discharge, the metallic zinc particles act as the anode electrode, if an electrical contact is established to the current collector. The active electrode surface area, and consequently the maximum discharge power density, then depend on the dynamic percolation network in the flowing slurry.

2 Model Description

The partial differential equations for momentum, species, charge and energy are discretized by the finite volume method and implemented in the OpenFOAM library [1]. The particle motion including multiple simultaneous particle contacts is described with the discrete element method using the LIGGGHTS library [2]. Coupling between the particle and fluid phase is realized with the CFD-DEM method using the CFDEM library [2], where an empirical description accounts for the momentum exchange between the viscous, non-Newtonian fluid and the densely distributed particles. A half-cell model for the anode part of the zinc-air

flow battery is implemented, which accounts for the flow characteristics via the described CFD-DEM coupling method. Simultaneously, the charge and species transport is considered according to the porous electrode theory as described by [3] and [4]. In contrast to previous models, the heterogeneous local porosities change temporally depending on the evolving particle distributions. Additionally, the active electrode surface area in each finite volume is dependent on the percolation network from the considered local point to the current collector surface. The percolation probability is estimated via statistical means from previously conducted CFD-DEM simulations for the prevalent flow conditions in the considered anode setups. Fig. 1 shows the instantaneous (a) and time-averaged (b) fraction of particles in contact with the current collector within flowing, pseudoplastic sample slurries.

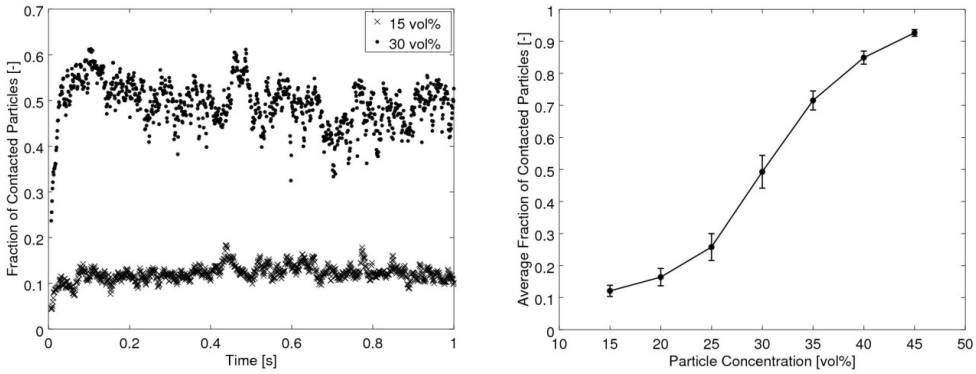

(a) Dynamic percolation for two particle concentrations

(b) Time-averaged percolation depending on concentration including the standard deviation from the mean value

Figure 1: Percolation behavior of uniform, spherical particles in a flowing slurry electrode

Acknowledgements

Funding by the Federal Ministry for Economic Affairs and Energy (BMWi) within the projects ZnPLUS (FKZ 03ESP217C) and ZnMobil (FKZ 03ET6090G) is gratefully acknowledged.

References

[1] H. G. Weller, G. Tabor, H. Jasak, C. Fureby, *A tensorial approach to computational continuum mechanics using object-oriented techniques*, COMPUT PHYS **12(6)** (1998) 620–631.

[2] C. Kloss, C. Goniva, A. Hager, S. Amberger, S. Pirker, *Models, algorithms and validation for opensource DEM and CFD-DEM*, PROG COMPUT FLUID DY **12(2/3)** (2012) 140–152.

[3] R. Smith, M. Bazant, *Multiphase Porous Electrode Theory*, J. Electrochem. Soc. **164(11)** (2017) E3291–E3310.

[4] J. Newman, K. Thomas-Alyea, *Electrochemical Systems*, 3rd ed. Wiley-Interscience, 2004.

Book of abstracts of the 7th International Conference
on Advanced Computational Methods
in Engineering, ACOMEN 2017
18–22 September 2017.

Stress simulation of phase-separating cathode materials

Tobias Hofmann[1], Ralf Müller[2], Heiko Andrä[1] and Jochen Zausch[1]

[1] *Material and flow simulation, Fraunhofer Institute of Industrial Mathematics ITWM, Kaiserslautern, Germany*

[2] *Chair of Applied Mechanics, University of Kaiserslautern, Germany*

e-mails: tobias.hofmann@itwm.fhg.de, ram@rhrk.uni-kl.de, heiko.andrae@itwm.fhg.de, jochen.zausch@itwm.fhg.de

Abstract

An electro-chemical Cahn-Hilliard model for the phase-separation in lithium iron phosphate is introduced. A linear elastic model describes small deformations of the electrode material due to intercalation. The coupling effects are studied on three-dimensional microstructures for different material parameters and boundary conditions.

Key words: phase-field model, Cahn-Hilliard equation, Butler-Volmer kinetics, intercalation, lithium-ion battery
MSC 2010: 35K59, 65M08, 74N25, 82B26, 82C26

1 Electro-chemical model

Some cathode materials in lithium-ion batteries show phase-separation during usage. The imbalanced intercalation of the lithium ions into the lattice causes large concentration gradients. The stresses resulting from these gradients can damage and destroy the battery cell. The computer simulation of the stresses during charging and discharging can support the development of battery cell structures.

A model coupling lithium-ion diffusion to the electric potential, Butler-Volmer interface currents and linear elasticity is shown. A phase-field method with the Cahn-Hilliard equation is used to model the phase-separation of lithium-rich and lithium-poor phases. The complex three-dimensional microstructure of the anode and cathode material in the liquid electrolyte is resolved. The phase separation dynamics of lithium ions is described based on a micromodel [1]. It is coupled to the electrolyte phase by Butler-Volmer interface currents [2]. Additionally mechanical stresses resulting from concentration-dependent strains [3] are computed.

2 Numerical method

A fast immersed boundary method is presented. A three-dimensional finite-volume discretization on a periodic regular voxel mesh is used in combination with fast elliptic solvers. The domain decomposition uses the explicit jump method [4]. The semi-implicit time discretization is stable and enables larger time steps [5] in the time integration.

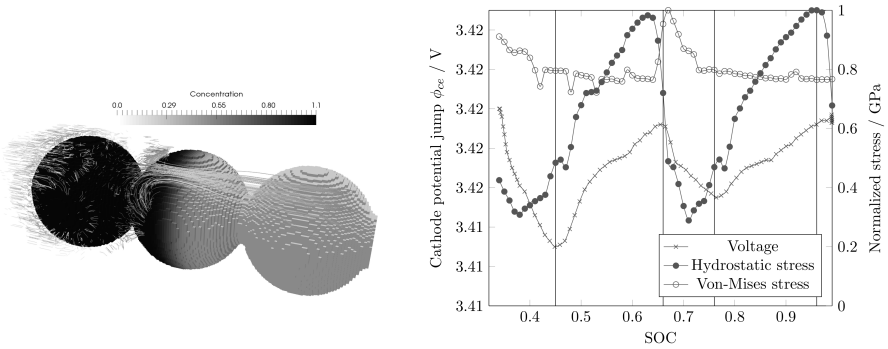

Figure 1: Left: Phase-separating cathode microstructure of three spherical particles. Depicted is the concentration inside the electrode and the lithium ion current in the electrolyte. Right: Cell voltage and maximum non-dimensionalized stress invariants occuring in the electrode during a charge cycle.

3 Numerical tests

Figure 1 shows on the left the phase separation in a cathode microstructure made from three spherical particles. On the right, the cell voltage and non-dimensionalized maximum stress invariants occuring in the electrode during a charge cycle are depicted. The simulation results of the phase separation are interpreted to allow for qualitative and quantitative prediction of damage and fracture resulting from multiple charge cycles by extension of the linear elastic model to e.g. include large deformations.

References

[1] Latz, A., Zausch, J., *Thermodynamic consistent transport theory of Li-ion batteries*, J. Power Sources **196 (6)** (2011) 3296-3302.

[2] Hofmann, T., Müller, R., Andrä, H., Zausch, J., *Numerical simulation of phase separation in cathode materials of lithium ion batteries*, Int. J. Solids and Structures Geom. **100-101** (2016) 456-469.

[3] Zhang, X., Shyy, W., Sastry, A.M., *Numerical simulation of intercalation-induced stress in Li-ion battery electrode particles*, J. Electrochem. Soc. **154 (12)** (2007) 661–692.

[4] Wiegmann, A., Bube., K.P., *The Explicit-jump immersed interface method: Finite difference methods for PDEs with piecewise smooth solutions*, SIAM J. Num. Anal. **37 (3)** (2000) 827-862.

[5] Eyre, D., *Unconditionally gradient stable time marching the Cahn-Hilliard equation*, MRS Proceedings **529** (1998)

Book of abstracts of the 7th International Conference on Advanced Computational Methods in Engineering, ACOMEN 2017 18–22 September 2017.

Spectral analysis and model reduction of Newman-type battery models for improved calibration and control

Matteo Icardi[1] **and Florian Theil**[1]

[1] *Mathematics Institute, University of Warwick, Coventry, UK*

e-mails: m.icardi@warwick.ac.uk,

Abstract

Lithium-ion batteries present many modelling challenges, including complex electrochemical reactions, transport in porous heterogeneous materials, multi-scale structures, etc. Several approaches have been developed to describe and numerically solve micro- or meso-scale equations. However, for practical applications such as hybrid vehicles, there is an increasing need of fast online, yet accurate, simple reduced models. State-of-the-art macroscopic models for battery applications are defined by system identification techniques and fail to capture the intrinsic functional dependence of the parameters on the material attributes and to predict irreversible and complex non-linear phenomena such as fast (dis)charge and degradation. We present an analytical approach for model reduction, based on spectral analysis of the underlying PDEs, to develop simple and efficient reduced order models, as an alternative to classical equivalent circuit models. Starting from the well-know porous electrode theory and Newman's model, we derive and solve simple differential equations that can retain the interesting features of the full model (e.g., solid diffusion, non-linearities). This model can easily be implemented in online battery management systems and can be coupled with data assimilation and control techniques. We also discuss the possibility of a full multi-scale approach by integrating pore-scale analysis of the porous micro-structures via fully resolved direct numerical simulations.

Key words: Lithium-ion batteries, Model reduction, Porous Media, Spectral analysis, Asymptotic expansion

1 Newman's model

Following [1], the electric potential in the solid and electrolyte phases is governed by:

$$\nabla \cdot \left(\sigma \nabla \phi_s\right) = A_s j_{BV}, \qquad \sigma \frac{\partial \phi_s}{\partial n}\Big|_{x=0} = \pm \frac{I}{A} \qquad \frac{\partial \phi_s}{\partial n}_{x=L} = 0 \tag{1}$$

$$\nabla \cdot \left(\kappa \nabla \phi_e + \kappa_D \nabla \log c_e\right) = -A_s j_{BV}, \qquad \frac{\partial \phi_e}{\partial n}\Big|_{x=0,L} = 0 \tag{2}$$

The equation for the ionic concentration c_e is

$$\frac{\partial c_e}{\partial t} - \nabla \cdot (D_e \nabla c_e) = \frac{1 - t_+^0}{F\varepsilon} j_{BV}, \qquad D_e \frac{\partial c_e}{\partial n}_{x=0,L} = 0 \tag{3}$$

where A is the surface area of the current collector, A_s is the specific surface area of the particles, and I is the applied current. F is the Faraday constant, t_+^0 is the transference number, ε is the porosity, ϕ are the potential fields and c is the ionic concentration where subscripts e represent electrolyte and s the solid phase. The reaction term j_{BV} that is the current source given by Butler-Volmer equation

$$j_{BV} = j_{BV}(x) = i_0 \sinh\left(\frac{\alpha F}{RT}\eta\right) \tag{4}$$

where R is the universal gas constant, F is the Faraday constant, α is the transfer coefficient for an electrode reaction (assumed equal for anode and cathode, equal to 0.5). i_0 and η are, respectively, the exchange current density of an electrode reaction, and the overpotential

$$i_0 = i_0(c_s, c_e) = K c_e^{\alpha}(c_{s,max} - c_s)^{\alpha} c_e^{\alpha} \tag{5}$$

$$\eta = \eta(\phi_e, \phi_s, c_s) = \phi_s - \phi_e - U_0\left[\frac{c_s}{c_{s,max}}\right] \tag{6}$$

with constants $c_{s,max}$, K and open-circuit potential function U_0. The solid surface concentration $c_s = c_s(x)$ in these expressions is given by the Dirichlet boundary value of:

$$\frac{\partial \gamma}{\partial t} - \nabla \cdot \left(D_s \nabla \gamma\right) = 0, \text{in } \Omega_s \qquad D_s \frac{\partial \gamma}{\partial n}|_{\Gamma_s} = \frac{1}{F} j_{BV} \tag{7}$$

2 Reduced model

Assuming spherical particles, neglecting c_e, and linearising the Butler-Volmer relation $j_{BV} = a_0 + a_c c_s + a_\phi \phi_s$ We can analytically obtain:

$$\phi_s(L_1, t) - \phi_s(0, t) = \int_0^t \mathcal{K}(t-\tau)\, I(\tau)\, \mathrm{d}\tau.$$

$$\mathcal{K}(t) = \sum_l \frac{L^2}{2\pi^2 l^2}\, \hat{\chi}_{2l}\, K_l', \qquad K_l' = \sum_k \mathrm{e}^{-\alpha_k(\theta_{2l})^2 t}$$

with $\alpha_k(\theta_l) > 0$ is k^{th} solution of $\theta \tan(\alpha) = \alpha$ with $\theta_l = \frac{Ra_c}{D_s F}\frac{1}{1+\frac{Aa_\phi L^2}{\sigma\pi^2 l^2}} + 1$ and $\hat{\chi}_l = \frac{2}{L}\frac{1}{A_s b + \sigma\pi^2 l^2}$

The kernels $\mathcal{K}$ and K_l' are the key quantities needed for understanding the full dynamics of the system for the macroscopic quantities of interest.

Acknowledgements

This work has been partially supported by AVL.

References

[1] M. Doyle, J. Newman, The use of mathematical modeling in the design of lithium/polymer battery systems, Electrochim. Acta **40** (1995) 2191–2196.

[2] M. Icardi, F. Theil, Spectral analysis and model reduction of Newman-type battery models, submitted.

Book of abstracts of the 7th International Conference on Advanced Computational Methods in Engineering, ACOMEN 2017
18–22 September 2017.

A chemo-mechanical model of the response of electrode particles in Li-ion batteries

Marco Magri[1], Alberto Salvadori[1], Robert McMeeking[2,3,4] and Davide Grazioli[5]

[1] *DICATAM - Dipartimento di Ingegneria Civile, Architettura, Territorio, Ambiente e di Matematica, Università di Brescia, via Branze 43, 25123 Brescia, Italy*

[2] *Materials and Mechanical Engineering Departments, University of California, Santa Barbara CA 93106, USA*

[3] *School of Engineering, University of Aberdeen, King's College, Aberdeen AB24 3UE, UK*

[4] *Leibniz Institute for New Materials, Campus D2 2, Saarbruecken, Germany*

[5] *Faculty of Civil Engineering and Geosciences, Delft University of Technology, P.O. Box 5048, 2600 GA Delft, The Netherlands*

e-mails: m.magri007@unibs.it, alberto.salvadori@unibs.it, rmcm@engineering.ucsb.edu, d.grazioli@tudelft.nl

Abstract

This work sets forth a new model of the response of active particles during insertion and extraction of lithium ions in the electrodes of Li-ion batteries. The phase changes during insertion are described via trapping of interstitial lithium with its own chemical kinetics. Non convex free energies are derived accordingly. Numerically obtained evolution of stored lithium will be presented.

Key words: Lithium batteries, trapping reaction, phase transition

1 Introduction

$LiCoO_2$ provides good capacity, high energy density, good power rates and cycle life. Such a favorable electrochemical behavior is associated with a sequence of phase transitions, which progressively change the crystal structure [1]. A recent formulation [3] of a fully coupled model for mass, mechanics, and chemical reactions applies well to the insertion and removal of a mobile guest species into a stable host crystal structure. Structural changes are modeled here through trapping of Li ions, which allows modeling phase segregation.

2 Modeling and Simulations

The trapping process of lithium is described as a chemical reaction:

$$\mathrm{Li}_L \leftrightharpoons \mathrm{Li}_T \tag{1}$$

which portrays the conversion of mobile (L) to trapped (T) species and vice-versa by the rate of reaction $w^{(1)}$. The mass and force balance equations yield:

$$\frac{\partial c_L}{\partial t} + \mathrm{div}\,[\mathbf{h}_\mathrm{L}] + \mathrm{w}^{(1)} = 0, \qquad \frac{\partial \mathrm{c_T}}{\partial \mathrm{t}} - \mathrm{w}^{(1)} = 0, \qquad \mathrm{div}\,[\boldsymbol{\sigma}] + \mathbf{b} = \mathbf{0}. \tag{2}$$

Symbols in equations (2) have the following meaning: c_β (with $\beta = L, T$) is the *molarity* of a generic species Li_β, $\mathbf{h}_L$ is the mass flux of species Li_L, $\boldsymbol{\sigma}$ is the stress tensor, and $\mathbf{b}$ is the body force.

Constitutive laws are derived from rigorous thermodynamic principles, assuming a visco-plastic response of the host material. The governing equations for mass, chemical reaction, and mechanics are fully coupled. They have been numerically solved through an Abaqus User Element Subroutine (UEL) to simulate the response of $LiCoO_2$ particles at different C-rates. The influence of material parameters on the lithium profiles and on the state of stress is investigated in realistic geometries and boundary conditions.

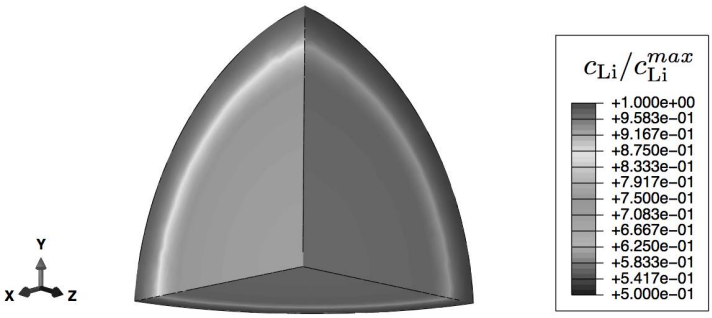

Figure 1: *Contour plot of Li concentration during Li insertion in a spherical particle under condition of radial symmetry. The lithium distribution shows two distinct phases separated by a steep gradient in space.*

References

[1] Reimers, Jan N. and Dahn, J. R., *Electrochemical and In Situ X - Ray Diffraction Studies of Lithium Intercalation in Li_xCoO_2*, J. Electrochem. Soc. **139** (1992) 2091–2097.

[2] Grazioli, D., Magri, M. and Salvadori, A., *Computational modeling of Li-ion batteries*, Comput. Mech. **58** (2016) 889–909.

[3] Salvadori, A., McMeeking, R., Grazioli, D. and Magri, M., *A coupled model of transport-reaction-mechanics with trapping. Part I-small strain analysis*, Submitted to International Journal of Engineering Science

Book of abstracts of the 7th International Conference on Advanced Computational Methods in Engineering, ACOMEN 2017
18–22 September 2017.

Consistent coupling of charge transport and fluid flow with application to nanopores

Wolfgang Dreyer[1], Jürgen Fuhrmann[1], Clemens Guhlke[1] and Rüdiger Müller[1]

[1] *Weierstrass Institute,*

e-mails: dreyer@wias-berlin.de, fuhrmann@wias-berlin.de, guhlke@wias-berlin.de, mueller@wias-berlin.de

Abstract

The coupling of ion transport by diffusion and migration to the fluid flow of a liquid electrolyte gives rise to subtle compatibility conditions for the constitutive equations. In the electrolyte model of [1] the coupling is realized by a free energy density that contains the elastic energy in addition to the well known contributions from configurational entropy. We discuss the implications of the coupling conditions and the resulting challenges for the solution of the system. For the application to the flow in a nanopore with charged pore walls, we present a numerical method and a dimension reduction approach for simple symmetric cases.

Key words: modeling, nanopores, Nernst-Planck, numerical methods

1 Electrolyte Model

We consider a liquid electrolyte and let n_α with $\alpha \in \{1, \dots, N\}$ denote the number densities of the different species in the solution while n_0 is the number density of the solvent. The total mass density is $\rho = \sum_{\alpha=0}^{N} m_\alpha n_\alpha$ and $\boldsymbol{v} = \rho^{-1} \sum_{\alpha=0}^{N} m_\alpha n_\alpha \boldsymbol{v}_\alpha$ is the barycentric velocity, where $\boldsymbol{v}_\alpha$ denotes the velocity of species α. The free charge is given by $q = \sum_{\alpha=0}^{N} z_\alpha n_\alpha$, where z_α is the charge number of species α. Let φ be the electrostatic potential such that the electric field is $E = -\nabla\varphi$. Independent of the specific material under consideration, there is a universal set of equations describing the evolution of the electrolyte that according to [1] reads for the isothermal case and with quasi-static momentum balance

$$\partial_t n_\alpha + \operatorname{div}(n_\alpha \boldsymbol{v} + \tfrac{1}{m_\alpha} \boldsymbol{J}_\alpha) = r_\alpha \qquad \text{for } 0 \neq \alpha = 1, 2, \dots, N, \tag{1}$$

$$\partial_t \rho + \operatorname{div}(\rho \boldsymbol{v}) = 0\,, \tag{2}$$

$$\operatorname{div}(\boldsymbol{\sigma}) = q \nabla\varphi\,, \tag{3}$$

$$-(1+\chi)\varepsilon_0 \Delta\varphi = q\,. \tag{4}$$

The newly introduced variables above are the diffusive fluxes $\boldsymbol{J}_\alpha$, the production rates r_α due to chemical reactions and the stress tensor $\boldsymbol{\sigma}$. They can be determined by the assumption of a free energy density $\rho\psi(T, n_0, \dots, n_N) - \chi \frac{\varepsilon_0}{2} |\nabla\varphi|^2$ and exploitation of the 2nd law of thermodynamics.

While the classical Poisson-Nernst Planck system consists only of the subsystem (1) and (4), the full set of equations above requires for a consistent coupling to fluid flow the compatibility of the flux $\boldsymbol{J}_0$ of the solvent that $\sum_{\alpha=0}^{N} \boldsymbol{J}_\alpha = 0$. Moreover, with the introduction of the chemical potentials as $\mu_\alpha := \frac{\partial \rho\psi}{\partial n_\alpha}$, the mass conservation requires to take the ion-solvent interaction into account, such that for the simple case of a diagonal mobility matrix the mass flux $\boldsymbol{J}_\alpha$ for $\alpha = 1, \ldots, N$ is

$$\boldsymbol{J}_\alpha = -M_\alpha(\nabla\mu_\alpha - \tfrac{m_\alpha}{m_0}\nabla\mu_0 + z_\alpha e_0 \nabla\varphi). \tag{5}$$

Introducing the pressure p by means of the Gibbs-Duhem relation $p = -\rho\psi + \sum_{\alpha=0}^{N} m_\alpha n_\alpha \mu_\alpha$, we see that in general the chemical potentials μ_α and the fluxes $\boldsymbol{J}_\alpha$ are functions of p, thereby linking the Nernst-Planck system to the fluid flow. We emphasize that incompressibility of a mixture in general does not imply constant mass density ρ leading to the usual divergence constraint $\operatorname{div}(\boldsymbol{v}) = 0$. Instead, incompressibility is characterized by a linear dependence of the chemical potentials μ_α on p, cf. [4].

2 Application to flow in nanopores

Biological as well as synthetic nanopores are used for various microfluidic applications, like e.g. sensing of large molecules like proteins and DNA strands. Since the pore walls are typically carrier of surface charge, there are space charge layers formed in the electrolyte. Due to the small diameter of the pores, these layers may occupy large portions of the pore volume. For the accurate numerical simulation of the charge layers, structure preserving finite volume discretizations of the Nerst-Planck system [2] are applied. Inside the space charge layers the electric field causes the pressure to rise to extremely high level. Thus, when coupling the charge transport to the fluid flow, novel so called pressure robust finite element methods [3] are used. Then, adequate post processing can in turn provide pointwise divergence free velocity fields as an input for the Nerst-Plack subsystem while keeping the structure of the Helmholtz decomposition.

Acknowledgements

This work is partially supported by funding from the Einstein Foundation Berlin within the Research Center Matheon under the ECMath Project CH11 “Sensing with Nanopores”.

References

[1] W. Dreyer, C. Guhlke, R. Müller *Overcoming the shortcomings of the Nernst-Planck model*, Phys. Chem. Chem. Phys. 15(19) (2013) 7075-7086

[2] J. Fuhrmann *A numerical strategy for Nernst-Planck systems with solvation effect* Fuel cells 16(6) (2016) 704–714

[3] V. John, A. Linke, C. Merdon, M. Neilan, and L. Rebholz *On the divergence constraint in mixed finite element methods for incompressible flows* SIAM Review, accepted, (2016)

[4] M. Landstorfer, C. Guhlke, W. Dreyer *Theory and structure of the metal-electrolyte interface incorporating adsorption and solvation effects*, Electrochim. Acta 201 (2016) 187–219

Book of abstracts of the 7th International Conference on Advanced Computational Methods in Engineering, ACOMEN 2017 18–22 September 2017.

MULTIBAT – Reduced Order Modelling of Lithium-Ion Battery Models with Resolved Electrode Geometry

Mario Ohlberger[1] **and Stephan Rave**[1]

[1] *Applied Mathematics and Center for Nonlinear Science, University of Münster*

e-mails: mario.ohlberger@uni-muenster.de, stephan.rave@uni-muenster.de

Abstract

In this contribution we present recent work on parametric model order reduction for lithium-ion battery cell models at the pore scale using reduced basis methods. We obtain a modelling and simulation workflow which enables fast parameter studies of highly resolved battery models that are able to capture microscale phenomena such as Lithium-plating. We give numerical examples which underline the potential of our approach.

Key words: lithium-ion batteries, microscale modelling, model order reduction, reduced basis method

1 Problem

A major cause for performance degradation and failure of rechargeable lithium-ion batteries is the disposition lithium (Li) as an additional metallic phase at the negative cell electrode (Li-plating). The conditions leading to the formation of this additional phase are still poorly understood, however. It is the aim of the interdisciplinary MULTIBAT[1] research project to gain new insights into the causes of this phenomenon through mathematical modelling and numerical simulation [1]. Since Li-plating is influenced by the local microscale geometry of the electrode, only high-resolution models which resolve the local pore-scale geometry of the electrode will be able to faithfully capture this phenomenon.

2 Model Order Reduction and the MULTIBAT Workflow

In MULTIBAT we have developed a unified simulation workflow based on micrometer-scale partial differential equation models [2] and stochastic parametrized modelling of electrode geometries. Subsequent discretization of these models using the finite volume method leads to large, highly nonlinear equation systems which can only be solved with substantial computational effort, making parameter studies of the cell's behavior, e.g. for different charging regimes, prohibitively expensive. Therefore, model order reduction is a crucial final ingredient in order to make this workflow feasible.

The reduced basis method (e.g. [3] and references therein) is a generic approach to the reduction of parametrized discrete problems based on the idea of projecting the original

[1] http://wwwmath.uni-muenster.de/num/ohlberger/research/projects/MULTIBAT/home.html

high-dimensional equation system onto a problem-adapted low-dimensional reduced space spanned by solution snapshots of the high-dimensional problem for certain well-chosen parameters. Unlike classical multiscale discretizations, this allows an efficient reduction of the computational complexity while retaining the characteristic local microscale features of the solution.

In this contribution we start with an overview of the MULTIBAT simulation workflow and give a brief introduction to the main ingredients of reduced basis methods. We then discuss the application of these methods in the context of MULTIBAT, as well as the technical realization based on our free model order reduction software library `pyMOR` [4]. Numerical examples will demonstrate the feasibility of our approach.

Acknowledgements

This work has been supported by the German Federal Ministry of Education and Research (BMBF) under contract number 05M13PMA.

References

[1] J. Feinauer, S. Hein, S. Rave, S. Schmidt, D. Westhoff, et al., *MULTIBAT: Unified workflow for fast electrochemical 3D simulations of lithium-ion cells combining virtual stochastic microstructures, electrochemical degradation models and model order reduction.* arXiv e-prints **1704.04139** (2016), submitted.

[2] A. Latz, J. Zausch, *Thermodynamic consistent transport theory of li-ion batteries*, J. Power Sources **196** (1982) 3296–3302.

[3] M. Drohmann, B. Haasdonk, M. Ohlberger, *Reduced basis approximation for nonlinear parametrized evolution equations based on empirical operator interpolation*, SIAM J. Sci. Comput. **34** (2012) A937–A969.

[4] R. Milk, S. Rave, F. Schindler *pyMOR - Generic algorithms and interfaces for model order reduction*, SIAM J. Sci. Comput. **38** (2016) 194–216.

Book of abstracts of the 7th International Conference on Advanced Computational Methods in Engineering, ACOMEN 2017 18–22 September 2017.

Optimal Control of Ion Transport in Solid Electrolytes

Simon Schardt[1,2], Katharina Becker-Steinberger[1,3], Marie Preusse[1,2] and Arnulf Latz[1,3,4]

[1] *Electrochemical Multiphysics Modelling, Helmholtz-Institute Ulm for Electrochemical Energy Storage (HIU)*

[2] *Karlsruhe Institute of Technology (KIT),*

[3] *Institute of Engineering Thermodynamics, German Aerospace Center (DLR)*

[4] *Institute of Electrochemistry, University of Ulm*

e-mails: simon.schardt@kit.edu, katharina.becker-steinberger@dlr.de, marie.preusse@kit.edu, arnulf.latz@dlr.de

Abstract

In this work a thermodynamically consistent model for lithium ion transport in solid electrolytes (SEs) is used as constraint for optimization. By solving a drift-diffusion Poisson (DDP) equation system and applying techniques from infinite dimensional optimization, we find optimal material configurations for certain favored physical properties.

Key words: batteries, drift-diffusion Poisson system, PDE constrained optimization, solid electrolyte

1 Introduction

As SEs allow to be promising candidates for future batteries, the simulation in this field becomes more and more relevant. The understanding of the fundamentals of the underlying equations is crucial. Through optimization we provide valuable information about optimal material properties with respect to charge-transfer resistance which is known to be a limiting factor of current all-solid-state batteries. Starting point is the partial differential equation (PDE) system derived in [1] consisting of a continuity equation for the cation concentration c_+, a Poisson equation for the electric potential ϕ and a momentum equation. Replacing the momentum equation by its quasi-static approximation allows us to reduce the PDE system in the incompressible limit. This results in our DDP equation system describing cation transport in a self consistent electric field:

$$\begin{aligned} \partial_t c_+ + \nabla \cdot \frac{\rho}{\rho_-} \boldsymbol{N}_+ &= 0 \\ -\nabla \cdot \varepsilon_0 (1+\chi) \nabla \phi &= q \end{aligned} \tag{1}$$

with generalized drift-diffusion flux for the cations

$$\boldsymbol{N}_+ = -\left(f(c_+)\nabla c_+ + g(c_+)\nabla\phi\right) \tag{2}$$

and suitable initial and boundary conditions. The cation concentration and the electric potential together introduce the state variable $\boldsymbol{y} = (c_+, \phi)$.

2 Optimal Control

We will present first optimization results with respect to different cost functionals and minimization problems of the form

$$\min_{(\boldsymbol{y},u)} J(\boldsymbol{y},u) \quad \text{s.t.} \quad (1), \tag{3}$$

where u denotes the control variable. One example for the control might be the dielectric susceptibility $u = \chi$. This choice is motivated by experiments [3] showing reduced charge-transfer resistance by dielectric material modifications. The solution is obtained via the adjoint approach [2] true to the mentality of 'first optimize, then discretize'. The PDE system itself is discretized by a finite volume method together with implicit time stepping. As soon as the functional gradient has been characterized, through the adjoint state and implicit function theorem / Lagrange functional, a gradient projection method coupled with line search is applied.

Acknowledgements

This work has been partially supported by the Federal Ministry of Education and Research (BMBF).

References

[1] S. Braun, C. Yada, A. Latz, *Thermodynamically Consistent Model for Space-Charge-Layer Formation in a Solid Electrolyte*, J. Phys. Chem. C, 2015, 119 (39), pp 22281–22288.

[2] M. Hinze, C. Pinnau, M. Ulbrich, S. Ulbrich, *Optimization with PDE Constraints*, Springer Science + Business Media B.V., 2009.

[3] C. Yada, A. Ohmori, K. Ide, H. Yamasaki, T. Kato, T. Saito, F. Sagane, Y. Iriyama, *Dielectric Modification of 5V-Class Cathodes for High-Voltage All-Solid-State Lithium Batteries*, Adv. Energy Mater., 4, 2014, 1301416. doi: 10.1002/aenm.201301416.

MS 8 Inverse source problems : recent developments

Organiser: Abdellatif El Badia

Description: In various fields of science, engineering and bio-engineering, many important problems can be formulated as inverse problems (IP) for partial differential equations. Among them, inverse source problems (ISP) which consist of determining external force terms, from additional informations (given data, measurements, observations) on the state of the corresponding to the direct problem. The inverse source problems have attracted great attention from many researchers over recent years of course of their applications to many practical examples, particularly in biomedical imaging techniques such as; electro-encephalography/magneto encephalography (EEG/MEG) problems, pollution in the environment, photo and thermo-acoustic tomography (PAT and TAT), bioluminescence and fluorescence. One of the objectives of this minisymposia is to give an overview of the state of the art of the topic.

Book of abstracts of the 7th International Conference
on Advanced Computational Methods
in Engineering, ACOMEN 2017
18–22 September 2017.

Electroencephalography inverse source problem in neonates

M. M. Diallo[1,2], M. Darbas[2], A. El Badia[1] and S. Lohrengel[3]

[1] *LMAC EA 2222, Université de Technologie de Compiègne*

[2] *LAMFA CNRS UMR 7352, Université de Picardie Jules Verne*

[3] *LMR EA 4535, Université de Reims Champagne-Ardenne*

e-mails: mohamadou-malal.diallo@utc.fr, marion.darbas@u-picardie.fr, abdellatif.elbadia@utc.fr, stephanie.lohrengel@univ-reims.fr

Abstract

We investigate the localization of the normal and pathological sources of electric cerebral activity in neonates from measures in Electro-Encephalo-Graphy (EEG). The specificity for neonates is the presence of fontanels in the skull. Mathematically, the forward EEG problem consists in computing the electric potential on the scalp for given electrical sources located in the brain and different head tissues' conductivities. The inverse EEG source problem is identifying the characteristics of current sources from the knowledge of the measured potentials on the scalp. We propose in this thesis a mathematical model for the forward EEG problem in neonates able to take into account the presence and ossification process of fontanels. We perform the theoretical and numerical analysis for the forward and inverse problems and discuss the impact of fontanels for realistic head model. We perform a sensitivity analysis of the model with respect to variations of the conductivity.

Key words: Electroencephalography (EEG), inverse problem, forward problem, source analysis, finite element method, realistic head model, neonates.

References

[1] M. Farah, *Problèmes inverses de sources et lien avec l'Electro-Encéphalo-Graphie*, Thèse de doctorat université de technologie de Compiègne, 2007.

[2] H. Azizolahi, M. Darbas, M. M. Diallo, A. El Badia, S. Lohrengel, *EEG in neonates: modeling and sensitivity analysis with respect to variations of the conductivity*, (submitted).

[3] M. Darbas, M. M. Diallo, A. El Badia, S. Lohrengel, *An inverse dipole source problem in inhomogeneous media: Application to the EEG source localization in neonates.*, (in preparation).

Book of abstracts of the 7th International Conference
on Advanced Computational Methods
in Engineering, ACOMEN 2017
18–22 September 2017.

Full discretization of an inverse source problem

M. Grimmonprez[1] and M. Slodička[1]

[1] *Research Group NaM², Department of Mathematical Analysis, Ghent University, Belgium*

e-mails: Marijke.Grimmonprez@UGent.be, Marian.Slodicka@UGent.be

Abstract

The reconstruction of a solely time-dependent source function in a semilinear parabolic problem is considered. The existence and uniqueness of a strong solution to the problem is proved. Moreover, a full-discrete numerical scheme is designed and some corresponding error estimates are derived. The results and proofs are collected in [1] and [2].

Key words: error estimates, full discretization, inverse source problem, semilinear parabolic equation
MSC 2010: 47J35, 65M12, 65M32

1 Problem formulation

This research aims to reconstruct the couple $\{p(t), u(t,\boldsymbol{x})\}$ in the semilinear parabolic problem

$$\begin{cases} \partial_t u(t,\boldsymbol{x}) - \Delta u(t,\boldsymbol{x}) &= p(t)f(\boldsymbol{x}) + g(u(t,\boldsymbol{x})) + r(t,\boldsymbol{x}), & (t,\boldsymbol{x}) \in (0,T]\times\Omega, \\ u(t,\boldsymbol{x}) &= 0, & (t,\boldsymbol{x}) \in (0,T]\times\Gamma, \\ u(0,\boldsymbol{x}) &= u_0(\boldsymbol{x}), & \boldsymbol{x}\in\Omega, \\ \int_\Omega u(t,\boldsymbol{x})\mathrm{d}\boldsymbol{x} &= m(t), & t\in[0,T], \end{cases}$$

with $T > 0$ the final time and $\Omega \subset \mathbb{R}^d$, $d \in \mathbb{N}$, the spatial domain with a Lipschitz continuous boundary Γ.

2 Methods

In [1], Rothe's method has been applied to prove the existence and uniqueness of a strong solution to the problem. This method also reveals a convergent time-discrete numerical scheme for approximations. A space discretization of the time-discrete problem has then been carried out in [2] using the finite element method.

3 Results

The following variational formulation has been proposed: find $\{p, u(t)\} \in L_2(0,T) \times V$, with $V := \left\{\varphi \in H^2(\Omega) : \varphi_{|\Gamma} = 0\right\} = H^2(\Omega) \cap H_0^1(\Omega)$, such that for almost all $t \in (0,T]$ and for all $\varphi \in V$ it holds that

$$(\nabla \partial_t u(t), \nabla \varphi) + (\Delta u(t), \Delta \varphi) = -p(t)(f, \Delta \varphi) - (g(u(t)), \Delta \varphi) - (r(t), \Delta \varphi),$$

with

$$p(t) = \frac{m'(t) - \int_\Omega \Delta u(t) - \int_\Omega g(u(t)) - \int_\Omega r(t)}{\int_\Omega f}.$$

Under appropriate conditions on the data, the existence and uniqueness of a strong solution $\{p, u\} \in L_2(0,T) \times C\left([0,T], H_0^1(\Omega)\right) \cap L_\infty\left((0,T), V\right)$ to the problem has been proved in [1]. Moreover, some full-discrete error estimates have been derived in different settings, cf. [2]. In the first setting a one-dimensional domain has been considered, Hermite finite elements have been used and the global interpolation operator has been applied for the projection onto the finite element space. This has led to full-discrete (squared) error estimates of $O\left(\tau + h^{s-1}\right)$ or $O\left(\tau^2 + h^{\min\{s, 2(s-2)\}}\right)$, $s = 3$ or 4, depending on both the regularity of the data and of the exact solution. These theoretically obtained convergence rates have been supported by a numerical experiment. Similar error estimates with $s = 3, 4, 5$ or 6 and with $s = 3, 4$ or 5 have been derived for a two-dimensional domain with the use of Argyris elements and Bell's triangles respectively. A direct consequence of the error estimates is the strong convergence of the Rothe functions $\left\{\overline{p}_\sigma, u_\sigma\right\}$ to $\{p, u\}$ in $L_2(0,T) \times C\left([0,T], H^1(\Omega)\right)$ under the acquired conditions on the data and on the exact solution. Moreover, if the data and the exact solution are sufficiently regular, it follows that $p_\sigma \to p$ in $C([0,T])$.

References

[1] M. Grimmonprez and M. Slodička. Reconstruction of an unknown source parameter in a semilinear parabolic problem. *Journal of Computational and Applied Mathematics*, 289:331 – 345, 2015.

[2] Marijke Grimmonprez and Marián Slodička. Error estimates for the full discretization of a semilinear parabolic problem with an unknown source. *Mathematics and Computers in Simulation*, 142:15 – 33, 2017.

Book of abstracts of the 7th International Conference
on Advanced Computational Methods
in Engineering, ACOMEN 2017
18–22 September 2017.

GPR data interpretation problem and Inverse Source Problem for wave equation

Balgaisha Mukanova[1]

[1] *Department of Mathematical and Computer Modeling, L.N. Gumilyov Eurasian National University, Astana, Kazakhstan*

e-mails: mbsha01@gmail.com

Abstract

It is shown that the Ground Penetrating Radar (GRR) data interpretation problem can be reduced to the inverse source problem in 1D wave equation. The non-iterative algorithm for reconstructing the unknown spacewise dependent source is developed. The algorithm is based on the explicit representation of the direct problem solution via the source function. The minimization problem for discrete form of the Tikhonov functional is solved numerically for noise free and noisy data.

Key words: GPR data interpretation, inverse source problem, wave equation
MSC 2010: 65N20, 47A52,35L05, 35L20, 35Q86

1 GPR mathematical model

The 1D inverse problem for the model of GPR technique is considered. It is assumed that the medium fills the half-space $z > 0$ and the half-space $z < 0$ corresponds to the air. Let the electrical permittivity ε of the medium depend on the coordinate z only, magnetic permittivity $\mu = \mu_0 = \text{const} > 0$ in the whole space, and the conductivity is negligible. Let the current source with intensity

$$j^{ex}(t) = \Phi(t)\delta(z),\ \Phi(t) = 0 \text{ if } t \le 0,\ \Phi(t) \in C^2[0,\infty),\ \Phi''(+0) \neq 0,$$

be placed at the boundary $z = 0$ and directed along the axis y. Then it follows from Maxwell's equations that the electromagnetic field depends on (z, t) only. The field has an electric component $E_2(z, t)$ along the axis y that satisfies the Cauchy problem:

$$\frac{\partial^2 E_2}{\partial z^2} = \mu_0\varepsilon(z)\frac{\partial^2 E_2}{\partial t^2} + \mu_0\delta(z)\Phi'(t), \qquad E_2|_{t<0} = 0. \tag{1}$$

Denote by $c(z) = 1/\sqrt{\mu_0\varepsilon(z)}$. Suppose that the function $c^{-2}(z)$ is presented in the following form

$$c^{-2}(z) = \begin{cases} c_0^{-2}, & \text{if } z < 0 \\ c_1^{-2} + F(z), & \text{if } z \ge 0, \end{cases} \qquad c_0, c_1 = const,\ F(z) \in C(R),\ |F(z)| \ll c_1^{-2},$$

where the function $F(z)$ has a finite support in $z \in (0, \infty)$ and values $c_0 > 0,\ c_1 > 0$ are given. Now represent the solution of the direct problem (1) in the form $E_2(z,t) = U(z,t) + u(z,t)$ where $U(z,t)$ is the generalized solution to the Cauchy problem:

$$U_{zz} = \frac{1}{\bar{c}^2(z)} U_{tt} + \mu_0 \Phi'(t)\delta(z), \quad (z \in \mathbb{R},\ t > -\infty), \quad U|_{t<0} \equiv 0, \quad \bar{c}(z) = \begin{cases} c_0, & \text{if } z < 0, \\ c_1, & \text{if } z \geq 0. \end{cases}$$

The linearization of the equation (1) with respect to $u(z,t)$ shows that this function is a solution to the following problem

$$\frac{\partial^2 u}{\partial t^2} - c_1^2 \frac{\partial^2 u}{\partial z^2} = F(z)H(t - z/c_1), \quad (z > 0, 0 < t \leq T); \quad \left(\frac{\partial u}{\partial t} - c_0 \frac{\partial u}{\partial z}\right)_{z=0} = 0, \quad u|_{t<0} = 0, \quad (2)$$

where the function $H(t)$ is defined as follows:

$$H(t) = \mu_0 c_0 c_1^3 (c_0 + c_1)^{-1} \Phi''(t), \tag{3}$$

In GPR method a sought-for function is the $F(z)$ and the electrical field $E_2(0,t)$ is measured. Then additional data for inverse problem are

$$u|_{z=0} = g(t) \equiv E_2|_{z=0} - U|_{z=0}, \quad t \in [0, T],\ T > 0. \tag{4}$$

2 Numerical method

The solution $u(z,t)$ at $z = 0$ is expressed via partial Fourier sum of $F(z)$ and basic functions $X_k(z)$ in the following form

$$u(0,t;F^N) = \mu_0 (c^{-1} + c_0^{-1})^{-2} \sum_{k=1}^{N} F_k \int_0^{ct/2} X_k(\xi)(\Phi'(t - 2\xi/c) - \Phi'(0))d\xi \equiv \sum_{k=1}^{N} F_k G_k(t).$$

Substituting this formula in the regularized cost functional

$$J_\alpha(F) := \|u(0,\cdot;F) - g(\cdot)\|^2_{L^2(0,T)} + \alpha \|F\|^2_{L^2(0,l)}, \quad \alpha > 0, \tag{5}$$

where $l = l(T)$, and taking first derivatives of (5) with respect to F_k, we get a system of algebraic equations, which solution gives Fourier coefficients of $F(z)$ and define approximate solution of the considered ISP ([1]). Note that some approximate practical ways to solve inverse problems arising in GPR techniques are represented in [2] and in the review [3].

Acknowledgements

This work has been partially supported by Ministry of Education and Science of the Republic of Kazakhstan through the grant the grant #316(2016).

References

[1] Balgaisha Mukanova, Vladimir G. Romanov, *Inverse source problem for wave equation and GPR data interpretation problem*, Eur. J. of Math.and Comp. Appl. **4(3)** (2016) 15-28.

[2] R.H. Stolt, *Migration by Fourier transform*, Geophysics **43** (1978) 23-43.

[3] Caner Özdemir, Fevket Demirci, Enes Yiğit, and Betül Yilmaz, *A Review on Migration Methods in B-Scan Ground Penetrating Radar Imaging*, Math. Pr. in Eng. **2014**, Article ID 280738, http://dx.doi.org/10.1155/2014/280738.

Book of abstracts of the 7th International Conference
on Advanced Computational Methods
in Engineering, ACOMEN 2017
18–22 September 2017.

Inverse Coefficient Problem for a Time Fractional Diffusion Equation

Amir Hossein Salehi Shayegan[1]

[1] *Faculty of Mathematics, K. N. Toosi University of Technology*

e-mails: ah.salehi@mail.kntu.ac.ir

Abstract

The existence of a quasi solution for an inverse coefficient problem is studied. In this way, it is proved that the convergence of solutions for the corresponding direct problem continuously depends on the coefficient convergence. Then, an appropriate class of admissible functions is given and shown that the inverse coefficient problem has at least one quasi solution in this class of functions.

Key words: Inverse coefficient problem, Quasi solution, Time fractional diffusion equation

MSC 2010: 35R30

1 Introduction

Consider the inverse coefficient problem of determining the unknown function k in the following time fractional diffusion equation

$$\begin{aligned} &{}^{C}D_t^{\alpha}u - \nabla\cdot(k(x)\nabla u) = f(x,t), && (x,t)\in Q=\Omega\times(0,T),\\ &u(x,t)=0, && (x,t)\in\partial\Omega\times(0,T),\\ &u(x,0)=\phi(x), && x\in\Omega, \end{aligned} \tag{1}$$

from knowledge of the final measured data

$$u(x,T)=\psi(x), \qquad x\in\Omega, \tag{2}$$

where $0<\alpha<1$, Ω is a bounded domain in $\mathbb{R}^N$, $N\geq 1$ with piecewise smooth boundary $\partial\Omega$. Here ${}^{C}D_t^{\alpha}u(x,t)$ denotes the left Caputo fractional derivative. For a given $k=k(x)$ the problem (1) is called *direct problem* (DP). In order to determine the unknown function k, one should solve the following functional equation

$$u(x,T;k)=\psi(x), \qquad x\in\Omega, \tag{3}$$

where $u(x,t;k)$ is the solution of DP. In general, instead of solving (3), one usually tries to find the quasi solution of (3), which is obtained from minimization problem

$$I(k)=\min_{\tilde{k}\in\Im} I(\tilde{k}), \tag{4}$$

where $I(\tilde{k}) = \int_\Omega \left(u(x,T;\tilde{k}) - \psi(x)\right)^2 dx$, and $\mathfrak{I}$ is a set of admissible functions. The set $\mathfrak{I}$ is introduced in the following

$$\mathfrak{I} = \{k \in C(\Omega) \ : \ 0 < k_0 \leqslant k(x) \leqslant k_1\},$$

which guarantees the existence and uniqueness of the solution of DP.

2 Main results

The main contribution of this study is to prove the existence of a quasi solution in the class of admissible functions $\mathfrak{I}$. Due to this, suppose that $k \in \mathfrak{I}$ is given, i.e. the problem (1) is a DP, and u is its corresponding solution. Moreover, for $n \in \mathbb{N}$, the solution of (1) is denoted by u_n, when $k_n \in \mathfrak{I}$ is substituted to k. Now, we prove that if $\{k_n\}$ converges pointwise to k, then $\{u_n\} \to u$ for $(x,t) \in Q$. This stability result implies that the functional I is continuous. Then by constructing a suitable compact subset of admissible initial data $\mathfrak{I}$, we can conclude that a solution of the problem (4) exists for the continuous functional I. This means the existence of a quasi solution to the inverse coefficient problem (1)-(2).

Define $B^\alpha(Q) := H_0^\alpha((0,T), L_2(\Omega)) \cap L_2((0,T), H_0^1(\Omega))$, which is a Banach space with respect to the norm

$$\|v\|_{B^\alpha(Q)} = \left(\|v\|_{H^\alpha((0,T),L_2(\Omega))} + \ \|v\|_{L_2((0,T),H_0^1(\Omega))}\right)^{1/2}.$$

Theorem *If $k \in \mathfrak{I}$, then DP (1) has a unique solution. In addition, if u is a solution of DP (1) and also $f \in L_2(Q)$ and $\phi \in L_2(\Omega)$, then*

$$\|u\|_{B^{\alpha/2}(Q)} \leqslant c(\|f\|_{L_2(Q)} + \frac{T^{1-\alpha}}{\Gamma(2-\alpha)}\|\phi\|_{L_2(\Omega)}),$$

where c is an arbitrary positive constant.

This theorem help us to prove the following stability result.

Theorem *Suppose that a sequence of functions $\{k_m\} \subset \mathfrak{I}$ converges pointwise to a function $k \in \mathfrak{I}$. Then the sequence of solutions $u_m = u(x,t;k_m)$ converges to the solution $u(x,t;k)$, i.e., $\|u_m - u\|_{B^{\alpha/2}(Q)} \to 0$ as $m \to \infty$.*

Now, we are ready to prove that the functional I is continuous on $\mathfrak{I}$.

Theorem *The functional $I(\tilde{k})$ is continuous on $\mathfrak{I}$ in the sense that a sequence of functions $\{k_m\} \subset \mathfrak{I}$ converges pointwise to a function $k \in \mathfrak{I}$, then $\left|I(\tilde{k}_m) - I(\tilde{k})\right| \to 0$ as $m \to \infty$.*

In order to construct a compact subset of $\mathfrak{I}$, we use Arzela-Ascoli Theorem. Therefore, in addition to assumptions on k, we assume that the subset $\mathfrak{I}_c$ of $\mathfrak{I}$ has the equicontinuity, that is for each $\varepsilon > 0$, there exists $\delta > 0$ such that if $k \in \mathfrak{I}_c$, $x_1, x_2 \in \mathbb{R}^N$ and $\|x_2 - x_1\| < \delta$ then $\|k(x_2) - k(x_1)\|_{L_2(\Omega)} < \varepsilon$. Consequently, one can conclude the following theorem.

Theorem *Suppose that $\mathfrak{I}_c$ be an equicontinuous subset of $\mathfrak{I}$. Then any sequence $\{k_m\}$ of functions in $\mathfrak{I}_c$ has a uniformly convergent subsequence $\{k_{m,m}\}$ such that $\lim_{m\to\infty} k_{m,m}(x) = k(x)$, $\forall x \in \Omega$ and $k \in \mathfrak{I}_c$.*

Theorem *The nonlinear inverse parabolic problem (1)-(2) has at least one quasi solution in the set of admissible coefficients $\mathfrak{I}_c$.*

Book of abstracts of the 7th International Conference
on Advanced Computational Methods
in Engineering, ACOMEN 2017
18–22 September 2017.

Recognition of a time-dependent source in a time-fractional wave equation

Katarína Šišková[1] and Marian Slodička[1]

[1] *Department of Mathematical Analysis, research group of Numerical Analysis and Mathematical Modeling (NaM^2), Ghent University*

e-mails: katarina.siskova@ugent.be, marina.slodicka@ugent.be

Abstract

An inverse source problem for a time-fractional wave equation in a bounded domain in $\mathbb{R}^d$ is studied. The equation contains Caputo fractional derivative in time with the order $\beta \in (1,2)$ and is accompanied with the boundary condition of Neumann type and initial conditions. The time-dependent source is determined from an additional measurement in the form of integral over the space subdomain. The existence, uniqueness and regularity of a weak solution are obtained. A numerical algorithm based on Rothe's method is proposed, a priori estimates are proved and convergence of iterates towards the solution is established. Moreover, we present some numerical experiments confirming the convergence results.

Key words: time-fractional wave equation, inverse source problem, reconstruction, convergence

1 Introduction

We consider a partial differential equation (PDE) with a fractional derivative in time t

$$\left(g_{2-\beta} * \partial_{tt} u(x)\right)(t) - \Delta u(x,t) = h(t)f(x) + F(x,t,u(x,t)), \qquad x \in \Omega,\ t \in (0,T), \tag{1}$$

where $\Omega \subset \mathbb{R}^d$ is a bounded domain with a Lipschitz boundary Γ (cf. [1]), $T > 0$, $g_{2-\beta}$ is the Riemann-Liouville kernel given by

$$g_{2-\beta}(t) = \frac{t^{1-\beta}}{\Gamma(2-\beta)}, \qquad t > 0,\ 1 < \beta < 2,$$

and $*$ denotes the convolution on the positive half-line, i.e.

$$(k * v)(t) = \int_0^t k(t-s)v(s)\,\mathrm{d}s.$$

Thus, the Caputo fractional derivative of order β, cf. e.g. [2, 3], defined by

$$\partial_t^\beta u(x,t) = \left(g_{2-\beta} * \partial_{tt} u(x)\right)(t),$$

appears in the equation (1). Note that the equation (1) is a classical diffusion or wave equation for $\beta = 1$ and $\beta = 2$, respectively. We supplement governing PDE (1) with the following initial and boundary conditions

$$\begin{aligned} u(x,0) &= u_0(x), && x \in \Omega, \\ \partial_t u(x,0) &= v_0(x), && x \in \Omega, \\ -\nabla u(x,t)\cdot \boldsymbol{\nu} &= g(x,t), && (x,t) \in \Gamma \times (0,T), \end{aligned} \tag{2}$$

where the symbol $\boldsymbol{\nu}$ denotes the outer normal vector assigned to the boundary Γ.

The *Inverse Source Problem* (ISP) studied in here consists of finding a couple $(u(x,t), h(t))$ obeying (1), (2) and

$$\int_\Omega u(\boldsymbol{x},t)\omega(\boldsymbol{x})\,\mathrm{d}\boldsymbol{x} = m(t), \qquad t \in [0,T], \tag{3}$$

where the weight function ω is just a space-dependent function [4]. Usually ω is chosen to be a function with compact support in Ω, and then this type of measurement represents the weighted average of u on a subdomain of Ω.

The fractional wave equation is used for example to model the propagation of diffusive waves in viscoelastics solids (cf. [5, 6]).

Acknowledgements

K. Šišková was financed by the BOF project no. 01D23414, Ghent University, Belgium. M. Slodička was partially supported by the IAP P7/02-project of the Belgian Science Policy.

References

[1] A. Kufner, O. John, S. Fučík, Function Spaces, Monograpfs and textbooks on mechanics of solids and fluids, Noordhoff International Publishing, Leyden, 1977.

[2] M. Caputo, Linear models of dissipation whose Q is almost frequency independent-ii, Geophysical Journal of the Royal Astronomical Society 13 (5) (1967) 529–539.

[3] I. Podlubný, Fractional Differential Equations: An Introduction to Fractional Derivatives, Fractional Differential Equations, to Methods of Their Solution and Some of Their Applications, Mathematics in science and engineering, Academic Press, 1999.

[4] A. Prilepko, D. Orlovsky, I. Vasin, Methods for solving inverse problems in mathematical physics, Vol. 222 of Monographs and textbooks in pure and applied mathematics, Marcel Dekker, Inc., New York-Basel, 2000.

[5] F. Mainardi, Fractional diffusive waves in viscoelastic solids, in: J.L. Wegner, F.R. Norwood (Eds.), Nonlinear Waves in Solids, ASME/AMR, Fairfield, (1995) 93–97.

[6] F. Mainardi, P. Paradisi, A model of diffusive waves in viscoelasticity based on fractional calculus, in: Decision and Control, 1997., Proceedings of the 36th IEEE Conference on, Vol. 5, 1997, pp. 4961–4966 vol.5.

Book of abstracts of the 7th International Conference
on Advanced Computational Methods
in Engineering, ACOMEN 2017
18–22 September 2017.

The identification of a space-dependent load source in isotropic thermoelastic systems: numerical experiments

Karel Van Bockstal[1] **and Liviu Marin**[2]

[1] *Department of Mathematical Analysis, Ghent University, Krijgslaan 281, Ghent, Belgium*

[2] *Department of Mathematics, Faculty of Mathematics and Computer Science, University of Bucharest, 14 Academiei, 010014 Bucharest, Romania*

[2] *Institute of Solid Mechanics, Romanian Academy, 15 Constantin Mille, 010141 Bucharest, Romania*

e-mails: karel.vanbockstal@ugent.be, marin.liviu@gmail.com

Abstract

In this talk, the numerical determination of a space-dependent load source in an isotropic thermoelastic system of type-III from the knowledge of an additional final time measurement is discussed. A convergent and stable iterative algorithm is proposed for the recovery of the unknown vector source in the linear case and, at the same time, a stopping criterion is also given. Several numerical experiments are considered to validate the properties of the proposed iterative procedure and the regularizing/stabilizing character of the corresponding stopping criterion. The numerical experiments carried out showed that it exists a certain limitation of the method with respect to the recovery of non-symmetric sources. The results of this research are published in [1].

References

[1] K. Van Bockstal and L. Marin. Recovery of a space-dependent vector source in anisotropic thermoelastic systems. *Computer Methods in Applied Mechanics and Engineering*, 321:269–293, 2017.

Book of abstracts of the 7th International Conference
on Advanced Computational Methods
in Engineering, ACOMEN 2017
18–22 September 2017.

The reconstruction of a time-dependent source from a surface measurement for full Maxwell's equations by means of the potential field method

Ran Wang[1], Karel Van Bockstal[2] and Tong Kang[1]

[1] *Department of Applied Mathematics, Communication University of China*

[2] *Department of Mathematical Analysis, research group of Numerical Analysis and Mathematical Modeling (NaM²), Ghent University*

e-mails: ranwang@cuc.edu.cn, karel.vanbockstal@ugent.be, kangtong@cuc.edu.cn

Abstract

This paper is devoted to the study of an inverse source problem governed by full Maxwell's equations by means of the potential field method (the $\boldsymbol{A}$-ϕ method). The source term is assumed to be separable in time and space, in which the unknown part is solely time-dependent and is recovered from a surface measurement. We prove that the solution to the inverse problem based on the $\boldsymbol{A}$-ϕ formulation is existing and unique. We suggest a constructive scheme for approximating the solution and discuss its convergence. Finally, a few examples are presented to verify the theoretical results.

Key words: Maxwell's equations, inverse source problem, $\boldsymbol{A}$-ϕ method, reconstruction, time discretization

MSC 2010: 35Q60, 65N30, 65M60

MS 9 A priori and a posteriori error analysis for the time-harmonic Maxwell's systems

Organiser: Serge Nicaise

Description: The finite element method is widely used to solve time-harmonic Maxwell's systems. Today one of the challenges is to evaluate the quality of the solution with the help of error estimates. Hence different authors focus either on a priori estimates, where some regularity results on the exact solutions are required, or a posteriori error analysis, where only the energy regularity is requested. My goal is to invite different specialists on both topics in order to share their recent results.

Book of abstracts of the 7th International Conference on Advanced Computational Methods in Engineering, ACOMEN 2017
18–22 September 2017.

About the gauge conditions arising in finite element eddy current problems

Emmanuel Creusé[1], Patrick Dular[2] and Serge Nicaise[3]

[1] *Laboratoire de Mathématiques Paul Painlevé, Université Lille 1 Sciences et Technologies & Inria Lille Nord-Europe, Cité Scientifique, 59655 Villeneuve d'Ascq Cedex, France*

[2] *Dpt of Electrical Engineering and Computer Science - Unit of Applied and Computational Electromagnetics, University of Liège, Montefiore Institute, B-4000 Liege, Belgium*

[3] *Laboratoire de Mathématiques et Applications de Valenciennes, Université de Valenciennes et du Hainaut-Cambrésis, Le Mont Houy, 59313 Valenciennes Cedex 09, France*

e-mails: emmanuel.creuse@math.univ-lille1.fr, patrick.dular@ulg.ac.be, serge.nicaise@univ-valenciennes.fr

Abstract

This contribution deals with eddy current problems considered in their magnetic vector potential formulations. In order to ensure the uniqueness of the solution, a gauge condition has to be imposed on the vector potential, and several possibilities occur. We show the mathematically equivalence between some of these choices in the context of finite element methods, for several kinds of configurations and boundary conditions, and paying attention to the discrete form of the source current density. We highlight their characteristic behaviors on some numerical benchmarks.

Key words: Finite Element Methods, gauge conditions, Maxwell equations.
MSC 2010: 35Q61; 65N30.

1 The eddy-current problem and its usual associated gauges

Let $\Omega \subset \mathbb{R}^3$ be an open simply connected domain with a Lipschitz boundary $\partial\Omega = \Gamma_b \cup \Gamma_h$ such that Γ_b is connected with a strictly positive measure. We consider the eddy current problem in its weak formulation that consist in looking for the magnetic induction $\mathbf{B} = curl\,\mathbf{A}$, with $\mathbf{A} \in X(\Omega)$ the magnetic vector potential, solution of :

$$\int_\Omega \mu^{-1} curl\,\mathbf{A} \cdot curl\,\mathbf{A}' dx - \int_{\Omega_s} \mathbf{j} \cdot \mathbf{A}'\, dx = 0 \quad \forall \mathbf{A}' \in X(\Omega), \tag{1}$$

where μ is the magnetic permeability of the material, $\mathbf{j}$ is the current density, defined as a fixed source distribution $\mathbf{j}_s$ in stranded coils $\Omega_s \subset \Omega$ and as an unknown distribution function of $\mathbf{A}$ in massive conductors $\Omega_c \subset \Omega$. $X(\Omega)$ is the functional space defined by :

$$X(\Omega) = \{\mathbf{u} \in H(curl, \Omega); \mathbf{n} \times \mathbf{u} = 0 \text{ on } \Gamma_b\},$$

where $\mathbf{n}$ is the unit outward normal to Ω. The focus is first given on the way $\mathbf{j}_s$ is defined, considering no other forms of $\mathbf{j}$ in (1), i.e. with Ω_c empty. Provided that $div\,\mathbf{j}_s = 0$ in Ω_s, it can be easily shown that problem (1) admits at least one solution. Nevertheless, to ensure its uniqueness, a gauge condition has to be imposed. Several possibilities occur [1]. A first way to proceed is to use the Coulomb gauge, which consists in looking for $\mathbf{A} \in X_0(\Omega) \subset X(\Omega)$ solution of (1) defined by :

$$X_0(\Omega) = \{\mathbf{u} \in X(\Omega); \int_\Omega \mathbf{u} \cdot \nabla\zeta \, dx = 0 \ \forall \zeta \in H^1_{\Gamma_b}(\Omega)\}, \text{ where } H^1_{\Gamma_b}(\Omega) = \{\zeta \in H^1(\Omega); \zeta_{|\Gamma_b} = 0\}.$$

Using some low-order $H(curl)$-Nédélec finite elements to obtain an approximation $\mathbf{A}_h$ of $\mathbf{A}$ with such a gauge is not convenient (except if the linear solver is well adapted [2]), hence we can also consider some Lagrange multipliers associated with a weak constraint on the divergence of $\mathbf{A}_h$, or to restrict the number of degrees of freedom belonging to the discrete space $X_h(\Omega) \subset X(\Omega)$ using a so-called "tree - co-tree" gauge.

2 Equivalences on characteristic configurations

In this talk, several configurations will be analyzed, and the mathematical equivalence between the different previous considered gauges will be adressed for each of them, to prove that all these choices lead to the same value of the magnetic induction $\mathbf{B} = curl\,\mathbf{A}$. We will treat in particular the case where Γ_b on which $\mathbf{B} \cdot \mathbf{n} = 0$ is not simply-connected. In that case, we have to introduce some "cuts" in Γ_b to make the problem well-posed. In addition to these theoretical developpements, some tests will be performed to hightlight the performances of all these gauges from the practical point of view and to illustrate their particular behaviors (see Figure 1), in particular with different discretization forms of $\mathbf{j_s}$.

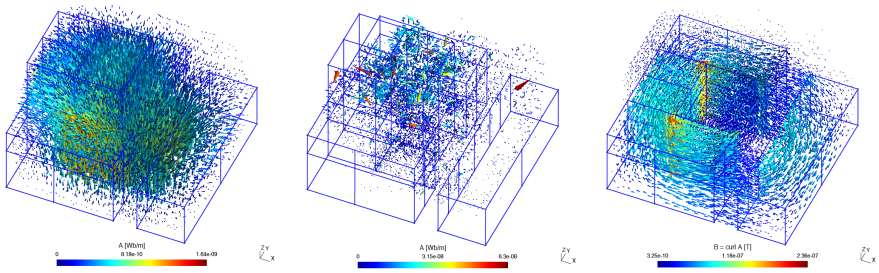

Figure 1: Magnetic vector potential $\mathbf{A}$ generated in a domain Ω using the Coulomb gauge (left), the tree-co-tree gauge (middle), and corresponding magnetic flux density $\mathbf{B} = curl\,\mathbf{A}$ being the same in both cases (right).

Acknowledgements

This work was supported in part by the Labex CEMPI (ANR-11-LABX-0007-01).

References

[1] A. Bossavit, *Computational electromagnetism*, Academic Press Inc, San Diego, CA, 1998.

[2] Z. Ren, *Influence of the R.H.S. on the convergence behaviour of the curl − curl equation*, IEEE Transactions on Magnetics, 32(3):655-658, 1996.

Book of abstracts of the 7th International Conference on Advanced Computational Methods in Engineering, ACOMEN 2017 18–22 September 2017.

A method to take into account a short-circuit in lamination stack

Ziani Smail[1], Thomas Henneron [1] and Yvonnick Le Menach[1]

[1] *Univ. Lille, Centrale Lille, Arts et Métiers Paris Tech, HEI, EA 2697 - L2EP -Laboratoire d'Electrotechnique et d'Electronique de Puissance, F-59000 Lille, France,*

e-mails: smail.ziani@ed.univ-lille1.fr, thomas.henneron@univ-lille1.fr, yvonnick.le-menach@univ-lille1.fr

Abstract

In this communication, a method in 2-D frequency domain is presented to simulate a laminated iron core with a short-circuit between several magnetic sheets. The idea consists to model the short-circuit with a classical formulation and to use a homogenization technique to model the lamination stack. The problem is the coupling between both approaches. Otherwise the problem is not linear and only the steady state is considered.

Key words: Electromagnetism, Harmonic Balance, Homogenization, Multi-scale, Non-linear

1 Introduction

To decrease the eddy current in the iron cores, the electrical devices are usually made of lamination stacks. Due to the symmetry of the stack and the *a priori* knowledge of electromagnetic phenomena inside the sheets, the homogenization techniques can be implemented [1]. The main interest is the reduction of the size of numerical problem. However, the small insulation defect can be broken the symmetry and a short-circuit between sheets appears [3]. In this case, the homogenization techniques cannot be used and the problem becomes multi-scale. Indeed, the size of defect is the very small behind the size of the lamination stack. The short circuit is modelled by a classical formulation. Consequently, a coupling between the homogenization approach and the classical formulations must be carried out [2]. Otherwise the problem is not linear and only the steady state is considered

2 Problem to solve

We consider a domain $\mathcal{D}$ with a boundary Γ ($\Gamma = \Gamma_b \cup \Gamma_{h1} \cup \Gamma_{h2}$) constituted of three part, a non conductive domain $\mathcal{D}_{nc}$, a conductive domain $\mathcal{D}_c$ and a homogenized domain $\mathcal{D}_h$ (figure 1). The sub-domains $\mathcal{D}_c$ and $\mathcal{D}_h$ are separated by the boundary Γ_c. In magneto-quasistatics, Maxwell's equations can be considered in the frequency domain under the following forms:

$$\begin{cases} \mathbf{rotH} = \mathbf{J} & in \quad \mathcal{D}_c \\ \mathbf{rotE} = -i\omega\mathbf{B} & in \quad \mathcal{D}_c \\ div\mathbf{B} = 0 & in \quad \mathcal{D} \end{cases}$$

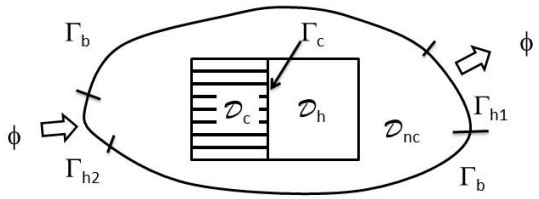

Figure 1: Studied domain

where **B** is the magnetic flux density, **H** the magnetic field, **E** the electric field and **J** the eddy current density. A magnetic flux Φ is imposed on the boundaries Γ_{h1} and Γ_{h2}. In order to complete these equations, the electric, the magnetic behavior laws and the boundary conditions must be introduced

$$\begin{cases} \mathbf{B} = \mu(H)\mathbf{H} & in \quad \mathcal{D}_c \\ \mathbf{B} = \mu\mathbf{H} & in \quad \mathcal{D}_{nc} \\ \mathbf{B} = \mu^*(H)\mathbf{H} & in \quad \mathcal{D}_h \\ \mathbf{J} = \sigma\mathbf{E} & in \quad \mathcal{D}_c \end{cases} \qquad \begin{cases} \mathbf{H}\times\mathbf{n} = 0\ |_{\Gamma_h} \\ \mathbf{B}.\mathbf{n} = 0\ |_{\Gamma_b} \\ \Phi = cte\ |\Gamma_{h1} \text{ and } \Gamma_{h2} \end{cases}$$

where σ is the electric conductivity and μ is the magnetic permeability. Moreover, in $\mathcal{D}_c$ and $\mathcal{D}_h$, the magnetic behaviour of the material is not linear. μ^* represents a homogenized permeability which takes into account the electromagnetic phenomena of the laminated stack. As Φ is a magnetic flux imposed, this represents the source term of the problem. The consequence of the short-circuit (in $\mathcal{D}_c$) is the establishing of current loop circulating in the domains $\mathcal{D}_c$ and $\mathcal{D}_h$ across the boundary Γ_c. Then, the continuity of all electromagnetic fields must be ensured on Γ_c. To solve this problem, the formulation in term of magnetic vector potential will be used. The non linear solver is based on the fixed-point method applied to the harmonic balance approach which imposes directly the steady-state. In the mini symposium, we will be presented the details of the computation, the obtained results and their numerical behaviour.

Acknowledgements

This work has been partially supported by University of Lille and the region Hauts de France.

References

[1] J. Gyselinck, R. V. Sabariego, and P. Dular, *A nonlinear time-domain homogenization technique for laminated iron cores in three-dimensional finite-element models*, IEEE Trans. Magn., vol. 42, no. 4, pp. 763–766, Apr. 2006.

[2] S. Ziani, T. Henneron, O. Puigdellivol, and Y. Le Menach, method coupling modified vector potential A* and homogenization formulations to model short-circuits in lamination stacks, Eur. Phys. J. Appl. Phys., vol. 75, no. 3, p. 30901, Sep. 2016.

[3] J. Muller, R. Romary, A. Benabou, T. Henneron, F. Piriou, J.P.A. Bastos, J.Y. Roger, Interlaminar short circuit detection: modeling and measurement, COMPEL - Int. J. Comput. Math. Electr. Electron. Eng., vol. 31, no. 5, pp. 1448–1457, Sep. 2012.

Book of abstracts of the 7th International Conference on Advanced Computational Methods in Engineering, ACOMEN 2017
18–22 September 2017.

Two guaranteed equilibrated error estimators for the eddy current problems solved by the finite element method

Emmanuel Creusé[1], Serge Nicaise[2] and Roberta Tittarelli[3]

[1] *Laboratoire de Mathématiques Paul Painlevé, University of Lille 1*

[2] *Laboratoire de Mathématiques et leurs Applications de Valenciennes , University of Valenciennes and Hainaut Cambrésis*

[3] *Institut Montpelliérain Alexander Grothendieck, University of Montpellier*

e-mails: emmanuel.creuse@math.univ-lille1.fr, serge.nicaise@univ-valenciennes.fr, roberta.tittarelli@umontpellier.fr

Abstract

Two guaranteed equilibrated error estimators are proposed. The system of interest is the harmonic magneto-dynamic Maxwell's system recasted into the classical $\mathbf{A} - \varphi$ potential formulation and approximated by the finite element method. The first estimator is built starting from a dual problem and is consequently available to estimate the error of both numerical resolutions. Its reliability and local efficiency without generic constants are showed. The second estimator is based on a flux reconstruction technique and estimates the error of the primal formulation. Its guaranteed reliability and its global efficiency are presented. Numerical tests illustrating the theoretical results and the performance of the estimators for adaptive refinement techniques conclude the communication.

Key words: Error bounds, Finite element methods, Maxwell equations.
MSC 2010: 65M15, 78M10, 35Q61.

1 Introduction

This communication is devoted to the developement and analysis of two equilibrated *a posteriori* error estimators for the harmonic eddy current problems. Therefore, the system of interest is given by the quasi-static approximation of Maxwell's equations in the magneto-harmonic regime completed by the constitutive laws: $\mathbf{B} = \mu\mathbf{H}$ in the whole domain $D \subset \mathbb{R}^3$ and $\mathbf{J}_e = \sigma\mathbf{E}$ in the conductor domain $D_c \subset D$. Here $\mathbf{B}$, $\mathbf{H}$, $\mathbf{J}_e$ and $\mathbf{E}$ represent, respectively, the magnetic flux density, the magnetic field, the eddy current density and the electric field, while μ stands for the magnetic permeability and σ for the electrical conductivity.

The numerical solution is obtained by the finite element method (FEM) with *regular* meshes $\mathcal{T}_h$ applied to the $\mathbf{A} - \varphi$ potential formulation [2, Section 2.1]. The approximation $(\mathbf{A}_h, \varphi_h)$ of $\mathbf{A}$ by the first order edge elements and φ by first order nodal elements, respectively, provides the numerical solution: $\mathbf{B}_h = \mathrm{curl}\mathbf{A}_h$ in D and $\mathbf{E}_h = -i\omega\mathbf{A}_h - \nabla\varphi_h$ in D_c.

We are insterested in building equilibrated error estimators which give at least a guaranteed upper bound for the energy norm of the error. So, we present two different ways to achieve it.

2 A posteriori error estimators

The idea consists in building error estimators based on the non-verification property of the constitutive laws for the numerical fields. Thus the two estimators η are defined as

$$\eta := \Big(\sum_{K \in \mathcal{T}_h} \eta_K^2 \Big)^{1/2}, \quad \text{with} \quad \eta_K^2 := ||\mu^{1/2}(\mathbf{H}_h - \mu^{-1}\mathbf{B}_h)||_K^2 + ||(\omega\sigma)^{-1/2}(\mathbf{J}_h - \sigma\mathbf{E}_h)||_K^2,$$

where the last norm is computed only if $K \subset D_c$. $(\mathbf{B}_h, \mathbf{E}_h)$ is the numerical solution from the $\mathbf{A} - \varphi$ formulation and $(\mathbf{H}_h, \mathbf{J}_h)$ represent a pair of *admissible* fields in the sense that $\mathbf{J}_h \in H(\mathrm{div}, D_c)$ is a divergence free vector and that $\mathbf{H}_h \in H(\mathrm{curl}, D)$ is a lowest order edge element satisfying (1) $\mathbf{H}_h = \Pi_h \mathbf{J}_s - \Pi_h \mathbf{J}_h$, with Π_h a suited projection onto the lowest order Raviart-Thomas space.

On one side, a **dual construction method** allows us to obtain a pair of *admissible* fields $(\mathbf{H}_h, \mathbf{J}_h)$ solving the dual potential formulation $\mathbf{T} - \Omega$ by the FEM [2, Section 2.1]. Therefore, the corresponding estimator estimates the following error energy norm ϵ:

$$\epsilon := \Big(\sum_{K \in \mathcal{T}_h} \epsilon_K^2 \Big)^{1/2}, \quad \text{with} \quad \epsilon_K^2 := \epsilon_{A,\varphi,K}^2 + \epsilon_{T,\Omega,K}^2,$$

where $\epsilon_{A,\varphi,K}^2 := ||\mu^{-1/2}(\mathbf{B} - \mathbf{B}_h)||_K^2 + ||\omega^{-1/2}\sigma^{1/2}(\mathbf{E} - \mathbf{E}_h)||_K^2$ and $\epsilon_{T,\Omega,K}^2 := ||\mu^{1/2}(\mathbf{H} - \mathbf{H}_h)||_K^2 + ||(\omega\sigma)^{-1/2}(\mathbf{J}_e - \mathbf{J}_h)||_K^2$. Naturally the two electric contributions in the local errors $\epsilon_{A,\varphi,K}$ and $\epsilon_{T,\Omega,K}$ are computed only if $K \subset D_c$. In [2, Theorems 3.5 and 3.6] we have proved that, up to some higher order terms, $\eta = \epsilon$ and $\eta_K \leq \sqrt{2}\epsilon_K$.

On the other side, a **flux reconstruction technique**, as the one proposed in [1], allows us to build the *admissible* field $\mathbf{J}_h$ and afterwards to prove that there exists an *admissible* field $\mathbf{H}_h$. In [3] we have proved that the upper bound $\epsilon_{A,\varphi} \leq \eta$ holds up to some higher order terms. Furthermore, computing the field $\mathbf{H}_h$ through the FEM to solve the magneto-static problem (1), we have obtained the lower bound $\eta \leq c\epsilon_{A,\varphi}$ up to some higher order terms, where the constant $c > 0$ does not depend on the mesh size.

3 Numerical tests

An analytical benchmark test confirms the theoretical predictions about the two estimators presented above. A physical benchmark shows their performance for some adaptive mesh refinements. It reveals in particular that the flux reconstructed estimator exhibits a locally efficient behavior, in spite of the fact that the lower bound has only been globally proved.

References

[1] S. Cochez-Dhondt and S. Nicaise, *A posteriori error estimators based on equilibrated fluxes*, Comput. Methods Appl. Math. **10** (2010) 49–68.

[2] E. Creusé, S. Nicaise and R. Tittarelli, *A guaranteed equilibrated error estimator for the $\mathbf{A} - \varphi$ and $\mathbf{T} - \Omega$ magnetodynamic harmonic formulations of the Maxwell system*, IMA Journal of Numerical Analysis **doi: 10.1093/imanum/drw026** (2016).

[3] R. Tittarelli, *Estimateurs d'erreur a posteriori pour les équations de Maxwell en formulation potentielle et temporelle*, Université de Lille 1 Sciences et Technologies, 2016.

Book of abstracts of the 7th International Conference
on Advanced Computational Methods
in Engineering, ACOMEN 2017
18–22 September 2017.

Optimal voltage control of non-stationary eddy current problems

Fredi Tröltzsch[1] **and Alberto Valli**[2]

[1] *Institut für Mathematik, Technische Universität Berlin, Germany*

[2] *Department of Mathematics, University of Trento, Italy*

e-mails: troeltz@math.tu-berlin.de, alberto.valli@unitn.it

Abstract

We propose and analyze a mathematical model that can be useful for controlled voltage excitation in time-dependent electromagnetism. The well-posedness of the model is proved and an associated optimal control problem is investigated. Here, the control function is a transient voltage and the aim of the control is the best approximation of desired electric and magnetic fields in suitable L^2-norms. Special emphasis is laid on an adjoint calculus for first-order necessary optimality conditions. Moreover, a peculiar attention is devoted to devise a formulation for which the computational complexity of the finite element solution method is substantially reduced.

Key words: optimal control problem, non-stationary eddy current system, optimality conditions, voltage excitation, well-posedness
MSC 2010: 49J20, 35Q60

In the last two decades, the optimal control of electromagnetic fields has received particular attention, and here we are interested in the analysis of controlled electric or magnetic fields in electrically conducting media. In the majority of the recent papers devoted to this subject steady or time-dependent electrical currents were considered as controls, while the control of electrical voltages has been only investigated in the time-harmonic case, thus resulting in a dynamical system of elliptic type.

Often, it is more realistic to control the electrical voltage in a time-dependent setting. To our best knowledge, only the papers [1], [2], [3] considered the optimal control of electromagnetic fields by the electrical voltage. A vector potential ansatz was applied to convert the standard magneto-quasistatic Maxwell equations in a (degenerate) parabolic system.

In our presentation, the mathematical analysis for the optimal control of voltages is the central aspect. The associated model for the electromagnetic fields is close to that proposed in [4]. We merge the modeling ideas of [4] with both a specific approach aiming at reducing the complexity of the Maxwell equations for given voltages and some ideas of adjoining in [5]. We should notice that, using our approach, specific difficulties arise in the process of adjoining. Here, differential operators on the boundary, namely, the surface gradient and the surface divergence, can be invoked to overcome this obstacle.

We devise the weak formulation of the problem and prove that it is well-posed. Then we furnish the formulation of the optimal control problem, and the adjoint problem and the necessary optimality conditions are derived. Some remarks on numerical approximation are also included.

References

[1] I. Yousept and F. Tröltzsch, *PDE-constrained optimization of time-dependent 3D electromagnetic induction heating by alternating voltages*, ESAIM Math. Model. Numer. Anal., **46** (2012) 709–729.

[2] S. Nicaise, S. Stingelin, and F. Tröltzsch, *On two optimal control problems for magnetic fields*, Comput. Methods Appl. Math., **14** (2014) 555–573.

[3] S. Nicaise, S. Stingelin, and F. Tröltzsch, *Optimal control of magnetic fields in flow measurement*, Discrete Contin. Dyn. Syst. Ser. S, **8** (2015) 579–605.

[4] A. Bermudez, B. López Rodríguez, R. Rodríguez, and P. Salgado, *Numerical solution of transient eddy current problems with input current intensities as boundary data*, IMA J. Numer. Anal., **32** (2012) 1001–1029.

[5] F. Tröltzsch and A. Valli, *Optimal control of low-frequency electromagnetic fields in multiply connected conductors*, Optimization, **65** (2016) 1651–1673.

MS 10 Numerical methods in electromagnetism

Organiser: M. Issa

Description: During the past decade, the computational electromagnetics has evolved rapidly to a point where various alternative modeling approaches and numerical methods are available for very general problems. This progress is due to the wide range of applications like Electric motors, transformers, microwave heating, optical fibers and wave-guides, eddy current, and antennas, etc. In this symposium, we consider the modelisation of particular electromagnetic problems and structures, as well as the numerical methods that contribute in modeling and solving them.

Book of abstracts of the 7th International Conference
on Advanced Computational Methods
in Engineering, ACOMEN 2017
18–22 September 2017.

Global solution of a mathematical model for the induction hardening with controlled Joule heat and nonlinear magnetic field: Potential formulation.

Jaroslav Chovan[1], Christophe Geuzaine[2] and Marián Slodička[1]

[1] *Department of Mathematical Analysis, Ghent University, Belgium*

[2] *Department of Electrical Engineering and Computer Science, University of Liege, Belgium*

e-mails: jaroslav.chovan@ugent.be, cgeuzaine@ulg.ac.be,
marian.slodicka@ugent.be

Abstract

We derive and analyze a mathematical model for the induction hardening process. The domain consists of a sphere where the electromagnetic field is present, coil which is connected to a source of an alternating electric current and a workpiece which is a subject to be heated by the process of the electromagnetic induction. We take into account that the magnetic permeability might behave differently in various materials e.g. in the air or in the workpiece.

We assume a nonlinear relation between the magnetic field and the magnetic induction field. For the electromagnetic part of our model, we consider a vector-scalar potential formulation of Maxwell's equation. Evolution of temperature in the coil and the workpiece is determined by the nonlinear heat transfer equation. The process of induction hardening creates Joule heat in the material. This term acts as a heat source in the heat transfer equation, therefore, in order to control it, we apply a truncation function. This formulation yields a system of three coupled equations. The coupling is provided through the electric conductivity function on the one hand and through the Joule heating term on the other hand.

We semi-discretize (time discretization) these equations and use the Rothe method to show the convergence of Rothe's functions towards a weak solution of the whole system. The nonlinearity in the electromagnetic part is handled by the theory of monotone operators. To supplement the theoretical results, we provide a numerical simulation where we estimate the order of convergence of our numerical scheme.

Key words: Maxwell's equation, Minty-Browder, Monotone operators, Rothe's method
MSC 2010: 35K61, 35Q61, 35Q79, 65M12

References

[1] J. Chovan, Ch. Geuzaine, M. Slodička, *A-ϕ formulation of a mathematical model for the induction hardening process with a nonlinear law for the magnetic field*, Computer Methods in Applied Mechanics and Engineering, 2017.

Book of abstracts of the 7th International Conference on Advanced Computational Methods in Engineering, ACOMEN 2017
18–22 September 2017.

Asymptotic Modelling for 3D Eddy Current Problems with a Conductive Thin Layer

Mohammad ISSA[1], Victor PÉRON[2] and Ronan PERRUSSEL[1]

[1] *Laboratoire Plasma et Conversion d'Énergie, UMR 5213 CNRS/INPT/UPS, Université de Toulouse, 31071 France*

[2] *LMAP CNRS UMR 5142 et Team MAGIQUE 3D INRIA, Université de Pau et des Pays de l'Adour, 64013 France*

e-mails: mohammad.issa@laplace.univ-tlse.fr, victor.peron@univ-pau.fr, perrussel@laplace.univ-tlse.fr

Abstract

In this work we derive and analyze an equivalent model for 3D Eddy Current problems with a conductive thin layer of small thickness ϵ. In our model, the conductive sheet is replaced by its mid-surface and their shielding behavior is satisfied by an equivalent transmission conditions on this interface. The transmission conditions are derived asymptotically for vanishing sheet thickness ϵ.

Key words: Asymptotic Expansions, Eddy-Current Problems, Thin Conducting Layers, Transmission Conditions

1 Introduction

We denote by $\Omega = \Omega^\epsilon_- \cup \overline{\Omega^\epsilon_0} \cup \Omega^\epsilon_+ \subset \mathbb{R}^3$ the domain of study, where Ω^ϵ_- corresponds to a non-conductive linear material, Ω^ϵ_+ the exterior of the structure domain, and Ω^ϵ_0 a conductive thin layer of constant thickness ϵ (see figure 1). The discretisation of the conducting sheet by FEM needs a very fine mesh due to the rapid decay of the field under high conductivity. For this, we approximate a new model defined in ϵ-independent domains. Let Σ be a smooth surface, we denote by $[v]_\Sigma$ and $\{v\}_\Sigma$ the jump and mean of v respectively across Σ

$$[v]_\Sigma = v_{|_{\Sigma^+}} - v_{|_{\Sigma^-}}, \quad \{v\}_\Sigma = \frac{1}{2}(v_{|_{\Sigma^+}} + v_{|_{\Sigma^-}}), \quad \text{for } v \in (C^\infty(\Omega_\pm))^3.$$

We consider the eddy current problem as follows

$$\begin{cases} \text{curl}H^\epsilon &= \sigma^\epsilon E^\epsilon + J_0 & \text{in} & \Omega \\ \text{curl}E^\epsilon &= iw\mu_0 H^\epsilon & \text{in} & \Omega \\ \text{div}(H^\epsilon) &= 0 & \text{in} & \mathbb{R}^3 \\ [E \times n] = [H \times n] &= 0 & \text{on} & \Gamma^\epsilon_\pm \end{cases}$$

$$\text{where } \sigma^\epsilon = \begin{cases} 0 & \text{in} \quad \Omega^\epsilon_\pm \\ \sigma_0 = \epsilon^{-2}\bar{\sigma} & \text{in} \quad \Omega^\epsilon_0 \end{cases}$$

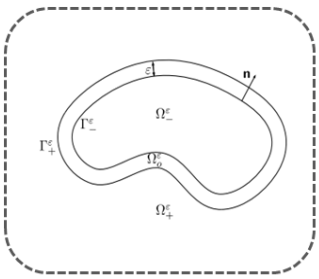

Figure 1: A cross Section of the domain Ω

Let u be a vector field on Γ, then we denote by $\gamma_D u = n \times (u \times n)$, and $\gamma_N u = \text{curl}u \times n$, the Dirichlet and Neumann data, respectively.

2 Multiscale Expansion

Assuming that Γ is a smooth surface, then E^ϵ and H^ϵ can be expanded with an asymptotic expansion in power series of the small parameter ϵ. [1]

$$\begin{aligned} E^\epsilon(x) &\approx E_0(x) + \epsilon E_1(x) + \epsilon^2 E_2(x) + \ldots + \mathcal{O}(\epsilon^k) \quad \text{in } \Omega^\epsilon_\pm \\ H^\epsilon(x) &\approx \boldsymbol{\mathcal{H}}_0(y_\alpha, \tfrac{h}{\epsilon}) + \epsilon \boldsymbol{\mathcal{H}}_1(y_\alpha, \tfrac{h}{\epsilon}) + \ldots + \mathcal{O}(\epsilon^k) \quad \text{in } \Omega^\epsilon_0 \end{aligned}$$

Here, $x \in \mathbb{R}^3$ are the cartesian coordinated, and (y_α, h) is the local normal coordinate system, $h \in (-\frac{\epsilon}{2}, \frac{\epsilon}{2})$ is the normal coordinate to Γ. The term $\boldsymbol{\mathcal{H}}_j$ is a profile defined on $\Gamma \times (-\frac{1}{2}, \frac{1}{2})$. The derivation is based on the expansion of the differential operators inside the thin layer Ω^ϵ_0, and the Taylor expansion of $E_j|_{\Gamma^\epsilon_\pm}$ around the mid-surface Γ.

3 Equivalent Model of Order 2

We introduce a problem satisfied by an approximation E^k_ϵ of the expression $E_0(x) + \epsilon E_1(x) + \epsilon^2 E_2(x) + \ldots + \epsilon^k E_k(x)$ up to a residual term $\mathcal{O}(\epsilon^{k+1})$.

The second order approximate solution E^1_ϵ, solves

$$\begin{aligned} \operatorname{curl}(\operatorname{curl} E^1_\epsilon) &= i\omega\mu J_0 && \text{in} \quad \Omega_\pm \\ \begin{pmatrix} [\gamma_D E^1_\epsilon]_\Gamma \\ \{\gamma_D E^1_\epsilon\}_\Gamma \end{pmatrix} &= \epsilon \begin{pmatrix} C_1 & 0 \\ 0 & C_2 \end{pmatrix} \begin{pmatrix} \{\gamma_N E^1_\epsilon\}_\Gamma \\ [\gamma_N E^1_\epsilon]_\Gamma \end{pmatrix} && \text{on} \quad \Gamma \end{aligned}$$

where

$$C_1 = -1 + \frac{2\tanh(\frac{\gamma}{2})}{\gamma} \quad , \quad C_2 = -\tfrac{1}{4} + \frac{\coth(\frac{\gamma}{2})}{2\gamma}$$
$$\gamma = exp(\tfrac{3i\pi}{4})\sqrt{\omega\mu_0\bar{\sigma}}.$$

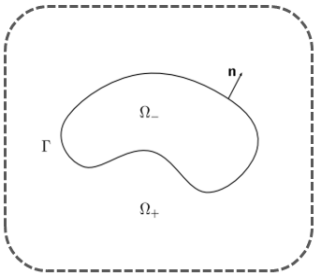

Figure 2: A cross section of the ϵ-independent subdomains

4 Numerical Results

Numerical experiments are performed to assess the accuracy of our model. The results are in particular compared to the model given in [2]. Complementary simulations will be conducted to study the robustness with respect to the sheet conductivity and the convergence of the modelling error.

Acknowledgements

We acknowledge the collaboration of B. BANNWARTH, O. CHADEBEC, and G. MEUNIER who participated in the implementation of the model, and the GDR SEEDS for the financial support.

References

[1] Victor Péron , *Impedence transmission conditions for eddy current problems.* 2017. https://hal.inria.fr/hal-01505612.

[2] Thanh-Trung Nguyen, Gérard Meunier, Jean-Michel Guichon, and Olivier Chadebec, *3-D Integral Formulation Using Facet Elements for Thin Conductive Shells Coupled With an External Circuit.* IEEE Transactions on Magnetics, Vol. 51, Issue 3, march 2015.

Book of abstracts of the 7th International Conference
on Advanced Computational Methods
in Engineering, ACOMEN 2017
18–22 September 2017.

Gradient-based optimization of the multilayer diffraction grating profile

A.A. Petukhov, D.A. Konyaev and A.V. Smirnov

e-mails: petukhov@physics.msu.ru, konyaev@physics.msu.ru,
smirnov.av14@physics.msu.ru

Abstract

In this work the application of the gradient-based optimization technique to multilayer diffraction grating optimization problem is discussed. The optimization problem is set as a merit function minimization problem. The merit function gradient is computed through obtaining the solution of the adjoint differential equation. The optimization problem is solved firstly for a-priori determined grating profile shapes (binary, triangular). The application of this method for shape-independent optimization is discussed, the possible grating parametrizations are discussed as well.

Key words: multilayer diffraction gratings, gradient-based optimization, adjoint equation.

1 Introduction

In most grating optimization problems the groove shape is given as an a-priori assumption [1-3]. Usually some simple profile shapes are chosen, such as rectangular, triangular or sinusoidal. However, it is not guaranteed that in some particular case the grating with one of these simple profile types is the optimal one. Gratings with a more complicated but still practically realizable groove profile shape can exhibit more decent properties than those with simple profile shapes. Moreover, it is important to make no special assumptions (except practical realizability) concerning the profile shape, so that it could be optimized as well. Thus, the grating groove shape can be given as a result of the optimization process. Such type of the optimization problem is referred to as shape-independent optimization (i.e. no a-priori assumption on the groove shape is given).

The optimization algorithm for such type of optimization problem, when almost any profile type has to be described by one and the same set of parameters, the number of optimization parameters is sufficiently large. Simple zero-order optimization methods (such as Nelder-Mead method [4]) turn to be unstable when the number of the optimization parameters increases. In this case efficient and reliable methods are required, such as gradient-based optimization methods. They are much more stable and much faster in case of a large number of optimization parameters, in comparison to zero-order methods.

2 Optimization problem and numerical approach

In this work the application of the gradient-based optimization technique to multilayer diffraction grating profile optimization problem is discussed. The multilayer diffraction grating consists of the grating itself with some groove shape (which is likely arbitrary) and the multilayer stack with homogeneous dielectric layers. All the structure is placed on a substrate. In this work we consider the case of one-dimensional dielectric gratings and waves with TE polarization (however generalizations are possible).

The optimization problem is set as a merit function minimization problem. Different types of merit functions are considered. The merit function gradient is computed through obtaining the solution of the adjoint differential equation [5]. The optimization problem is solved firstly for a-priori determined grating profile shapes. The application of this method for shape-independent optimization is discussed, the possible grating parametrizations are discussed as well.

At each step the merit function as well as its gradient are evaluated by obtaining the solution of a full-vectorial diffraction problem for Maxwell equations (or adjoint ones), which is obtained by means of a combination of the incomplete Galerkin's method and scattering matrix method [6]. This hybrid method provides efficient solution of the problem of wave diffraction on a multilayer grating.

Acknowledgements

This work has been supported by RFBR, research project №16–31–00477 mol_a.

References

[1] K. Hehl, J. Bischoff et al., *High-efficiency dielectric reflection gratings: design, fabrication and analysis*, J. Appl. Opt. **38(30)** (1999) 6257–6271.

[2] A.A. Petukhov, M.K. Trubetskov, A.N. Bogolyubov, *Grating profile optimization for reflection 1st order Littrow mounting*, Proceedings of SCEE-2012 Conference Zurich, 2012, 187–188.

[3] A.N. Bogolyubov, A.A. Petukhov and M.K. Trubetskov, *Mathematical modeling of multilayer diffraction gratings*, Physical Bases of Instrumentation **3(4)** (2014) 20–27.

[4] D.M. Himmelblau, *Applied Nonlinear Programming*, The McGraw-Hill Companies, 1972.

[5] R.P. Fedorenko, *Approximate solution of optimal control problems*, Nauka, Moscow (Russian), 1971.

[6] A.A. Petukhov, *Joint Application of the Incomplete Galerkin Method and Scattering Matrix Method for Modeling Multilayer Diffraction Gratings*, Mathematical Models and Computer Simulations **6(1)** (2014) 92–100.

Book of abstracts of the 7th International Conference
on Advanced Computational Methods
in Engineering, ACOMEN 2017
18–22 September 2017.

Application of a hybrid numerical technique for solving direct and inverse problems of light diffraction on multilayer gratings

A.V. Smirnov, A.A. Petukhov and D.A. Konyaev

e-mails: smirnov.av14@physics.msu.ru, petukhov@physics.msu.ru, konyaev@physics.msu.ru

Abstract

In this paper a hybrid numerical technique for solving direct and inverse problems of light diffraction on multilayer gratings is presented. This technique suggests using a combination of two methods: scattering matrix method and finite elements method (FEM). The proposed hybrid numerical method is used for solving direct problem while obtaining the solution of the inverse grating optimization problem. One-dimensional multilayer reflection gratings with different groove shapes are considered and optimized for maximum diffraction efficiency in the minus first order in Littrow mounting. Nelder-Mead method is applied for the optimization process.

Key words: multilayer diffraction gratings, finite elements method, scattering matrix method, hybrid method.

1 Introduction

Multilayer diffraction gratings are extensively applied in many fields of modern engineering and applied science, in optics, photonics and laser technology [1]. Wide application of multilayer gratings requires efficient numerical tools for their modeling. Within this paper we propose a hybrid numerical technique based on a combination of finite elements method (FEM) and scattering matrix method for solving direct problems of wave diffraction on multilayer gratings. The hybrid method takes the advantages of both techniques and thus allows to obtain more accurate solution. The proposed method is further used for solving multilayer grating optimization problems.

2 Problem statement and proposed numerical approach

Within this paper entirely dielectric one-dimensional multilayer reflection gratings with binary and triangular groove shapes are considered (however the grating geometry can be much more complicated). As the dielectric grating itself provides only redistribution of the incident wave energy between several diffraction orders, a multilayer dielectric mirror should be used for obtaining high reflectance. The grating is placed on top of the multilayer dielectric mirror, which is situated on a substrate. A plane wave is considered to be incident on a multilayer

grating at some given angle θ and diffracted into discrete directions (i. e. diffraction orders). Within this paper waves with TE-polarization are considered.

We propose a hybrid approach for solving the direct problem of multilayer grating modeling. As the grating can have rather complicated geometry we suggest using FEM [2] for this part of the grating since FEM suits well for arbitrary geometries. At the same time using FEM for homogeneous layers demands unnecessarily fine mesh and is time-consuming. For homogeneous layers in the multilayer stack (multilayer mirror) the use of the scattering matrix method is suggested. The grating itself is considered to be the first layer (an inhomogeneous one) and the FEM is used to compute the scattering matrix of this layer. Then the two methods are coupled together via global scattering matrix (S-matrix). Such combined approach makes the computations faster and more accurate.

3 Computations and grating optimization

In this work a free software package FreeFem++ [3] is used as a FEM-solver and allows to calculate the S-matrix for the grating layer. The global S-matrix is calculated in MATLAB environment.

We provide grating optimization for achieving maximal diffraction efficiency in minus first diffraction order for a given wavelength range in case of minus first order Littrow mount, i.e for the case when the incident and reflected light directions are coincident. The grating optimization is based on a merit function minimization. The multilayer mirror parameters are optimized independently, providing almost 100% reflectance for a given wavelength range and for a desired angle of incidence θ. The merit function minimization algorithm is based on the Nelder-Mead (simplex) optimization [4]. At each step the merit function is evaluated by obtaining the solution of a full diffraction problem for Maxwell equations, which is obtained by means of the proposed hybrid technique. This technique provides efficient solution of the direct and inverse problems of wave diffraction on a multilayer grating. The optimization problem is solved for binary and triangular gratings. The results are compared with those, presented in [5].

Acknowledgements

This work has been supported by RFBR, research project №16–31–00477 mol_a.

References

[1] Ch. Palmer, E. Loewen, *Diffraction Grating Handbook*, Newport Corporation, sixth edition, 2005.

[2] J. Jianming, *The Finite Element Method in Electromagnetics*, A Wiley-Interscience, Publication, 2002.

[3] F. Hecht, *New development in FreeFem++*, J. J. Numer. Math. **20** (2012) 251–265.

[4] D.M. Himmelblau, *Applied Nonlinear Programming*, The McGraw-Hill Companies, 1972.

[5] A.A. Petukhov, M.K. Trubetskov, A.N. Bogolyubov, *Grating profile optimization for reflection 1st order Littrow mounting*, Proceedings of SCEE-2012 Conference. Zurich, 2012, 187–188.

Book of abstracts of the 7th International Conference
on Advanced Computational Methods
in Engineering, ACOMEN 2017
18–22 September 2017.

Nonasymptotic and Nonlocal Homogenization of Electromagnetic Metamaterials

Igor Tsukerman[1] **and Vadim A. Markel**[2]

[1] *Department of Electrical and Computer Engineering, The University of Akron, OH 44325-3904, USA*

[2] *University of Aix-Marseille, Institute Fresnel, France,, and Departments of Radiology and Bioengineering (on leave), University of Pennsylvania, Philadelphia, PA 19104, USA*

e-mails: igor@uakron.edu, vmarkel@fresnel.fr

Abstract

The proposed homogenization methodology applies to periodic electromagnetic structures (photonic crystals and metamaterials), treated on two main spatial scales in the frequency domain. Fields on the fine and coarse scales are approximated via Trefftz bases, i.e. by functions satisfying the underlying equations and boundary conditions (Bloch modes on the fine scale and generalized plane waves on the coarse scale). Numerical examples demonstrate that nonlocal models can improve the accuracy of homogenization by an order of magnitude.

Key words: Electromagnetic waves, homogenization, metamaterials, photonic crystals, Trefftz approximations

1 Introduction

We present a framework for non-asymptotic and nonlocal homogenization of periodic electromagnetic structures. The methodology applies to any (reasonable) size and composition of the lattice cell, not necessarily vanishingly small relative to the vacuum wavelength. Central in this approach is a special construction of fields on the scale coarser that the lattice cell size, so that the dispersion relations and – importantly – the interface boundary conditions are satisfied as accurately as possible.

The formulation of the problem is as follows. A given periodic structure is to be replaced with a homogeneous sample of the same geometric shape and size, with some material tensor $\mathcal{M}$ to be defined, in such a way that reflection and transmission of monochromatic waves (or, equivalently, their far-field pattern) remain, to the extent possible, unchanged. This description is made more precise in [3].

The problem has two principal scales (levels). *Fine-level* fields are the exact solutions of Maxwell's equations for given illumination conditions and for a given sample. *Coarse-level* fields are constructed as some smoothed (averaged) versions of the fine-level ones. These auxiliary fields do depend on the respective fine-scale fields. Although the latter are not known *a priori*, suitable approximations can be used in their stead. Fields on the fine and

coarse scales are approximated via Trefftz bases, i.e. by functions satisfying the underlying equations and boundary conditions. Details of this construction for the local theory are given in [3]. It is important to note that the coarse-level fields are in general *not* volume averages of the fine-level ones. This approach is further extended to produce a nonlocal theory.

Fine-level Trefftz functions can be chosen as a set of Bloch waves traveling in different directions. On the coarse scale, a natural counterpart of the fine-scale Bloch basis is a set of generalized plane waves. To satisfy boundary conditions as accurately as possible, the **EH** amplitudes are taken as boundary averages of the periodic factors of the respective fine-scale Bloch modes. Least-squares approximation of the dispersion relation then yields an optimized material tensor [3].

In [3, 1], we introduced several benchmark examples of layered media and explored their non-asymptotic but *local* homogenization. Here we extend this to *nonlocal* homogenization using Example A of these papers. The medium consists of a finite number of stacked inversion-symmetric lattice cells each of which contains three intrinsically nonmagnetic layers of widths $a/4$, $a/2$ and $a/4$ and scalar permittivities ϵ_1, ϵ_2, and ϵ_1, respectively ($\epsilon_1 = 4+0.1i$ and $\epsilon_2 = 1$). We assume that λ is fixed and a changes. The numerical results depend only weakly on the kernel width parameter τ_0 when it varies within a reasonable range from ~10–20% of the cell size a to several cell sizes. The fine-scale basis consisted of $2n_{\text{dir}}$ Bloch modes traveling at $n_{\text{dir}} = 7$ different angles in $(-\pi/2, \pi/2)$ (two Bloch waves – "back" and "forth" – per angle).

The accuracy of the nonlocal homogenization is much higher than that of local homogenization and of the standard static (asymptotic) homogenization [2]. As one particular example, for a metamaterial slab with a 10-cell thickness in the normal direction, nonlocal homogenization reduces the absolute errors in the reflection coefficient by an order of magnitude uniformly as a function of a/λ, and also as a function of $\sin\theta_{inc}$ for a fixed $a/\lambda = 0.2$.

It should be noted that the relative simplicity of layered media is deceiving; their homogenization is notoriously difficult (e.g. [4]). Our conference presentation will also show examples of non-asymptotic and nonlocal homogenization for photonic crystals (2D-periodic structures).

Acknowledgements

This research was supported in part by the US National Science Foundation Grants DMS-1216927, DMS-1620112, and by A*MIDEX via Project ANR-11-IDEX-0001-02.

References

[1] Vadim A. Markel and Igor Tsukerman, *Current-driven homogenization and effective medium parameters for finite samples,* Phys. Rev. B, **88** (2013) 125131.

[2] Igor Tsukerman, *Classical and non-classical effective medium theories: New perspectives,* Physics Letters A, **381** (2017) 1635–1640.

[3] Igor Tsukerman and Vadim A. Markel, *A nonasymptotic homogenization theory for periodic electromagnetic structures,* Proc Royal Society A, **470** (2014) 2014.0245.

[4] Vladislav Popov, Andrei V. Lavrinenko, Andrey Novitsky, *Operator approach to effective medium theory to overcome a breakdown of Maxwell Garnett approximation,* Phys. Rev. B **94** (2016) 085428.

MS 11 Fast Helmholtz solvers for acoustics, electromagnetics and elastodynamics

Organiser: Christophe Geuzaine

Description: Time-harmonic wave problems arise in a variety of scientific and industrial problems, with far reaching applications in domains as diverse as radar scattering from airplanes, medical imaging, electromagnetic compatibility, geophysical exploration or acoustic noise simulations. The underlying mathematical model for such problems is the Helmholtz equation. In recent years the need has arisen to solve very large-scale Helmholtz problems with billions of unknowns, for both (piecewise) homogeneous or inhomogeneous media. This minisymposium will showcase several recent approaches to tackle such challenging problems, both from a mathematical and from a computational point of view.

Book of abstracts of the 7th International Conference
on Advanced Computational Methods
in Engineering, ACOMEN 2017
18–22 September 2017.

Recent advances in High-Order FEM for acoustics applications

Hadrien Bériot[1], **Alice Lieu**[1] **and Gwenael Gabard**[2]

[1] *Vibro-Acoustic Solver Team, Siemens Industry Software NV.*
Interleuvenlaan 68 B-3001 Leuven, Belgium

[2] *LAUM, CNRS, Université du Maine, Av. O. Messiaen, 72085 Le Mans, France*

e-mails: hadrien.beriot@siemens.com, alice.lieu@siemens.com,
gwenael.gabard@univ-lemans.fr

Abstract

Computational modelling remains key to the acoustic design of a wide range of products across many industries. Numerical models must be able to efficiently predict the performance of large systems across the whole audible range, which raises severe difficulties. Recently, high-order finite element methods have regained interest in the computational acoustics community, due to its flexibility, robustness and computational efficiency. This paper examines several challenges in the development of high-order FEM for solving large-scale Helmholtz problems.

Key words: high-order FEM; Helmholtz problems; acoustics; p-FEM; Domain Decomposition Methods; FETI

1 Performance of high-order FEM for acoustics

Classical low-order finite elements are not appropriate for resolving large-scale oscillatory problems arising in acoustics or in vibro-acoustics. They are known to be hindered by some large phase errors which, in practice, restricts their usage to the low frequency regime. Two common strategies to address this issue are to resort to high-order polynomial shape functions (e.g. *hp*-FEM), or to use Trefftz methods where the shape functions are local solutions of the problem (typically plane waves). Both strategies have been actively developed over the past decades and both lead to significantly reduced resolution requirements for a specific problem. However, the global matrices originating from high-order models are more densely populated and the relation between the numerical model (element size, polynomial order), the computational cost (memory and time) and the accuracy is not well documented. In a recent study, authors have compared higher-order polynomial approximations (*p*-FEM with hierarchic polynomials) and the wave-based discontinuous Galerkin method for two-dimensional Helmholtz problems [1]. Different benchmark problems are examined to perform a detailed and systematic assessment of the relative merits of these two methods in terms of interpolation properties, performance and conditioning. It is generally assumed that a wave-based method naturally provides better accuracy compared to polynomial methods since the plane

waves or Bessel functions used in these methods are exact solutions of the Helmholtz equation. However, the results in [1] indicate that this expectation does not necessarily translate into a clear benefit. The differences in performance, accuracy and conditioning are in fact more nuanced than generally assumed. This confirms that high-order FEM based on hierarchic polynomials stands among the most competitive approaches for solving practical Helmholtz problems at high-frequency on unstructured grids.

2 Efficient parallel solvers

The performance of the high-order FEM method relies heavily on the design of efficient solving procedures for the resulting large, sparse, complex linear systems. On the one hand, continued efforts are deployed to develop efficient iterative solvers for this purpose. These methods scale well with the problem size, are highly parallelizable and generally require a limited amount of computational resources. However, due to the properties of the underlying operator, the design of robust iterative solvers for Helmholtz problems remains a challenge. On the other hand, direct solving procedures do not scale well with respect to problem size and frequency. In practice, the amount of computational resources available is often not sufficient to tackle the frequency range of interest. An alternative to iterative or direct solving procedures is to resort to domain decomposition methods. While the performance of these methods is well documented for conventional FEM, the effect of increasing the polynomial order remains to be examined. In this study, a non-overlapping domain decomposition method called the Finite Element Tearing and Interconnecting method (FETI-2LM) is analysed [3]. This method employs Lagrange multipliers to recover the connections between the sub-domains. An iterative procedure is used to solve an interface problem whereas a direct solver is employed to factorize the local problems. The performance of the method is compared against a parallel sparse multifrontal solver using the same number of partitions. Preliminary results indicate that the use of FETI-2LM allows a better load balancing over all the processors. Another important finding is that, for a given number of processor and polynomial order, FETI-2LM requires much less memory as compared to the algebraic approach.

Acknowledgements

This work was performed as part of the CRANE project (www.crane-eid.eu) funded by the European Union under the Seventh Framework Programme (Grant 606844).

References

[1] Lieu, A., Gabard, G., Bériot, H., *A comparison of high-order polynomial and wave-based methods for Helmholtz problems.*, 321, 105-125, (2016).

[2] Bériot, H., Prinn, A., & Gabard, G. , *Efficient implementation of high-order finite elements for Helmholtz problems*, International Journal for Numerical Methods in Engineering, Volume 106, Issue 3, 213-240, (2015).

[3] Farhat, C., Macedo, A., Lesoinne, M., Roux, F. X., Magoulés, F., & de La Bourdonnaie, A., *Two-level domain decomposition methods with Lagrange multipliers for the fast iterative solution of acoustic scattering problems*, Computer methods in applied mechanics and engineering, 184(2), 213-239, (2000).

Book of abstracts of the 7th International Conference
on Advanced Computational Methods
in Engineering, ACOMEN 2017
18–22 September 2017.

On the efficiency of an $\mathcal{H}$–matrix based direct solver for the Boundary Element Method in 3D elastodynamics

Stéphanie Chaillat[1], Luca Desiderio[1] and Patrick Ciarlet[1]

[1] *Laboratoire POEMS (CNRS-INRIA-ENSTA), ENSTA Paristech, Université Paris-Saclay, France*

e-mails: chaillat@ensta.fr, desiderio@ensta.fr, ciarlet@ensta.fr

Abstract

The main advantage of the Boundary Element Method (BEM) is that only the domain boundaries are discretized leading to a drastic reduction of the total number of degrees of freedom. In traditional BE implementation the dimensional advantage with respect to domain discretization methods is offset by the fully-populated nature of the BEM coefficient matrix. In the present work, we propose a fast method to solve the BEM system in 3-D frequency-domain elastodynamics. Using the $\mathcal{H}$-matrix arithmetic and low-rank approximations (performed with Adaptive Cross Approximation), we derive a fast direct solver and we study the efficiency of low-rank approximations when the frequency is increased. We assess the numerical efficiency and accuracy on the basis of numerical results obtained for problems having known solutions. The efficiency of the method is also illustrated to study seismic wave propagation in 3-D domains.

Key words: boundary element method, elastodynamics, hierarchical matrices, low-rank approximations

1 Context

The main advantage of the Boundary Element Method (BEM) is that only the domain boundaries (and possibly interfaces) are discretized leading to a drastic reduction of the total number of degrees of freedom (DOFs). In traditional BE implementation the dimensional advantage with respect to domain discretization methods is offset by the fully-populated nature of the BEM coefficient matrix, with set-up and solution times rapidly increasing with the problem size.

The Fast Multipole Method (FMM) allows one to overcome the drawback of the fully-populated matrix by introducing a fast, reliable and approximate method to compute the linear integral operator. The efficiency of the method has been demonstrated in various fields including in 3D elastodynamics [1]. The FMM requires analytic closed-form expression of the fundamental solution to approximate the integral operator and is defined together with the use of an iterative solver. In 3D elastodynamics, the iteration count becomes the main limitation to use the Fast Multipole accelerated BEM (FM-BEM) on realistic seismological problems [2] (even though algebraic preconditioners can be developed to accelerate the convergence of the iterative solver).

2 Methodology

Other accelerated BEMs, based on hierarchical matrices ($\mathcal{H}$-matrices), have been proposed in the literature [4]. $\mathcal{H}$-matrices permit to approximate the fully-populated BEM matrix by a data-sparse matrix. When used in conjunction with an efficient rank revealing algorithm (for example Adaptive Cross Approximation, ACA) it leads to a data-sparse and memory efficient approximation of the original fully-populated BEM matrix. Contrary to the FM-BEM it is a purely algebraic tool which does not require *a priori* knowledge of the closed-form expression of the fundamental solutions. Such fast BEMs can be used in conjunction with an iterative solver. In computational mechanics, the method has successfully been applied to various problems. For example Coulier et al. [3] have applied the method to the layered half-space elastodynamic fundamental solutions to study soil-structure interaction. Milazzo et al. [5] have applied the method to study anisotropic elastodynamic media. Recent works (for example [6]) have proposed the development of fast direct solvers based on $\mathcal{H}$-matrices.

In the present work, we extend the ACA to problems with unknown vectors and propose iterative and direct solvers based on $\mathcal{H}$-matrices for 3-D frequency-domain elastodynamic BEMs (based on the full-space fundamental solutions). In addition, we study the expected efficiency of low-rank approximations in the low and high frequency regimes.

3 Numerical efficiency of the fast BEM

The numerical efficiency and accuracy of the method are assessed on the basis of numerical results obtained for problems having known solutions. In particular, a numerical study of the efficiency of low rank approximations when the frequency is increased is presented. Finally, the efficiency of the method to study seismic wave propagation in 3-D domain is demonstrated.

References

[1] S. Chaillat, M. Bonnet, J.F. Semblat. A multi-level fast multipole BEM for 3-D elastodynamics in the frequency domain. *Computer Methods in Applied Mechanics and Engineering*, Vol. **197**, 4233–4249, 2008.

[2] S. Chaillat, J.F. Semblat, M. Bonnet. A preconditioned 3-D multi-region fast multipole solver for seismic wave propagation in complex geometries. *Communications in Computational Physics*, Vol. **11**, 594–609, 2012.

[3] P. Coulier, S. François, G. Lombaert, G. Degrande. Application of hierarchical matrices to boundary element methods for elastodynamics based on Green's functions for a horizontally layered halfspace. *Engineering Analysis with Boundary Elements*, Vol. **37**, 1745–1758, 2013.

[4] W. Hackbusch. A Sparse Matrix Arithmetic Based on $\mathcal{H}$-Matrices. Part I: Introduction to $\mathcal{H}$-Matrices. *Computing*, Vol. **62**, 89–108, 1999.

[5] A. Milazzo, I. Benedetti, M.H. Aliabadi. Hierarchical fast BEM for anisotropic time-harmonic 3-D elastodynamics. *Computers & Structures*, Vol. **96**, 9–24, 2012.

[6] J. Shaeffer. Direct solve of electrically large integral equations for problem sizes to 1M unknowns. *IEEE Transactions on Antennas and Propagation*, Vol. **56**, 2306–2313, 2008.

Book of abstracts of the 7th International Conference
on Advanced Computational Methods
in Engineering, ACOMEN 2017
18–22 September 2017.

Analytic preconditioners for 3D high-frequency elastic scattering problems

Stéphanie Chaillat[1], Marion Darbas[2] and Frédérique Le Louër[3]

[1] *Laboratoire POEMS (CNRS-INRIA-ENSTA), Université Paris-Saclay, ENSTA-UMA, 91762 Palaiseau Cedex FRANCE*

[2] *LAMFA UMR CNRS 7352, Université de Picardie Jules Verne, 80039 Amiens Cedex, FRANCE*

[3] *LMAC EA 2222, Université de Technologie de Compiègne, 60205 Compiègne Cedex, FRANCE*

e-mails: stephanie.chaillat@ensta-paristech.fr, marion.darbas@u-picardie.fr, frederique.le-louer@utc.fr

Abstract

We propose to combine an approximate Dirichlet-to-Neumann (DtN) map as an analytic preconditioner with a fast multipole accelerated boundary element method (FM-BEM) to treat Dirichlet exterior scattering problems in 3D elasticity. The resulting boundary integral equations are preconditioned Combined Field Integral Equations (CFIEs). We provide various numerical illustrations of the efficiency of the method for different smooth and non smooth geometries. In particular, the number of iterations is shown to be completely independent of the number of degrees of freedom and of the frequency for convex obstacles.

Key words: time-harmonic elastic waves, Boundary Element Method, Fast Multipole Method, Analytical Preconditioner, approximate local DtN map.

1 Motivations

The aim of this work is to solve numerically 3D high-frequency elastic scattering problems by a bounded rigid obstacle, namely the exterior Navier problem with a Dirichlet boundary condition. To deal with the unbounded characteristic of the computational domain, we choose to apply the integral equation method. The advantage is to reformulate equivalently, through the potential theory, the exterior boundary-value problem as an integral equation on the boundary of the scatterer. The dimension of the problem is thus reduced by one. However, the discretization by BEM of boundary integral equations (BIE) leads to the solution of large and fully-populated complex linear systems. The solution of these systems is handled by the GMRES iterative method. To decrease the overall cost of the solver, two complementary ways are investigated: fast methods for the computation of matrix-vector products and preconditioners to speed up the convergence of the solver. The FMM permits to overcome the drawback of the fully-populated matrix by introducing a fast and approximate method to compute the linear integral operator. In 3D elastodynamics the FM-BEM has been shown to

be efficient [2] with solution times of order $O(N \log N)$ per iteration (where N is the number of BE degrees of freedom). However, the number of iterations in GMRES can significantly hinder the overall efficiency. Preconditioning the FM-BEM is therefore an important practical issue. Preconditioners are prescribed to yield fast convergence independently of both mesh size and frequency.

2 Methodology and results

A possible approach consists in constructing analytic preconditioners. The idea is to consider a judicious integral representation of the scattered field which naturally incorporates a regularizing operator. This operator is an approximation of the DtN map. The BIEs arising from this representation are compact perturbations of the identity operator. They are preconditioned Combined Field Integral Equations (CFIEs). Several well-conditioned integral equations based on this formalism have already been proposed in acoustics and electromagnetism. In [1], a pseudo inverse of the principal classical symbol of the single layer boundary integral operator - or equivalently the principal classical symbol of the Neumann trace of the double layer boundary integral operator - is used to approach the DtN map in the framework of the On-Surface Radiation Condition method. A preparatory theoretical work has been proposed to adapt such a preconditioning technique to solve 3D high-frequency elastic scattering problems [4]. The authors suggest strategies to overcome difficulties inherent in elasticity, in particular the fact that the double layer boundary integral operator and its adjoint are not compact even for sufficiently smooth boundaries. To this end, the tangential Günter derivative plays an important role.

We combine an approximate DtN map as an analytic preconditioner with a FM-BEM solver. The approximations of the DtN map are derived using tools proposed in [4]. They are expressed in terms of surface differential operators, square-root operators and their inverse. Complex Padé rational approximants provide local and uniform representations of the square-root operators. The numerical efficiency of the different proposed preconditioned CFIEs is illustrated for several more or less complex geometries. An analytical study for the spherical case underlines an "ideal" eigenvalue clustering around the point $(1, 0)$ for the preconditioned CFIEs. This is not the case for the standard CFIE which has small eigenvalues close to zero. The number of GMRES iterations is drastically reduced when the preconditioned CFIEs are considered, independently of the frequency [3].

References

[1] X.Antoine, M. Darbas, *Generalized combined field integral equations for the iterative solution of the three-dimensional Helmholtz equation*, M2AN **41** (2007) 147–167.

[2] S. Chaillat, M. Bonnet, J.F. Semblat, *A multi-level fast multipole BEM for 3-D elastodynamics in the frequency domain*, Comput. Methods Appl. Mech. Engrg. **197** (2008) 4233–4249.

[3] S. Chaillat, M. Darbas, F. Le Louër, *Fast iterative boundary element methods for high-frequency scattering problems in 3D elastodynamics*, Journal of Computational Physics **341** (2017) 429–446.

[4] M. Darbas, F. Le Louër, *Analytic preconditioners for the iterative solution of elasticity scattering problems*, M2AS **38** (2015) 1705–1733.

Book of abstracts of the 7th International Conference on Advanced Computational Methods in Engineering, ACOMEN 2017
18–22 September 2017.

Considerations on the Magnitude of the Shift in the Shifted Laplace Preconditioner for the Helmholtz Equation Combined with Deflation

D. Lahaye[1] **and C. Vuik**[1]

[1] *Delft Institute of Applied Mathematics, Delft University of Technology*

e-mails: d.j.p.lahaye@tudelft.nl, c.vuik@tudelft.nl

Abstract

In recent work we showed that the performance of the complex shifted Laplace preconditioner for the discretized Helmholtz equation can be significantly improved by combining it multiplicatively with a deflation procedure that employs multigrid vectors. In this contribution we argue that in this combination the preconditioner improves the convergence of the outer Krylov acceleration through a new mechanism. This mechanism allows for a much larger damping and facilitates the approximate solve with the preconditioner. The convergence of the outer Krylov acceleration is not significantly delayed and occasionally even accelerated. To provide a basis for these claims, we analyze for a one-dimensional problem a two-level variant of the method in which the preconditioner is applied after deflation and in which both the preconditioner and the coarse grid problem are inverted exactly. We show that in case that the mesh is sufficiently fine to resolve the wave length, the spectrum after deflation consists of a cluster surrounded by two tails that extend in both directions along the real axis. The action of the inverse of the precondioner is to shrink the length of the tails while at the same time rotating them and shifting the center of the cluster towards the origin. A much larger damping parameter than in algorithms without deflation can be used.
Key words: shifted Laplace preconditioner, deflation, Helmholtz equation

1 Deflating the Shifted Laplace Preconditioned Operator

The advent of the complex shifted Laplacian in [1] led to a breakthrough in capabilities in solving the Helmholtz equations. This preconditioner introduces damping and shifts small eigenvalues away from the origin such that the outer Krylov method converges faster. For a survey we refer to the recent monograph [2] and the references cited therein.

As the wavenumber increases while the number of grid points per wavelength is kept constant however, the number of small eigenvalues becomes too large for the preconditioner to handle effectively. This motivated the further development in [3] of a deflation approach aiming at removing small eigenvalues using a projection procedure. In this paper we combine a multigrid deflation technique and the complex shifted Laplacian multiplicatively. This construction allows to

- add a term to the deflation operator to shift a set of eigenvalues away from zero without significantly disturbing the non-zero eigenvalues. This in turn allows to extend the deflation method to multiple levels in a multigrid hierarchy. This multilevel extension can be interpreted as a multigrid method in which at least formally the complex shifted Laplacian acts as a smoother. As in [3], the method requires a Krylov acceleration at each level of the multigrid hierarchy;
- deduce the algebraic multiplicity of the zero eigenvalue of the deflated operator in a model problem analysis. This facilitates the computation of the non-zero eigenvalues;
- re-use implementations of the multigrid approximate inversion of the complex shifted Laplacian to code the operation with the deflation operator. In this re-use one has to construct the coarser grid operators by Galerkin coarsening, to provide a Krylov acceleration on the intermediate coarse levels and to provide a flexible Krylov method on the finest level.

We perform a model problem analysis of the preconditioned operator. The spectrum is real-valued in case that only the deflation is applied. It consists of a tight cluster surrounded by two tails. These tails spread in opposite directions along the real axis as the wavenumber increases. Elements in each tail correspond to the elements in the near-kernel of the Helmholtz operator on either side of zero. The role of the preconditioner is to scale and rotate the eigenvalues of the deflated operator. The spectrum of the operator after applying both deflation and preconditioning is complex-valued and consists of a cluster surrounded by two tails. These tails spread along a line in opposite directions in the complex plane away from the cluster with increasing wavenumber. The abscissa and slope of this line as well as the spread of the eigenvalues along this line are functions of the damping parameter in the preconditioner. Our results convincingly show that the use of deflation allows to significantly increase the damping parameter. Results in [3] give evidence for the fact using deflation results in a reduction of outer Krylov iterations and leads to a significant speed-up of the computations.

References

[1] Y. A. Erlangga, C. W. Oosterlee, and C. Vuik. A novel multigrid based preconditioner for heterogeneous Helmholtz problems. *SIAM J. Sci. Comput*, 27:1471–1492, 2006.

[2] D. Lahaye, J. Tang and C. Vuik. Modern Solvers for Hemholtz Problems, Springer, 2017.

[3] A. H. Sheikh, D. Lahaye, L. Garcia Ramos, R. Nabben and C. Vuik. Accelerating the shifted Laplace preconditioner for the Helmholtz equation by multilevel deflation. Journal of Computational Physics, 322: 473–490, 2016.

Book of abstracts of the 7th International Conference
on Advanced Computational Methods
in Engineering, ACOMEN 2017
18–22 September 2017.

Performance study of the Beyn method for the solution of lossy electromagnetic cavity problems

Nicolas Marsic[1], Felix Wolf[1], Sebastian Schöps[1] and Herbert De Gersem[1]

[1] *Institut für Theorie Elektromagnetischer Felder, Technische Universität Darmstadt*

e-mails: marsic@temf.tu-darmstadt.de, wolf@gsc.tu-darmstadt.de,
schoeps@temf.tu-darmstadt.de, degersem@temf.tu-darmstadt.de

Abstract

Since a few years, contour integral techniques for solving non-linear eigenvalue problems have become an active field of research. This work proposes to benchmark a particular method, known as the Beyn method, in the context of lossy electromagnetic cavities modelled by an impedance boundary condition.

Key words: finite element method, non-linear eigenvalue problem, surface impedance boundary condition.

1 Introduction

Contour integral methods for solving non-linear eigenvalue problems have gained in popularity in recent years. This approach allows to compute all the eigenvalues enclosed in a given contour in the complex plane by integrating some quantities on this path. Many algorithms taking advantage of this strategy have been proposed, by varying the computed integrals and how they are combined. In this work, the algorithm proposed in [1], usually referred to as the *Beyn method*, is used and tested on lossy electromagnetic cavity problems.

2 The Beyn method

Let us consider the following (potentially non-linear) eigenvalue problem:

$$\boldsymbol{T}(\omega)\boldsymbol{v} = \boldsymbol{0} \quad \text{with } \boldsymbol{v} \in \mathbb{C}^m \backslash \{\boldsymbol{0}\} \text{ and } \omega \in \Omega \subset \mathbb{C}, \tag{1}$$

where $\boldsymbol{T} : \Omega \to \mathbb{C}^{m,m}$ is an holomorphic matrix-valued function in Ω. As an illustration, in the classical linear case $\boldsymbol{T}(\omega) = \boldsymbol{A} - \boldsymbol{I}\omega$, where $\boldsymbol{I}$ is the identity matrix. The keystone of the Beyn method is the following identity [1]:

$$\frac{1}{2\jmath\pi}\int_\Gamma f(\omega)\boldsymbol{T}(\omega)^{-1}\mathrm{d}\omega = \sum_{n=1}^{N} f(\lambda_n)\boldsymbol{v}_n\boldsymbol{w}_n^\star, \tag{2}$$

where $\jmath$ is the imaginary unit, Γ the boundary of Ω, f an holomorphic scalar function, $\boldsymbol{v}_n$ (resp. $\boldsymbol{w}_n$) the n^{th} right (resp. left) eigenvector of $\boldsymbol{T}$, λ_n its n^{th} eigenvalue and N the number of

eigenvalues enclosed by Γ. It is then possible to extract the eigenvalues of $\boldsymbol{T}$ in Ω by probing (2) by a random matrix $\hat{\boldsymbol{V}} \in \mathbb{C}^{m,k}$, which satisfies some rank conditions [1]. In particular, the two following matrices are constructed:

$$\boldsymbol{A}_i = \frac{1}{2\jmath\pi} \int_\Gamma f^i(\omega) \boldsymbol{T}(\omega)^{-1} \hat{\boldsymbol{V}} \mathrm{d}\omega \quad \text{with } i \in \{0, 1\}, \tag{3}$$

where the number k of column of $\hat{\boldsymbol{V}}$ is chosen such that $\boldsymbol{A}_0$ exhibits a rank drop. By taking $f(\omega) = \omega$, these matrices can then be combined to construct a small matrix $\boldsymbol{B}$ with the same spectrum as the one of $\boldsymbol{T}$ in Ω.

The integrals of (3) are computed by using a quadrature rule. Thus the computation of the $\boldsymbol{A}_i$s accounts to the solution of many linear systems with the columns of $\hat{\boldsymbol{V}}$ as right-hand-sides and different values of ω. Obtaining these solution is the most time consuming part of the algorithm. Fortunately, since these linear systems are independent from each other, this integration step can be efficiently parallelized.

3 Application to lossy electromagnetic cavity simulations

In this work, the simulation of electromagnetic cavities with lossy walls is considered to test the performance of the Beyn method. By discretizing Maxwell's equation with the finite element method (FEM), and by using the Leontovich impedance boundary condition to model the wall losses, the following operator $\boldsymbol{T}$ can be constructed [2]:

$$\boldsymbol{T}(\omega) = \boldsymbol{K} - \omega^2 \boldsymbol{M} - \omega \Re(\omega)^{-1/2} \boldsymbol{C}, \tag{4}$$

where the matrices $\boldsymbol{K}$, $\boldsymbol{M}$ and $\boldsymbol{C}$ are given by the FEM, and where $\Re$ is the real part operator.

The behaviour of the Beyn method to solve the non-linear eigenvalue problem (1) with (4) will studied and analysed. Furthermore, since the construction of the matrices $\boldsymbol{A}_0$ and $\boldsymbol{A}_1$ in (3) requires only the solution of direct problems at known frequencies, the use of a domain decomposition method for electromagnetic waves will also be shortly discussed.

Acknowledgements

This research is funded by the German Bundesministerium für Bildung und Forschung as the project BMBF-05P15RDRBB "Ultra-Sensitive Strahlstrommessung für zukünftige Beschleunigeranlagen".

References

[1] W.-J. Beyn, "An integral method for solving nonlinear eigenvalue problems," *Linear Algebra and its Applications*, vol. 436, no. 10, pp. 3839–3863, 2012.

[2] S. Yuferev and N. Ida, *Surface impedance boundary conditions: a comprehensive approach*. CRC Press, 2009.

Book of abstracts of the 7th International Conference on Advanced Computational Methods in Engineering, ACOMEN 2017
18–22 September 2017.

Transmission Conditions for Non-Overlapping Schwarz Domain Decomposition Methods Applied to Elastic Waves

Christophe Geuzaine[1] **and Vanessa Mattesi**[1]

[1] *Departement of Electrical Engineering and Computer Science, University of Liège*

e-mails: cgeuzaine@ulg.ac.be, vanessa.mattesi@ulg.ac.be

Abstract

We focus on the construction of transmission conditions for optimized Schwarz domain decomposition methods applied to time-harmonic elastic wave scattering problems solved numerically with finite element methods.

Key words: Scattering, elastic waves, optimized Schwarz method, approximate DtN map

1 Introduction

The aim of this ongoing work is to solve time-harmonic elastodynamic scattering problems for which the scatterer is inhomogeneous. Direct sparse solvers do not scale well for such problems and iterative solvers exhibit poor convergence or even diverge. Domain decomposition methods provide an alternative, combining direct sparse solvers on subproblems of smaller sizes with an iterative Krylov solver. In this paper we investigate the impact of the transmission conditions used between the subdmains on the convergence of the iterative algorithm.

2 Problem statement

Mono-domain elastic wave problem Let us consider $\Omega^- := \{\mathbf{x} \in \mathbb{R}^2 : |\mathbf{x}| \leq r_{int}\}$ with boundary Γ and its complementary $\Omega^+ := \mathbb{R}^2 \backslash \Omega^-$. When illuminated by a time-harmonic incident wave $\mathbf{u}^{inc}$, the scattering problem is formulated as follows: find the displacement $\mathbf{u}$ in Ω^+ solution to the Navier equation such that $\mathbf{u} = -\mathbf{u}^{inc}$, on Γ, and satisfying the Kupradze radiation conditions at infinity. In view of a finite element discretization, Ω^+ is truncacted by an artificial boundary Γ^∞, which delimits the bounded domain Ω under study.

Domain decomposition We split the domain Ω into N_{dom} sub-domains Ω_i without overlap. Let us denote $\Gamma_i := \Gamma \cap \Omega_i$, $\Gamma_i^\infty := \Gamma^\infty \cap \Omega_i$ and $\Sigma_{ij} := \overline{\Omega_i} \cap \overline{\Omega_j}$ the transmission boundary. At iteration $n+1$ for a sub-domain Ω_i, the classical additive Schwarz domain decomposition method can be described as follows.

- First, find the volume solution $\mathbf{u}_i^{n+1}$ such that $\begin{cases} \mathrm{div}\sigma(\mathbf{u}_i^{n+1}) + \rho\omega^2\mathbf{u}_i^{n+1} = 0, & \text{on } \Omega_i, \\ \mathbf{u}_i^{n+1} = -\mathbf{u}^{inc}, & \text{on } \Gamma_i, \\ \partial_{n_i}\mathbf{u}_i^{n+1} + \mathcal{B}\mathbf{u}_i^{n+1} = 0, & \text{on } \Gamma_i^{\infty}, \\ \partial_{n_i}\mathbf{u}_i^{n+1} + \mathcal{T}\mathbf{u}_i^{n+1} = g_{ij}^n, & \text{on } \Sigma_{ij}, \end{cases}$

where n_i is the outgoing normal of Ω_i, $\mathcal{B}$ is the operator describing boundary conditions at infinity, $\mathcal{T}$ is the transmission operator and g_{ij}^n is the surface field given by the previous iteration.

- Then update the interface unknowns: $g_{ji}^{n+1} = -g_{ij}^n + 2\mathcal{T}\mathbf{u}_i^{n+1}, \quad \text{on } \Sigma_{ij}.$

3 Transmission operators

Multiple choices are possible for the transmission operator $\mathcal{T}$, the optimal operator being the Dirichlet-to-Neumann map associated to the complementary of the subdomain. This operator being nonlocal (and thus computationally expensive), we investigate two approximations:

- Lysmer and Kuhlemeyer condition: $\mathcal{T}_0\mathbf{u} = -\mathrm{i}[(\lambda + 2\mu)k_p\mathbf{u}_p + \mu k_s\mathbf{u}_s]$, with k_p and k_s the wavenumbers associated with $\mathbf{u}_p$ (the longitudinal pressure wave with a vanishing curl), and $\mathbf{u}_s$ (the transverse shear wave with a vanishing divergence) respectively.
- Square-root condition: $\mathcal{T}_1\mathbf{u} = -\mathrm{i}[(\lambda + 2\mu)k_p(\frac{\Delta_\Sigma}{k_{p,\epsilon}^2} + \mathrm{I})^{1/2}\mathbf{u}_p + \mu k_s(\frac{\Delta_\Sigma}{k_{s,\epsilon}^2} + \mathrm{I})^{1/2}\mathbf{u}_s]$, with Δ_Σ the tangential Laplacian operator and $k_{\alpha,\epsilon} := k_\alpha + 0.39\mathrm{i}k_\alpha^{1/3}\mathcal{H}^{2/3}$, $\alpha = s, p$. This condition is then localized using complex Padé approximants [1, 2].

4 Preliminary results

We consider an annulus-shaped domain Ω, split into two concentric subdomains with $\rho = 1\,\mathrm{kg.m^{-3}}$, $\omega = 2\pi\,\mathrm{s^{-1}}$ and $\lambda = \mu = 1\,\mathrm{Pa}$. The figure displays the eigenvalues of the iteration operator for the two transmission conditions. These spectra lead respectively to 49 and 23 GMRES iterations in the domain decomposition algorithm as implemented in [1].

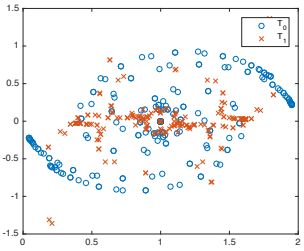

Acknowledgements

This work has been supported by the University of Liège.

References

[1] B. Thierry, A. Vion, S. Tournier, M. El Bouajaji, D. Colignon, N. Marsic, X. Antoine and C. Geuzaine, *GetDDM: An open framework for testing optimized Schwarz methods for time-harmonic wave problems Computer Physics Communications*, Elsevier, **203** (2016) pp. 309-330.

[2] F.A. Milinazzo, C.A. Zala and G.H. Brooke, *Rational square-root approximations for parabolic equation algorithms Acoustical Society of America*, J. Diff. Geom. **17** (1997) 661–692.

Book of abstracts of the 7th International Conference on Advanced Computational Methods in Engineering, ACOMEN 2017
18–22 September 2017.

High-order absorbing boundary conditions with edge and corner compatibility for the Helmholtz equation

Axel Modave[1], Vanessa Mattesi[2] and Christophe Geuzaine[2]

[1] *Team POEMS, CNRS-ENSTA-INRIA, Université Paris-Saclay, France*

[2] *Electrical Engineering and Computer Science, University of Liège*

e-mails: axel.modave@ensta-paristech.fr, vanessa.mattesi@ulg.ac.be, cgeuzaine@ulg.ac.be

Abstract

We deal with the finite element solution of 3D time-harmonic acoustic wave problems defined on unbounded domains, but computed using cuboidal computational domains with artificial boundaries. We combine a standard finite element method for the Helmholtz equation with high-order absorbing boundary conditions *(on the faces of the domain)* and compatibility relations *(on the edges and the corners)* that provide an arbitrary high accuracy.

Key words: Helmholtz equation, Finite element method, Radiation boundary condition, Corner compatibility
MSC 2010: 35J05, 35J25

The finite element methods must be combined with specific boundary techniques, such as perfectly matched layers and non-reflective boundary conditions, to accurately simulate the radiation of wavefields at the artificial boundaries of truncated computational domains. Padé-type high-order absorbing boundary conditions (HABCs) can provide an arbitrary high accuracy [2], but they are generally limited to regions with smooth boundaries. We propose a comprehensive strategy for cuboidal domains, with treatments for the edges and the corners.

Let the field $u(\mathbf{x})$ governed by the Helmholtz equation $\Delta u + k^2 u = 0$ on the cube $\Omega = [-L, L]^3$. On the faces of Ω, we consider the HABC obtained by approximating the square root in the exact non-reflective boundary operator thanks to the $(2N+1)^{\text{th}}$-order Padé expansion with a θ-rotation of the branch cut [2]. On the face belonging to the plane $x = L$, the HABC can then be written as

$$\partial_x u = \imath k e^{\imath\theta/2}\left(u + \frac{2}{M}\sum_{n=1}^{N} c_n\,(u + u_n)\right), \quad \text{with } c_n = \tan(n\pi/M) \text{ and } M = 2N+1. \tag{1}$$

This condition involves N auxiliary fields u_n defined only on the face and governed by

$$k^2\left(e^{\imath\theta}c_n + 1\right)u_n + k^2 e^{\imath\theta}\,(c_n+1)\,u + \left[\partial_{yy} + \partial_{zz}\right]u_n = 0, \quad n = 1\ldots N. \tag{2}$$

Because of the spatial partial derivatives in Eq. 2, boundary conditions must be prescribed on the boundary of the face (*i.e.* on the edges of the cube) for each auxiliary field u_n.

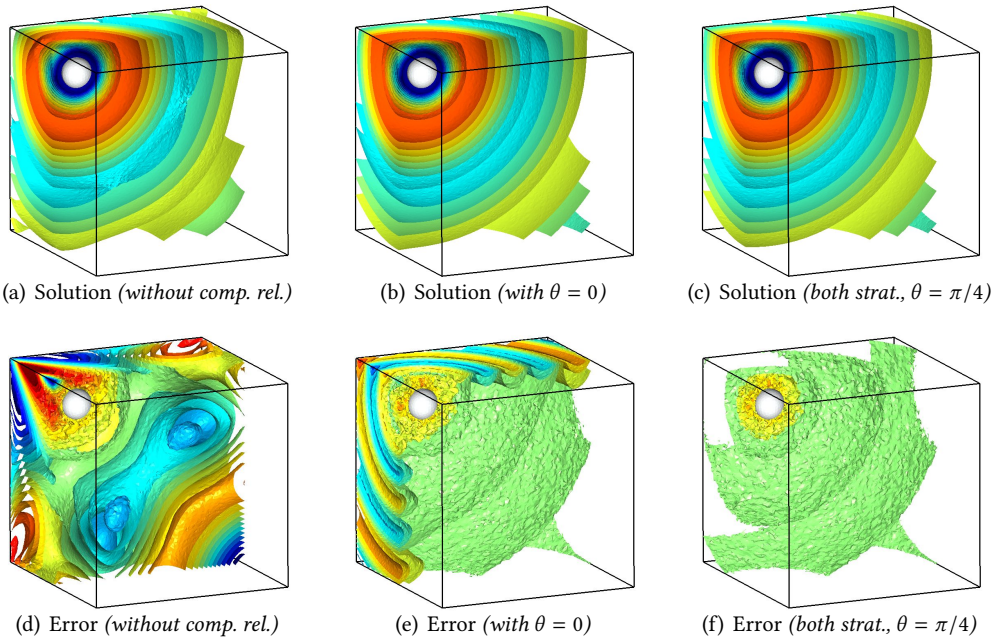

(a) Solution *(without comp. rel.)* (b) Solution *(with $\theta = 0$)* (c) Solution *(both strat., $\theta = \pi/4$)*

(d) Error *(without comp. rel.)* (e) Error *(with $\theta = 0$)* (f) Error *(both strat., $\theta = \pi/4$)*

Figure 1: Solutions and errors for the benchmark with HABCs ($N = 4$). Three cases are shown: without compatibility relations *(left)*, without rotating branch cut *(middle)*, with both strategies *(right)*. Isosurfaces of the solutions (scale: [-0.2,0.2]) and the errors (scale: [-0.015,0.015]) are represented in only half the domain. We use a mesh made of approx. 10^6 tetrahedron and P1 elements.

In our strategy, we introduce new relations that close the system and that ensure its compatibility without any supplementary approximation. They are derived by manipulating the equations (Eqs. 1-2) corresponding to the different faces, and by introducting auxiliary fields and auxiliary equations on each edge (N^2 per edge) and each corner (N^3 per corner). The result is a multi-dimensional solver with equations to be solved on the volume, the faces, the edges and the corners of Ω. See [1] for a time-dependent version of this solver.

As preliminary 3D finite element results, we present simulations of a spherical wave generated inside a cubic domain (Fig. 1). HABCs are prescribed on all the faces of the domain. By comparing the three cases, we see the positive effect of both the compatibility relations and the rotating branch cut on the quality of the solution. When using both strategies (Fig. 1f), the remaining error corresponds to the classical numerical dispersion caused by the mesh.

References

[1] A. Modave, A. Atle, J. Chan, T. Warburton, *A GPU-accelerated nodal discontinuous Galerkin method with high-order absorbing boundary conditions and corner/edge compatibility*, To appear in International Journal for Numerical Methods in Engineering

[2] R. Kechroud, X. Antoine, A. Soulaïmani, *Numerical accuracy of a Padé-type non-reflecting boundary condition for the finite element solution of acoustic scattering problems at high-frequency*, International Journal for Numerical Methods in Engineering 64.10 (2005): 1275-1302.

Book of abstracts of the 7th International Conference
on Advanced Computational Methods
in Engineering, ACOMEN 2017
18–22 September 2017.

Optimized Schwarz Methods for Electromagnetic Time-Harmonic Wave Propagation Problems

Bertrand Thierry[1], Xavier Antoine[2], Mohamed El Bouajaji[2] and Christophe Geuzaine[3]

[1] *CNRS - Laboratoire Jacques-Louis Lions, University Pierre and Marie Curie, Paris, France*

[2] *Institut Elie Cartan de Lorraine, University of Lorraine, Nancy, France*

[3] *Applied Computational Electromagnetics, University of Liège, Belgium*

e-mails: thierry@ljll.math.upmc.fr, xavier.antoine@univ-lorraine.fr, melbouaj@gmail.com, cgeuzaine@ulg.ac.be

Abstract

We present a non-overlapping optimized Schwarz method for the vector Helmholtz equation, based on a Padé approximation of the Magnetic-To-Electric map. It exhibits a quasi-optimal convergence in terms of both the wavenumber and the mesh refinement. We also show numerical results highlighting this behavior and sumarize the last developments of GetDDM, the software we built that is designed to solve large time-harmonic wave propagation problems in parallel and using domain decomposition method.

Key words: Domain Decomposition Method, Time-harmonic wave propagation

1 Introduction

In terms of computational methods, solving three-dimensional time-harmonic acoustic or electromagnetic wave problems is known to be challenging, especially in the high frequency regime. Among the various approaches that can be used to solve them, the Finite Element Method (FEM) with an Absorbing Boundary Condition (ABC) or a Perfectly Matched Layer (PML) is widely used for its ability to handle complex geometrical configurations and materials with non-homogeneous properties. However, the brute-force application of the FEM in the high-frequency regime leads to the solution of very large, complex-valued and possibly indefinite linear systems. Direct sparse solvers do not scale well for such problems, and Krylov subspace iterative solvers exhibit slow convergence or even diverge. Domain decomposition methods provide an alternative, iterating between subproblems of smaller sizes, amenable to sparse direct solvers.

2 Optimized Schwarz Method

We consider a perfectly conducting obstacle Ω^- with a smooth boundary Γ surrounded by a (fictitious) absorbing boundary Γ^∞ with a simple ABC, and denote by Ω the domain of boundary $\Gamma \bigcup \Gamma^\infty$. When illuminated by a time-harmonic incident electric field $\mathbf{E}^{\text{inc}}$, the obstacle generates a scattered field $\mathbf{E}$, solution of the exterior electromagnetic scattering problem:

$$\left\{\begin{array}{rcll} \text{curl curl}\,\mathbf{E} - k^2\mathbf{E} & = & 0, & \text{in } \Omega, \\ \gamma^T(\mathbf{E}) & = & -\gamma^T(\mathbf{E}), & \text{on } \Gamma, \\ \gamma^t(\text{curl}\,\mathbf{E}) + \imath k(\gamma^T(\mathbf{E})) & = & 0, & \text{on } \Gamma^\infty, \end{array}\right. \tag{1}$$

where $k := 2\pi/\lambda$ is the wavenumber, λ the wavelength, $\mathbf{n}$ is the outward unit normal to Ω, $\gamma^T\mathbf{v} = \mathbf{n}\times(\mathbf{v}\times\mathbf{n})$, $\gamma^t\mathbf{v} = \mathbf{n}\times\mathbf{v}$ and $\text{curl}\,\mathbf{a} := \nabla\times\mathbf{a}$. The propagation domain Ω is now decomposed in N subdomains Ω_i, $i = 1,\dots,N$, without overlap. The iterative Jacobi algorithm for the computation of the electric fields $(\mathbf{E}_i^{n+1})_{1\le i\le N}$ at iteration $n+1$ involves, first, the solution of the N following problems ($i = 1,\dots,N$)

$$\left\{\begin{array}{rcll} \text{curl curl}\,\mathbf{E}_i^{n+1} - k^2\,\mathbf{E}_i^{n+1} & = & \mathbf{o}, & \text{in } \Omega_i, \\ \gamma_i^T(\mathbf{E}_i^{n+1}) & = & -\gamma_i^T(\mathbf{E}^{\text{inc}}), & \text{on } \Gamma_i, \\ \gamma_i^t(\text{curl}\,\mathbf{E}_i^{n+1}) + \imath k(\gamma_i^T(\mathbf{E}_i^{n+1})) & = & \mathbf{o}, & \text{on } \Gamma_i^\infty, \\ \gamma_i^t(\text{curl}\,\mathbf{E}_i^{n+1}) + \mathcal{S}(\gamma_i^T(\mathbf{E}_i^{n+1})) & = & \mathbf{g}_{ij}^n, & \text{on } \Sigma_{ij} := \partial\Omega_i \bigcap \partial\Omega_j,\ \forall j \neq i, \end{array}\right. \tag{2}$$

and then forming the quantities $\mathbf{g}_{ji}^{n+1}$ through

$$\mathbf{g}_{ji}^{n+1} = \gamma_i^t(\text{curl}\,\mathbf{E}_i^{n+1}) + \mathcal{S}(\gamma_i^T(\mathbf{E}_i^{n+1})) = -\mathbf{g}_{ij}^n + 2\mathcal{S}(\gamma_i^T(\mathbf{E}_i^{n+1})), \quad \text{on } \Sigma_{ij}. \tag{3}$$

The operator $\mathcal{S}$ is the transmission operator through the interfaces Σ_{ij} and plays a major role in the convergence speed of the algorithm. Problems (2) and (3) could be rewritten in a linear system based on the interface quantities $\mathbf{g}$ only, and solved using a Krylov subspace solver. In [1], we propose a new transmission operator $\mathcal{S}$, given by approximating the MtE operator with a complex Padé expansion (C_0, A_ℓ and B_ℓ are given by the expansion):

$$\mathcal{S}_{\text{GIBC}(N_p,\,\alpha,\,\varepsilon)}(\gamma^T(\mathbf{E})) = \imath k\left(C_0 + \sum_{\ell=1}^{N_p} A_\ell X\,(\mathcal{I} + B_\ell X)^{-1}\right)^{-1}\left(\mathcal{I} - \text{curl}_\Sigma\frac{1}{k_\varepsilon^2}\text{curl}_\Sigma\right)(\gamma^T(\mathbf{E})), \tag{4}$$

with $X := \nabla_\Sigma\frac{1}{k_\varepsilon^2}\text{div}_\Sigma - \text{curl}_\Sigma\frac{1}{k_\varepsilon^2}\text{curl}_\Sigma$, and where $k_\varepsilon = k + \imath\varepsilon$.

After a review of the transmission conditions proposed in the literature, we will see that condition (4) leads to a quasi-optimal algorithm, in terms of both the wavenumber and the mesh refinement. The numerical results that will be presented have been achieved with GetDDM [2], an open-source software that we built, dedicated to solve in parallel time-harmonic wave propagation problems using the domain decomposition method. Problems with several billion degrees of freedom have been successfully solved on massively parallel computers using GetDDM. The last improvements of our software will also be presented.

References

[1] M. El Bouajaji, B. Thierry, X. Antoine and C. Geuzaine, *A quasi-optimal domain decomposition algorithm for the time-harmonic Maxwell's equations*, Journal of Computational Physics, 2015.

[2] B. Thierry, A. Vion, S. Tournier, M. El Bouajaji, D. Colignon, N. Marsic, X. Antoine and C. Geuzaine, *GetDDM: An open framework for testing optimized Schwarz methods for time-harmonic wave problems*, Computer Physics Communications, 2016.

MS 12 Computational methods in fractional PDEs

Organiser: Rob De Staelen

Description: In recent decades, fractional calculus has found a large number of profound applications, which have triggered the development of methods for more reliable discretisation and approximations of the dynamics of continuous systems. From a pragmatic point of view, fractional order models provide better descriptions and, ultimately, a better understanding of underlying complex phenomena in sciences and technology. To that end, novel analytical methods to investigate qualitative features of the solutions of these nonlocal systems as well as more general results on the existence and the uniqueness of suitable solutions are desirable tools in the study of fractional systems. At the same time, continuous models based on systems of partial differential equations have been investigated via various criteria of discretisation. Novel numerical methods to approximate the solutions of fractional systems have emerged in the literature. However, the search for discrete techniques which are faster and stable, which possess a higher order of convergence at lower computational costs, and which preserve the main features of the solutions of interest, is a constant pursuit in the numerical analysis. In particular, the design of discretisation of continuous fractional systems that preserve important characteristics, such as positivity, boundedness, convexity, monotonicity, and energy, is a fruitful area of research that merits a closer attention. In light of these facts, the purpose of this mini-symposium is to present original high-quality research that address the latest progress on analytical methods of fractional systems or that analyse new numerical schemes for fractional differential equations arising in science and technology. Rather than mere applications of standard analytical and numerical techniques, our emphasis is on novel theoretical results and the analysis of new methodologies.

Book of abstracts of the 7th International Conference on Advanced Computational Methods in Engineering, ACOMEN 2017
18–22 September 2017.

Analysis of $L1$-difference methods for time-fractional nonlinear parabolic problems with delay

R. H. De Staelen[1] **and A. S. Hendy**[2]

[1] *Department of Mathematical Analysis, Ghent University, Gent 9000, Belgium*

[2] *Department of Mathematics, Faculty of Science, Benha University, Benha 13511, Egypt*

e-mails: rob.destaelen@ugent.be, ahmed.hendy@fsc.bu.edu.eg

Abstract

This work is concerned with numerical solutions of time-fractional nonlinear parabolic problems by a class of $L1$-difference methods. The analysis of $L1$ methods for time-fractional nonlinear problems with delay is limited mainly due to the lack of a fundamental Gronwall type inequality. We establish such a fundamental inequality for the $L1$ approximation to the Caputo fractional derivative. In terms of the Gronwall type inequality, we will provide error estimates of a fully discrete linearized difference scheme for this kind of problems.

Key words: time-fractional nonlinear parabolic problems with delay, L1-difference scheme, error estimates, Gronwall inequality, linearized schemes

1 Introduction

We study numerical solutions of the time-fractional nonlinear parabolic equation with delay

$$ {}^{C}D_t^{\alpha} u - \frac{\partial^2 u}{\partial x^2} = f(x,t,u,u(x,t-s)), \ \ (x,t) \in \Omega \times (0,T], \tag{1a} $$

with the following initial and boundary conditions

$$ u(x,t) = \phi(x,t), \quad (x,t) \in \Omega \times [-s,0], \tag{1b} $$

$$ u(x,t) = 0, \quad (x,t) \in \partial\Omega \times [0,T], \tag{1c} $$

where $\Omega = [a,b]$ and $s > 0$ is a fixed delay parameter. The fractional derivative ${}^{C}D_t^{\alpha}$ of order $0 < \alpha \leq 1$ is defined in Caputo sense.

In the past decades, developing effective numerical methods and rigorous numerical analysis for the time-fractional PDEs have been a hot research spot, see e.g. [2]. Numerical methods can be roughly divided into two categories: indirect and direct methods. The former is based on the solution of an integro-differential equation by some proper numerical schemes since time-fractional differential equations can be reformulated into integro-differential equations in general, while the latter is based on a direct (such as piecewise polynomial) approximation to the time-fractional derivative [1]. Direct methods are more popular in practical computations due to its ease of implementation. One of the most commonly used direct methods

is the so-called $L1$-scheme, which can be viewed as a piecewise linear approximation to the fractional derivative and which has been widely applied for solving various time-fractional PDEs [3]. However, numerical analysis for direct methods is limited, even for a simple linear model (1) where $s = 0$ and $f(u) = L_0 u$.

The analysis of $L1$-type methods for the linear model was studied by several authors, while the convergence and error estimates were obtained under the assumption that $L_0 \leq 0$ in general, see [4]. Recently, this condition was improved in [6], in which a time-fractional nonlinear predator-prey model was studied by an $L1$ finite difference scheme and $f(u)$ was assumed to satisfy a global Lipschitz condition. The stability and convergence were proved under the assumption $T^\alpha < \frac{1}{L\Gamma(1-\alpha)}$ where L denotes the Lipschitz constant. This restriction condition implies that the scheme is convergent and stable only locally in time.

It is well known that the classical Gronwall inequality plays an important role in analysis of parabolic PDEs ($\alpha = 1$) and the analysis of corresponding numerical methods also relies heavily on the discrete counterpart of this inequality. Clearly, the analysis of $L1$-type numerical methods for time-fractional nonlinear differential equations ($0 < \alpha < 1$) has not been well done mainly due to the lack of such a fundamental inequality. In [5], the authors aimed to present the numerical analysis for several fully discrete $L1$ Galerkin FEMs for the general nonlinear equation 1 at $s = 0$ with any given $T > 0$. The key to their analysis is to establish a Gronwall type inequality for a positive sequence satisfying

$$D_\tau^\alpha \omega^k \leq \lambda_1 \omega^k + \lambda_2 \omega^{k-1} + g^k.$$

As an extension to the work of [5], the main purpose of our contribution is to discuss the numerical analysis for fully discrete L_1 difference schemes for the general nonlinear equation (1) with fixed delay with any given $T > 0$. Our analysis is done by constructing a new Gronwall type inequality for a positive sequence satisfying

$$D_\tau^\alpha \omega^k \leq \lambda_1 \omega^{k-1} + \lambda_2 \omega^{k-2} + \lambda_3 \omega^{k-n} + g^k,$$

where D_τ^α denotes an $L1$ approximation to ${}^C D_t^\alpha$, and λ_1, λ_2 and λ_3 are all positive constants.

References

[1] W. Cao, Z. Zhang, G. Karniadakis, *Time-splitting schemes for the fractional differential equations I: smooth solutions*, SIAM. J. Sci. Comput. **37** (2015) 1752–1776.

[2] C. Chen, F. Liu, V. Anh, I. Turner, *Numerical methods for solving a two-dimensional variable-order anomalous subdiffusion equation*, Math. Comput. **81** (2012) 345–366.

[3] G. Gao, Z. Sun, *A compact finite difference scheme for the fractional sub-diffusion equations*, J. Comput. Phys. **230** (2011) 565–586.

[4] B. Jin, R. Lazarov, Z. Zhou, *An analysis of the L1 scheme for the subdiffusion equation with nonsmooth data*, IMA. J. Numer. Anal. **36** (2016) 197–221.

[5] D. Li, H.-L. Liao, W. Sun, J. Wang, J. Zhang, *Analysis of L1-Galerkin FEMs for time-fractional nonlinear parabolic problems*, arXiv:1612.00562.

[6] Y. Yu, W. Deng, Y. Wu, *Positivity and boundedness preserving schemes for space time fractional predator prey reaction diffusion model*, Comput. Math. Appl. **69** (2015) 743–759.

Book of abstracts of the 7th International Conference
on Advanced Computational Methods
in Engineering, ACOMEN 2017
18–22 September 2017.

Time fractional derivatives and maximal regularity results for evolution equations

Davide Guidetti[1]

[1] *Department of Mathematics, University of Bologna (Italy)*

e-mails: davide.guidetti@unibo.it

Abstract

We discuss some results of maximal regularity for abstract evolution equations containing a fractional time derivative.

Key words: Abstract evolution equations, Fractional derivatives, Maximal regularity
MSC 2010: 26A33, 34G10.

1 Introduction

We consider linear abstract evolution equations of the form

$$D^\alpha u(t) = Au(t) + f(t), \quad t \in [0,T] \tag{1}$$

where we indicate with D^α the time derivative of order α, belonging to $[0,2]$ in the sense of Riemann-Liouville or of Caputo. (1) is supplemented by suitable initial conditions in $t = 0$. A is a linear unbounded operator in the Banach space X. We illustrate results of maximal regularity in spaces of continuous and Hölder continuous functions. We recall that a maximal regularity result establishes a linear and topological isomorphism between spaces of data and spaces of solutions. The abstract results are applicable to mixed boundary values problems, where, typically, A is the realization of a linear partial differential operator in a space domain, with suitable boundary conditions.

Book of abstracts of the 7th International Conference on Advanced Computational Methods in Engineering, ACOMEN 2017 18–22 September 2017.

Numerical methods for solving of the Dirichlet boundary value problem for the fractional Allers' equation

Fatimat Karova[1]

[1] *Department of Computational Mathematics, Institute of Applied Mathematics and Automation*

e-mails: karova.fatimat@mail.ru

Abstract

Solution of the Dirichlet boundary value problem for the fractional Allers' equation in differential and difference settings are studied. By the method energy inequalities a priori estimate is obtained for the solution of the problems. The obtained results are supported by the numerical calculations carried out for test problem.

Key words: a priori estimate, difference scheme, fractional derivative, numerical analysis, stability and convergence.

1 Introduction

Moisture movement in is capillary porous environment is described by the equation of Aller [1]. Boundary value problems for classical Allers' equation is studied in [2]. However, it was found that the fractional derivatives are more effective in describing the properties of viscoelastic fluid. In this regard, there are models for fractional Allers' equation. The method of energy inequalities has been applied for the numerical solution of boundary value problems for differential equations of fractional order with variable coefficient [3] and [4]. The stability and convergence of the numerical scheme for solving the boundary value problem for generalized Allers' equation are analysed [5] by energy method.

2 Dirichlet boundary value problem

In rectangle $\overline{Q}_T = \{(x,t):\ 0 \le x \le l, 0 \le t \le T\}$ let us study the boundary value problem

$$\partial_{0t}^{\alpha} u = \frac{\partial}{\partial x}\left(k(x,t)\frac{\partial u}{\partial x}\right) + \partial_{0t}^{\alpha}\frac{\partial}{\partial x}\left(\eta(x,t)\frac{\partial u}{\partial x}\right) - q(x,t)u + f(x,t), \tag{1}$$

$$u(0,t) = 0,\ u(l,t) = 0,\ 0 \le t \le T, \tag{2}$$

$$u(x,0) = u_0(x),\ 0 \le x \le l, \tag{3}$$

where $\partial_{0t}^{\alpha} u(x,t) = \frac{1}{\Gamma(1-\alpha)}\int\limits_0^t u_s(x,s)(t-s)^{-\alpha}\,ds$ is a Caputo fractional derivative of order α, $0 < \alpha < 1$, $0 < c_1 \le k(x,t), \eta(x,t) \le c_2$, $\eta_t(x,t) \ge 0$, $q(x,t) \ge 0$ on $\overline{Q}_T$.

Theorem *If* $k(x,t) \in C^{1,0}\left(\overline{Q}_T\right), \eta(x,t) \in C^{1,1}\left(\overline{Q}_T\right), q(x,t), f(x,t) \in C\left(\overline{Q}_T\right), 0 < c_1 \le k(x,t), \eta(x,t) \le c_2, \eta_t(x,t) \ge 0$, *then the solution* $u(x,t)$ *of the problem (1)–(3) is satisfies the a priori estimate*

$$||u||^2_{W_2^1(0,l)} + D_{0t}^{-\alpha}\,||u_x||_0^2 \le M\left(D_{0t}^{-\alpha}||f||_0^2 + ||u_0||^2_{W_2^1(0,l)}\right), \tag{4}$$

where $M > 0$ *– is a known constant independent from* T.

3 Difference schemes for the Dirichlet boundary value problem

Let $\eta(x,t) = \eta(x)$. In rectangle $\overline{Q}_T$ we introduce the grid $\overline{\omega}_{h\tau} = \overline{\omega}_h \times \overline{\omega}_\tau$, where

$$\overline{\omega}_h = \{x_i = ih,\ i = 0,1,\dots,N,\ hN = l\},$$
$$\overline{\omega}_\tau = \left\{t_j = j\tau,\ j = 0,1,\dots,j_0,\ \tau j_0 = T\right\}.$$

To problem (1)–(3) we assign the difference scheme:

$$\Delta^{\alpha}_{0t_{j+\sigma}} y = \Lambda_1 y^{(\sigma)} + \Delta^{\alpha}_{0t_{j+\sigma}}\Lambda_2 y + \varphi,\ 1 \le i \le N-1,\ 1 \le j \le j_0 - 1, \tag{5}$$

$$y(0,t) = 0, \quad y(l,t) = 0, \quad 0 < t \le T, \tag{6}$$

$$y(x,0) = u_0(x), \quad 0 \le x \le l, \tag{7}$$

where $\sigma = 1 - \frac{\alpha}{2}$, $\varphi = f\left(x_i, t_{j+\sigma}\right)$, $\Delta^{\alpha}_{0t_{j+\sigma}} y$ is the difference analogue of the Caputo fractional derivative of order [4].

The difference scheme (5)–(7) has the order of approximation $O\left(\tau^2 + h^2\right)$ [4].

Theorem *The difference scheme (5)–(7) is absolutely stable and its solution satisfies a priori estimate*

$$\|y^{j+1}\|_1^2 \le \|y^0\|_1^2 + \frac{l^2 T^{\alpha}\Gamma(1-\alpha)}{4c_1}\max_{0\le j\le j_0}\|\varphi^j\|_0^2, \tag{8}$$

where

$$\|y\|_1^2 = \|y\|_0^2 + \|\sqrt{b}y_{\bar{x}}]\|_0^2, \quad \|y\|_0^2 = (y,y), \quad \|y]\|_0^2 = (y,y],$$
$$(y,v) = \sum_{i=1}^{N-1} y_i v_i h, \quad (y,v] = \sum_{i=1}^{N} y_i v_i h.$$

References

[1] A.F. Chudnovsky, *Thermophysics Soil*, Moscow, 1976.

[2] M.Kh. Shkhanukov-Lafishev,, *About boundary value problems for equation of the third order*, J. Diff. Eq. **18** (1982) 1785–1795.

[3] A.A. Alikhanov, *Boundary value problems for the diffusion equation of the variable order in differential and difference settings*, J. Appl. Math. Comput. **219** (2012) 3938–3946.

[4] A.A. Alikhanov, *A new difference scheme for the time fractional diffusion equation*, J. Comput. Phys. **280** (2015) 424–438.

[5] Ch. Wu, *Numerical solution for Stokes' first problem for a heated generalized second grade fluid with fractional derivative*, J. Appl. Num. Math. **59** (2009) 2571–2583.

Book of abstracts of the 7th International Conference on Advanced Computational Methods in Engineering, ACOMEN 2017
18–22 September 2017.

Structure-preserving methods to solve a nonlinear parabolic equation with fractional diffusion and advection

Jorge E. Macías-Díaz[1]

[1] *Departamento de Matemáticas y Física, Universidad Autónoma de Aguascalientes*

e-mails: jemacias@correo.uaa.mx

Abstract

This work is motivated by an extension of both the two-dimensional Burgers–Fisher and Burgers–Huxley equations, that considers Riesz fractional diffusion and advection. Initial-boundary conditions which are positive and bounded are imposed on a closed and bounded interval, and a finite-difference method is proposed to approximate the solutions of the fractional model. The methodology is a linear and implicit technique which is based on fractional centered differences. We show in this manuscript that the method can be expressed in vector form using a Minkowski matrix under suitable conditions. The main properties of Minkowski matrices are used then to establish the existence and the uniqueness of the solutions of the finite-difference method, as well as the capability of the technique to preserve the positivity and the boundedness. Additionally we show that the method is a second-order consistent technique which is stable and convergent, with first order of convergence in time and second order in space. Some illustrative simulations show that the scheme is capable of preserving the positivity and the boundedness of the numerical approximations.

Key words: advection-diffusion-reaction partial differential equations, Riesz space-fractional equation, structure-preserving numerical method, fractional centered differences, stability and convergence analyses

MSC 2010: 65N06, 65C20, 35C05, 35K20

1 Introduction

Throughout we will assume that $a, b \in \mathbb{R}$ satisfy $a < b$, and suppose that γ, λ and T are positive numbers such that $\gamma < 1$. Let $\phi : [a, b] \to \mathbb{R}$ and $\psi_1, \psi_2 : [0, T] \to \mathbb{R}$ be continuously differentiable functions whose ranges are all subsets of $(0, \gamma)$ or of $(0, 1)$. Assume additionally that the compatibility conditions $\phi(a) = \psi_1(0)$ and $\phi(b) = \psi_2(0)$ are satisfied. Let $1 < \alpha \leq 2$ and $0 < \beta < 1$, and define $\Omega = (a, b) \times (0, T)$. In this work, we will suppose that $u : \overline{\Omega} \to \mathbb{R}$ is a sufficiently smooth function that satisfies the initial-boundary-value problem with fractional diffusion

$$\frac{\partial u}{\partial t}(x,t) = \frac{\partial^\alpha u}{\partial |x|^\alpha}(x,t) - \lambda u(x,t)\frac{\partial^\beta u}{\partial |x|^\beta}(x,t) + u(x,t) f(u(x,t)), \quad \forall (x,t) \in \Omega,$$
$$\text{such that } \begin{cases} u(x,0) = \phi(x), & \forall x \in (a,b), \\ u(a,t) = \psi_1(t), & \forall t \in (0,T), \\ u(b,t) = \psi_2(t), & \forall t \in (0,T), \end{cases} \tag{1}$$

for each $(x,t) \in \Omega$. For practical purposes, the function f adopts the form of Huxley's reaction,

$$f(u(x,t)) = (1-u(x,t))(u(x,t)-\gamma), \quad \forall (x,t) \in \Omega, \tag{2}$$

of Fisher's reaction law,

$$f(u(x,t)) = 1-u(x,t), \quad \forall (x,t) \in \Omega, \tag{3}$$

2 Aims and scope

Some efforts have been done already to discretize (1) considering fractional or integer derivatives. For instance, some linear discretizations have been published in [1]. In that report, the authors provide a positivity- and boundedness-preserving discretization of the Burgers–Huxley equation. The method reported in that work requires solving computationally a linear system represented by a sparse square matrix with number of rows equal to the number of spatial nodes of the discretization. On the other hand, other papers have considered a nonlinear approach which has resulted in more efficient numerical methods that preserve the positivity, the boundedness and the monotonicity of solutions for diffusive partial differential equations of the Burgers–Huxley and Burgers–Fisher types [2].

ur present work is motivated by the linear approach in view that more numerical properties can be guaranteed using such discretizations. In this manuscript, we will consider a two-dimensional generalization of (1) with diffusion and reaction terms that include Riesz space-fractional derivative. We will also consider a generalized reaction term that extends many particular models from mathematical biology and physics, including equations from population dynamics and nuclear physics [3, 4].

References

[1] J. E. Macías-Díaz, J. Ruiz-Ramírez, and J. Villa. The numerical solution of a generalized Burgers–Huxley equation through a conditionally bounded and symmetry-preserving method. *Computers and Mathematics with Applications*, 61:3330–3342, 2011.

[2] A. Szafrańska and J. E. Macías-Díaz. On the convergence of a finite-difference discretization à la Mickens of the generalized Burgers–Huxley equation. *Journal of Difference Equations and Applications*, 20(10):1444–1451, 2014.

[3] R. A. Fisher. The wave of advance of advantageous genes. *Annals of Eugenics*, 7(4):355–369, 1937.

[4] A. N. Kolmogorov, I. G. Petrovskii, and N. S. Piskunov. A study of the equation of diffusion with increase in the quantity of matter, and its application to a biological problem. *Bjul. Moskovskogo Gos. Univ*, 1(7):1–26, 1937.

Book of abstracts of the 7th International Conference on Advanced Computational Methods in Engineering, ACOMEN 2017
18–22 September 2017.

An explicit and dissipative method to solve a Riesz space-fractional wave equation with damping

Adan J. Serna[1] **and Jorge E. Macías-Díaz**[1]

[1] *Departamento de Matemáticas y Física, Universidad Autónoma de Aguascalientes*

e-mails: ajserna@correo.uaa.mx, jemacias@correo.uaa.mx

Abstract

In this manuscript, we consider an initial-boundary-value problem governed by a $(1+1)$-dimensional hyperbolic partial differential equation with constant damping that generalizes many nonlinear wave equations from mathematical physics. The model considers the presence of a spatial Laplacian of fractional order which is defined in terms of Riesz fractional derivatives, as well as the inclusion of a generic continuously differentiable potential. It is known that the undamped regime has an associated positive energy functional, and we show here that it is preserved throughout time under suitable boundary conditions. To approximate the solutions of this model, we propose an explicit finite-difference discretization based on fractional centered differences. Some discrete quantities are proposed in this work to estimate the energy functional, and we show that the numerical method is capable of conserving the discrete energy under the same boundary conditions for which the continuous model is conservative. Moreover, we establish suitable computational constraints under which the discrete energy of the system is positive. The method is consistent of second order, and is both stable and convergent. The numerical simulations shown here illustrate the most important features of our numerical methodology.

Key words: dissipative fractional wave equation, Riesz space-fractional equations, dissipation-preserving method, fractional centered differences, stability and convergence analyses
MSC 2010: 65N06, 65C20, 35C05, 35K20

1 Introduction

In this manuscript we let $T > 0$ and $\gamma \in \mathbb{R}^+ \cup \{0\}$, and suppose that $a, b \in \mathbb{R}$ satisfy $a < b$. Throughout this work we will assume that $1 < \alpha \leq 2$ and let $\Omega = (a,b)\times(0,T) \subseteq \mathbb{R}^2$. We will employ here the notation $\overline{\Omega}$ to represent the closure of Ω in $\mathbb{R}^2$ under the standard topology, and will assume that $G : \mathbb{R}^2 \to \mathbb{R}$, that $\phi, \psi : [a,b] \to \mathbb{R}$ and that $f, g : [0,T] \to \mathbb{R}$ are all continuously differentiable functions that satisfy the compatibility conditions $\phi(a) = f(0)$, $\phi(b) = g(0)$, $\psi(a) = f'(0)$ and $\psi(b) = g'(0)$. Moreover, we will suppose that G is nonnegative, that G'' is bounded and that $u : \overline{\Omega} \to \mathbb{R}$ is a sufficiently smooth function that satisfies the

initial-boundary-value problem

$$\frac{\partial^2 u}{\partial t^2}(x,t) - \frac{\partial^\alpha u}{\partial |x|^\alpha}(x,t) + \gamma \frac{\partial u}{\partial t}(x,t) + G'(u(x,t), u_x(x,t)) = 0, \quad \forall (x,t) \in \Omega,$$
$$\text{such that } \begin{cases} u(x,0) = \phi(x), & \forall x \in (a,b), \\ \dfrac{\partial u}{\partial t}(x,0) = \psi(x), & \forall x \in (a,b), \\ u(a,t) = f(t), & \forall t \in (0,T), \\ u(b,t) = g(t), & \forall t \in (0,T). \end{cases} \tag{1}$$

For the sake of convenience, we let $u(x,t) = 0$ for each $x \in (\mathbb{R} \setminus [a,b]) \times [0,T]$ and define

$$\frac{\partial^\alpha u}{\partial |x|^\alpha}(x,t) = \frac{-1}{2\cos(\frac{\pi\alpha}{2})\Gamma(2-\alpha)} \frac{\partial^2}{\partial x^2} \int_{-\infty}^{\infty} \frac{u(\xi,t)}{|x-\xi|^{\alpha-1}} d\xi, \quad \forall (x,t) \in \Omega. \tag{2}$$

2 Aims and scope

In the present work, we will consider problem (1), for which some positive energy functional is preserved under suitable boundary and parameter conditions. Motivated by the early works by L. Vázquez [1, 2] and D. Furihata [3, 4], we will design an explicit and structure-preserving method that conserves the dissipation of the energy of the system. More concretely, our approach will be based on the use of fractional centered differences, and we will provide discrete schemes for both the solution of the problem and the total energy of the system. We will show here that, under appropriate conditions on the computational parameters, the total energy of the discretized system is likewise a positive function of the time. To that end, various alternative expressions of the energy invariants will be derived. The preserved quantities will be used then to show that the method proposed in this manuscript is not only consistent but also stable and convergent of second order. Some simulations will show the capability of the method to preserve the energy under the analytic conditions derived in this work.

References

[1] Guo Ben-Yu, Pedro J Pascual, María J Rodriguez, and Luis Vázquez. Numerical solution of the sine-Gordon equation. *Applied Mathematics and Computation*, 18(1):1–14, 1986.

[2] Zhang Fei and Luis Vázquez. Two energy conserving numerical schemes for the sine-Gordon equation. *Applied Mathematics and Computation*, 45(1):17–30, 1991.

[3] Daisuke Furihata. Finite-difference schemes for nonlinear wave equation that inherit energy conservation property. *Journal of Computational and Applied Mathematics*, 134(1):37–57, 2001.

[4] Takayasu Matsuo and Daisuke Furihata. Dissipative or conservative finite-difference schemes for complex-valued nonlinear partial differential equations. *Journal of Computational Physics*, 171(2):425–447, 2001.

Open Session

Book of abstracts of the 7th International Conference on Advanced Computational Methods in Engineering, ACOMEN 2017 18–22 September 2017.

Implementing adequate subsonic boundary conditions in the Spectral Difference Method for the compressible Navier-Stokes equations

Takfarines Ait-Ali[1], Noureddine Hannoun[2] and Fateh Boukria[1]

[1] *Fluid Mechanic's Laboratory, Polytechnic Military School, Algiers*

[2] *Department of Mathematics, University of Science and Technology Houari Boumediene*

e-mails: takfarine.aitali@gmail.com, n.hannoun@gmail.com,

Abstract

External flows around obstacles such as airfoils or cylinders involve a wake which consists of a vortex street. These vortices prevail in the flow even far downstream. In a numerical simulation for such flows, it is often necessary to restrict the size of the calculation domain in order to limit the computational resources needed for the calculations. As a result, the outflow boundary requires appropriate boundary conditions, which allow the vortices to leave the computational domain without distortion or reflection. In the present work, we implement the well-known non-reflecting boundary condition algorithm (NSCBC: Navier-Stokes Characteristic Boundary Conditions) which has been proposed by Poinsot and Lele [2] , in a two-dimensional compressible Navier-Stokes solver based on the Spectral Difference Method [1]. The simulation program, which uses an unstructured triangular grid, has been designed at the EMP MDF Laboratory for the numerical simulation of compressible external flows. The implementation of the non-reflecting boundary condition involves the solution of a modified system of equations, which suppresses incoming waves that are traveling normal to the boundary. Space discretization of this system of equations is performed via polynomial interpolation. The validation of the boundary condition implementation algorithm in the subsonic case is performed by carrying out a series of tests involving the perturbation of a uniform flow with an entropy wave , an acoustic wave, and a convected vortex. The reflection level of the waves at the outflow boundary is investigated and some results are shown in figure (1) and figure (2) .

Key words: acoustic wave, characteristic boundary conditions, spectral difference, unstructured grid, viscous flow

References

[1] Y. Liu, M. Vinokur, Z.J. Wang, *Spectral difference method for unstructured grids I: Basic formulation*, J. Comput. Phys. **216** (2006) 780-801.

[2] T. J. Poinsot, S.K. Lele, *Boundary conditions for direct simulations of compressible viscous flows*, Journal of Computational Physics, vol. 101, no. 1, July 1992, p. 104–129.

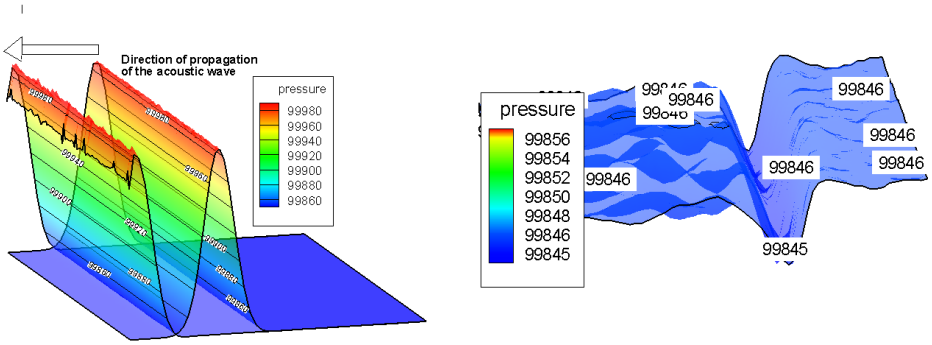

(a) (b)

Figure 1: Involving acoustic wave through the outlet boundary on (a) and the reflected wave shown on (b) is about 1% of the incoming wave.

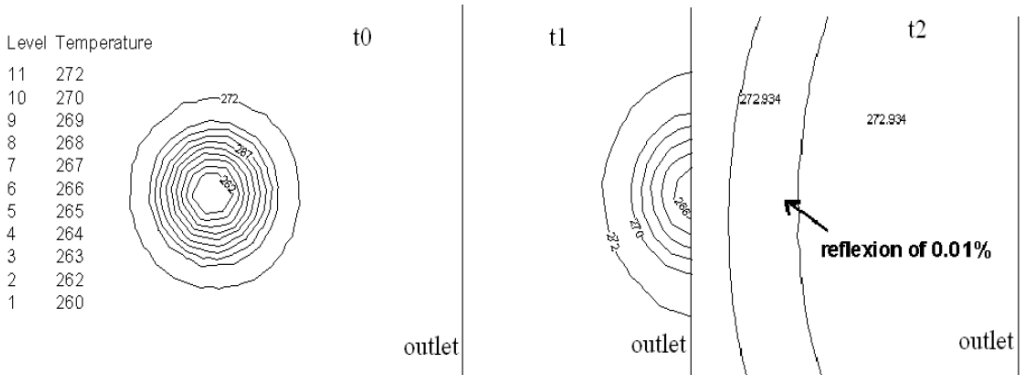

Figure 2: Involving entropy wave through outlet boundary

Book of abstracts of the 7th International Conference
on Advanced Computational Methods
in Engineering, ACOMEN 2017
18–22 September 2017.

Development of two dimensional Finite Surface Discretization for Fluid Flows

Arpiruk Hokpunna[1]

[1] *Department of Mechanical Engineering, Faculty of Engineering, Chiang Mai University*

e-mails: a.Hokpunna@eng.cmu.ac.th

Abstract

The sixth-order accurate finite-surface discretization for the incompressible Navier-Stokes equations are presented. This discretization retains all the advantage of the staggered without needing to define the staggered cell or co-volume and it is 6X faster than the fourth-order compact finite volume method.

Key words: finite volume method, Navier-Stokes equations, finite surface method, staggered grid, high-order schemes

1 Introduction

The work on higher-order methods applied to turbulent flows on collocated grid were discourage at first as the early adopter found that the improvement over the second-order scheme were small [1, 2]. Later, a fourth-order compact scheme is reported to deliver the same predictions as the second-order scheme while using the total grid points 8X lesser [3]. At this comparable level of accuracy, the fourth-order deliver the result 10X faster. The reason why staggered grid is much better than the collocated grid at solving turbulent flow was further investigated in [4]. It was found that half-a-cell distance of the staggered is the reason which means it can resolve the high-frequency components better and thus the high-frequency components of the flow are kept at the momentum instead of diverted to the pressure by the fractional-time-stepping method. In another word, the staggered grid satisfies the mass-conservation better than the collocated one. Thus, what would happen if we could have the exact equation for the mass-conservation?

Consider the arrangement of the flow variables in staggered finite volume discretization (Fig.1(a)) showing the positions of the u and v momentums relative to the pressure cell. If we shrink the control volumes of the momentum cells towards the boundary of the pressure cell, the momentums become the surfaces defined on the faces of the pressure cell as the thicknesses approach zero. It is obvious that the sum of these momentum flux is the mass balance over the pressure cell. The finite surface method (FSM) defines the velocities as surfaced-averaged values living on a set of connected volumes where the mass is set to be conserved similar to finite volume method. The equation for the mass balance becomes an analytical discrete equation. Therefore the only equation left to approximate is the momentum equation. We present the sixth-order approximation of the FSM with three variants of pressure treatments and its validation in the next section.

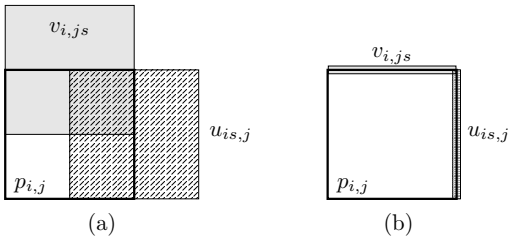

Figure 1: (a) Arrangement of flow variables on staggered grids consisting of pressure cells (clear), u-momentum (dash) and v-momentum (gray) cells. (b) The finite surface discretization constricts the momentum control volumes on to the surfaces of the pressure cell.

N	FSM6:PE$_4$			FSM6:PCO$_4$			FVM$_4$:P$_4$E		
	t_m	t_p/n_{it}	n_{it}	t_m	t_p/n_{it}	n_{it}	t_m	t_p/n_{it}	n_{it}
128^2	**21.1**	1.07	88	**21.6**	1.78	55	**31**	0.94	406
256^2	**78.1**	7.24	41	**86.4**	10.26	46	**130.2**	11.96	96
512^2	**396.0**	34.80	25	**440.0**	47.50	32	**524.0**	43.88	100

Table 1: Number of iteration needed to reach 10^{-6} relative volumetric imbalance, the CPU-time (t_m) in millisecond spent in the momentum equation and the time used for projection step per pressure iteration (t_p/n_{it}).

2 Results

In this work, we repeat the same doubly periodic shear layer widely used in the literature. The sixth-order FSM with 170^2 cells can match the result of the FVM on 256^2 cell. The proposed method, not only more accurate than the fourth-order FVM (which it should), it is also significantly faster than the fourth-order Tab.1. This table suggests that in two dimensions, the newly developed sixth-order FSM is 4.5X faster than the fourth-order FVM per time step which is translated to 6X times faster in a time-dependent problem.

References

[1] J. Gullbrand, An evaluation of a conservative fourth order DNS code in turbulent channel, Tech. rep., Center for Turbulence Research,Stanford University (2000).

[2] O. Shishkina, C. Wagner, A fourth order finite volume scheme for turbulent flow simulations in cylindrical domains, Computers & Fluids 36 (2) (2007) 484–497.

[3] A. Hokpunna, M. Manhart, Compact fourth-order finite volume method for numerical solutions of Navier–Stokes equations on staggered grids, Journal of Computational Physics 229 (20) (2010) 7545–7570.

[4] W. Rojanratanangkule, A. Hokpunna, Performance of high-order schemes on collocated and staggered grids, Journal of Research and Applications in Mechanical Engineering 3 (1) (2015) 22–28.

Book of abstracts of the 7th International Conference on Advanced Computational Methods in Engineering, ACOMEN 2017
18–22 September 2017.

Multipoint flux mixed finite element methods for slightly compressible flow in porous media

Andrés Arrarás[1] **and Laura Portero**[1]

[1] *Department of Engineering Mathematics and Computer Science, Public University of Navarre*

e-mails: andres.arraras@unavarra.es, laura.portero@unavarra.es

Abstract

In this work, we propose numerical approximation methods for a nonlinear parabolic problem describing slightly compressible Darcy flow in porous media. The problem is discretized by multipoint flux mixed finite element methods, which have been successfully applied earlier to the incompressible case. The convergence of the proposed methods and related computational results are discussed in detail.

Key words: mixed finite element, multipoint flux approximation, nonlinear parabolic equation, slightly compressible flow
MSC 2010: 35K55, 65M60, 76M10, 76S05

1 Problem formulation

Slightly compressible single-phase Darcy flow in porous media is governed by the following nonlinear parabolic initial-boundary value problem

$$\partial_t(\phi\rho(p)) + \nabla\cdot\mathbf{u} = f \qquad \text{in } \Omega\times(0,T], \tag{1a}$$

$$\mathbf{u} = -\frac{\rho(p)}{\mu}K(\nabla p - \rho(p)\mathbf{g}) \qquad \text{in } \Omega\times(0,T], \tag{1b}$$

$$p = g \qquad \text{on } \Gamma_D\times(0,T], \tag{1c}$$

$$\mathbf{u}\cdot\mathbf{n} = 0 \qquad \text{on } \Gamma_N\times(0,T], \tag{1d}$$

$$p = p_0 \qquad \text{in } \Omega\times\{0\}, \tag{1e}$$

where $\Omega\subset\mathbb{R}^2$ is a convex polygonal domain with Lipschitz continuous boundary given by $\partial\Omega = \overline{\Gamma}_D\cup\overline{\Gamma}_N$ such that $\Gamma_D\cap\Gamma_N = \emptyset$. In this formulation, p is the fluid pressure, $\mathbf{u}$ represents the Darcy velocity, ϕ is the porosity of the medium, $\rho(p)$ denotes the fluid density, μ is the kinematic viscosity, K is a symmetric and positive definite tensor representing the rock permeability, $\mathbf{g}$ is the gravitational vector, and $\mathbf{n}$ denotes the outward unit normal on $\partial\Omega$. The nonlinear relationship between ρ and p is given by

$$\rho(p) = \rho_{\text{ref}}\, e^{c_f(p-p_{\text{ref}})},$$

where ρ_{ref} and p_{ref} are the reference density and pressure, respectively, and c_f is the fluid compressibility constant.

In this work, we propose and analyze multipoint flux mixed finite element (MFMFE) methods to approximate the solution to (1). In doing so, we extend the results reported in [1] for the incompressible problem using the techniques discussed in [2].

2 Full discretization

Let $\mathcal{T}_h$ be a conforming, shape-regular and quasi-uniform partition of Ω into convex quadrilateral elements, where $h = \max_{E\in\mathcal{T}_h} \operatorname{diam}(E)$. The spatial discretization of problem (1) is based on the MFMFE method, which considers the lowest order Brezzi-Douglas-Marini mixed finite element spaces, V_h and W_h, for the velocity and pressure variables, respectively. The no-flow boundary condition (1d) is imposed by introducing the subspace $V_h^0 \subset V_h$ as $V_h^0 = \{\mathbf{v} \in V_h : \mathbf{v}\cdot\mathbf{n} = 0 \text{ on } \Gamma_N\}$.

On the other hand, we define the equidistant time grid $0 = t_0 < t_1 < \ldots < t_N = T$, where $t_n = n\tau$ and $\tau = T/N$, for $n = 0, 1, \ldots, N \in \mathbb{N}$. As for the the time integration, we consider the backward Euler method. The fully discrete scheme yields approximations p_h^{n+1} and $\mathbf{u}_h^{n+1}$ to the solution of (1) at time t_{n+1}, namely: for $n = 0, 1, \ldots, N-1$, find $(\mathbf{u}_h^{n+1}, p_h^{n+1}) \in V_h^0 \times W_h$ such that

$$\left(\phi\,\frac{\rho(p_h^{n+1}) - \rho(p_h^n)}{\tau}, w\right) + (\nabla\cdot\mathbf{u}_h^{n+1}, w) = (f^{n+1}, w), \qquad w \in W_h, \tag{2a}$$

$$\left(\frac{\mu}{\rho(p_h^{n+1})}K^{-1}\mathbf{u}_h^{n+1}, \mathbf{v}\right)_Q = (p_h^{n+1}, \nabla\cdot\mathbf{v}) + (\rho(p_h^{n+1})\,\mathbf{g}, \mathbf{v}) - \langle g, \mathbf{v}\cdot\mathbf{n}\rangle_{\Gamma_D}, \qquad \mathbf{v} \in V_h^0, \tag{2b}$$

$$p_h^0 = \mathcal{S}_h p_0, \tag{2c}$$

where $f^{n+1} = f(\cdot, t_{n+1})$ and $\mathcal{S}_h p_0$ denotes the $L^2(\Omega)$-projection of p_0 onto W_h. The notation $(\cdot,\cdot)_Q$ in equation (2b) stands for the application of a numerical integration formula. This formula is based on the trapezoidal rule applied on the reference element, and can be either symmetric or non-symmetric. Two variants of the method are thus obtained: a symmetric MFMFE scheme, which applies to smooth quadrilateral meshes, and a non-symmetric MFMFE method, designed to preserve the accuracy on general quadrilateral grids (see [1] for details). Newton's method is used to solve the nonlinear system of equations arising from (2).

We discuss the convergence of the proposed methods, and present computational experiments illustrating their numerical behaviour.

Acknowledgements

This work has been partially supported by the grant MTM2014-52859 awarded by MINECO.

References

[1] A. Arrarás, L. Portero, I. Yotov, *Error analysis of multipoint flux domain decomposition methods for evolutionary diffusion problems*, J. Comput. Phys. **257** (2014) 1321–1351.

[2] M.-Y. Kim, E.-J. Park, S. G. Thomas, M. F. Wheeler, *A multiscale mortar mixed finite element method for slightly compressible flows in porous media*, J. Korean Math. Soc. **44** (2007) 1103–1119.

Book of abstracts of the 7th International Conference
on Advanced Computational Methods
in Engineering, ACOMEN 2017
18–22 September 2017.

Mixed finite element solution of radiative transfer equation

M. A. Badri[1,2], Y. Favennec[2], H. Digonnet[3], S. Le Corre[2] and B. Rousseau[2]

[1] *Institut de Recherche Technologique Jules Verne, 44340 Bouguenais, France*

[2] *Laboratoire Thermocinétique de Nantes (UMR CNRS 6607), University of Nantes, France*

[3] *Institut de Calcul Intensif, Ecole Centrale de Nantes, 44300 Nantes, France*

e-mails: mohd-afeef.badri@irt-jules-verne.fr, Yann.Favennec@univ-nantes.fr, hugues.digonnet@ec-nantes.fr, Steven.Lecorre@univ-nantes.fr, Benoit.Rousseau@univ-nantes.fr

Abstract

The radiative transfer equation (RTE) for participating medium has been solved using mixed finite element approach. Using such method a banded-sparse matrix system is formed. Such matrix systems are proven to be advantageous over the more typical block-matrix systems formed using traditional finite element methods, while solving the RTE.

Key words: radiative transfer equation, vectorial finite element, mixed finite element

1 Introduction

Radiative transfer equation (RTE) is often modeled in its discrete form, using discrete set of ordinates ($\boldsymbol{s}_m$) and discrete set of radiative intensities I_m [1]:

$$(\boldsymbol{s}_m \cdot \nabla + \kappa + \sigma_s)\, I_m(\boldsymbol{x}) = \sigma_s \sum_{n=1}^{N_a} \omega_n I_n(\boldsymbol{x}) \Phi_{m,n} + \kappa I_b \quad \forall m = 1, \ldots, N_a \tag{1}$$

Each equation in this set of N_a equations depicts the transport of radiative intensity through a participating media. Left hand side of the equations sums up the losses due to absorption, scattering and transport, while on the right hand side summation term represents source due to in-scattering effect and the Plank's black body source at a given temperature T.

Mixed and traditional finite element solution of RTE

Computation of radiative field using this set of coupled equations requires spatial discretization, in order to form a solvable linear system. Among other approaches, SUPG-FEM has proven to be a good candidate. Iterative application of such method for each equation yields a huge block matrix composed of $N_a \times N_a$ submatrices, a matrix structure classical to coupled system of equations. Using a trial function $v \in \mathcal{V}_h \subset H^1(\mathcal{D})$ the diagonal submatrix of this huge block matrix is given by variation formulation of left hand side of (1), while the off-diagonal submatrices are formulated using variation formulation of the first term on right hand side. Naturally, one can see that the same finite element space $\mathcal{V}_h$ has to be used in an iterative manner to formulate the full block matrix.

Alternative to this traditional approach, we introduce SUPG based on mixed finite element method ($\mathcal{M}$FEM). This notion was first introduced in 1967 by Herrmann [2], in connection with elastic theory, in which both stresses and strains were simultaneously calculated. Based on the same principle, using $\mathcal{M}$FEM, N_a radiative intensities (I_m) are simultaneously calculated. The problem consists in searching a vector of radiative intensities $\mathbb{I} = [I_1\ I_2\ \cdots\ I_{N_a}]^T$ utilizing a vectorial test function $\mathbb{V} = [v_1\ v_2\ \cdots\ v_{N_a}]^T$. The chosen functional space which contains this vectorial test function is given by $H^1(\mathcal{D})^{N_a} = H^1(\mathcal{D}) \times H^1(\mathcal{D}) \times \ldots \times H^1(\mathcal{D}) = \prod_{i=1}^{N_a} H^1(\mathcal{D})$. The SUPG-$\mathcal{M}$FEM weak formulation can be built using the vectorial trial function $\mathbb{H} = \mathbb{V} + \gamma \mathbb{S} \cdot \nabla \mathbb{V}$, $\gamma : \Omega \mapsto \mathbb{R}^+$, over the domain of interest $\mathcal{D}$:

$$\int_{\mathcal{D}} [(\mathbb{S} \cdot \nabla \mathbb{I} + \beta \mathbb{I}) : (\mathbb{H})]\, \mathrm{d}\boldsymbol{x} - \int_{\mathcal{D}} [(\Theta \mathbb{I}) : (\mathbb{H})]\, \mathrm{d}\boldsymbol{x} = \int_{\mathcal{D}} [(\kappa I_b \mathbb{1}) : (\mathbb{H})]\, \mathrm{d}\boldsymbol{x} \tag{2}$$

2 Results

The use of SUPG-$\mathcal{M}$FEM formulation yields a sparse matrix structure contrary to ordinary SUPG-FEM which results into a huge block matrix structure (See Figure 1). This proposed SUPG-$\mathcal{M}$FEM method has various advantages: the obtained banded sparsed matrix system can be much efficiently solved using LU factorization, faster matrix building is observed, parallelization in angles and space is applicable in a straight forward manner etc. All these advantages that will be presented at the conference prove the superiority of SUPG-$\mathcal{M}$FEM method for solving RTE.

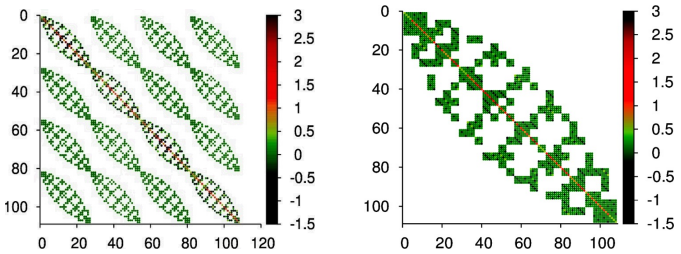

Figure 1: Matrix obtained by ordinary FEM (left) and by Mixed FEM (right).

Acknowledgements

M.A. Badri would like to thank IRT JV (French Institute in Research and Technology in Advance Manufacturing Technologies for Composite, Metallic and Hybrid Structures) for funding his research. He also wishes to associate the industrial and academic partners of the project: Airbus Group Innovations, Dassault Aviation, Safran Composites, GeM (Institut de Recherche en Génie Civil et Mécanique) and LTeN (Laboratoire de Thermique et Ènergie de Nantes).

References

[1] Modest M. F. , *Radiative heat transfer*, Academic press,2013

[2] Herrmann Leonard R. , *Finite-element bending analysis for plates*, ASCE, 1967.

Book of abstracts of the 7th International Conference
on Advanced Computational Methods
in Engineering, ACOMEN 2017
18–22 September 2017.

Strong stability preserving transformed GLMs with RK stability

Califano Giovanna[1], Izzo Giuseppe[2] and Jackiewicz Zdzislaw[3]

[1] *Department of Mathematics, University of Salerno*

[2] *Department of Mathematics and Applications, University of Naples Federico II*

[3] *Department of Mathematics, Arizona State University*

e-mails: gcalifano@unisa.it, giuseppe.izzo@unina.it, jackiewicz@asu.edu

Abstract

We investigate the strong stability preserving (SSP) transformed general linear methods (GLMs) with Runge-Kutta (RK) stability properties. We present examples of SSP transformed GLMs with RK stability, which have order p and stage order q=p, number of the external approximations r and number of the internal approximations s=r=p+1. We find that they are better than the others SSP methods.

Key words: general linear methods, inherent Runge-Kutta stability, Runge-Kutta stability, strong stability preserving

1 Introduction

Aim of this work is to continue the investigation of SSP GLMs already started by Spijker in [4], and by Izzo and Jackiewicz in [2], to solve systems of ordinary differential equations (ODEs). In order to increase the probability to find SSP GLMs, we multiply a classic GLM (see [2]) by a nonsingular trasformation matrix $\mathbf{T} \in \mathbb{R}^{r\times r}$, and so we obtain a new class of transformed GLMs of the form

$$\begin{cases} Y^{[n]} = h(\overline{\mathbf{A}} \otimes \mathbf{I}) f\left(t_{n-1} + \mathbf{c}h, Y^{[n]}\right) + (\overline{\mathbf{U}} \otimes \mathbf{I})\overline{y}^{[n-1]}, \\ \overline{y}^{[n]} = h(\overline{\mathbf{B}} \otimes \mathbf{I}) f\left(t_{n-1} + \mathbf{c}h, Y^{[n]}\right) + (\overline{\mathbf{V}} \otimes \mathbf{I})\overline{y}^{[n-1]}, \end{cases} \tag{1}$$

$n = 1, 2, \ldots, N$, where the transformed coefficient matrices $\overline{\mathbf{A}}, \overline{\mathbf{U}}, \overline{\mathbf{B}}$, and $\overline{\mathbf{V}}$ are defined as follows

$$\overline{\mathbf{A}} = \mathbf{A}, \quad \overline{\mathbf{U}} = \mathbf{U}\,\mathbf{T}^{-1}, \quad \overline{\mathbf{B}} = \mathbf{T}\,\mathbf{B}, \quad \overline{\mathbf{V}} = \mathbf{T}\,\mathbf{V}\,\mathbf{T}^{-1},$$

with $\mathbf{A}, \mathbf{U}, \mathbf{B}$ and $\mathbf{V}$ coefficient matrices of the original GLM. Moreover, $\mathbf{I}$ is the identity matrix of dimension m, the dimension of the initial ODEs and the transformed vector of the approximated solution in t_n is given by

$$\overline{y}^{[n]} = (\mathbf{T} \otimes \mathbf{I})\, y^{[n]}.$$

For such methods the vector of the internal approximations or stages satisfies

$$Y^{[n]} = y(t_{n-1} + \mathbf{c}h) + O(h^{q+1}),$$

and the vector of the external approximations, which propagates to the next step t_n satisfies

$$y^{[n]} = \sum_{k=0}^{p} (\mathbf{q}_k \otimes \mathbf{I}) h^k y^{(k)}(t_n) + O(h^{p+1}),$$

with the same vectors $\mathbf{q}_k, k = 0, \ldots, p$ used to determinate $y^{[n-1]}$ at previous step.

2 SSP transformed GLMs with RK stability

In order to construct SSP transformed GLMs with RK stability we use the approach by Spijker, [4]. So, we assume that they satisfy the following SSP relations

$$\begin{array}{ll} (\mathbf{I} + \gamma \overline{\mathbf{A}})^{-1} \overline{\mathbf{U}} \geq 0, & \mathbf{I} - (\mathbf{I} + \gamma \overline{\mathbf{A}})^{-1} \geq 0, \\ \overline{\mathbf{V}} - \gamma\, \overline{\mathbf{B}} (\mathbf{I} + \gamma \overline{\mathbf{A}})^{-1} \overline{\mathbf{U}} \geq 0, & \gamma\, \overline{\mathbf{B}} (\mathbf{I} + \gamma \overline{\mathbf{A}})^{-1} \geq 0, \end{array} \tag{2}$$

where γ is some constant, and where these inequalities should be interpreted componentwise. Then, we compute the SSP coefficient defined by

$$C = C(\mathbf{c}, \mathbf{A}, \mathbf{U}, \mathbf{B}, \mathbf{V}) = \sup \big\{ \gamma \in \mathbb{R} : \ \gamma \text{ satisfies } (2) \big\},$$

by solving the constrained minimization problem

$$F(\gamma) := -\gamma \longrightarrow \min,$$

with a very simple objective function $F(\gamma) = -\gamma$, subject to the nonlinear constrains (2).

Acknowledgements

This research was starting during the visit of the first author (GC) to Arizona State University in the Sprinhg semester of 2017. This author wish to express her gratitude to the School of Mathematical and Statistical Sciences for hospitality during the visit.

References

[1] G. Califano, G. Izzo and Z. Jackiewicz, *Strong stability preserving*, submitted to J. Sci. Comput.

[2] G. Izzo and Z. Jackiewicz, *Strong stability preserving general linear methods*, J. Sci. Comput. **65** (2015) 271–298.

[3] G. Izzo and Z. Jackiewicz, *Strong stability preserving transformed DIMSIMs*, submitted to J. Comput. Appl. Math.

[4] M.N. Spijker, *Stepsize conditions for general monotonicity in numerical initial value problems*, J. Numer. Anal. **45** (2007) 1226–1245.

Book of abstracts of the 7th International Conference
on Advanced Computational Methods
in Engineering, ACOMEN 2017
18–22 September 2017.

In Silico Modeling for the Risk Assessment of Toxicity in Cells

Qasim Ali Chaudhry[1], Muqaddas Asif[1], Amna Abbas[2] and Ayesha Noor[3]

[1] *Department of Mathematics, University of Engineering and Technology, Lahore*

[2] *Department of Mathematics, Govt. Post Graduate College for Women, Samanabad, Lahore*

[2] *Department of Mathematics, Govt. Post Graduate College for Women, Wahdat Colony, Lahore*

e-mails: chqasim@uet.edu.pk, muqaddas.pari1@gmail.com, amnaabbas25@yahoo.com, ashi_aquarious@yahoo.com

Abstract

A cell is a complex biochemical reactor. Various biochemical reactions take place in it to carry out different tasks. One such task is metabolism of the ubiquitous environmental carcinogenic compounds namely PAHs into biological cells which is crucial to model. These PAHs are lipophilic which partition into membranes and diffuse through them to target the DNA and thereby cause toxicity or tumor. Therefore, there is a dire need of the development of the model for the assessment of these carcinogenic chemical compounds. Earlier, a 3D model was developed in order to investigate the cellular fate after being affected by PAHs but this model was lacking the presence of Nucleolemma with its enzymatic reactions, which is an important factor to be considered. Thus, a new 3D model was developed which in addition to the other domains, consists of Nucleolemma along with its enzymatic reactions. Homogenization approach was used for the numerical treatment of cytoplasm to scale down the complexity of the model. The numerical results of the extended model were validated against the numerical results of old model and the experimental results, where the results of extended model clearly show the improvement and convergence to the experimental results not only qualitatively but quantitatively as well.

Key words: Mathematical Modeling, PAHs, Nucleolemma, Homogenization, Reaction, Diffusion, Cell

1 Introduction

Because of the complex real-world problems, mathematical models are now proceeding in almost all the scientific fields including biology and medicine. In many eras computational simulations have become an important aspect to understand the mathematical modeling of the given systems. To make good grasp of the cell related issues such a diffusion, restrain synergy and chastise prodigy illustration of a bio-chemical processes, such as membrane transport, different theoretical studies and computational models are in progress. Mathematical modeling of a biological cell is complex due to its schematic structure. When these biological cells are exposed to the harmful environmental pollutants, they undergo a series of reaction- diffusion processes. In our previous paper [1], the process of the first phase of metabolism was partially

studied and modeled whereas the process of the second phase of metabolism was included in [2]. The first model mimics the cellular fate after being affected by the foreign toxic chemical compounds. The model was developed in 2D considering the shape of a cell as a ball. Later, the model was extended by considering the different cellular shapes. Then the model was developed in 3D where only five subdomains namely extracellular medium, cellular membrane, cytoplasm, nuclear membrane and nucleus were considered, where Nucleolemma and perinuclear space were not included. Nucleolemma is a highly regulated membrane barrier which controls the inward and outward transportation of the compounds and protects the nucleus. In this study, our aim is to develop a 3D mathematical model including Nucleolemma and its enzyme reactions, which narrates reaction-diffusion mechanism within and outside the cell due to these carcinogenic factors. Also, the homogenization technique will be used in cytoplasm for the numerical simulation.

2 Materials and Methods

In this model, we are considering seven subdomains. We considered that the extracellular medium contains water where hydrolysis process takes place. It was assumed that no reaction takes place in membranous structure, only diffusivity was considered. Cytoplasm consists of aqueous part (cytosol) and the small bodies of the cell (mitochondrion, endoplasmic reticulum and vacuoles etc.). PAH undergoes three reactions in cytoplasm, firstly; the hydrolysis process, secondly; reacting with proteins present in cytoplasm leaving protein-adductsand thirdly; Glutathione conjugation. Similarly, reactions take place in perinuclear space and finally in the nucleus where DNA-adducts are formed due to which mutation or the demolition of the cell may cause. The diffusion-reaction process gives rise to the system of Partial Differential Equations, which were handled numerically using finite element method.

3 Results and Discussion

The formulated model is executed on a software COMSOL MULTIPHYSICS [3] which is based on the principle of FEM. The numerical results of the extended model were validated against the numerical results of old model and the experimental results, where the results of newly developed model clearly show the improvement and convergence to the experimental results not only qualitatively but quantitatively as well. The aim of this research work is to set a stage for a comprehensive computational approach that can be refined against exact measures of enzyme and molecular behavior in cells.

References

[1] D. Dreij, *et al.*, *A method for efficient calculation of diffusion and reactions of lipophilic compounds in complex cell geometry*, PLoS One, **6** (2011) e23128.

[2] Q. A. Chaudhry, *et al.*, *Surface reactions on the cytoplasmatic membranes – Mathematical modeling of reaction and diffusion systems in a cell*, Journal of Computational and Applied Mathematics, **262** (2011) 244–260.

[3] AB. COMSOL, *Comsol Multiphysics*, Stockholm, 2010.

Book of abstracts of the 7th International Conference on Advanced Computational Methods in Engineering, ACOMEN 2017
18–22 September 2017.

Data-driven discovery of the nonlinear dynamics in an electromechanical drivetrain using mixed norm inverse solver

Guillaume Crevecoeur[1]

[1] *Department of Electrical Energy, Metals, Mechanical Constructions and Systems, Ghent University*

e-mails: Guillaume.Crevecoeur@ugent.be

Abstract

Inverse problems have been attracting much attention because of their ability to recover unknown parameter values in a given system starting from measurements. A fixed structure of the physical behavior within the system is each time provided by means of a behavioral model. This paper describes a methodology for uncovering the structure of the system and thus of the models starting from measurement data in a complex nonlinear dynamic mechatronic system. We propose the use of a mixed norm inverse problem solver that is reformulated as a second order cone programming problem. An electromechanical drivetrain is considered as case study where the proposed methodology is validated upon.

Key words: dynamical systems, data-driven modeling, inverse problems, optimization, sensing

1 Introduction and problem statement

Mechatronic systems such as electromechanical drivetrains are exhibiting increasing complexity making the modelling of their behavior starting from first principles difficult. Due to advances in low cost sensor technology and the advantages that can be reached by exploiting interconnectivity these so-called cyberphysical systems give rise to increasing data in their application fields [1]. Industrial applications can benefit from the data to increase their performance and moreover, correct interpretation of the measurement data is required to enable further advancements in the operation of these systems. This paper discusses the possibility of discovering the governing equations in an exemplary electromechanical drivetrain exhibiting strong nonlinear behavior.

The application that is considered is an electromechanical drivetrain, as depicted in Fig. 1. It consists of an electrical machine driving a mechanical load consisting of a flywheel having a certain unknown intertia and mechanical links such as cam follower components. Measurement data can be captured by means of an encoder measuring the angular displacement (ϕ) and velocity ($\dot{\phi}$). In a state space formulation with the time-varying state vector (dimensionality $p = 2$) $\mathbf{x}(t) = [\dot{\phi}(t), \phi(t)]$ we have following nonlinear ordinary differential equation $\dot{\mathbf{x}}(t) = \mathbf{f}(\mathbf{x}(t))$. We assume here that the measurements $\mathbf{y}(t) \equiv \mathbf{x}(t)$ and thus the states are perfectly observable. A measurement matrix is defined as the consecutive n measurements of the states: $\mathbf{X} = [\mathbf{x}_1, \ldots, \mathbf{x}_n]$ and a matrix $\mathbf{Y} \equiv \dot{\mathbf{X}}$.

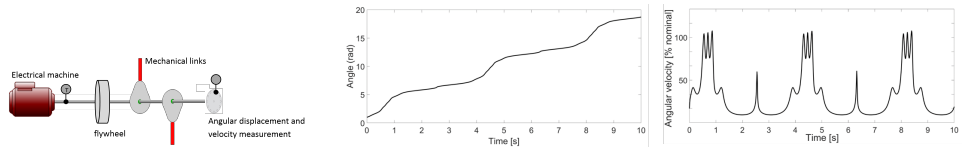

(a) (b)

Figure 1: (a) Electromechanical drivetrain consisting of a flywheel having inertia, mechanical links and encoder. (b) Measurement data of the angular displacement and velocity of the considered electromechanical drivetrain.

2 Methods and conclusions

The aim of this study is to uncover the function $\mathbf{f}(\cdot)$ of the nonlinear dynamics in an electromechanical drivetrain. First steps to enable the identification of the governing equations was proposed by [2] using so-called symbolic regression. It balances the complexity of the model with model accuracy. A reduction in the complexity of finding the structure of the underlying phenomena was presented in [3]. The methodology makes use of a library of m pre-defined candidate basis functions that are gathered in $\mathbf{F}(\mathbf{X})$ and a sparse regression on the candidate functions is carried out: $\dot{\mathbf{X}} = \mathbf{F}(\mathbf{X})\mathbf{\Lambda}$. $\mathbf{\Lambda} = [\boldsymbol{\lambda}_1, \ldots, \boldsymbol{\lambda}_p]$ contains vectors that determine which candidate function is active and need to be sparse for balancing model complexity and accuracy. In this paper we investigate the optimization problem for finding proper λ values as being a formulation of mixed $l_1 l_2$ norm inverse solver:

$$\mathbf{\Lambda}^* = \arg\min_{\mathbf{\Lambda}} \|\mathbf{Y} - \mathbf{F}(\mathbf{X})\mathbf{\Lambda}\|_F^2 + \alpha|\mathbf{\Lambda}|_{l_1}^{l_2} \tag{1}$$

The regularization term is $|\Lambda|_{l_1}^{l_2} = \sum_{n=1}^{N} \sqrt{\sum_{k=1}^{K} \Lambda_{nk}^2}$ and $\|\cdot\|_F$ is the Frobenius norm of a matrix. We reformulate (1) as a second-order cone programming problem. The advantage of this problem formulation is that it allows to recover time-dependent variations on $\mathbf{f}(\cdot)$ because l_1 sparsity is enforced in the basis functions domain and l_2 on the state space domain.

Figure 1b depicts the measured angular displacement and velocity of the considered drivetrain. We defined a library of functions consisting of polynomial functions ($\mathbf{x}$, $\mathbf{x}^2$, etc.), and sinusoidal functions ($\sin(\mathbf{x})$, $\sin(\mathbf{2x})$, etc.). For various regularization parameter values for α, optimal Λ^* are found, each time corresponding with a certain structure for the function $\mathbf{f}(\cdot)$. The effect of the regularization parameter, i.e. larger α correspond with more sparse regularization, on the recovered nonlinear dynamical system is analyzed. From the optimization (1) the following nonlinear ordinary differential equation was derived $\ddot{\phi} = Q - g(\phi)\dot{\phi}^2 - c\dot{\phi}$ with $g(\phi) = \sum_{k_1=1}^{6} \sum_{k_2=1}^{6} a_{k_1 k_2} \sin(k_1\phi) \sin(k_2\phi)$ with constants Q, c $a_{k_1 k_2}$.

References

[1] R.C. Luo, C.C. Chang, C.C. Lai *Multisensor fusion and integration: theories, applications, and its perspectives* IEEE Sens. Journ. **11** (2011) 3122–3138.

[2] M. Schmidt, H. Lipson, *Distilling free-form natural laws from experimental data*, Science **324** (2009) 81–85.

[3] S.L. Brunton, J.L. Proctor, N. Kutz, *Discovering governing equations from data by sparse identification of nonlinear dynamical systems*, Proc. Natl. Acad. Sci. USA **113** (2016) 3932–3937.

Book of abstracts of the 7th International Conference on Advanced Computational Methods in Engineering, ACOMEN 2017 18–22 September 2017.

Accurate Field Reconstruction by Kirchhoff Integrals on Unstructured Finite-Element Meshes

Wolfgang Ackermann[1], Herbert De Gersem[1] and Thomas Weiland[1]

[1] *Institut für Theorie Elektromagnetischer Felder (TEMF), Technische Universität Darmstadt, Germany*

e-mails: ackermann@temf.tu-darmstadt.de, degersem@temf.tu-darmstadt.de, thomas.weiland@temf.tu-darmstadt.de

Abstract

FE field simulation results for accelerator cavities on unstructured meshes exhibit numerical fluctuations which are unacceptable when studying high-precision beam dynamics in an accelerator cavity. An improvement is obtained by post-processing the field by applying Kirchhoff integrals including the Green function associated with the electromagnetic wave equation.

Key words: finite-element method, electromagnetic-field simulation, accelerator cavities

1 Introduction

Relativistic particles are accelerated along the axis of a superconducting cavity with the help of a resonating electric field. The eigenmode is solved from the eigenvalue problem related to Maxwell's wave equation, discretrised by a 3D higher-order finite-element (FE) method (Fig. 1). Asymmetries in almost cylindrically symmetric cavities, e.g., due to power couplers, are responsible for transverse electric fields which are by orders of magnitude smaller than the accelerating field but nevertheless generate transverse kicks causing an unacceptable deflection of the beam. An accurate characterisation of the transverse components is challenging because of numerical fluctuations introduced by the FE method and by an unstructured mesh (grey in Fig. 2a).

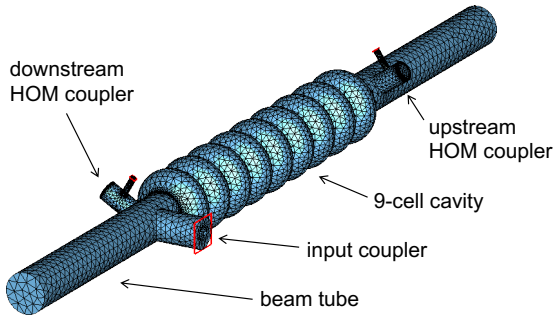

Figure 1: TESLA cavity (exemplary mesh of 136.443 tetrahedra).

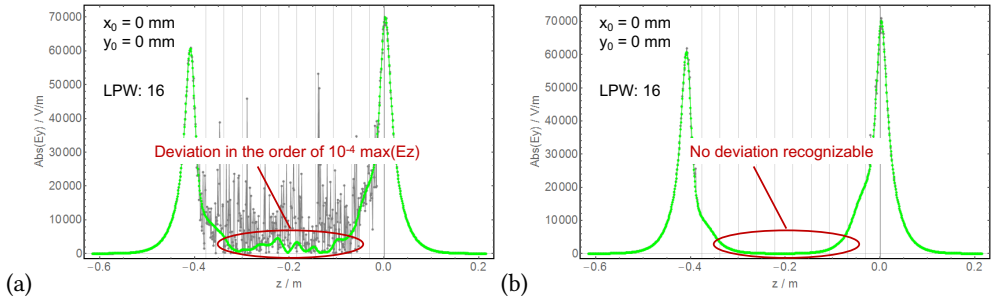

Figure 2: Transversal y-component of the electric field strength: (a) results from FE simulation for a mesh with 16 lines per wavelength (LPW) before and after post-processing using Kirchhoff integrals; (b) results for a symmetric mesh and after post-processing using Kirchhoff integrals.

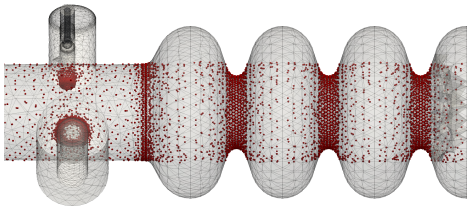

Figure 3: Source points $\mathbf{r}_q$ used for evaluating Kirchhoff integrals at a closed hull S. For visualisation reasons, only one collocation point per surface triangle is displayed.

2 Kirchhoff Integrals

A smooth field distribution is reached by evaluating the Kirchhoff integral for the electric field strength, i.e.,

$$\mathbf{E} = \int_S ((\mathbf{n} \times jc\mathbf{B})kG - (\mathbf{n} \times \mathbf{E}) \times \nabla G - (\mathbf{n} \cdot \mathbf{E})\nabla G) \, \mathrm{d}S$$

with Green function

$$G = \frac{e^{-jkr}}{4\pi r}, \quad r = |\mathbf{r}_P - \mathbf{r}_Q|, \tag{1}$$

wave number $k = \frac{\omega}{c}$, angular frequency ω, speed of light c, observation point $\mathbf{r}_P$ within the examined volume and source point $\mathbf{r}_Q \in S$, at a closed surface S embedding the respective volume. For convenience, a cylindrical surface S slightly inside the cavity is chosen (Fig. 3). The results are shown in green in Fig. 2a.

3 Symmetric Mesh

A tetrahedral mesh constructed as to reflect as much as possible the cylindrical symmetry of central parts of the cavity structure allows to further improve the results (Fig. 2b).

Acknowledgements

This work is funded by Deutsches Elektronen-Synchrotron (DESY) in Hamburg, Germany and by DFG through GRK 2128.

Book of abstracts of the 7th International Conference
on Advanced Computational Methods
in Engineering, ACOMEN 2017
18–22 September 2017.

Accelerated numerical simulations of a heaving floating body by coupling a motion solver with a two-phase fluid solver

Brecht Devolder[1,2,*], Peter Troch[1] and Pieter Rauwoens[2]

[1] *Department of Civil Engineering, Ghent University*

[2] *Department of Civil Engineering, Technology Cluster Construction, KU Leuven*

e-mails: Brecht.Devolder@UGent.be, Peter.Troch@UGent.be,
pieter.rauwoens@kuleuven.be

Abstract

Numerical simulations of floating bodies, heaving under wave loading, are performed by coupling a fluid solver and a motion solver. During each time step in the transient simulation, a converged solution is needed between the wave-induced fluid field around and the motion of the body. For some geometries in particular, a very slow converging or unstable solution is found. The mechanism for this non-physical instability is identified and an accelerated coupling scheme is derived for speeding up the simulations.

Key words: CFD, two-phase flow, rigid body motion, accelerated coupling scheme
MSC 2010: 65L20, 70E15, 76T10

1 Introduction

This paper presents a study on the coupling between a fluid solver and a motion solver by interchanging the total force F acting on a floating body. The two-phase fluid solver with dynamic mesh handling, interDyMFoam, is a part of the Computational Fluid Dynamics (CFD) toolbox OpenFOAM. The incompressible Navier-Stokes (NS) equations are solved together with a conservation equation for the Volume of Fluid (VoF). In this paper, that fluid solver is coupled to a rigid body motion solver, restricted to the heave motion only.

We were able to identify the mechanism for a numerical instability between the fluid and motion solver and to derive an accelerated coupling scheme, which are explained below.

2 Governing equations

The acceleration of the body a is derived from Newton's second law: $F = ma$ and subsequently integrated to the velocity v and position z respectively. In general, the fluid solver calculates the total force F by a discrete sum of the pressure forces p and the viscous forces τ over the faces of the body completed with body's total weight. In order to identify the source of the instability, the total force acting on the body is not calculated by solving the NS equations. Instead, a 1D simplified mass-spring-damper system is used in which the damping contribution is neglected ($b = 0$). Its equation of motion is explicitly formulated in terms of a by:

$$F^{n+1} = ma^{n+1} = -m_a a^n - bv^n - k(z^n - z^{eq}) \tag{1}$$

$$a^{n+1} = -\frac{m_a}{m}a^n - \frac{k}{m}(z^n - z^{eq}) \tag{2}$$

in which m_a is the added mass, b the damping coefficient, v the body's velocity, k the spring constant representing the hydrostatic restoring force and $z^n - z^{eq}$ the distance between the Centre of Mass (CoM) at the previous time step n and the CoM in equilibrium.

A linear stability analysis proves that (2) is only stable if $m_a < m$. Otherwise, an implicit formulation is needed for a (3a) using a relaxation method with relaxation factor α (3b).

$$a_{i+1}^{n+1} = -\frac{m_a}{m}a_i^{n+1} - \frac{k}{m}(z_i^{n+1} - z^{eq}) \tag{3a}$$

$$a_{i+1}^{n+1} = \alpha a_{i+1}^{n+1} + (1-\alpha)a_i^{n+1} \tag{3b}$$

in which $i+1$ and i are the current and previous iteration during the same time step $n+1$.

3 Accelerated coupling scheme

The coupling between motion and fluid solver is accelerated by using an optimal value for α (4a). Consequently, only one sub-iteration is needed for (3b) if m_a is known. However, in general m_a is unknown and varies from time to time (e.g a floating body in an irregular sea-state). Therefore Newton's second law $F = ma$ is linearised and m_a is estimated by (4b).

$$\alpha_{optimal} = \frac{1}{1 + m_a/m} \tag{4a}$$

$$m_a = -\frac{F_i^{n+1} - F_{i=1}^{n+1}}{a_i^{n+1} - a_{i=0}^{n+1}} \tag{4b}$$

As a result, the new acceleration is obtained by substituting (4b) in (4a) and apply (3b). As an example, the accelerated scheme is applied for a free decay test of a 2D floating block for which $m_a = 3m$ and compared to (3b) using α equal to 0.05 and 0.45. It is clearly shown in Fig. 1, that (4a) accelerates the convergence significantly between the fluid and motion solver.

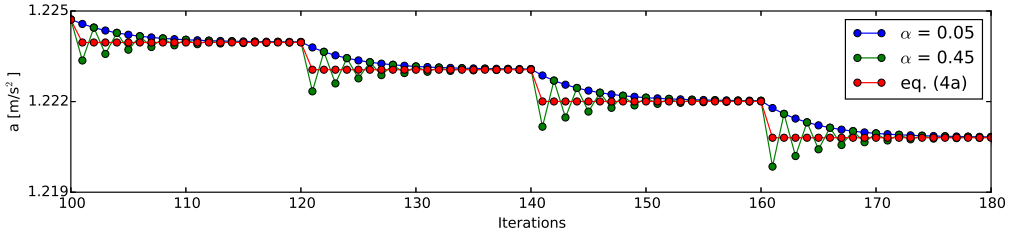

Figure 1: Acceleration as a function of the number of iterations for different values of α and eq. (4a). During each time step, 20 iterations are performed.

Acknowledgements

The first author is Ph.D. fellow of the Research Foundation-Flanders (FWO), Belgium (Ph.D. fellowship 1133815 N).

Book of abstracts of the 7th International Conference
on Advanced Computational Methods
in Engineering, ACOMEN 2017
18–22 September 2017.

Water artificial circulation for eutrophication control

Francisco J. Fernández[1], Aurea Martínez[2] and Lino J. Álvarez Vázquez[2]

[1] *Centro Universitario de la Defensa, Escuela Naval Militar, 36920 Marín, Spain*

[2] *Depto. Matemática Aplicada II, Universidade de Vigo, E.I. Telecomunicación 36310 Vigo, Spain*

e-mails: fjavier.fernandez@cud.uvigo.es, aurea@dma.uvigo.es, lino@dma.uvigo.es

Abstract

This work analyzes, from a mathematical point of view, the artificial mixing of water - by means of several pairs collector/injector that set up a circulation pattern in the waterbody - in order to prevent the undesired effects of eutrophication. The environmental problem is formulated as a constrained optimal control problem of partial differential equations, where the state system is related to the velocity of water and to the concentrations of the different species involved in the eutrophication processes, and the cost function to be minimized represents the volume of recirculated water.

Key words: Optimal control, Partial differential equations, Eutrophication, Water circulation, Restoration
MSC 2010: Primary: 49M25, 35Q93; Secondary: 90C56

1 Introduction

This work deals with artificial circulation as a shallow water aeration technique. Large waterbodies (for instance, lakes or reservoirs) get much of their oxygen from the atmosphere through diffusion processes. Artificial circulation increases water's oxygen by forcefully circulating the water to expose more of it to the atmosphere. Two techniques are the most common: air injection and mechanical mixing. The former has been analyzed, from an optimal control viewpoint in a few works (see, for instance, [3] and the references therein). However, in this work we will focus our attention on the latter that, as far as we know, has remained unaddressed in the mathematical literature.

In this work we will introduce a mathematical formulation of the environmental problem as a control/state constrained optimal control problem of partial differential equations. Then, we will analyze the optimal control problem and finally, we will deal with the numerical resolution of the problem, presenting a complete numerical algorithm and a realistic computational example.

2 Mathematical formulation of the control problem

In order to address the mitigation of the harmful effects of eutrophication by controlling the flow pumped by the injectors/collectors, we assume that their geometry and position are fixed

beforehand, and that we can only act on the pumped flow rate. Thus, the following optimal control problem needs to be solved:

$$(\mathcal{P}_B)\ \min\{J(\mathbf{g}):\ \mathbf{g}\in\mathcal{U}_{ad} \text{ and } \frac{1}{\mu(\Omega_C)}\int_{\Omega_C}\mathbf{u}(t)\,d\mathbf{x}\in K_C,\ \forall t\in[0,T]\}, \tag{1}$$

where $\mathbf{g}(t) = (g^1(t), g^2(t), g^3(t), g^4(t))$ is the flow rate in each group (see figure 1), $\mathcal{U}_{ad} = \{\mathbf{g}\in\mathcal{U}:\ -c_1\le g^k(t)\le c_2,\ \forall t\in[0,T],\ \forall k=1,\dots,4\}$, with $\mathcal{U}$ a suitable functional space, $K_C = [\lambda_1^m,\lambda_1^M]\times\cdots\times[\lambda_5^m,\lambda_5^M]$, $J(\mathbf{g}) = \int_0^T g(t)^2/2\,dt$ is the cost functional and $\mathbf{u} = (u^1,u^2,u^3,u^4,u^5)$, with u^1, u^2, u^3, u^4 and u^5 the concentration of, respectively, nitrogen, phytoplankton, zooplankton, organic detritus, and dissolved oxygen, is the solution of a Michaelis-Menten kinetics eutrophication model (see, for instance, [1]) coupled with a modified Navier-Stokes equations hydrodynamic model (see, for instance, [2]).

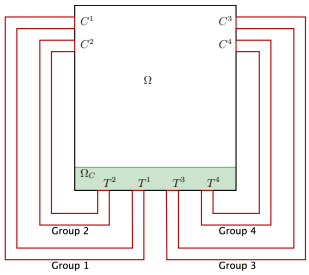

Figure 1: Physical domain Ω, showing the control domain Ω_C and the four pumping groups

Acknowledgements

This work was supported by funding from project MTM2015- 65570-P of Ministerio de Economía y Competitividad (Spain)/FEDER.

References

[1] L.J. Álvarez-Vázquez, F.J. Fernández and R. Muñoz-Sola, *Mathematical analysis of a three-dimensional eutrophication model* J. Math. Anal. Appl., **349** (2009), 135-155.

[2] M.D. Gunzburger, O.A. Ladyzhenskaya and J.S. Peterson, *On the global unique solvability of initial-boundary value problems for the coupled modified Navier-Stokes and Maxwell equations*, J. Math. Fluid Mech., **6** (2004), 462-482.

[3] R.C. Haynes, *Some ecological effects of artificial circulation on a small eutrophic lake with particular emphasis on phytoplankton*, Hydrobiologia, **43** (1973), 463-504.

[4] F. Hecht, *New development in Freefem++*, J. Numer. Math., **20** (2012), 251-265.

[5] A. Wachter and L.T. Biegler, *On the implementation of an interior-point filter line-search algorithm for large-scale nonlinear programming*, Math. Program., **106** (2006), 25-57.

Book of abstracts of the 7th International Conference
on Advanced Computational Methods
in Engineering, ACOMEN 2017
18–22 September 2017.

Gmsh 3.0: Gmsh goes boolean!

Christophe Geuzaine[1]

[1] *Dept. of Electrical Engineering and Computer Science, University of Liège*

e-mails: cgeuzaine@ulg.ac.be

Abstract

Gmsh is an open-source three-dimensional finite element mesh generator with a build-in CAD engine and post-processor. Its design goal is to provide a fast, light and user-friendly meshing tool with parametric input and advanced visualization capabilities. After 20 years of development, Gmsh enjoys a thriving community of several thousand users and developers worldwide. Its continuing development is driven by the need of researchers and engineers in academia and industry alike for a small, open-source pre- and post-processing solution for grid-based numerical methods. In this talk I will give a brief overview of the Gmsh project, present the new constructive solid geometry features introduced in Gmsh 3.0, and highlight some features currently under development.

Book of abstracts of the 7th International Conference
on Advanced Computational Methods
in Engineering, ACOMEN 2017
18–22 September 2017.

A pyramid scheme for three-dimensional diffusion equations on general polyhedral meshes

Xudeng Hang[1], Shuai Wang [1];[2] and Guangwei Yuan[1];[2]

[1] *Beijing 100094, China, Institute of Applied Physics and Computational Mathematics*

[2] *P.O.Box 8009, Beijing, 100088, China, Laboratory of Computational Physics*

e-mails: hang_xudeng@iapcm.ac.cn, wang_shuai@iapcm.ac.cn, yuan_guangwei@iapcm.ac.cn

Abstract

A new cell-centered finite volume scheme called the pyramid scheme (P-scheme) is proposed for three-dimensional diffusion equations on general polyhedral meshes with nonplanar faces.

Key words: Finite volume scheme, polyhedrons with nonplanar faces, 3D diffusion equation.

1 The pyramid scheme

Consider the stationary diffusion problem :$-\nabla\cdot(\kappa\nabla u) = f, \quad \text{in} \quad \Omega \subset R^3, u(x) = g, \quad \text{on} \quad \partial\Omega,$ For $\sigma = ABCD$, the expression of the normal flux across σ of P-scheme reads

$$F_{K,\sigma} = \frac{1}{2}\tau_\sigma|\overrightarrow{AC}\times\overrightarrow{BD}|(u_K - u_L + \alpha(u_C - u_A)) + \beta(u_D - u_B))). \tag{1}$$

where $\alpha = (\overrightarrow{K'L'}, \overrightarrow{n}_{BD})/(\overrightarrow{A'C'}, \overrightarrow{n}_{BD}), \quad \beta = (\overrightarrow{K'L'}, \overrightarrow{n}_{AC})/(\overrightarrow{B'D'}, \overrightarrow{n}_{AC})$. and $\overrightarrow{n}_{AC}$ (or $\overrightarrow{n}_{BD}$) is obtained by rotating $\overrightarrow{AC}$ (or $\overrightarrow{BD}$) anticlockwise by $\frac{\pi}{2}$ with respect to the vector $\overrightarrow{AC}\times\overrightarrow{BD}$. The cell-vertex unknowns u_A, u_B, u_C and u_D should be eliminated by the method in [1].

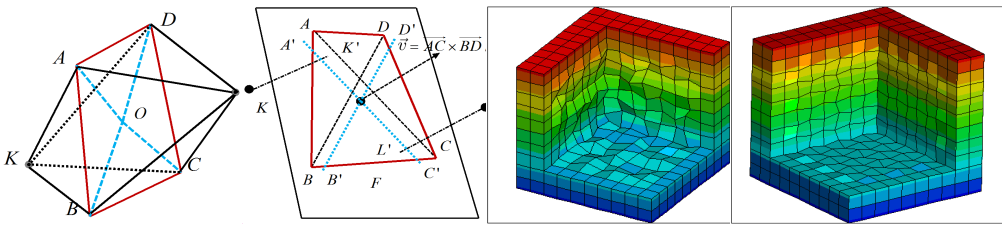

Figure 1: the face(left), the stencil(middle left),rand3D mesh (middle right), 3D distorted mesh (right)

2 Numerical results

Consider the meshes as shown in Figure1. Let the problem be as follows:

$$u(x,y) = \begin{cases} (x^2+10)(y-y^2)(z-z^2), & x < 0.5, \\ (5x^2+9)(y-y^2)(z-z^2), & \text{else}, \end{cases} \qquad \kappa = \begin{cases} 5, & x < 0.5, \\ 1, & \text{else}. \end{cases}$$

The precission is shown in Table 1,compared with the O-scheme in [1].The discretization cost of the O-scheme is almost 20 times more than that of the O-scheme as shown in Table 2.

Table 1: Errors of the P-scheme solutions compared with the O-scheme solutions

	3D distorted mesh			rand3D mesh		
number of cells	P-scheme	O-scheme	difference	P-scheme	O-scheme	difference
$4 \times 4 \times 4$	2.09e-02	2.10e-02	1.0e-04	2.21e-02	2.20e-02	1.0e-04
$8 \times 8 \times 8$	5.57e-03	5.39e-03	1.8e-04	5.75e-03	5.73e-02	2.0e-05
$16 \times 16 \times 16$	1.42e-03	1.32e-03	1.0e-04	1.49e-03	1.47e-03	2.0e-05
$32 \times 32 \times 32$	3.55e-04	3.20e-04	3.5e-05	3.73e-04	3.68e-04	5.0e-06
$64 \times 64 \times 64$	8.87e-05	7.86e-05	1.0e-05	9.36e-05	9.22e-05	1.4e-06

Table 2: The comparison of the CPU time (seconds) of discretization on the 3D distorted mesh.

	smooth coefficient		discontinuous coefficient	
number of cells	P-scheme	O-scheme	P-scheme	O-scheme
$64 \times 64 \times 64$	2.0e-02	5.3e-01	3.0e-02	5.6e-01

3 Acknowledge

This work was partially supported by the CAEP developing fund of science and technology(no.2014A0202009), and the National Science Foundation of China (11571048, 11401034).

References

[1] S. Wang, X. Hang, G. Yuan, A positivity-preserving finite volume scheme for diffusion equations on polyhedral meshes, Mathematica numerica sinica 37 (2015) 247–263.

[2] J. Droniou, Finite volume schemes for diffusion equations: Introduction to and review of modern methods, Mathematical Models and Methods in Applied Sciences 24 (08) (2014) 1575–1619.

[3] Z. Sheng, G. Yuan, A nine point scheme for the approximation of diffusion operators on distorted quadrilateral meshes, SIAM Journal on Scientific Computing 30 (3) (2008) 1341–1361.

[4] M. K.Lipnikov, G.Manzini, Mimetic finite difference metod, Journal of Computational Physics 257 (12) (2014) 1163 – 1227.

Book of abstracts of the 7th International Conference on Advanced Computational Methods in Engineering, ACOMEN 2017 18–22 September 2017.

Quality of the ruin probabilities approximation using the regenerative processes approach regarding to large claims

S. Hocine[1], Z. Benouaret[1] and D. Aïssani[1]

[1] *Recherche unit LaMOS, University of Bejaia*

e-mails: hsafia4@gmail.com, benouaret$_z$@yahoo.fr, djamil$_a$issani@hotmail.com

Abstract

Risk models, recently studied in the literature, are becoming increasingly complex. It is rare to find explicit analytical relations to calculate the ruin probability (see [2]). Indeed, the stability issue (see [1, 7]) occurs naturally in ruin theory, when parameters in risk can not be estimated than with uncertainty. However, in most cases, there are no explicit formulas for the ruin probability. Hence, the interest to obtain explicit stability bounds for these probabilities in different risk models (see [4, 6]). In this study, we are interested to the stability bounds of the univariate classical risk model established by Kalashnikov (2000) (see [6]) via the regenerative processes approach (see [5]). By adopting an algorithmic approach, we have implemented this approximation and determined numerically the bound of ruin probability in the case of large claims (heavy-tailed distribution (see [3, 8, 9])). After presenting numerically and graphically the stability bounds, an interpretation and comparison of the results have been done.

Keywords: Heavy-tailed distribution, large claims, regenerative process, risk model, ruin probability, stability.

References

[1] D. Aïssani and N. V. Kartashov. Ergodicity and stability of Markov chains with respect to operator topology in the space of transition kernels. *Compte Rendu Academy of Sciences U. S. S. R, ser. A, 11.* 3-5, 1983.

[2] S. Asmussen and H. Albrecher Ruin Probabilities. vol. 14 of Advanced Series on Statistical Science Applied Probability, World Scientific, 2010.

[3] S. Coles. An introduction to statistical modeling of extreme values. Springer, 2001.

[4] F. Enikeeva, V. Kalashnikov and D. Rusaityte. Continuity estimates for ruin probabilities. Scandinavian Actuarial Journal. 18-39, vol 10, 2001.

[5] V. Kalashnikov. *Topics on Regenerative Process.* CRC Press, Boca Raton, 1994.

[6] V. Kalashnikov. The Stability concept for stochastic risk models. *Working Paper Nr 166. Lab. of Actuarial Mathematics. University of Copenhagen*, 2000.

[7] N. V. Kartashov. Strong Stable Markov Chains. VSP, Utrecht, 1996.

[8] D.G. Konstantinidis. Comparison of ruin probability estimates in the presence of heavy tails. Journal of Mathematical Sciences, Vol. 93, No. 4, 552-562, 1999.

[9] D.G. Konstantinidis. Risk models with extremal subexponentiality. Brazilian Journal of Probability and Statistics, 21, 63-83, 2007.

Book of abstracts of the 7th International Conference
on Advanced Computational Methods
in Engineering, ACOMEN 2017
18–22 September 2017.

Numerical modeling of heat exchange in unsaturated porous media

J. Kačur[1], **P. Mihala**[1] **and M. Tóth**[1]

[1] *Department of Mathematical analysis and Numerical mathematics, Comenius University*

e-mails: jozef.kacur@fmph.uniba.sk, p.mihala@gmail.com, m.toth82@gmail.com

Abstract

We discuss the heat exchange between the infiltrated water and matrix of unsaturated porous media. This contribution is motivated by thermal isolation properties of facades. The mathematical model consists of coupled nonlinear system of parabolic-elliptic equations representing the conservation of heat energy and water mass balance. Mathematical model for water transport in unsaturated porous media is represented by Richard's type equation. Heat transport by water includes water flux, molecular diffusion and dispersion. Heat exchange in pours is modeled by temperature jumps between water and matrix, transmission coefficient and saturation. A successful experiment scenario is suggested to measure the transmission coefficient.

Book of abstracts of the 7th International Conference
on Advanced Computational Methods
in Engineering, ACOMEN 2017
18–22 September 2017.

A Framework for the Generation and Descritization of Heterogeneous Polydisperse Material Microstructures

Elizabeth R. Livingston[1], Peter J. Vonk[2] and Masoud Safdari[2]

[1] *Department of Mechanical Science and Engineering, University of Illinois at Urbana-Champaign*
[2] *Illinois Rocstar LLC, 1800 South Oak St., Suite 108, Champaign, IL 61820*
e-mails: eliving2@illinois.edu, vonk@illinoisrocstar.com, msafdari@illinoisrocstar.com

Abstract

A novel methodology that generates simulation-ready general-purpose material microstructure models is presented. A computational framework is devised to (i) generate random packs of convex inclusions, (ii) obtain accurate geometric representations for the pack, and (iii) create a high-quality conformal mesh. This approach is innovative because of its simplicity, ease of automation, and potential to account for uncertainties such as the effect of a material's microstructure. A variation of the Lubachevsky-Stillinger algorithm with collision detection is used to produce polydisperse random distributions and orientations of particles. The framework generates packs from a number of inclusion shapes into one of four different geometric domains. Several pre-processing options are available such as the ability to enforce periodic boundary conditions, take a 2D cross-section, and manipulate particles. Several examples are presented to demonstrate applications including the modeling of solid propellants, energetic materials, composites, and granular materials.

Key words: 3D mesh generation, materials microstructure, particle packing

1 Introduction

The macroscopic properties of materials can be directly linked to their characteristic microstructure through modeling an appropriate representative volume element (RVE). RVE-based modeling techniques have been used to predict fracture in solid propellants [1], understand damage in concrete [2], and study the surface remodeling of trabecular bone [3]. We present an engineering solution for generating and discretizing simulation-ready microstructures comprised of convex-shaped inclusions based on known information such as the inclusion geometry and volume fractions.

2 Methods

In the first step, a digital representation of a material's microstructure that has the desired properties is generated. This was done using a random packing algorithm previously implemented in the software package *Rocpack* [4]. Inclusions with radii of zero are randomly assigned to the periodic or fixed-boundary domain at time $t = 0$ with random velocities. Each mode (type of inclusion) grows linearly in time with a rate distribution across all modes that is based on the input size fractions. Inclusions stop growing when the desired volume fraction

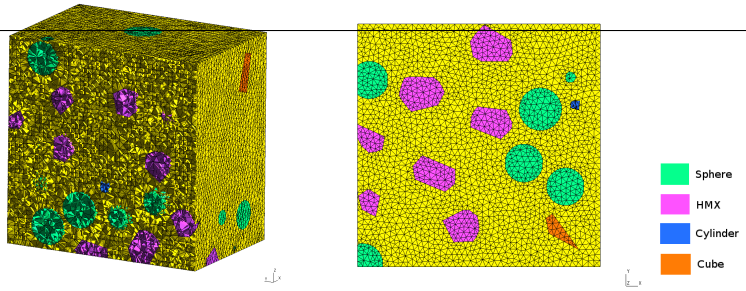

(a) (b)

Figure 1: Arbitrary inclusions in a RVE. a) conforming volumetric mesh, and b) cross-section of the same mesh at $z = 0.5$. (Periodicity is not enforced)

(the total volume of inclusions to the volume of the domain) is reached for all phases or after the interval between collisions becomes too small to continue.

To develop a conformal volumetric mesh, a pre-processing step is then applied to the pack. The *Rocpack* output is modeled using the *OpenCASCADE* geometry kernel of the software *GMSH* [5]. The particles may touch in a jammed pack, which may lead to singularities during numerical analysis or technical challenges during the discretization step, causing excessive number of elements. To avoid these pitfalls, an optional uniform shrinkage in particle radius can be applied. The resulting reduction in volume fraction is insignificant.

The tool also enables cross section analysis of the microstructure. First, inclusions are translated to standard STL representation. A slicing algorithm then intersects a plane with the facets of the model. This slice is then processed further to remove collinear points and smooth sharp corners. The simplified geometry is still representative of the randomly packed microstructure and can be used for 2D analyses.

In the last step, the generated pack is discretized using *GMSH* into a conforming mesh in either 2D or 3D. A sample conforming mesh is shown in Figure 1-a. Each mode from the packing algorithm is defined in a set for simulation purposes, as shown in Figure 1-b. The output mesh then can be written into a variety of standard formats supported by *GMSH* for subsequent analysis and simulation steps.

Acknowledgements

This work has been partially supported by Illinois Rocstar and through the grant #DE-SC0013278 awarded by the Department of Energy.

References

[1] K. Matous, H.M. Inglis, et. al., *Multiscale modeling of solid propellants: From particle packing to failure*, Compos. Sci. Technol. **67** (2007) 1694–1708.

[2] P. Wriggers, S.O. Moftah, *Mesoscale models for concrete: Homogenisation and damage behavious*, Fin. Elem. Anal. and Des. **42** (2006) 623–636.

[3] T. Adachi, K. Tsubota, et. al., *Trabecular Surface Remodeling Simulation for Cancellous Bone Using Microstructural Voxel Finite Element Models*, J. Biomech. Eng. **123** (2001) 403–409.

[4] D.S. Stafford, T.L. Jackson, *Using level sets for creating virtual random packs of non-spherical convex shapes*, J. Comp. Phys. **229** (2010) 3295–3315.

[5] C. Geuzaine, J.-F. Remacle, *Gmsh: a three-dimensional finite element mesh generator with built-in pre- and post-processing facilities*, Int. J. Numer. Meth. Engrg. **79(11)** (2009) 1309–1331.

Book of abstracts of the 7th International Conference
on Advanced Computational Methods
in Engineering, ACOMEN 2017
18–22 September 2017.

Numerical methods of a mixed problem for a nonlinear Kirchhoff model with moving boundary

Mohamed Mbehou[1]

[1] *Department of Mathematical Sciences, University of South Africa*

e-mails: mohamm@unisa.ac.za

Abstract

With the use of the coordinate transformation which fixes the boundaries, the finite element formulation is presented for the space variable. Its convergence and error bounds in the energy norm and for the first time derivative in the L^2-norm are established. In particular, the error in the energy norm and for the first time derivative in the L^2-norm is shown to converge with the optimal order $O(h^r)$ with respect to the mesh size h and the polynomial degree $r \geq 1$. To obtain the fully discrete solution, the generalized-α method is adapted to the semidiscrete formulation . Finally, some numerical simulations that validated the theoretical findings are exhibited.

Key words: Galerkin finite element method, generalized-α method, Kirchhoff model, moving boundaries, Newmark schemes.
MSC 2010: 65N12, 65N30, 35K65, 35J65.

1 Introduction

The following Kirchhoff-Carrier model for the hyperbolic-parabolic equations has been considered in this work.

$$\begin{aligned} &(\rho_1 u_t)_t + \rho_2 u_t - (1 + M(t, \int_{\Omega_t} |Du|^2 dx))D^2 u = f(x,t) \quad \text{in} \quad Q_t \\ &u(\alpha(t), t) = u(\beta(t), t) = 0 \qquad \text{on} \quad (0,T) \\ &u(x,0) = u_0(x) \quad u_t(x,0) = u_1(x) \quad \text{in} \quad \Omega_0 = (\alpha(0), \beta(0)), \end{aligned} \tag{1}$$

where Q_t is a bounded noncylindrical domain defined by

$$Q_t = \{(x,t) \in \mathbb{R}^2 \, : \alpha(t) < x < \beta(t), \quad \text{for all} \quad 0 < t < T\},$$

$$\Omega_t = \{x \in \mathbb{R} \, : \alpha(t) < x < \beta(t), \quad 0 < t < T\}.$$

$\rho_1(.)$ and $\rho_2(.)$ are two positive functions. $\alpha(.)$ and $\beta(.)$ are two functions such that $\alpha(t) < \beta(t) \quad$ for all $\quad t \in [0,T]$. D^k ($k \in \mathbb{N}$) denotes the differential operator $\frac{\partial^k}{\partial z^k}$ (z is a generic one spatial dimensional variable).
Benabidallah and Ferreira [1] investigated the global existence, uniqueness and asymptotic behavior of regular solutions to problem (1). In [2], Bisognin proved the existence of local

solution of (1) in a bounded or unbounded domain of $\mathbb{R}^n$. The existence of global solutions to problem (1) with analytic initial data was firstly investigated by Pokhozhaev [3] and Arosio and Spagnolo [4].
The goal of this research work is to use the coordinate transformation to fix the boundaries and then propose the numerical algorithm based on generalized-α method in the fixed domain problem.

References

[1] R. Benabidallah and J. Ferreira, *On hyperbolicŰparabolic equations with nonlinearity of kirchhoffŰcarrier type in domains with moving boundary,* Nonlinear Analysis: Theory, Methods and Applications, **37** (1999) 269–287.

[2] E. Bisognin, *Hyperbolic parabolic equations with nonlinearity of kirchhoff-carrier type,*Revista Matemťatica Complutense **8** (1995) 401–430.

[3] S. I. Pokhozhaev, *On a class of quasilinear hyperbolic equations,* Matematicheskii Sbornik, **138** (1975) 152–166.

[4] A. Arosio and S. Spagnolo, *Global Solution of the Cauchy Problem for a Non-linear Hyperbolic Equation.* Universit'a di Pisa. Dipartimento di Matematica, 1982.

[5] K. Nishihara, *Degenerate quasilinear hyperbolic equation with strong damping,* Funkcialaj Ekvacioj, **27**(1984) 125–145.

Book of abstracts of the 7th International Conference on Advanced Computational Methods in Engineering, ACOMEN 2017
18–22 September 2017.

Adjoint sensitivity for ODE based statistical models

Valdemar Melicher[1], Tom Haber[2] and Wim Vanroose[1]

[1] *Department of Mathematics and Computer Science, Middelheimlaan 1, 2020 Antwerp, Belgium, University of Antwerp*

[2] *Expertise Centre for Digital Media, Wetenschapspark 2, 3590 Diepenbeek, Belgium, Hasselt University*

e-mails: Valdemar.Melicher@UAntwerpen.be, Tom.Haber@UHasselt.be, Wim.Vanroose@UAntwerpen.be

Abstract

We consider statistical models constrained by ordinary differential equations (ODEs) and present and analyze an *adjoint state method* (ASM) framework for an efficient computation of likelihood sensitivities with respect to the parameters of the underlying ODE model.

In the statistical context, the discrete time series data have to be coupled with the continuous ODE model. We interface the discrete and continuous worlds at the level of the likelihood. We show rigorously that the resulting methodology is locally well-posed under reasonable assumptions about the ODE model.

Further, we present a highly optimized implementation of the results and its benchmarks on a number of problems.

Key words: Algorithm, Mathematical Statistics, Ordinary Differential Equations, Sensitivity Analysis, Statistical Computing

1 Introduction

In [1] we employ the *adjoint state method* (ASM) for an efficient computation of the first and the second derivatives of likelihood functionals constrained by ODEs with respect to the parameters of the underlying ODE model.

Essentially, the gradient can be computed with a cost (measured by model evaluations) that is independent of the number of the parameters and the Hessian with a linear cost in the number of the parameters instead of the quadratic one. The sensitivity analysis becomes feasible even if the parametric space is high-dimensional.

We consider time series vector data $\boldsymbol{y}_i \in \mathbb{R}^n$ for $i = 1, \ldots, N$, where n is the dimension of the observation space and N is the number of corresponding measurements times t_i in interval $I := [0, T]$ with some positive final time $T > 0$. Very often in science the underlying structural model for such data is the following initial-value problem

$$\begin{aligned} d_t \boldsymbol{u} &= \boldsymbol{f}(t, \boldsymbol{u}, \boldsymbol{\phi}), \quad t \in [0, T], \\ \boldsymbol{u}(0) &= \boldsymbol{u}_0(\boldsymbol{\phi}), \end{aligned} \tag{1}$$

where $\boldsymbol{u}_0$ is the initial condition, dependent only on the parameter vector $\boldsymbol{\phi} \in \mathbb{R}^p$. In general non-linear r.h.s. $\boldsymbol{f}$ of the governing equation represents the time derivative of the model variable $\boldsymbol{u}(t)$. It depends on the current time t, the model parameters $\boldsymbol{\phi}$ and the current values of $\boldsymbol{u} \in \mathbb{R}^m$.

The predictor $\hat{\boldsymbol{y}}$ of the data $\boldsymbol{y}$ is a result of integration of the dynamical system (1) and a possible subsequent post-processing, for example aggregation. This can be expressed in mathematical terms as $\hat{\boldsymbol{y}} = \mathcal{P}(\boldsymbol{u}(t,\boldsymbol{\phi})) =: \boldsymbol{g}(t,\boldsymbol{\phi})$, where $\mathcal{P} : \mathbb{R}^m \to \mathbb{R}^n$ is the post-processing operator relating the solution $\boldsymbol{u}$ to data.

We aim to efficiently compute the first and the second derivatives of functionals of the following form

$$l(\boldsymbol{\phi}) = \pm \sum_i d(\boldsymbol{y}_i, \boldsymbol{g}(t_i,\boldsymbol{\phi})) \tag{2}$$

with respect to $\boldsymbol{\phi}$. Here $d : \mathbb{R}^n \times \mathbb{R}^n \to [0,\infty)$ is a sufficiently smooth distance function (metric) on $\mathbb{R}^n$. Equation (2) measures the fidelity between the model and the data.

2 Connecting the worlds

Measurements $\boldsymbol{y}_i$ are acquired at discrete time points t_i. In statistics, these measurements should not be tempered with in any way, e.g. they cannot be interpolated, which stands for augmentation.

On the other hand the model (1) is a continuous one and since the ASM deals extensively with the model and the functional (2), it is necessary to work in continuous setting.

In [1] we connect the discrete data and the continuous model on the level of the likelihood functional. One can write

$$\sum_i d(\boldsymbol{y}_i, \boldsymbol{g}(t_i,\boldsymbol{\phi})) = \int_0^T \delta\{t - t_i\} d(\boldsymbol{y}(t), \boldsymbol{g}(t,\boldsymbol{\phi}))\, \mathrm{d}t \tag{3}$$

where, by the classical misuse of notation, $\delta\{t - t_i\}$ is the Dirac delta function of the set of all measurement times t_i. In order to achieve that the above integral is well-defined, we will consider a small positive ϵ, such that the functions $\boldsymbol{y}(t) := \boldsymbol{y}_i$, $t \in (t_i - \epsilon, t_i + \epsilon)$ for all measurement times t_i are well defined. We emphasize, that by doing so, we do not generate new measurements. We merely assume an infinitesimally small interval of their validity.

Acknowledgements

The work of the first two authors was supported by IWT O&O project 130406 – ExaScience Life HPC.

References

[1] V. Melicher, T. Haber, and W. Vanroose, *Fast derivatives of likelihood functionals for ODE based models using adjoint-state method*, ArXiv e-prints (2016).

Book of abstracts of the 7th International Conference
on Advanced Computational Methods
in Engineering, ACOMEN 2017
18–22 September 2017.

Localization of polynomial eigenvalues

Aaron Melman[1]

[1] *Department of Applied Mathematics, Santa Clara University, USA*

e-mails: amelman@scu.edu

Abstract

We present localization results for the eigenvalues of matrix polynomials, which are encounterered in a wide range of engineering applications, and that are expressed in the standard power basis as well as in generalized bases, some of which are generalizations of little known or very recent (scalar) polynomial bounds. We illustrate these bounds with examples from the engineering literature.

Key words: bound, matrix polynomial, polynomial eigenvalue
MSC 2010: 30C15, 47A46, 65F15

1 Introduction

Matrix polynomials appear in generalized eigenvalue problems where a nonzero complex vector v and a complex number z are sought such that $P(z)v = 0$, with

$$P(z) = A_n z^n + A_{n-1} z^{n-1} + \cdots + A_0 \,, \tag{1}$$

and the coefficients A_j are $m \times m$ complex matrices. We will assume throughout that P is *regular*, namely, that $\det P(z)$ is not identically zero. If A_n is singular then there are infinite eigenvalues and if A_0 is singular then zero is an eigenvalue. There are nm eigenvalues, including possibly infinite ones. The finite eigenvalues are the solutions of $\det P(z) = 0$. The familiar (linear) eigenvalue problem is obtained as a special case when $n = 1$ and $A_n = I$.

Bounds on polynomial eigenvalues are useful, e.g., for their computation by iterative methods, when computing pseudospectra, or, especially, in the analysis of engineering problems. They are much more difficult to compute than polynomials zeros, making bounds on such eighenvalues more valuable. An extensive list of bounds can be found in [2], in which the authors systematically generalize results for scalar polynomials to correponding results for matrix polynomials. What we propose follows a similar pattern, although we consider apparently relatively unknown results for scalar polynomials, refine and extend some of them, and then generalize them to matrix polynomials. Contrary to almost all existing bounds, these eigenvalue localization results can be further improved iteratively to achieve significant improvements of existing bounds, like the ones in [2], sometimes by orders of magnitude.

2 Eigenvalue localization results

We begin by reviewing a few results for scalar polynomials before generalizing them to matrix polynomials, where our true interest lies. We cannot list all of the results we will present due to page limitations, but the following should at least illustrate the general idea.

A classical result by Cauchy (1829) states that all the zeros of p (defined in the introduction) lie in $|z| \leq r$, where r is the unique positive solution of $|a_n|x^n - |a_{n-1}|x^{n-1} - \cdots - |a_1|x - |a_0| = 0$. We define r as the *"Cauchy radius"* of p. A much less known improvement of this result, obtained by using a polynomial multiplier, was published in [5] in 2002. Specifically, it was shown there that the Cauchy radius of $\left(a_n z^k - a_{n-k}\right) p(z)$ is not larger than that of p, where k is the smallest positive integer such that $a_{n-k} \neq 0$. At the moment this is the only known multiplier guaranteed to improve the Cauchy radius. Here we present a different multiplier and show that, in the simplest case when $a_{n-1}a_{n-2} \neq 0$, the Cauchy radius of $\left(a_n z^2 - a_{n-1}z - (a_{n-2} - a_{n-1}^2)\right) p(z)$ is also not larger than the Cauchy radius of p. Although this Cauchy radius is not necessarily better than the one from [5], in practice, it almost always outperforms it. When $a_{n-1}a_{n-2} = 0$, a simple modification of the multiplier preserves this result. In addition, the multipliers can be repeatedly applied to improve the bounds.

Cauchy's result was generalized to matrix polynomials in [1], [2], and [3], where it was shown that the eigenvalues of P in (1) (when A_n is nonsingular) are contained in the disk $|z| \leq r$, where r is the unique positive solution of $\|A_n^{-1}\|^{-1}x^n - \|A_{n-1}\|x^{n-1} - \cdots - \|A_1\|x - \|A_0\| = 0$ and $\|.\|$ can be any matrix norm. As before, r is the *Cauchy radius* of P. In [4], it was shown that this generalization can also be improved by using a multiplier, namely that the Cauchy radii of $(A_n z^k - A_{n-k})P(z)$ and $P(z)(A_n z^k - A_{n-k})$ are not larger than the Cauchy radius of P. Likewise, we will show here that the Cauchy radii of $\left(A_n z^2 - A_{n-1}z - (A_{n-2} - A_{n-1}^2)\right) P(z)$ and $P(z)\left(A_n z^2 - A_{n-1}z - (A_{n-2} - A_{n-1}^2)\right)$ are also not larger than that of P.

This same pattern of scalar polynomial results that can be generalized to matrix polynomials also extends to another classical result, namely, Pellet's theorem, which sometimes allows polynomial zeros to be separated from each other according to their moduli, and also to results expressed in generalized bases. We present those results as well.

Several examples drawn from the engineering literature will be used to illustrate the usefulness of the above results.

References

[1] D. A. Bini, V. Noferini, M. Sharify, *Locating the eigenvalues of matrix polynomials.* SIAM J. Matrix Anal. Appl. **34** (2013) 1708–1727.

[2] Higham, N.J. and Tisseur, F. *Bounds for eigenvalues of matrix polynomials.* Linear Algebra Appl., 358 (2003), 5–22.

[3] Melman, A. *Generalization and variations of Pellet's theorem for matrix polynomials.* Linear Algebra Appl., 439 (2013), 1550âĂŞ1567.

[4] Melman, A. *Bounds for eigenvalues of matrix polynomials with applications to scalar polynomials.* Linear Algebra Appl., 504 (2016), 190âĂŞ203.

[5] Rahman, Q.I., and Schmeisser, G. *Analytic Theory of Polynomials* London Mathematical Society Monographs. New Series, 26. The Clarendon Press, Oxford University Press, Oxford, 2002.

Book of abstracts of the 7th International Conference
on Advanced Computational Methods
in Engineering, ACOMEN 2017
18–22 September 2017.

The implementation of a new method for the approximation of integrals using Bernstein operators

Dan Micläuş[1]

[1] *Department of Mathematics and Computer Science, Technical University of Cluj-Napoca, North University Center at Baia Mare*

e-mails: dan.miclaus@cunbm.utcluj.ro

Abstract

In the present paper we establish the theoretical framework of a new method in order to approximate a definite integral of a given function by Bernstein quadrature formula. Some numerical examples will be given for supporting of the theoretical aspects.

Key words: Bernstein operators, Bernstein quadrature formula, Integrals approximation.
MSC 2010: 65D32.

1 Introduction

In the real daily applications arise different situations where it is necessary to solve certain definite integrals, much more complicated than those presented in the courses of mathematical analysis. Thus, some integrals are so complex that they can not be solved analytically, or solving them requires a great deal of computation and time. In order to solve such of integrals in a efficient way, numerous numerical methods have been developed, called quadrature formulas. The most known method of numerical integration is obtained by integrating the Lagrange interpolation formula resulting the class of Newton-Cotés quadrature formulas.
Knowing the fact that in the approximation process of certain definite integrals using the Newton-Cotés quadrature formulas, we can not get a desired a priori error, we ask whether there are simple quadrature formulas with this property. Some recent studies [1], [2], [3] confirm that the Bernstein operator

$$B_n(f;x)=\sum_{k=0}^{n}\binom{n}{k}x^k(1-x)^{n-k}f\left(\frac{k}{n}\right)$$

can be a way to solve this problem.

Acknowledgements

The results presented in this paper were obtained with the support of the Technical University of Cluj-Napoca through the research Contract no. 2011/12.07.2017, Internal Competition CICDI-2017.

References

[1] U. Abel, M. Ivan, *New representation of the remainder in the Bernstein approximation*, J. Math. Anal. Appl. **381** (2011), No. 2, 952–956.

[2] D. Bărbosu, D. Micláuş, *On the composite Bernstein quadrature formula*, Rev. Anal. Numér. Théor. Approx. **39** (2010), No. 1, 3–7.

[3] D. Bărbosu, G. Ardelean, *The Bernstein quadrature formula revised*, Carpathian J. Math. **30** (2014), No. 3, 275–282.

Book of abstracts of the 7th International Conference
on Advanced Computational Methods
in Engineering, ACOMEN 2017
18–22 September 2017.

Determination of transmission and matrix heat conduction coefficients at heat exchange in unsaturated porous media

J. Kačur[1], P. Mihala[1] and M. Tóth[1]

[1] *Department of Mathematical analysis and Numerical mathematics, Comenius University*

e-mails: jozef.kacur@fmph.uniba.sk, p.mihala@gmail.com, m.toth82@gmail.com

Abstract

We discuss the efficient experimental scenario for determination of transmission coefficient and matrix heat conduction via solution of inverse problem. The infiltrated water in pours exchange heat energy with matrix. This exchange depends on the temperature jump, saturation and transmission coefficient. Because of microstructure, one cannot measure temperature jump and therefore a special experimental scenario is suggested, which enables to determine the transmission coefficient and moreover the heat conduction coefficient of matrix. The sample used in experiments is 3D. This experimental scenario is based on suitable choice of initial and boundary conditions for water and heat in the sample. The numerical experiments support efficiency of this scenario for reliable determination of required coefficients.

Book of abstracts of the 7th International Conference on Advanced Computational Methods in Engineering, ACOMEN 2017 18–22 September 2017.

Analysis of the semi-smooth Newton method for 3D contact problems with the Tresca friction

Kučera Radek[1] **and Motyčková Kristina**[1]

[1] *IT4Innovations, VŠB - Technical University of Ostrava, 17. listopadu 15/2172, 708 33 Ostrava-Poruba, Czech Republic*

e-mails: radek.kucera@vsb.cz, kristina.motyckova@vsb.cz

Abstract

The semi-smooth Newton method for solving discretized contact problems with Tresca friction in three space dimensions is analyzed. The slanting function is approximated to get symmetric inner linear systems. The primal-dual algorithm is transformed into the dual one so that the conjugate gradient method can be used. The R-linear convergence rate is proved for an inexact globally convergent variant of the method.

Key words: Contact problem, Tresca friction, Semi-smooth Newton method, Conjugate gradient method, Gradient projection, Convergence rate

MSC 2010: 65K10, 65N22, 49M29, 74M15, 74M10

1 Introduction

The dual algebraic formulation of discretized contact problems with Tresca friction in three space dimensions (3D) belongs to the class of problems called QCQP (Quadratically Constrained Quadratic Program) with a specific structure: the minimized function is strictly convex and quadratic subject to simple inequality bounds and separable quadratic constraints (spherical for isotropic and elliptical for orthotropic Tresca friction). The active set optimization algorithm for solving such problems has been proposed in [5, 6] as a generalization of the algorithm for simple bounds [3]. In this context, the active set is an index subset of components for which the constraints are satisfied as equalities in the current iteration. The CG (Conjugate Gradient) method generates iterations for non-active components and, when the progress is not sufficient, the active set is changed by a gradient projection step. The algorithm seeks the active set at the minimizer by generating iterations lying in the feasible set and examines if the sequence of the function values is monotonously decreasing. In contrast to 2D case, the algorithm in 3D does not exhibit any finite termination property due to the presence of the quadratic constraints but still it enjoys the same R-linear convergence rate.

Another way how to introduce active set strategies for solving contact problems is an active set implementation of the semi-smooth Newton (SSN) method. It is based on the primal-dual formulation of contact problems which uses projections onto convex sets to formulate the nonpenetration and friction conditions. The SSN method may be interpreted as a primal-dual active set algorithm. This approach has been used in [8] for solving 3D frictional contact

problems in which projections are replaced by appropriate nonlinear complementarity functions. The convergence analysis uses typically the slant differentiability concept [1] leading to the local superlinear convergence rate.

The projective formulation presented in this paper seems to be natural since it can be directly derived from the weak formulation of contact problems [4]. The respective slanting function is given by non-symmetric matrices and this property can not be eliminated by simple linear algebra tools. Fortunately, the slanting function at the minimizer does not contain some terms so that a symmetrization is possible. Neglecting these terms a-priori we get a symmetric approximation of the slanting function. Then 3D contact problems can be treated analogously as 2D ones [7]. First we propose a dual implementation of the SSN method with inexact solving inner linear systems by few CG steps. Note that exact solving is unrealistic for large-scale problems. Although numerical experiments indicate a high computational efficiency, the superlinear convergence result does not hold. Therefore we propose a monotonous globalization strategy guaranteeing the R-linear convergence rate of the algorithm. Although this result is similar to 2D case, its proof differs in many points. The globally convergent variant of the SSN method is closely related to the above mentioned active set algorithms [6, 2].

Acknowledgements

This work was supported by The Ministry of Education, Youth and Sports from the National Programme of Sustainability (NPU II) project "IT4Innovations excellence in science - LQ1602".

References

[1] *X. Chen, Z. Nashed, L. Qi*: Smoothing methods and semismooth methods for nondifferentiable operator equations. SIAM J. Numer. Anal. **38** (2000), 1200–1216.

[2] *Z. Dostál, T. Kozubek*: An optimal algorithm and superrelaxation for minimization of a quadratic function subject to separable convex constraints with applications. Mathematical Programming **135** (2012), 195–220.

[3] *Z. Dostál, J. Schöberl*: Minimizing quadratic functions over non-negative cone with the rate of convergence and finite termination. Comput. Optim. Appl. **30** (2005), 23–44.

[4] *J. Haslinger, I. Hlaváček, J. Nečas*: Numerical methods for for unilateral problems in solid mechanics. In Handbook of Numerical Analysis, vol. IV, Ciarlet, P.G. and Lions, J.L. eds., North-Holland, Amsterdam, 1996, 313–485.

[5] *R. Kučera*: Minimizing quadratic functions with separable quadratic constraints. Optim. Methods Soft. **22** (2007), 453–467.

[6] *R. Kučera*: Convergence rate of an optimization algorithm for minimizing quadratic functions with separable convex constraints. SIAM J. Optim. **19** (2008), 846–862.

[7] *R. Kučera, K. Motyčková, A. Markopoulos*: The R-linear convergence rate of an algorithm arising from the semi-smooth Newton method applied to 2D contact problems with friction. Comput. Optim. Appl., **61** (2015), 437–461.

[8] *S. Hüeber, G. Stadler, B. Wohlmuth*: A primal-dual active set algorithm for three-dimensional contact problems with Coulomb friction. SIAM J. Sci. Comput. **30** (2008), 572-596.

Book of abstracts of the 7th International Conference
on Advanced Computational Methods
in Engineering, ACOMEN 2017
18–22 September 2017.

TNL: Framework for numerical computing on modern parallel architectures

T. Oberhuber[1], J. Klinkovský[1], V. Žabka[1] and R. Fučík[1]

[1] *Department of Mathematics, Faculty of Nuclear Sciences and Physical Engineering, Czech Technical University in Prague*

e-mails: tomas.oberhuber@fjfi.cvut.cz, klinkjak@fjfi.cvut.cz, zabkav@gmail.com, radek.fucik@fjfi.cvut.cz

Abstract

We present new numerical library (TNL, Template Numerical Library) which is an abstract layer for development of numerical solvers on modern parallel architectures. Currently it supports multi-core CPUs and GPUs via CUDA. The library is written in C++ and it uses C++ templates extensively. The template design of TNL allows to write only one code and to run it on both CPU and also GPU without any knowledge of the GPU design. The library has native support for several sparse matrix formats optimized for GPUs together with iterative solvers for large linear systems and Runge-Kutta solvers. It also has a native implementation of structured and unstructured numerical meshes. We will briefly explain the design of TNL, the interface for implementation on PDE solvers and we will show scalability on multi-core CPUs together with speed-up on GPUs.

Book of abstracts of the 7th International Conference
on Advanced Computational Methods
in Engineering, ACOMEN 2017
18–22 September 2017.

A robust Riemann solver without artificial intervention

Jian REN[1], Zhijun SHEN[12], Wei YAN[1] and Guangwei YUAN[1]

[1] *Division of Computational Physics, Institute of Applied Physics and Computational Mathematics*

[2] *Center for Applied Physics and Technology, HEDPS, Peking University*

e-mails: ren_jian@iapcm.ac.cn, shen_zhijun@iapcm.ac.cn, wyanmath01@sina.com, yuan_guangwei@iapcm.ac.cn

Abstract

In order to improve the multi-fluid-channel scheme on the average of volume (MFCAV) and overcome its artificial intervention in the actual application, a new HLLCM scheme has been designed on a moving mesh, which can reduce false distortion of mesh. Numerical results show that the HLLCM scheme have better numerical effects in energy conservation in the complex applications than the MFCAV scheme.

Key words: Artificial intervention, HLLCM scheme, Riemann solver, Godunov method, Arbitrary Lagrangian-Eulerian method
MSC 2010: 76M12, 35L65, 65M06

1 Introduction

The multi-fluid-channel scheme on the average of volume (MFCAV)[1], an two-dimensional Arbitrary Lagrangian and Eulerian (ALE) method, is widely applied in computational studies for multi-material compressible fluid flows. The main assumption of MFCAV method is that the physical variables (density, energy, pressure and velocity) are cell-centered, hence named Cell-Centered Grid Hydrodynamics(CGH).

However, MFCAV method easily suffers from a numerical shock instability problem: the discrete computational mesh might become very stretched and distorted, which always need artificial intervention such as mesh adjustment, even fixed the Lagrangian mesh moving. Althought artificial intervention can improve the robustness of MFCAV method, these eventually result in large numerical errors in real applications, such as energy conservation error.

In this work, a robust HLLC-type Riemann solver named HLLCM has been designed[2], which is capable of preserving sharp contanct surface and avoid the numerical shock instability. The numerical experiments of real application demonstrate that HLLCM scheme have better energy conservation than MFCAV scheme.

2 Numerical schemes and experiments

When solving compressing Euler equations in ALE formulation, we need know the entire structure and wave speeds of an approximate Riemann solver in order to determine where the flux lies in state space. The HLLC[3] approximate Riemann solver consistent of three waves propagating at some speeds and four states, see Fig.1(a). Compared with the original HLLC method, we construct a new HLLC-type Riemann solver: HLLCM, in which only the contact wave S^*_{HLLC} is remained and the shear wave v^*_L, v^*_R is smeared by v^*, see Fig.1(b).

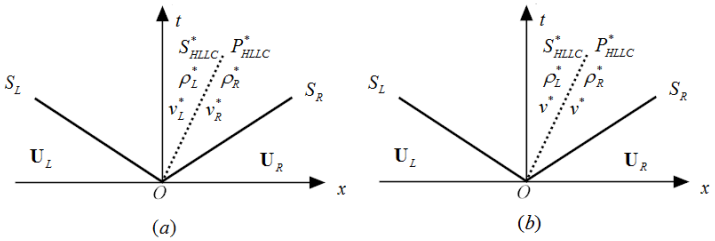

Figure 1: Wave structures of HLLC and HLLCM approximate Riemann solvers for the x-split two dimensional equations. (a) HLLC, (b) HLLCM.

Numerical experiments of application demonstrate that the HLLCM have better mesh quality than MFCAV. Moreover, the density calculated by HLLCM have been improved than MFCAV, especially above the interface between two immiscible fluids. In fact, densities of meshes above interface have always lead to the negative $\frac{\partial p}{\partial \rho}$, which break the thermodynamics law and make calculation terminate abnormally. So the MFCAV scheme have to introduce several artificial intervention, such as mesh rezoning, interface adjustment, for robustness in applications. Unfortunately, these intervention always increase the error of energy conservation. The error of energy conservation calculated by HLLCM scheme is less than MFCAV in applications.

3 Conclusion

The HLLCM scheme smears the shear velocities of the HLLC solver but remains almost all other states in the HLLC solver. Numerical results of applications demonstrate that HLLCM scheme have better numerical effects in keeping mesh quality and energy conservation than MFCAV.

References

[1] D. Li, G. Xu, H. Shui, et al., *Numerical Methods for Two-Dimensional Non-Steady Hydrodynamics*, Chinese Academic Publisher, 1987, 264–288.(in Chinese)

[2] Z. J. Shen, W. Yan, G. W. Yuan, *A robust HLLC-type Riemann solver for strong shock.*, J. Comput. Phys. **309** (2016) 185–206.

[3] E. F. Toro,M. Spruce and W. Speares, *Restoration of the contact surface in the HLL-Riemann solver.*, Shock Wave **4** (1994) 25–34.

Book of abstracts of the 7th International Conference on Advanced Computational Methods in Engineering, ACOMEN 2017
18–22 September 2017.

A fast solver for two-dimensional shallow water equations over erodible beds with multiple sediments

Thomas Rowan[1] **and Mohammed Seaid**[2]

[1] *School of Engineering and Computing Sciences,x, University of Durham, South Road, Durham DH1 3LE, UK*

e-mails: thomas.rowan@durham.ac.uk, m.seaid@durham.ac.uk

Abstract

A two-dimensional model of shallow water flow over erodible beds is presented. A novel approach is adopted for the treatment of multiple sediment types, both in packed beds and suspended sediment. An interface tracking tool is developed from one dimension and utilised on various different bed types and structures to demonstrate its capabilities. Two numerical solvers are developed and tested in this paper, the first consists of the standard Roe solver that is first order accurate, but time consuming compared to the other. Secondly a faster finite volume of characteristics (FVC) solver is used. In this method the Riemann problem is avoided using a two step approach. The two solvers are contrasted and tested against several benchmark tests as well as novel situations designed to explore the capabilities of the sediment handling tools implemented.

Key words: Finite volume method, Modified method of characteristics, Shallow water flows, Sedimentary layers, Suspended sediment, Roe Solver.

1 Introduction

The ability to model sediment interaction with water flows is crucial to planning and development. Building on the model in[2], we develop sediment handling tools to handle multiple sediments. In our model the coupled governing equations consist of the three two-dimensional shallow water equations for flow, a transport equation for suspended sediment, a bed Exner equation and empirical equations for sediment erosion and deposition. Two methods are compared in this work, a 1st order Roe Solver and the Finite Volume Characteristic (FVC) method used in [1]. The FVC method uses two steps; firstly the fluxes are reconstructed using the method of characteristics and then in he corrector stage the conservation equations are recovered. This method is conservative and well balanced.

2 Modelling of multiple sediments

In this study we consider non-cohesive sediment only. We utilise standard equations for Erosion E_α and Deposition D_α for each sediment type ($\alpha = 1, 2, 3 \ldots . m$) which are shown:

$$D_\alpha = w_\alpha (1 - C_\alpha)^{1.2} C_\alpha, \qquad E_\alpha = \varphi_\alpha \frac{\theta - \theta_\alpha}{h} u d_\alpha^{-0.2}. \tag{1}$$

where w_α is settling velocity, C_α is near bed concentration, φ_α is an erosion coefficient, θ is the near bed shear stress, θ_c is the critical shear stress for the initiation of motion, h is fluid height, u fluid speed, and d is sediment diameter. We utilise a novel approach for handling sediment in both suspended concentration and the bed. This consists of a three dimensional discretised bed coupled with a two dimensional discretised fluid flow. The height of the 3D bed cells are crucial when working out what the required resolution of the model. As these cells can either be overfilled, totally eroded, in flux or undergo armouring.

3 Preliminary Results

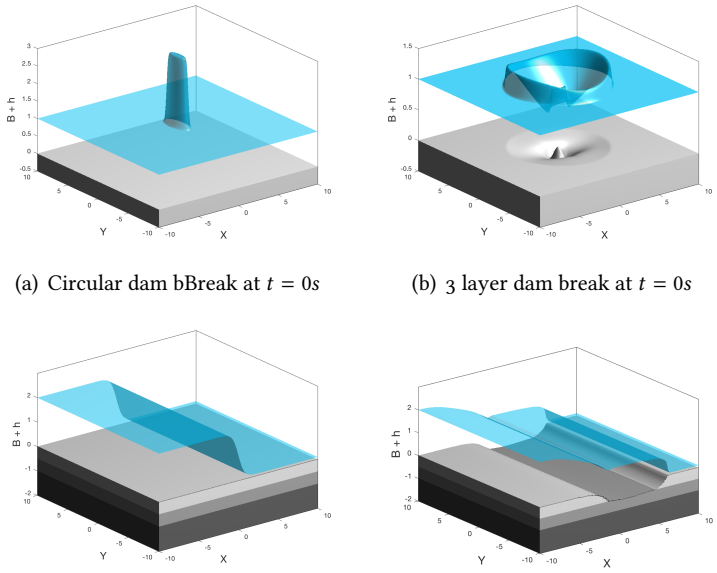

(a) Circular dam bBreak at $t = 0s$

(b) 3 layer dam break at $t = 0s$

(c) Circualr dam break at $t = 1s$

(d) 3 layer dam break at $t = 5s$

Figure 1: A circular dam break with mixed sediments, and a 3 sediment layer dam break.

This new approach to multi-sediment handling allows us to consider both mixed sediment types as shown in the circular dam break as well as discrete bed layers, as shown in Figure 1. This model enables the user to much more accurately assess real world sedimentary problems, with mixed sediments or discrete sediment layers. For example in Equation 1, the user no longer has to rely on an averaged value for d (like d_{50}), instead they can use multiple sediments mixed into the same three-dimensional bed cell that better represent the sediment grading.

References

[1] F. Benkhaldoun, M. Seaid, *A simple finite volume method for shallow water equations*, Jounral of Computational and Applied Mathematics, 2009. **234** (2010) 58-72.

[2] T. Rowan, M. Seaid, *Development and verification of a finite volume model for hydraulics over multi-layered erodible beds*, Scour and Erosion: Proceedings of the 8th International Conference on Scour and Erosion, (2016) 119-130.

Book of abstracts of the 7th International Conference
on Advanced Computational Methods
in Engineering, ACOMEN 2017
18–22 September 2017.

Accuracy enhancement for higher order non isoparametric finite-element simulations in curved domains

Vitoriano Ruas[1]

[1] *Institut Jean Le Rond d'Alembert, Sorbonne Universités, UPMC, CNRS - UMR 7190, France*

e-mails: vitoriano.ruas@upmc.fr, ruas.vitoriano@gmail.com

Abstract

The isoparametric version of the finite element method for meshes consisting of curved triangles or tetrahedra is widely employed to solve PDEs posed in curved domains. It allows to recover optimal approximation properties that hold for higher order elements in the case of polytopic domains. However, besides a geometric complexity, this technique requires the manipulation of rational functions and the use of numerical integration. We consider a simple alternative to deal with Dirichlet boundary conditions that bypasses these drawbacks, without eroding qualitative approximation properties.

Key words: curved domain, finite elements, high order, N-simplex, polynomial algebra.

1 Introduction

This work deals with a finite element technique for solving boundary value problems posed in two- or three-dimensional domains, with a smooth curved boundary. Its conception is close to the interpolated Dirichlet boundary condition method studied in [1]. The latter technique is intuitive and is known since the seventies, but has been of limited use so far. Among the reasons for this lies its difficult implementation, the lack of an extension to three-dimensional problems and restrictions on the choice of boundary nodal points to reach optimal convergence rates. In contrast our method is simple to implement in both two- and three-dimensional geometries. Moreover optimality is attained in both cases for a wide choice of boundary nodal points. The new method also bypasses the inconveniences of the isoparametric technique pointed out in the abstract. Moreover it is particularly handy, whenever a finite element method has normal component or normal derivative degrees of freedom, for in this case the definition of isoparametric finite element analogs is not always simple or clear. Our method was first studied in [4], in connection with triangular Lagrange finite elements of arbitrary order. In this work we address the case of tetrahedral Lagrange elements for second order elliptic PDEs, besides some Hermite elements.

2 Method's short description with a numerical example

Referring to [4] for further details, here we endeavor to illustrate our new method, by solving a simple model problem as follows. Let Ω be a smooth two-dimensional domain and Γ be its

boundary. Given a function $f \in H^1(\Omega)$ we wish to find a function $u \in H^3(\Omega)$ that solves $-\Delta u = f$ in Ω with $u = 0$ on Γ.
Let $\mathcal{P} = \{\mathcal{T}_h\}_h$ be a uniformly regular family of partitions of Ω into (straight) triangles respecting the usual intersection rules for finite element meshes. For every partition $\mathcal{T}_h \in \mathcal{P}$, h represents the maximum diameter of all triangles therein. Further we denote by Ω_h the union of triangles in $\mathcal{T}_h$, and by Γ_h the boundary of Ω_h. Now we denote by V_h the finite-element space consisting of continuous functions that vanish on Γ_h, whose restriction to each triangle $T \in \mathcal{T}_h$ is a polynomial of degree less than or equal to two, and set $a_h(u,v) := \int_{\Omega_h} \mathbf{grad}\, u \cdot \mathbf{grad}\, v \, d\mathbf{x}$ and $L_h(v) := \int_{\Omega_h} f_h v \, d\mathbf{x}$, where f_h is an extension of f in $H^1(\Omega_h)$ to $\Omega_h \setminus \Omega$. If we search for

$$u_h \in V_h \text{ such that } a_h(u_h, v) = L_h(v) \; \forall v \in V_h, \tag{1}$$

it is well-known that the energy norm $\| \cdot \|_{e,h}$ of $u - u_h$ in Ω_h, that is $\| u - u_h \|_{e,h} := [\int_{\Omega_h} |\mathbf{grad}(u - u_h)|^2 d\mathbf{x}]^{1/2}$, will be only an $O(h^{1.5})$.
In order to recover an optimal $O(h^2)$ for the energy norm of such an error function, we propose the following. Let W_h be a space defined exactly like V_h, except for the fact that every $w \in W_h$ necessarily vanishes only at the vertices of Γ_h and at points P of Γ arbitrarily located between two neighboring vertices of Γ_h. To make implementation more straightforward, such points can be chosen for instance as the (nearest) intersections with Γ of the perpendicular to an edge of Γ_h passing through its mid-point. Now instead of solving (3) we search for

$$\tilde{u}_h \in W_h \text{ such that } a_h(\tilde{u}_h, v) = L_h(v) \; \forall v \in V_h, \tag{2}$$

According to [4], $\| \tilde{u}_h - u \|_{e,h}$ is an $O(h^2)$.
Let us illustrate this by solving problems (3) and (4) in case Ω is the unit disk centered at the origin, and a uniformly regular family of meshes consisting of $8n^2$ triangles for $n = 2^m$, with $m = 1, 2, \ldots$ is constructed. In these experiments we take $f(x,y) = 9(x^2 + y^2)^{1/2}$, and hence the exact solution is given by $u(x,y) = 1 - (x^2 + y^2)^{3/2}$. Owing to symmetry only the quarter disk corresponding to $x > 0$ and $y > 0$ is taken into account in the computations, and therefore only meshes containing $2n^2$ elements are employed.

Taking $m = 2, 3, 4, 5$ and 6 and observing that $h = 1/n$, we display in the table below the quantities $\| \tilde{u}_h - u \|_{e,h}$ and $\| u_h - u \|_{e,h}$ for the resulting decreasing values of h.

Observation of this table confirms second order convergence in the energy norm for the

h	$\longrightarrow$	1/4	1/8	1/16	1/32	1/64
$\| \tilde{u}_h - u \|_{e,h}$	$\longrightarrow$	0.1329×10^{-1}	0.3343×10^{-2}	0.8381×10^{-3}	0.2097×10^{-3}	0.5245×10^{-4}
$\| u_h - u \|_{e,h}$	$\longrightarrow$	0.5434×10^{-1}	0.1969×10^{-1}	0.7042×10^{-2}	0.2503×10^{-2}	0.8870×10^{-3}

approach advocated in this paper, while the traditional approach yields only $O(h^{1.5})$ approximations in the same norm, as predicted in classical books.

References

[1] S. Brenner, R. Scott, *The Mathematical Theory of Finite Element Methods, Texts in Applied Mathematics 15*, Springer, 2008.

[2] V. Ruas, *Optimal simplex finite-element approximations of arbitrary order in curved domains circumventing the isoparametric technique.* arXiv **1701.00663** (2017)

Book of abstracts of the 7th International Conference
on Advanced Computational Methods
in Engineering, ACOMEN 2017
18–22 September 2017.

DRBEM Solution of MHD Flow in Pipes with Partly Insulated Partly Perfectly Conducting Slipping Walls

P. Senel[1] **and M. Tezer-Sezgin**[1]

[1] *Department of Mathematics, Middle East Technical University*

e-mails: psenel@metu.edu.tr, munt@metu.edu.tr

Abstract

In this study, the influence of the slipping and partly insulated, partly perfectly conducting walls on the fully developed, pressure driven MHD pipe flow is investigated numerically by using the DRBEM. The flow is subjected to a horizontally applied uniform magnetic field $\mathbf{B_0} = B_0\mathbf{e_x}$. The walls parallel to the magnetic field (side walls) are perfectly conducting and the vertical walls (Hartmann walls) are partly insulated, partly perfectly conducting that admit slip. It is shown that, the slip is effective as weakening the boundary layers as Hartmann number increases.

Key words: DRBEM, MHD pipe flow, slip velocity condition.

1 Mathematical Model

The coupled non-dimensional partial differential equations modeling the problem are [1]

$$\begin{aligned} \nabla^2 V + Ha\frac{\partial B}{\partial x} &= -1 \\ \nabla^2 B + Ha\frac{\partial V}{\partial x} &= 0 \end{aligned} \qquad -1 \le x, y \le 1 \tag{1}$$

with the boundary conditions

$$\begin{gathered} V = 0, \quad \frac{\partial B}{\partial y} = 0 \quad -1 \le x \le 1,\ y = \pm 1 \\ V \pm \alpha\frac{\partial V}{\partial x} = 0,\ B = 0 \text{ (insulated part)},\ \frac{\partial B}{\partial x} = 0 \text{ (perfectly conducting part)},\ x = \pm 1 \end{gathered} \tag{2}$$

where $V(x, y)$ and $B(x, y)$ are the velocity and the induced magnetic field in the pipe-axis direction, respectively. Ha is the Hartmann number and α is the dimensionless slip length.

2 DRBEM Application

The MHD flow problem (1)-(2) does not have an analytical solution due to its boundary conditions. Thus, the solution is obtained by using the DRBEM (dual reciprocity boundary element method) which is a numerical method providing both the solution and its normal derivative

necessary on the slip boundary. The MHD equations in (1) are transformed to boundary integral equations using the fundamental solution of the Laplace equation ($u^* = (1/2\pi)ln(1/r)$) [2]. All the terms other than Laplacian, are taken as inhomogeneity and approximated by the radial basis functions $f_j(r)$'s. The DRBEM discretized coupled system of differential equations are combined into a large system as

$$\bar{\mathbf{H}} \begin{Bmatrix} V \\ B \end{Bmatrix} = \bar{\mathbf{G}} \begin{Bmatrix} \frac{\partial V}{\partial n} \\ \frac{\partial B}{\partial n} \end{Bmatrix} + \bar{\mathbf{S}} \begin{Bmatrix} -1 \\ 0 \end{Bmatrix} \tag{3}$$

where

$$\bar{\mathbf{H}} = \begin{bmatrix} \mathbf{H} & \mathbf{o} \\ \mathbf{o} & \mathbf{H} \end{bmatrix} + Ha \begin{bmatrix} \mathbf{o} & \mathbf{M} \\ \mathbf{M} & \mathbf{o} \end{bmatrix}, \qquad \bar{\mathbf{G}} = \begin{bmatrix} \mathbf{G} & \mathbf{o} \\ \mathbf{o} & \mathbf{G} \end{bmatrix}, \qquad \bar{\mathbf{S}} = \begin{bmatrix} \mathbf{S} & \mathbf{o} \\ \mathbf{o} & \mathbf{o} \end{bmatrix}$$

$\mathbf{S} = (\mathbf{H}\hat{\mathbf{U}} - \mathbf{G}\hat{\mathbf{Q}})\mathbf{F}^{-1}$ and $\mathbf{M} = \mathbf{S}\frac{\partial \mathbf{F}}{\partial x}\mathbf{F}^{-1}$. $\bar{\mathbf{H}}$, $\bar{\mathbf{G}}$, $\bar{\mathbf{S}}$ are $2(N+L) \times 2(N+L)$ sized matrices and [2]

$$\mathbf{H}_{ij} = c_i\delta_{ij} + \int_{\Gamma_j} q^* d\Gamma_j, \quad \mathbf{H}_{ii} = c_i,$$

$$\mathbf{G}_{ij} = \int_{\Gamma_j} u^* d\Gamma_j, \quad \mathbf{G}_{ii} = \frac{l}{2\pi}(\ln(\frac{2}{l}) + 1)$$

$$\mathbf{F}_{ij} = f_j(r_i)$$

l is the length of the boundary element, $q^* = \partial u^*/\partial n$ and N and L are the numbers of boundary and interior nodes, respectively. $c_i = \theta/2\pi$ where θ is the internal angle at point i. The matrices $\hat{\mathbf{U}}$, $\hat{\mathbf{Q}}$ are constructed by taking the particular solutions $\hat{u}_j$'s ($\nabla^2\hat{u}_j = f_j$) and their normal derivatives as columns, respectively.
The system (3) is solved once without an iterative procedure which reduces the computational cost and provides the solution in one stroke.

3 Numerical Results

The obtained solution is validated with the one in [3] which is the case of all the walls are insulated. The numerical results show the significant effect of slip on the Hartmann walls when the slip ratio $s = \alpha Ha$ is greater than one as diminishing the Hartmann layers. The slip is more effective on the insulated portions of the vertical walls as Hartmann number increases.

References

[1] U. Muller, L. Buhler, *Magnetohydrodynamics in Channels and Containers*, Springer, 2001.

[2] P.W. Partridge, C.A. Brebbia, L.C. Wrobel, *The Dual Reciprocity Boundary Element Method*, Computational Mechanics Publications, 1992.

[3] S. Smolentsev, *MHD duct flows under hydrodynamic 'slip' condition*, Theoretical and Computational Fluid Dynamics **23** (2009) 557-570.

Book of abstracts of the 7th International Conference
on Advanced Computational Methods
in Engineering, ACOMEN 2017
18–22 September 2017.

Use of QGD-based parallel program complex for hypersonic flows simulation

Evgeny Shilnikov[1], **Alexander Davydov**[1] **and Tatiana Elizarova**[1]

[1] *Keldysh Institute of Applied Mathematics RAS, Moscow, Russia*

e-mails: shilnikov@imamod.ru, alexander.a.davydov@gmail.com, telizar@mail.ru

Abstract

This paper presents an experience in using a program complex Express-3D, based on quasi gas dynamic equation system. The method of difference scheme construction on non-orthogonal grids in 3D formulation basing on the finite volume method is described. The program complex showed a good efficiency and scalability in solving a set of problems including subsonic and supersonic flows. Here we present some new results of using this program complex for the problems of hypersonic flow/boundary layer interaction. The simulations results are discussed and compared with known experimental data.

Key words: explicit scheme, hybrid computer clusters, hypersonic flows, quasi gas dynamic equations, shock–boundary layer interaction.

Currently, there is a rapid progress in the growth of the computer performance. It is planned that the Exaflops performance will be overcome by 2024. It is expected that the increased capabilities of computer systems will make a strong support in solving problems of fundamental science, technology development etc. Mathematical modeling of hypersonic flows, based on the multi-disciplinary models, requires the detailed spatial and time resolution for the adequate description. This leads to the need of high-performance technology. A priori estimations show that, in the near future it will be necessary to use several petaflops performance in one simulation run. Unfortunately, at present, despite of the existence of systems with a performance of several petaflops, the number of tasks that use 100 TFlops and more simultaneously is small. This problem is fundamental and is related to the difficulties in algorithms and software adaptation to the systems architecture with extra massively parallelism. Note that the efforts of scientists and experts in many countries are directed to the solution of this problem. Modern HPC systems require software being created to take into account different types of processing units and a hybrid structure of memory. In this regard very promising are the explicit schemes, which can be easily adapted to the computer systems with different architectures.

This paper presents an experience in using a program complex Express-3D, oriented on heterogeneous GPU-based computer systems. Our program complex uses the explicit variant

of kinetically consistent finite difference schemes based on quasi gas dynamic (QGD) equation system [1], [2]. This system, proposed in Keldysh institute of applied mathematics RAS, is essentially based on the fundamental relationship between kinetic and gas dynamic continuum descriptions. QGD equation system differs from Navier-Stokes equations in specific additional dissipative terms. These terms serve as efficient numerical stabilizers. Note that the algorithm used here permits to simulate gas flows in a wide diapason of Mach numbers with minimum changes in program code. Our program complex was tested on a large number of problems including subsonic and supersonic flows. The efficiency of parallel implementation on different massively parallel computer systems was investigated. Good scalability is achieved up to a very large number of computational nodes. For example, weak scalability was more than 90% when 1024 GPUs were used in the calculations.

New version of program complex Express-3D uses multi block non orthogonal structured hexahedral grids. This permits to solve problems with complex geometry. Transition to non-orthogonal grids, in addition to complication of computing algorithms, demands storage of large volumes of additional information and ensuring access to it. This leads to a loss of efficiency when the GPUs of previous generation are used, such as Tesla C20xx with small number of registers on thread. However, upon transition to modern graphic processors with architecture of Kepler it is possible to achieve the acceptable acceleration.

The program complex was used for the numerical simulation of the problems connected with the hypersonic flows, in particular boundary layer/shock wave interaction. These problems are:

- hypersonic flow over edge compression corner under the different angles of attack ($M_\infty = 6.01, Re = 6 \times 10^5$);
- hypersonic flow in the ramjet air intake ($M_\infty = 4.9, Re = 1.9 \times 10^6$).

The comparison of calculations results (flow pictures, positions of the shock waves, separation and reattachment points, wall pressure distributions) with the results of other authors and the experimental data (see [3], [4]) was held and showed a good coincidence. The simulation results will be presented at the Conference.

Acknowledgements

This work has been partially supported by Russian Foundation for Basic Research (Grants No 15-01-03654-a, 15-01-03445-a and 16-07-00206-a).

References

[1] B.N. Chetverushkin, *Kinetic Schemes and Quasi-Gasdynamic System of Equations*, CIMNE, Barcelona, 2008.

[2] T.G. Elizarova, *Quasi-Gas Dynamic Equations*, Springer-Verlag, 2009.

[3] V. Zapryagaev1, I. Kavun, and I. Lipatov, *Supersonic laminar separated flow structure at a ramp for a free-stream Mach number of 6*, Progress in Flight Physics **5** (2013) 349–362.

[4] J. Wagner, K. Yuceil, A. Valdivia, N. Clemens and D. Dolling, *Experimental investigation of unstart in an inlet/isolator model in Mach 5 flow*, AIAA J. **47** (2009) 1528–1542.

Book of abstracts of the 7th International Conference
on Advanced Computational Methods
in Engineering, ACOMEN 2017
18–22 September 2017.

Acceptance Tail Method for Sampling from Univariate and Multivariate Distributions

Efraim Shmerling[1]

[1] *Department of Mathematics, Ariel University, Israel*

e-mails: efraimsh@ariel.ac.il

Abstract

A new efficient method named acceptance tail (AT) for generating univariate and multivariate continuous random variables with unbounded range and infinite-valued discrete random variables is introduced. Different versions of the AT method are presented. Validity of the AT method is proved. Theorems that enable one to estimate the efficiency of the method are formulated and the proof of the theorems given.

Key words: Random number generator, sampling method, multivariate distribution.

1 Introduction and Description of the AT Method

Acceptance tail (AT) method is a universal sampling method designed for generating random variables (rv's) of different types: univariate and multivariate, continuous and discrete, that satisfy certain weak conditions, which makes it applicable for vast majority of widely used distributions. Three versions of the AT method have been developed: continuous unimodal univariate (UNAT), multivariate continuous (MAT) and discrete (DAT). Implementation of these versions enables one to design random number generators (RNGs) for sampling from many specific distributions which are much more efficient than the RNGs which have been developed to date. Note that for Gaussian, exponential and some other distributions the performance of currently used generators can't be improved significantly in terms of speed. These generators implement the ziggurat method designed for rv's with monotonously decreasing and unimodal symmetric probability density functions (see [2]), grid method for multivariate rv's with bounded range and alias table method for finite-valued discrete rv's (see [1]). Unfortunately, these algorithms do not extend to other types of rv's. However, we have proved that algorithms implementing the AT method which extend to non-symmetric unimodal, infinite-valued discrete and multivariate continuous rv's with unbounded range are as fast as the algorithms implementing ziggurat, grid and alias table methods. These three fastest methods developed to date are based on the same idea: covering the density region (region below the graph of the probability density function) by a set of equi-length (equi-area, equi-volume) coverage units (CUs), such that generating a random point within any of them is very simple, selecting one of CUs utilizing a uniform integer RNG and generating a point in the selected CU. The AT method is based on the similar idea which is covering the bounded

main part ("head") of the density region H by a set of m CUs with common length (area, volume) 1/n, m less than or equal to n, and selecting randomly an integer in the range 1:n. If the selected integer i which is the index of one of the CUs is less than or equal to m, a random point P=(P1;P2) is generated within the chosen CU. If the generated point P belongs to H, P1 is âĂIJacceptedâĂİ as a generated value of the "target" rv X; otherwise, a point is generated randomly in the unbounded "tailâĂİ" T of the density region. If the covering set satisfies the requirement of the AT method (m/n is very close to one), with very high probability only one generation of a point within the chosen CU will be required for a generated value of X which makes the AT method extremely fast.

2 Concluding Remarks

1) The theorems on the existence of a required set of CUs in the case where the distribution satisfies certain conditions and the theorems enabling one to estimate the efficiency of the presented versions of the AT method are proved.

2) RNGâĂŹs implementing the presented versions of the AT method for some specific distributions have been developed and tested in experimental sampling.

3) Due to the advantages of the AT method which is fast, universal and simple, we predict that in the nearest future generators implementing the method will be incorporated as standard generators for many rv's in some of the most widely used platforms.

References

[1] L. Devroye, *Non-Uniform Random Value Generation*, Springer-Verlag,New York ,1986,Ch.9(3).

[2] G. Marsaglia, W.W Tsang, *The Ziggurat Method for Generating Random Variables*, J. Stat. Soft. **5 (8)** (2000) 1–7.

Book of abstracts of the 7th International Conference
on Advanced Computational Methods
in Engineering, ACOMEN 2017
18–22 September 2017.

p-adaptation strategies for a Flux Reconstruction based Compressible Navier Stokes solver

Vikram Singh[1] **and Steven Frankel**[1]

[1] *Department of Mechanical Engineering, Technion, Israel Institute of Technology*

e-mails: vikram@campus.technion.ac.il, frankel@technion.ac.il

Abstract

With high order methods increasingly becoming prominent, it has become necessary to employ adaptation strategies to reduce cost while maintaining accuracy. The flux reconstruction (FR) method is an arbitrary high order method for solving PDE's on unstructured meshes. In the present work we study various p-adaptation strategies in the FR method to solve the compressible Navier Stokes (CNS) equation in 2D and present the advantages and disadvantages of each.

Key words: flux reconstruction, compressible flow, p-adaptation, error indicator

1 Introduction

Over the past few years, research in unstructured high order methods for computational fluid dynamics has been gaining prominence. The discontinuous Galerkin (DG) and more recently, the flux reconstruction (FR) methods [1] can handle both unstructured meshes and arbitrary high order. Flows governed by the compressible Navier Stokes (CNS) equation, especially wall bounded flows, are in general characterized by high gradients. Low order methods generally dissipate away gradients including vortices that need to be advected for accurate flow physics. Therefore we need high order methods.

On the other hand, increasing order exponentially increases the degrees of freedom for the problem. Therefore a price has to be paid in terms of cost of computation. Adaptation methods such as h-adaptation, where the mesh is refined, and p-adaptation, where the order of the polynomial in the cell is increased, are therefore necessary to manage the trade-off between cost and accuracy. They allow us to control where in the domain we want to lower dissipation and thus increase accuracy. In the present work we study various strategies towards p adaptation to improve the cost of computations while preserving the high order of computations.

2 Numerical method

The compressible Navier Stokes (CNS) equation can be written in 2D as,

$$\frac{\partial \mathbf{u}}{\partial t} + \frac{\partial \mathbf{f}_i}{\partial x} + \frac{\partial \mathbf{g}_i}{\partial y} - \frac{\partial \mathbf{f}_v}{\partial x} - \frac{\partial \mathbf{g}_v}{\partial y} = 0 \tag{1}$$

where $\mathbf{u}, \mathbf{f}_i, \mathbf{f}_v$ are the conserved variable, the Euler flux and viscous flux vector respectively. In the flux reconstruction method, the domain is divided into mesh elements. Inside each element we have solution points for the solution vector and flux points at the boundary for calculating correction functions. In 1D, the solution and flux are represented as a polynomial inside each cell.

$$\begin{aligned} u^h &= \sum_{i=1}^{K} (u^h)^i l_i(x) \\ f^h &= \sum_{i=1}^{K} (f^h)^i l_i(x) \end{aligned} \tag{2}$$

where K is the order of the polynomial, h signifies that this is a discretized representation and l_i are the Lagrange polynomials. To account for the interaction between cells, a common solution is calculated at the flux points and the correction polynomial is constructed.

$$f^C = (f_L^I - f_L^D) g_L + (f_R^I - f_R^D) g_R \tag{3}$$

Here f^I, f^D, g_L, g_R are the interaction flux and discontinuous flux at the flux points and the correction polynomials. Interaction fluxes can be calculated by Riemann solvers for the inviscid term and DG schemes for the viscous term. This procedure is extended into multiple dimensions by performing a tensor product of the polynomials.

p-adaptation requires that different cells have different polynomial orders which means having different number of solution and flux points in each cell. In the present work, p-adaptation is implemented by calculating common values on the flux points of the cell having higher order and constructing the correction polynomial using these values. More important is the issue of error indicators. There are various ways of estimating errors such as feature-based, residual-based and adjoint based indicators [2]. Each of these error indicators come with their own trade-offs. In the present work, we present an algorithm for a dynamic p-adaptation based FR and compare results obtained from the various error indicators for different test cases in 2D.

Acknowledgements

This work has been partially supported by ISF-NSFC joint research program (ISF Grant No. 2232/15).

References

[1] H. T. Huynh, *A reconstruction approach to high-order schemes including discontinuous Galerkin for diffusion*, AIAA Paper 2009-403, 2009.

[2] Yi Li, S. Premasuthan, A. Jameson, *Comparison of h- and p- Adaptations for Spectral Difference Methods*, AIAA Paper 2010-4435, 2010.

Book of abstracts of the 7th International Conference on Advanced Computational Methods in Engineering, ACOMEN 2017
18–22 September 2017.

Moving rigid body with perfect contact with surrounding area: Direct and Inverse source problem

Marián Slodička[1] and Karel Van Bockstal[1]

[1] *Department of Mathematical Analysis, Ghent University, Krijgslaan 281, Ghent, Belgium*

e-mails: marian.slodicka@ugent.be, karel.vanbockstal@ugent.be

Abstract

We study a direct and an inverse source problem for a moving rigid body, which has a perfect contact with the neighbourhood.

Let Ω be a bounded fixed domain of $\mathbb{R}^n$, where $n \geq 1$, with Lipschitz boundary Γ. Suppose a moving rigid subdomain $\Omega_1(t)$ of Ω for all $t \in [0,T]$, which is traveling with a given velocity $v(x,t)$. We assume that

$$\bigcup_{t\in[0,T]} \overline{\Omega_1(t)} \subset \Omega,$$

which means that the traveling part $\Omega_1(t)$ allways stays at a safe distance from the boundary Γ. The rest of the domain Ω is denoted by $\Omega_2(t) := \Omega \setminus \Omega_1(t)$.

We study the following direct problem

$$\begin{array}{rcll} \partial_t u(x,t) - \nabla\cdot(K(x)\nabla u(x,t)) &=& f(x) & \text{in} \quad \Omega_1(t)\times(0,T] \\ -\nabla\cdot(K(x)\nabla u(x,t)) &=& f(x) & \text{in} \quad \Omega_2(t)\times(0,T] \\ u(x,t) &=& 0 & \text{in} \quad \Gamma\times(0,T] \\ u(x,0) &=& u_0(x) & \text{in} \quad \Omega. \end{array} \tag{1}$$

We assume the ideal contact on $\partial\Omega_1(t)$, which can be described by the following transmission conditions

$$[u(x,t)]_{\partial\Omega_1(t)} = 0, \qquad [K(x)\nabla u(x,t)\cdot\nu]_{\partial\Omega_1(t)} = 0, \tag{2}$$

where $[w]_{\partial\Omega_1(t)}$ denotes the jump of w across $\partial\Omega_1(t)$. These conditions represent continuity of the potential (temperature, etc.) and the flux across the interface $\partial\Omega_1(t)$.

The inverse source problem we consider is to reconstruct the source $f(x)$ in (1) from the additional final time measurement $u(x,T)$.

Book of abstracts of the 7th International Conference
on Advanced Computational Methods
in Engineering, ACOMEN 2017
18–22 September 2017.

MATSLISE, a Matlab package for solving Sturm-Liouville and Schrodinger equations

Marnix Van Daele[1]

[1] *Department of applied mathematics, computer science and statistics, Ghent University*

e-mails: marnix.vandaele@ugent.be

Abstract

Matslise [1] is a graphical Matlab software package for the interactive numerical study of Sturm-Liouville problems (SLPs), which can generally be written as

$$(p(x)\,y'(x))' + q(x)\,y(x) = E\,w(x)\,y(x) \quad x \in (a,b)$$

The package allows the fast and accurate computation of the eigenvalues E and the visualization of the corresponding eigenfunctions y. It is built upon high-order piecewise constant perturbation methods, also called the CP methods. Many researchers, in particular the ones from applied fields, prefer to use the user friendly problem solving environment Matslise over Fortran subroutines, like SLEDGE and SLEIGN2, although these latter packages can deal with a larger range of singular problems.

Recently, we developed the successor code Matslise 2.0 [2]. This new release is developed to work for a broad class of singular problems. This is realized by including the recent extension of the CP algorithm from problems in Liouville normal form to the general Sturm-Liouville form and by using specially adapted algorithms in a narrow interval around the singularity.

In the present talk, I will focuss on some important ideas that have lead to the success of the Matslise package, such as shooting, coefficient approximation, perturbative corrections, the Liouville transformation, the Prüfer transformation, ...and some new ideas that are included in the new release.

References:

[1] V. Ledoux and M. Van Daele, Matslise: a Matlab package for the numerical solution of Sturm-Liouville and Schrödinger equations, ACM. T. Math. Software 31 (2005) 612 – 619.

[2] V. Ledoux and M. Van Daele,MATSLISE 2.0 : a Matlab toolbox for Sturm-Liouville computations, ACM. T. Math. Software 42 (4), article 29 (2016)

Book of abstracts of the 7th International Conference on Advanced Computational Methods in Engineering, ACOMEN 2017
18–22 September 2017.

Optimal management of an urban road network with an environmental perspective

Miguel E. Vázquez-Méndez[1], Lino J. Alvarez-Vázquez[2], Nestor García-Chan[3] and Aurea Martínez[2]

[1] *Departamento de Matemática Aplicada, Universidade de Santiago de Compostela (Spain)*

[2] *Departamento de Matemática Aplicada II, Universidade de Vigo (Spain)*

[3] *Departamento de Física, Universidad de Guadalajara (Mexico)*

e-mails: miguelernesto.vazquez@usc.es, lino@dma.uvigo.es, nestor.gchan@academicos.udg.mx, aurea@dma.uvigo.es

Abstract

In this paper the management of an urban road network is formulated as an optimal control problem associated to a system of partial differential equations. The problem is analyzed from a mathematical viewpoint, and a complete numerical algorithm to solve it is proposed. Finally, some numerical results for a realistic situation in the Guadalajara Metropolitan Area (Mexico) are presented.

Key words: Air pollution, Optimal control, Partial differential equations, Traffic flow
MSC 2010: 49M25, 35Q93

1 Numerical simulation: the state system

We consider an urban domain $\Omega \subset \mathbb{R}^2$ where we want to simulate pollution levels due to vehicular traffic in the time interval $[0, T]$. We take, for example, carbon monoxide (CO) as air pollution indicator, and we propose to obtain the CO concentration $\Phi(x, t)$ by solving the following system of partial differential equations (see [1]):

$$\frac{\partial \rho_i}{\partial t} + \frac{\partial f_i(\rho_i)}{\partial s} = 0 \qquad \text{in } (a_i, b_i) \times (0, T), \tag{1a}$$

$$\rho_i(., 0) = \rho_i^0 \qquad \text{in } [a_i, b_i], \tag{1b}$$

$$\rho_s(a_s, .) = \rho_s^{in} \qquad \text{in } (0, T), \tag{1c}$$

$$\rho_t(b_t, .) = \rho_t^{out} \qquad \text{in } (0, T), \tag{1d}$$

$$\beta_{kl}^j f_{v_j(n_j+l)}(\rho_{v_j(n_j+l)}(a_{v_j(n_j+l)}, .)) = \alpha_{lk}^j f_{v_j(k)}(\rho_{v_j(k)}(b_{v_j(k)}, .)) \qquad \text{in } (0, T), \tag{1e}$$

$$\frac{\partial \phi}{\partial t} + \mathbf{v} \cdot \nabla \phi - \nabla \cdot (\mu \nabla \phi) + \kappa \phi = \sum_{i=1}^{N_R} \xi_{A_i} \qquad \text{in } \Omega \times (0, T), \tag{1f}$$

$$\phi(., 0) = \phi^0 \qquad \text{in } \Omega, \tag{1g}$$

$$\mu \frac{\partial \phi}{\partial n} - \phi\, \mathbf{v} \cdot \mathbf{n} = 0 \qquad \text{on } S^-, \tag{1h}$$

$$\mu \frac{\partial \phi}{\partial n} = 0 \qquad \text{on } S^+, \tag{1i}$$

where $\rho_i(x,t)$ is the density of cars in the road $A_i \subset \Omega$ represented by the 1D segment (a_i, b_i), f_i is a suitable known function giving the flux on that avenue, ρ_i^0 is the initial density, ρ_s^{in} and ρ_t^{out} are, respectively, boundary conditions for incoming and outgoing avenues, parameters $\alpha_{lk}^j \in [0,1]$ represent the preferences of drivers arriving to the junction j (α_{lk}^j gives the percentage of drivers that arriving at junction j from the avenue A_k are going to take the avenue A_l), parameters $\beta_{kl}^j \in [0,1]$ represent the ingoing capacity in outgoing avenues (β_{kl}^j gives the percentage of vehicles that coming at junction j from A_k can enter the outgoing avenue A_l), $\mathbf{v}(x,t)$ is the horizontal wind velocity, μ is the CO molecular diffusion coefficient, κ is a CO extinction rate, ϕ^0 is the initial CO concentration, and $\mathbf{n}$ denotes the unit outward normal vector to the boundary $\partial\Omega = S^- \cup S^+$, where $S^- = \{(x,t) \in \partial\Omega \times (0,T)$ such that $\mathbf{v}\cdot\mathbf{n} < 0\}$ represents the inflow boundary, and $S^+ = \{(x,t) \in \partial\Omega \times (0,T)$ such that $\mathbf{v}\cdot\mathbf{n} \geq 0\}$ represents the outflow boundary. Finally, N_R is the number of unidirectional roads in the network and ξ_{A_i} represents the source of pollution due to vehicular traffic on the avenue A_i. From a mathematical viewpoint, ξ_{A_i} is a Radon measure given, from a 2D parametrization of A_i, in terms of the car density ρ_i (see [1] for further details).

2 Optimal management of a network: the optimal control problem

The model (1) is very useful in order to study what consequences will have, in terms of atmospheric pollution, any action taken on vehicular traffic. This model is also very useful for designing operations on the road network, which are good (optimal), not only in terms of traffic flow, but also in terms of pollution levels. From a mathematical point of view, the search of these optimal operations (the optimal management of a network) consists of solving an optimal control problem where model (1) is the state system. This problem can be formulated as:

$$\min_{\mathbf{u}\in U_{ad}} \mathbf{J}(\rho_{\mathbf{u}}, \phi_{\mathbf{u}}), \tag{2}$$

where $\mathbf{u}$ (control variable) represents the parameters of the road network what can be managed, U_{ad} collects all the admissible operations, and $\mathbf{J}$ includes traffic and environmental objectives. $\mathbf{J}$ is a given function (possibly a vector function) of $(\rho_{\mathbf{u}}, \phi_{\mathbf{u}})$ solution of the state system (1) for the network defined by the control $\mathbf{u}$.

Acknowledgements

This work was supported by funding from project MTM2015-65570-P of Ministerio de Economía y Competitividad (Spain)/FEDER. The second author also thanks the support from Sistema Nacional de Investigadores SNI-52768 and Programa para el Desarrollo Profesional Docente PRODEP/103.5/16/8066 (Mexico).

References

[1] L.J Alvarez-Vázquez, N. García-Chan, A. Martínez, M.E. Vázquez-Méndez, *Numerical simulation of air pollution related to traffic flow in urban networks*, J. Comput. Appl. Math. (in press).

Book of abstracts of the 7th International Conference
on Advanced Computational Methods
in Engineering, ACOMEN 2017
18–22 September 2017.

A $1/t$ Algorithm with the Density of Two States for Estimating Multidimensional Integrals

Wanyok Atisattapong[1]

[1] *Department of Mathematics and Statistics, Thammasat University, Thailand*

e-mails: awanyok@tu.ac.th

Abstract

In this work we developed a $1/t$ algorithm [1, 2] for numerical integration in high dimensions. A large amount of computation time is wasted when a random walker is unable to reach a rare state at the sharp peak of an integrand, and becomes trapped after falling through that state. In this study, the density of states was divided into only two levels by sampling an arbitrary point in the range of the integrand, rather than into many levels using a fixed bin width (grid discretization on continuous space). The technique is quite straightforward and easy to implement. It avoids the need to determine the exact boundaries of the integrand, which is often a non-trivial task. Simulations show that our method [3] is able to significantly reduce the number of Monte Carlo trials required, and therefore the simulation time. The potential of the proposed method was demonstated by application to two multidimensional integrals: the Gaussian ring, adapted from the toy problem [4], and the setting sun Feynman diagram [5]. The results confirm that the proposed method can be applied to the calculation of multidimensional integrals without error saturation, yielding accurate values in applications where other numerical methods fail.

Key words: Gaussian integrals, Monte Carlo integration, Wang-Landau algorithm
MSC 2010: 65C05, 65D30

References

[1] R. E. Belardinelli and V. D. Pereyra, *Fast algorithm to calculate density of states*, Phys. Rev. E **75** (2007) 046701.

[2] R. E. Belardinelli and V. D. Pereyra, *Analysis of the convergence of the $1/t$ and Wang-Landau algorithms in the calculation of multidimensional integrals*, Phys. Rev. E **78** (2008) 067701.

[3] W. Atisattapong and P. Maruphanton, *Obviating the bin width effect of the $1/t$ algorithm for multidimensional numerical integration*, Appl. Numer. Math. **104** (2016) 133–140.

[4] B. C. Allanach and C. G. Lester, *Sampling using a bank of clues*, Comput. Phys. Commum. **179** (2008) 256–266.

[5] A. Tröster and C. Dellago, *Wang-Landau sampling with self-adaptive range*, Phys. Rev. E **71** (2005) 066705.

Book of abstracts of the 7th International Conference
on Advanced Computational Methods
in Engineering, ACOMEN 2017
18–22 September 2017.

Parallel iteration algorithms for 3T equations

Yunlong Yu[1] **and Yanzhong Yao**[2]

[1] *Institute of Applied Physics and Computational Mathematics,*

[2] *Laboratory of Computational Physics,*

e-mails: yu_yunlong@iapcm.ac.cn, yao_yanzhong@iapcm.ac.cn

Abstract

Aimed to the parallel computation of the three-temperature(3T) diffusion equations, we design two parallel iteration algorithms by using local and global interface prediction method. The numerical results show that the two algorithms obtain second order accuracy, unconditional stability and good scalability. Besides, the algorithm with global prediction is more efficient than the one with local prediction when calculating the 3T problems with strong nonlinearity.

Key words: Domain decomposition, Parallel iteration algorithm, Three-temperature equations.

1 Introduction

Three-temperature(3T) diffusion equations are commonly encountered in engineering, such as the inertial confinement fusion. When solving the 3T equations numerically, the parallel technique is always necessary because of the huge cost. In [1], the author construct a parallel iteration algorithm with the local interface prediction to solve nonlinear single-temperature diffusion equations on structured quadrilateral meshes. The algorithm is unconditionally stable, conservative, and obtains linear speed-up.

In this paper, we will design some new parallel algorithms for 3T problems by following the idea of [1]. At first, we extend the algorithm in [1] to 3T equations on the unstructured meshes. Then, we design a new parallel algorithm by using the global prediction and extrapolation estimation for the nonlinear coefficients. At last, we perform some numerical experiments to test the two algorithms.

2 The parallel iteration schemes

For 3T equations, we use the implicit nine point scheme and the Picard iteration. Take the electronic equation for example, the scheme is

$$\rho_K^{n+1}(c_{ve})_K^s \frac{u_K^{e,s+1} - u_K^{e,n}}{\tau} S_K + \sum_{\sigma_j \in \varepsilon_K} F_{K,\sigma_j}^{e,s+1} |\sigma_j| = f_K^{e,s+1} S_K, \tag{1}$$

where

$$F_{K,\sigma_j}^{e,s+1} = -\kappa_{\sigma_j}^{s}\left[\frac{u_L^{e,s+1}-u_K^{e,s+1}}{d_{L,\sigma_j}+d_{K,\sigma_j}} - D_{\sigma_j}\left(\frac{u_{\alpha_{j+1}}^{e,s}-u_{\alpha_j}^{e,s}}{|\sigma_j|}\right)\right]. \tag{2}$$

The computational domain is divided into many subdomains. In order to solve the above discrete equations in parallel, the prediction value $\tilde{u}_L^{e,s+1}$ is needed if cell L is located in neighboring subdomain. When $s > 0$, we take $\tilde{u}_L^{e,s+1} = u_L^{e,s}$; When $s = 0$, we use the following two methods to predict the value $\tilde{u}_L^{e,1}$.
(1) $\tilde{u}_L^{e,1} = \tilde{u}_L^{e,n}$., $Algorithm1$.
(2) All the unknowns at the first iteration step are predicted by Jacobi scheme. The nonlinear coefficients, such as $C_{ve}(u)$, are calculated by using the extrapolated value $2u^n - u^{n-1}$, i.e., $\tilde{C_{ve}}(u^{n+1}) = C_{ve}(2u^n - u^{n-1})$. $Algorithm2$.

3 Numerical results

We calculate a nonlinear 3T model[2] by the two parallel algorithms. There are two materials SiO_2 and CH in this model, and a strong source is put on the outer boundary.

Tab.1 show the parallel efficiencies and the average nonlinear iteration numbers $it^\sharp$. We can see that both algorithms have good parallel scalability, but the algorithm 2 has a better performance than algorithm 1.

Table 1: The parallel efficiencies and the average numbers of the nonlinear iterations

CPU	4	8	16	32
		Algorithm 1		
time(s)	2824.6	1422.9	700.6	336.9
efficiency	1	99.2%	100.7%	104.8%
$it^\sharp$	38.1	38.5	38.1	36.1
		Algorithm 2		
time(s)	1962.7	976.2	482.3	227.7
efficiency	1	100.5%	101.7%	107.7%
$it^\sharp$	26.7	26.7	26.5	24.9

References

[1] G.W. Yuan, Y.Z. Yao, L. Yin, *A conservative domain decomposition procedure for nonlinear diffusion problems on arbitrary quadrilateral grids*, SIAM J. Sci. Comput. **33** (2011) 1352-1368.

[2] Z.Y. Mo, L.J. Shen, W. Gabriel, *Parallel adaptive multigrid algorithm for 2-D 3-T diffusion equations*, Intern. J. Comput. Math. **81** (2004) 361-374.

Poster Session

Book of abstracts of the 7th International Conference on Advanced Computational Methods in Engineering, ACOMEN 2017 18–22 September 2017.

The Numerical Simulation of a Microscale Model for Li-Ion Batteries

Fabian Castelli[1] **and Willy Dörfler**[1]

[1] *Institute of Applied and Numerical Mathematics, Karlsruhe Institute of Technology (KIT)*

e-mails: fabian.castelli@kit.edu, willy.doerfler@kit.edu

Abstract

We consider the thermodynamic consistent microscale model from [4] for modeling the Lithium and charge transport during the discharge of a Li-ion battery. By assuming a constant temperature we neglect thermal dependencies. The work [3] gives references to experimental evidences, which shows that the intercalation process of Li-ions in the active particles of the cathode (e. g. $LiCoO_2$) should be described in a more complex manner than with the Fickian diffusion law. In papers like [6] one uses for the intercalation a two-phase diffusion model, which reduces mathematically to a Stefan-problem in the active particles.

The elliptic-parabolic system of partial differential equations with a strong nonlinear (exponential) coupling at the electrode-electrolyte-interface, which describes the transport in the microscale model, can be extended by a two-phase diffusion model for the active particles. For the numerical approximation one can reformulate the extended equations in an enthalpy-formulation. A Finite-Element approach for solving these transport equations was developed in [2]. For the time discretization there was used a theta-Euler-scheme and additionally a semi-implicit scheme proposed in [5]. Hereby the full system was decomposed in an elliptic and a parabolic subproblem and solved successively.

The main point of the algorithm is to compensate the missing regularity of the enthalpy function by a regularization to still solve the nonlinear system with Newton's method.

Due to the reformulation with the enthalpy one has the advantage that the change of the diffusion model is simulated without any additional information. Furthermore through the enthalpy-formulation the resulting algorithm is fully independent of the geometry and the space dimension.

The numerical scheme for solving that problem was implemented with the open source Finite-Element library deal.II [1] and validated for some one and two dimensional problems with a one-phase diffusion model.

Key words: Li-ion battery, modeling, numerical simulation

References

[1] W. Bangerth, R. Hartmann, G. Kanschat, *deal.II—A General Purpose Object Oriented Finite Element Library*, ACM Transactions on Mathematical Software (TOMS) **33**(4) (2007) 24/1–24/27.

[2] F. Castelli, *Die Numerische Simulation eines Mikroskalenmodells für Li-Ionen-Batterien*, Master thesis, Karlsruher Institut für Technologie (KIT), Karlsruhe, 2016.

[3] M. Kespe, *Numerische Untersuchungen zur Interkalation bei Lithium-Ionen Batterien*, Diplomarbeit, Karlsruher Institut für Technologie (KIT), Karlsruhe, 2012.

[4] A. Latz, J. Zausch, *Thermodynamic consistent transport theory of Li-ion batteries*, Journal of Power Sources **196**(6) (2011) 3296–3302.

[5] M. Maier, *The Mathematical Analysis of a Micro Scale Model for Lithium-Ion Batteries*, PhD thesis, Karlsruher Institut für Technologie (KIT), Karlsruhe, 2016.

[6] Q. Zhang, R. E. White, *Moving Boundary Model for the Discharge of a $LiCoO_2$ Electrode*, Journal of the Electrochemical Society **154**(6) (2007) A587–A596.

Book of abstracts of the 7th International Conference
on Advanced Computational Methods
in Engineering, ACOMEN 2017
18–22 September 2017.

Autocatalytic Reaction as a Building Block for Describing the Typical Dependencies of Chemical Kinetics

Zoë Gromotka[1], Denis Constales[1] and Gregory Yablonsky[2]

[1] *Department of Mathematical Analysis, Ghent University*

[2] *Parks College of Engineering, Aviation and Technology, Saint Louis University*

e-mails: zoe.gromotka@ugent.be, denis.constales@ugent.be, gyablons@slu.edu

Abstract

Mathematically the chemical kinetics of a reversible reaction is shown to be equivalent to the chemical kinetics of several autocatalytic reactions, happening in parallel. This is specifically interesting for first order reversible reactions, as one can now incorporate the properties of first order kinetics with the ideas of collision theory. As such these autocatalytic reactions can be viewed as a simple alternative to the Lindemann mechanism. As for higher order reversible reactions, the approach of multiple autocatalytic reactions simplifies mathematical descriptions of the chemical kinetics to a product of two polynomials with at least one polynomial being linear. To conclude, by using autocatalytic reactions as building blocks for chemical kinetics there can be a better mathematical as well as physical understanding of reversible chemical reactions and by extension irreversible reactions.

Key words: autocatalytic reaction, chemical kinetics, reversible reaction

References

[1] G.S. Yablonsky, D. Constales, G.B. Marin, *Equilibrium relationships for non-equilibrium chemical dependencies*, Chem. Eng. Sci. **66** (2011) 111–114.

[2] D. Constales, G.S. Yablonsky, G.B. Marin, *Thermodynamic time invariances for dual kinetic experiments: nonlinear single reactions and more*, Chem. Eng. Sci. **73** (2012) 20–29.

Book of abstracts of the 7th International Conference
on Advanced Computational Methods
in Engineering, ACOMEN 2017
18–22 September 2017.

POD based reduced order modelling of a non-linear eddy current problem

MD Rokibul Hasan[1] **and Ruth V. Sabariego**[1]

[1] *Department of Electrical Engineering, KU Leuven, Belgium*

e-mails: rokib.hasan@kuleuven.be, ruth.sabariego@kuleuven.be

Abstract

In this paper reduced order model of a non-linear model is developed by proper orthogonal decomposition method. The reduced model is compared with the reference model when applied to an eddy current problem. A classical magnetodynamic finite element formulation is used as reference and as starting point of the reduced models.

Key words: Eddy currents, Non-linear, Proper orthogonal decomposition, Reduced order modelling

1 Introduction

The accurate modelling of electromagnetic devices taking eddy current effects, movement, non-linearities,... into account are a major concern from the early design stage. The finite element method is widely used and versatile for modelling these phenomena. However, it maybe extremely cumbersome and expensive in terms of computational time and memory in case of 3D geometries, high working frequency, non-linearities (possibly hysteresis), a long transient behaviour. Reduced Order (RO) techniques are a feasible and efficient alternative, which are gaining interest in electromagnetic field problem to approximate the full system accurately in a reduced manner. RO techniques implementation on the linear and non-parametric dynamic systems have already been reached at a mature level [1]. However, a few works have addressed the RO modelling of non-linear problem taking into account the eddy currents. The major challenge of RO modelling of a non-linear problem lies on the large computational time requirement due to the regular update of the non-linear term in the iterative loop and full system matrix multiplication at each parametric values. The model order reduction of a non-linear magnetostatic problem is proposed in [2], where the discrete empirical interpolation (DEI) method is used combined with the proper orthogonal decomposition (POD) method to interpolate the non-linear terms of the full system in order to speed up the computational process. In this paper, we propose POD based RO technique to accurately model a non-linear eddy current problem. To achieve furthermore computational efficiency, we aim at implementing the DEI method along with the POD.

2 Model order reduction and Results

As a test case we consider the single-phase power transformer. Let us consider a bounded domain $\Omega = \Omega_c \cup \Omega_c^C \in \mathbb{R}^3$ with boundary Γ. The conducting and non-conducting parts of Ω are denoted by Ω_c and Ω_c^C, respectively. The (modified) magnetic-vector-potential ($a-$) magneto-dynamic formulation (weak form of Ampère's law) reads: find a, such that

$$(\sigma \partial_t a, a')_{\Omega_c} + (\nu \operatorname{curl} a, \operatorname{curl} a')_{\Omega} + \langle \hat{n} \times h, a' \rangle_{\Gamma} = (j_s, a')_{\Omega_s}\,, \ \forall a' \tag{1}$$

with a' test functions in a suitable function space; $b = \operatorname{curl} a$ the magnetic flux density; j_s a prescribed current density and $\hat{n}$ the outward unit normal vector on Γ. The derivative with respect to time is denoted by ∂_t. The ferromagnetic non-linear isotropic material with reluctivity ν (magnetic field $h = \nu b$) and conductivity σ is considered. The discretization of the weak form of (1) leads to the following matrix system:

$$A\partial_t x(t) + B[x(t)]x(t) = C(t)\,. \tag{2}$$

The POD method reduces the order of the system (2) from $x \in \mathbb{R}^{N\times 1}$ to $x_r \in \mathbb{R}^{M\times 1} (M \ll N)$ by means of a projector operator Ψ. The POD generates Ψ with a snapshot technique [3]. In Fig. 1, the joule loss of the transformer core and relative error results for ROM with two basis M = 29 and M = 39 are shown. We observe that only M = 29 number of basis can approximate the full system (4816 number of unknowns) very accurately. Details on the test model, the RO theory and the more efficient RO modelling will be provided in the full paper.

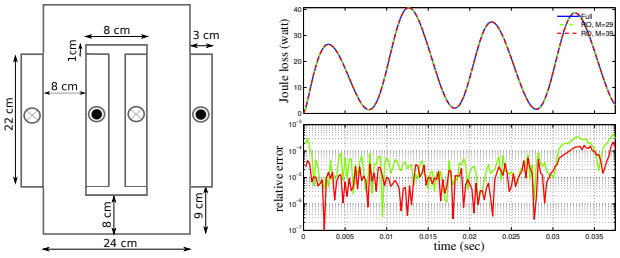

(a) (b)

Figure 1: (a) geometry of a single phase transformer, (b) Joule loss (up) and relative error (down) between full and RO models

3 Acknowledgements

Work supported by the Belgian Science Policy (IAP P7/02).

References

[1] BENNER, P., GUGERCIN, S.; *A Survey of Projection-Based Model Reduction Methods for Parametric Dynamical Systems*, SIAM J. S CI. COMPUT., (2011).

[2] HENNERON, T., STEPHANE C.; *Model order reduction of non-linear magnetostatic problems based on POD and DEI methods*, IEEE Trans. on Mag., (2014).

[3] HASAN, R., MONTIER, L., HENNERON, T., SABARIEGO, R.; *POD-based reduced-order model of an eddy current levitation problem*, Springer Journal, (2017).

Book of abstracts of the 7th International Conference
on Advanced Computational Methods
in Engineering, ACOMEN 2017
18–22 September 2017.

Operator splitting Fourier spectral methods for the Swift–Hohenberg equation

Hyun Geun Lee[1]

[1] *Department of Mathematics, Kwangwoon University*

e-mails: leeh1@kw.ac.kr

Abstract

The Swift–Hohenberg (SH) equation has been widely used as a model for the study of pattern formation. The SH equation is a fourth-order nonlinear partial differential equation and cannot generally be solved analytically. Therefore, computer simulations play an essential role in understanding of nonequilibrium processing. The aim of this research is to present accurate and efficient approaches for solving the SH equation. The methods are based on the operator splitting method and are to split the SH equation into linear and nonlinear subequations. The linear and nonlinear subequations have closed-form solutions in the Fourier and physical spaces, respectively. The methods are simple to implement and computationally cheap to achieve high-order time accuracy. Numerical experiments are presented demonstrating the accuracy and efficiency of proposed methods.

Key words: First- and second-order convergence, Fourier spectral method, Operator splitting method, Swift–Hohenberg equation

Acknowledgements

This research was supported by Basic Science Research Program through the National Research Foundation of Korea (NRF) funded by the Ministry of Education (2016R1A6A3A11935668, 2017R1D1A1B03034619).

References

[1] J. Swift, P.C. Hohenberg, *Hydrodynamic fluctuations at the convective instability*, Phys. Rev. A **15** (1977) 319–328.

[2] G. Strang, *On the construction and comparison of difference schemes*, SIAM J. Numer. Anal. **5** (1968) 506–517.

[3] D. Goldman, T.J. Kaper, *Nth-order operator splitting schemes and nonreversible systems*, SIAM J. Numer. Anal. **33** (1996) 349–367.

Book of abstracts of the 7th International Conference on Advanced Computational Methods in Engineering, ACOMEN 2017 18–22 September 2017.

Towards Accelerated Optimal Control with Black-Box System Simulators using an Adaptive Surrogate Model Refinement Trust Region Management Framework

Tom Lefebvre[1], Frederik De Belie[1] and Guillaume Crevecoeur[1]

[1] *Department of Electrical Energy, Metals, Mechanical Constructions & Systems, Ghent University*

e-mails: tom.lefebvre@ugent.be, frederik.debelie@ugent.be, guillaume.crevecoeur@ugent.be

Abstract

This abstract presents a framework for accelerated solution of discrete time optimal control problems considering the presence of a computationally expensive black-box system simulator. The conventional solution methodology is concisely reviewed and an adapative surrogate model refinement trust region framework is conceptualized. A trust region update rule is proposed, based on assessing the capability of the local surrogate models to correctly predict descent of the local Lagrangian cost contribution of the highly constrained optimization problem.

Key words: black-box simulators, direct multiple shooting, optimal control, surrogate models, trust region framework

1 Introduction

We consider problems of the form (1), which defines a generic discrete time optimal control problem. The optimization variable s consists of $N+1$ discrete time state values, $s = (s_0^{\mathrm{t}} \cdots s_N^{\mathrm{t}})^{\mathrm{t}}$, and q of N corresponding control parametrizations, $q = (q_0^{\mathrm{t}} \cdots q_{N-1}^{\mathrm{t}})^{\mathrm{t}}$. The functions $c^+ : \mathbb{R}^{n_x} \times \mathbb{R}^{n_u} \to \mathbb{R}$ and $x^+ : \mathbb{R}^{n_x} \times \mathbb{R}^{n_u} \to \mathbb{R}^{n_x}$ correspond the cost contribution and final state value associated to each piecewise trajectory respectively, function $c : \mathbb{R}^{n_x} \to \mathbb{R}$ accounts for a final cost contribution associated to the end state. In this context, we assume that the functions c^+ and x^+ are jointly evaluated by addressing a function $p^+ : \mathbb{R}^{n_x} \times \mathbb{R}^{n_u} \to \mathbb{R}^{n_x+1}, p^+(s_i, q_i) = (x^+(s_i, q_i)^{\mathrm{t}}\ c^+(s_i, q_i))^{\mathrm{t}}$, which evaluation coincides with calling a (computationally expensive) black-box simulator. Hence, it is further assumed that we do not dispose over (direct) gradient information, $\partial p^+ / \partial s_i$ nor $\partial p^+ / \partial q_i$.

$$\min_{s,q} \sum_{i=0}^{N-1} c^+(s_i, q_i) + c(s_N), \text{ subject to } \begin{cases} x_0 - s_0 = 0 \\ s_{i+1} - x^+(s_i, q_i) = 0, \ \forall i \in \{0, \ldots, N-1\} \end{cases} \tag{1}$$

Under these circumstances, conventional solution would result in excessive evaluation of the simulator p^+ and corresponding time consumption. We propose to facilitate acceleration of the overall solution speed by ruling out direct communication between the solver and the system simulator, p^+. That by introducing N data-based surrogate models which adaptive refinement is managed by a trust region surrogate model management framework [1].

2 Sequential Quadratic Programming in Optimal Control

Generally, such problems are solved by performing a Sequential Quadratic Programming (SQP) minimization of the Lagrangian cost function, $\Phi(v) : \mathbb{R}^{n_s+n_q+n_s} \rightarrow \mathbb{R}$, with $v = (s^{\mathrm{t}}\, q^{\mathrm{t}}\, \lambda^{\mathrm{t}})^{\mathrm{t}}$ and λ^{t} the Lagrangian multipliers [2]. The SQP method then generates a series $\{v^j\}_{j=0}^{n}$ which converges to a solution v^* of the first-order Karush-Kuhn-Tucker conditions: $\partial\Phi/\partial v = 0$.

$$\Phi\left(v^j\right) = f\left(s^j, q^j\right) + \lambda^{j,\mathrm{t}} \cdot g\left(s^j, q^j\right) = \sum_{i=0}^{N-1} \Phi_i\left(v^j\right) + c\left(s_N^j\right) + \lambda_0^{j,\mathrm{t}} \cdot \left(x_0^j - s_0^j\right) \tag{2}$$

Here, we defined the local Lagrangian cost contribution, $\Phi_i(v^j)$, which is completely dependent on a single call of $p^+(w_i^j)$ at the local joint optimization variable $w_i^{j,\mathrm{t}} = (s_i^{j,\mathrm{t}}\, q_i^{j,\mathrm{t}})^{\mathrm{t}}$:

$$\Phi_i\left(v^j\right) = c^+\left(s_i^j, q_i^j\right) + \lambda_{i+1}^{j,\mathrm{t}} \cdot \left(s_{i+1}^j - x^+\left(s_i^j, q_i^j\right)\right) \tag{3}$$

3 A Concept Trust Region Framework

We propose to replace the global and computationally expensive black-box simulator p^+ during the SQP iterations by N local iterate dependent data-based surrogate models $\tilde{p}_i^{+,j}$. We assume these local models to generate quality predictions within the corresponding Euclidean balls $B(w_i^j; \Delta_i^j) = \{w_t \in \mathbb{R}^{n_x+n_u} : \|w_t - w_i^j\| \leq \Delta_i^j\}$. The SQP series is propagated using these local models (for which direct gradient information is readily available) until the iterates lie no longer within the balls $B(w_i^j; \Delta_i^j)$, from where the local models and corresponding trust radii should be updated. The prediction quality after k successful iterations is assessed by accuracy metric r_i^j, which is understood as the capability of model $\tilde{p}_i^{+,j}$ (corresponding approximate Lagrangian contribution, $\tilde{\Phi}_i$) to correctly predict descent of the actual contribution, Φ_i.

$$r_i^j = \frac{\Phi_i\left(s_i^j, q_i^j, s_{i+1}^j, \lambda_{i+1}^j\right) - \Phi_i\left(s_i^{j+k}, q_i^{j+k}, s_{i+1}^{j+k}, \lambda_{i+1}^{j+k}\right)}{\Phi_i\left(s_i^j, q_i^j, s_{i+1}^j, \lambda_{i+1}^j\right) - \tilde{\Phi}_i\left(s_i^{j+k}, q_i^{j+k}, s_{i+1}^{j+k}, \lambda_{i+1}^{j+k}\right)} \tag{4}$$

The trust region radii, Δ_i^j, are updated according to a conventional update rule [3] and new local models $\tilde{p}_i^{+,j+k}$ are built within the neighbourhoods $B(w_i^{j+1}; \Delta_i^{j+k})$. This procedure is then repeated until convergence of the governing SQP series is achieved.

Acknowledgements

This work has been supported by the Strategic basic research project EMODO of the Flanders Make Strategic Research Centre and the FWO Research project G.0D93.16N.

References

[1] N. Alexandrov, J. Dennis, R. Lewis, V. Torzcon, *A Trust Region Framework for managing the use of Approximation Models in Optimization*, Structural and Multidisciplinary Optimization. 15(1) (1998) 16–23

[2] B. Chauchat, *Nonlinear and Dynamic Optimization: from theory to practice*, 2007.

[3] A. Conn, K. Scheinberg, L. Vicente, *Global Convergence of General Derivative-Free Trust Region Algorithms to First- and Second-Order Critical Points*, SIAM Journal on Optimization. 20(1) (2009) 387–415

Book of abstracts of the 7th International Conference
on Advanced Computational Methods
in Engineering, ACOMEN 2017
18–22 September 2017.

A new Steffensen-Homeier iterative method for solving nonlinear equations

Laurian Ioan Pişcoran[1] **and Dan Miclăuş**[1]

[1] *Department of Mathematics and Computer Science, Technical University of Cluj-Napoca, North University Center at Baia Mare*

e-mails: plaurian@yahoo.com, dan.miclaus@cunbm.utcluj.ro

Abstract

In this paper we present a new family of efficient iterative methods, in order to approximate the simple roots of various nonlinear equations. By some numerical examples we test the accuracy of our methods making a comparative study with other well known iterative methods.

Key words: Iterative methods, Nonlinear equation, Order of convergence.
MSC 2010: 49M15.

1 Introduction

One of the most important problem in all the history of mathematics was to solve the nonlinear equation $f(x) = 0$. We can not always find an exact solution to this equation, but we can obtain some approximative solutions using iterative methods. Newton's method is the best known iterative method for solving nonlinear equations, given by

$$x_{n+1} = x_n - \frac{f(x_n)}{f'(x_n)}, \quad n = 0, 1, 2, \cdots \tag{1}$$

which converges quadratically. In order to improve the order of convergence many researchers introduced and studied some modifications of Newton's iterative method, based especially on the expense of additional evaluations of the functions, derivatives and changes in the point of iterations. A modification in this sense was done by Homeier [1], which studied the following iterative method

$$x_{n+1} = x_n - \frac{f(x_n)}{f'\left(x_n - \frac{f(x_n)}{2f'(x_n)}\right)}, \tag{2}$$

with cubic convergence. This method is suitable if the computation of the derivative has a similar or lower cost than that of the function itself. Although Newton iterative method is the most used in solving nonlinear equations, there exists a disadvantage concerning the application, because it depends upon derivatives which are sometimes restricted in engineering. This disadvantage which appears in application of Newton iterative method was eliminated

by Steffensen [2]. He replaced the derivative $f'(x_n)$ form the relation (1) by forward-difference approximation

$$f'(x_n) \approx \frac{f(x_n + f(x_n)) - f(x_n)}{f(x_n)} \tag{3}$$

and got the famous Steffensen's iterative method

$$x_{n+1} = x_n - \frac{f^2(x_n)}{f(x_n + f(x_n)) - f(x_n)}, \tag{4}$$

free from any derivative of the function. Steffensen iterative method (4) is also quadratically and require two functional evaluations per iteration, but in contrast with Newton method (1) is free from any derivative of the function. Following the idea of Steffensen, in many research articles have been developed and studied new derivative-free iterative methods, with the aim to improve the order of convergence.

The main focus of our paper is to present a new family of iterative methods depending on a real parameter, constructed as a linear combination of Steffensen, respectively Homeier method. These methods require two functional evaluations per iteration. We will prove that each family member converges quadratically. In the last part, by some numerical examples we put in evidence the performance of our methods, making a comparative study with other methods of the same order.

Acknowledgements

The results presented in this paper were obtained with the support of the Technical University of Cluj-Napoca through the research Contract no. 2011/12.07.2017, Internal Competition CICDI-2017.

References

[1] H.H.H. Homeier, *A modified Newton method for root finding with cubic convergence*, J. Comput. Appl. Math. **157** (2003) 227–230.

[2] J.F. Steffensen, *Remarks on iteration*, Skand. Aktuarietidskrift **16** (1933) 64–72.

Book of abstracts of the 7th International Conference
on Advanced Computational Methods
in Engineering, ACOMEN 2017
18–22 September 2017.

A Sigmoidal Type Weight Function for Fourier Series Approximation to Discontinuous Functions

Beong In Yun[1]

[1] *Department of Mathematics, Kunsan National University, Rep. Korea*

e-mails: paulllyun@gmail.com

Abstract

We introduce a sigmoidal type non-linear function $w_m(r;x)$ on a given interval $[a,b]$ with a threshold at $x = r \in (a,b)$. Using the proposed function w_m, we develop a weighted averaging method to improve Fourier partial sum approximation for a function having a jump-discontinuity. The method is based on the decomposition of the target function into the left-hand and the right-hand part extensions. The resultant approximate function is composed of the Fourier partial sums of each part extension. The uniform convergence of the presented method is proved and the efficiency of the method is shown by some numerical example.

List of participants

Name	Country	e-mail
Adi-Kusumo Fajar	Indonesia	f_adikusumo@ugm.ac.id
Ait-Ali Takfarines	Algeria	takfarine.aitali@gmail.com
Ambroz Martin	Slovakia	ambroz.martin.ml@gmail.com
Andriulli F. P.	France	francesco.p.andriulli@gmail.com
Anlamlert Wanwarat	Thailand	wanwarat@tu.ac.th
Arrarás Andréas	Spain	andres.arraras@unavarra.es
Atisattapong Wanyok	Thailand	wanyok@mathstat.sci.tu.ac.th
Bériot Hadrien	Belgium	hadrien.beriot@siemens.com
Badri M. A.	France	mohd-afeef.badri@univ-nantes.fr
Bause Markus	Germany	bause@hsu-hh.de
Becker-Steinberger Katharina	Germany	katharina.becker-steinberger@dlr.de
Boscarino Sebastiano	Italy	boscarino@dmi.unict.it
Both Jakub W.	Norway	jakub.both@uib.no
Brenner Susanne C.	USA	brenner@math.lsu.edu
Brzeźniak Zdzisław	United Kingdom	zdzislaw.brzezniak@york.ac.uk
Burger Martin	Germany	martin.burger@wwu.de
Califano Giovanna	Italy	gcalifano@unisa.it
Carraro Thomas	Germany	thomas.carraro@iwr.uni-heidelberg.de
Casati Daniele	Switzerland	daniele.casati@sam.math.ethz.ch
Castelli Fabian	Germany	fabian.castelli@kit.edu
Chaillat Stéphanie	France	stephanie.chaillat@ensta-paristech.fr
Chaudhry Qasim Ali	Pakistan	chqasim@uet.edu.pk
Chovan Jaroslav	Belgium	jaroslav.chovan@ugent.be
Cimrák Ivan	Slovakia	ivan.cimrak@fri.uniza.sk
Constales Denis	Belgium	Denis.Constales@UGent.be
Cools Kristof	United Kingdom	kristof.cools@nottingham.ac.uk
Creusé Emmanuel	Belgium	emmanuel.creuse@math.univ-lille1.fr
Crevecoeur Guillaume	Belgium	guillaume.crevecoeur@ugent.be
Dörfler Willy	Germany	willy.doerfler@kit.edu
Darbas Marion	France	marion.darbas@u-picardie.fr
De Gersem Herbert	Germany	degersem@temf.tu-darmstadt.de
De Staelen Rob	Belgium	rob.destaelen@ugent.be
Devolder Brecht	Belgium	brecht.devolder@ugent.be
Diallo Malal	France	mohamadou-malal.diallo@utc.fr
El Badia Abdellatif	France	abdellatif.elbadia@utc.fr
Elliot Charles	United Kingdom	c.m.elliott@warwick.ac.uk
Evcin Cansu	Belgium	cbilgir@metu.edu.tr
Farzam Far Mehrnaz	Finland	mehrnaz.farzam.far@aalto.fi
Feierabend Lukas	Belgium	l.feierabend@zbt-duisburg.de
Fiorina Carlo	Switzerland	carlo.fiorina@epfl.ch
Francisco Fernández	Spain	fjavier.fernandez@cud.uvigo.es
Frolkovič Peter	Slovakia	peter.frolkovic@gmail.com
Galba Michal	Belgium	michal.galba@ugent.be

Gaspar Francisco	Netherlands	F.J.Gaspar@cwi.nl
Geuzaine Christophe	Belgium	cgeuzaine@ulg.ac.be
Gossye Michiel	Belgium	michiel.gossye@ugent.be
Grimmonprez Marijke	Belgium	marijke.grimmonprez@ugent.be
Gromotka Zoë	Belgium	zoe.gromotka@ugent.be
Guidetti Davide	Italy	davide.guidetti@unibo.it
Hahn Jooyoung	Austria	JooyoungHahn@gmail.com
Hamada Rinako	Japan	ri.bado.1227.choco@gmail.com
Hang Xudeng	China	hang_xudeng@iapcm.ac.cn
Hasan Rokibul	Belgium	rokib.hasan@kuleuven.be
Henneron Thomas	Belgium	thomas.henneron@univ-lille1.fr
Hiptmair Ralf	Switzerland	hiptmair@sam.math.ethz.ch
Hocine Safia	Algeria	hsafia4@gmail.com
Hofmann Tobias	Germany	tobias.hofmann@itwm.fhg.de
Hokpunna Arpiruk	Thailand	arpiruk.hok@eng.cmu.ac.th
Icardi Matteo	United Kingdom	m.icardi@warwick.ac.uk
Inoue Kazuya	Japan	mornel@kobe-u.ac.jp
Issa Mohammad	France	issa@laplace.univ-tlse.fr
Jain Shobhit	Switzerland	shjain@ethz.ch
Jančigová Iveta	Slovakia	iveta.jancigova@fri.uniza.sk
Jantarakhajorn Khajee	Thailand	jantarakhajorn@gmail.com
Jaust Alexander	Belgium	alexander.jaust@uhasselt.be
Kačur Jozef	Slovakia	Jozef.Kacur@fmph.uniba.sk
Kaiser Klaus	Germany	kaiser@igpm.rwth-aachen.de
Kang Tong	China	kangtong@cuc.edu.cn
Kanschat Guido	Germany	kanschat@uni-heidelberg.de
Karasözen Bülent	Turkey	bulent@metu.edu.tr
Karova Fatimat	Russian Federation	karova.fatimat@mail.ru
Kim Byeong Hun	Korea, Republic of	b.hoon.kim@samsung.com
Klibanov Michael	USA	mklibanv@uncc.edu
Knabner Peter	Germany	peter.knabner@math.fau.de
Kongnuan Supachara	Thailand	suputchara@yahoo.com
Kucera Radek	Czech Republic	radek.kucera@vsb.cz
Kudryashova Tatiana	Belgium	kudryashova@imamod.ru
Lahaye Domenico	Netherlands	d.j.p.lahaye@tudelft.nl
Le Menach Yvonnick	Belgium	yvonnick.le-menach@univ-lille1.fr
Lee Hyun Geun	Korea, Republic of	leeh1@kw.ac.kr
Lefebvre Tom	Belgium	tom.lefebvre@ugent.be
Livingston Elizabeth	USA	eliving2@illinois.edu
Müller Rüdiger	Germany	mueller@wias-berlin.de
Macías-Díaz Jorge E.	Mexico	jemacias@correo.uaa.mx
Magri Marco	Italy	m.magri007@unibs.it
Marsic Nicolas	Germany	marsic@temf.tu-darmstadt.de
Mattesi Vanessa	Belgium	vanessa.mattesi@ulg.ac.be
Mbehou Mohamed	South Africa	mohamm@unisa.ac.za
Melicher Valdemar	Belgium	valdemar.melicher@uantwerpen.be
Melman Aaron	USA	amelman@scu.edu
Miclăuş Dan	Romania	dan.miclaus@cunbm.utcluj.ro
Mihala Patrik	Slovakia	p.mihala@gmail.com
Mitra Koondanibha	Netherlands	k.mitra@tue.nl
Modave Axel	France	axel.modave@ensta-paristech.fr
Motyčková Kristina	Czech Republic	kristina.motyckova@vsb.cz
Mukanova Balgaisha	Kazakhstan	mbsha01@gmail.com
Mumtaz Faisal	Qatar	faimumtaz@hbku.edu.qa
Nicaise Serge	France	serge.nicaise@univ-valenciennes.fr

Nigro Alessandra	Italy	alessandra.nigro@unibz.it
Oberhuber Tomáš	Czech Republic	tomas.oberhuber@fjfi.cvut.cz
Oliveira Diana	Portugal	diana.oliveira@tecnico.ulisboa.pt
Ondrušová Mariana	Slovakia	mariana.ondrusova@fri.uniza.sk
Pacheenburawana Archara	Thailand	archara@mathstat.sci.tu.ac.th
Patthanangkoor Poonchayar	Thailand	p.patthanangkoor@gmail.com
Pels Andreas	Germany	pels@gsc.tu-darmstadt.de
Petukhov Andrey	Russian Federation	petukhov@physics.msu.ru
Pişcoran Laurian-Ioan	Romania	plaurian@yahoo.com
Pop Iuliu Sorin	Belgium	sorin.pop@uhasselt.be
Quarteroni Alfio	Switzerland	alfio.quarteroni@epfl.ch
Radu Florin Adrian	Norway	florin.radu@uib.no
Rave Stephan	Germany	stephan.rave@uni-muenster.de
Ren Jian	China	ren_jian@iapcm.ac.cn
Rogier Hendrik	Belgium	Hendrik.Rogier@UGent.be
Rowan Thomas	Belgium	thomas.rowan@durham.ac.uk
Ruas Vitoriano	France	vitoriano.ruas@upmc.fr
Safdari Masoud	USA	msafdari@gmail.com
Salehi Shayegan Amir Hossein	Iran, Islamic Republic of	ah.salehi@mail.kntu.ac.ir
Sanghavi Chaitanya	Belgium	chaitanya.sanghavi@siemens.com
Schütz Jochen	Belgium	jochen.schuetz@uhasselt.be
Schardt Simon	Germany	simon.schardt@kit.edu
Senel Pelin	Turkey	psenel@metu.edu.tr
Serna-Reyes Adan Jair	Mexico	ajserna@correo.uaa.mx
Shilnikov Evgeny	Russian Federation	shilnikov@imamod.ru
Shin Jaemin	Korea, Republic of	jmshin@ewha.ac.kr
Shmerling Efraim	Israel	efraimsh@yahoo.com
Singh Vikram	Israel	vikram@campus.technion.ac.il
Slodička Marián	Belgium	marian.slodicka@ugent.be
Smirnov Alexey	Russian Federation	smirnov.av14@physics.msu.ru
Šisková Katarína	Belgium	katarina.siskova@ugent.be
Tertrais Hermine	Belgium	hermine.tertrais@ec-nantes.fr
Thierry Bertrand	France	thierry@ljll.math.upmc.fr
Tittarelli Roberta	France	roberta.tittarelli@umontpellier.fr
Tsukerman Igor	USA	igor@uakron.edu
Urbán Jozef	Slovakia	jozo.urban@gmail.com
Vázquez-Méndez Miguel E.	Spain	miguelernesto.vazquez@usc.es
Valli Alberto	Italy	alberto.valli@unitn.it
Van Bockstal Karel	Belgium	karel.vanbockstal@ugent.be
Van Daele Marnix	Belgium	Marnix.VanDaele@UGent.be
Vande Ginste Dries	Belgium	dries.vandeginste@ugent.be
Vazquez Sabariego Ruth	Belgium	ruth.sabariego@kuleuven.be
Wang Ran	China	ranwang@cuc.edu.cn
Yu Yunlong	China	yu_yunlong@iapcm.ac.cn
Yun Beong In	Korea, Republic of	paulllyun@gmail.com
Zeifang Jonas	Germany	jonas@zeifang.net